



University of
Nottingham

UK | CHINA | MALAYSIA

Glass on The Silk Roads:

An SEM-EDS study of Islamic Period artifacts from
Rayy, Iran: their manufacture and trade connections.

Originally submitted June 2024, in partial fulfillment of the conditions for the
award of the degree MRes Archaeology.

Emily Bell MRes

20516001

Supervised by Dr Julian Henderson

School of Humanities

University of Nottingham, University Park

I hereby declare that this thesis is all my own work, except indicated in the text:

Word Count: 24,966.

Signature: *Emily Bell*

Date: 27/06/2024

Contents

| | |
|---|-----|
| List of Figures | iii |
| List of Tables..... | v |
| Chapter 1: Introduction..... | 1 |
| 1.1 The Site, Rayy | 1 |
| 1.2 Preservation at the site | 2 |
| 1.3 Layout of the city..... | 3 |
| 1.4 Previous Excavations | 4 |
| 1.4.1 19 th Century Survey..... | 4 |
| 1.4.2 20 th Century Excavations..... | 7 |
| 1.5 The Silk Roads..... | 8 |
| 1.6 The Historical Setting | 9 |
| 1.6.1 The Pre-Islamic Era..... | 9 |
| 1.6.2 The Islamic Era..... | 9 |
| 1.6.3 The Umayyad Caliphate | 10 |
| 1.6.4 The Abbasid Caliphate | 10 |
| 1.6.5 Persian Resistance and the Buyid Period | 11 |
| 1.7 The Glass Samples R.01-R.57..... | 13 |
| Chapter 2: Glass | 17 |
| 2.1 Glass Composition..... | 17 |
| 2.2 The Scientific Analysis of Glass..... | 19 |
| 2.3 Islamic Glass | 20 |
| 2.3.1 Flux Agent | 20 |
| 2.3.2 Production Model..... | 21 |
| 2.4 Sasanian Glass..... | 24 |
| 2.5 Regional Fingerprints..... | 25 |
| Chapter 3: Methodology | 30 |
| 3.1 Sample Preparation | 31 |
| 3.2 Analysis..... | 33 |
| 3.3 Analysis of The Data..... | 34 |
| 3.3.1 Data Cleaning | 34 |
| 3.3.2 Standard Deviation..... | 34 |
| 3.3.3 Cluster Analysis | 35 |
| 3.3.4 Principal Component Analysis | 37 |
| 3.3.5 Data Visualisation | 37 |
| 3.4 Regional Comparison..... | 38 |
| 3.5 Limitations of The Study..... | 39 |

| | |
|---|----|
| Chapter 4: Comparative Data, The Case Studies | 40 |
| 4.1 Rayy | 40 |
| 4.2 The Serçe Limani Shipwreck | 41 |
| 4.3 Al Raqqa..... | 43 |
| 4.4 Samarra | 45 |
| 4.5 Gorgan..... | 46 |
| 4.6 Siraf..... | 47 |
| 4.7 Nishapur | 48 |
| Chapter 5: Results | 51 |
| 5.1 Element Maps..... | 51 |
| 5.2 SEM-EDS Analysis Results | 53 |
| 5.3 R.28..... | 54 |
| 5.4 Standard Deviation | 55 |
| 5.4.1 Regional Comparison..... | 56 |
| 5.5 Cluster Analysis..... | 58 |
| 5.6 Principal Component Analysis | 59 |
| 5.7 Regional Comparison..... | 63 |
| 5.7.1 Cluster 1-3 | 65 |
| 5.7.2 Cluster 2 | 65 |
| 5.7.3 Cluster 4 | 66 |
| 5.8 Schibille et al. 2022 S1/S2 | 66 |
| 5.9 Schibille et al. 2022 Group 3/Mesopotamian | 68 |
| 6.1 Materials Composition..... | 70 |
| 6.2 Technological Variance | 71 |
| 6.3 Cluster Analysis and Principal Component Findings..... | 72 |
| 6.4 Comparative Typology with Mesopotamian and Eastern Mediterranean Glasses..... | 74 |
| 6.4.1 Cluster 1/3 (C1/3) | 74 |
| 6.4.2 Cluster 2 (C2) | 75 |
| 6.4.3 Cluster 4 (C4) | 76 |
| 6.5 Conclusions | 77 |
| 6.5.1 Proposals for Further Study | 78 |
| Bibliography | 80 |
| Appendix 1: A Catalogue of the Rayy Glass..... | 90 |
| Appendix 2: Table Comprising all Data Considered | 91 |

List of Figures

| | |
|--|----|
| Figure 1: A Map of the Silk Roads across Eurasia indicating the location of Rayy (adapted from Schibille et al. 2022: 2)..... | 2 |
| Figure 2: A topographical view of the citadel showing the portion destroyed by the cement factory (Rante, 2015: 39)..... | 2 |
| Figure 3: Topographical plan of the site Rayy (Rante, 2008: 191)..... | 3 |
| Figure 4: Photograph of the southern rampart (Rante, 2008: 194)..... | 4 |
| Figure 5a: (left) Plan of Rayy by Ker Porter circa 1820 (Rante, 2015: 27). B: (right) Plan of Rayy by Pascal Coste circa 1840 (Rante, 2015: 29). | 6 |
| Figure 6: Topographical map of the Češmeh ‘Alī (Rante, 2014: 33). | 7 |
| Figure 7: Carved stucco from Samara demonstrating the vegetal and geometric designs (Abdullahi & Rashid Bin Embi, 2013: 245)..... | 11 |
| Figure 8: R.42.1/R.41.2, an aqua coloured glass vessel (image taken by author). | 14 |
| Figure 9a: (left) R.33 a colourless glass rim, b: (right) R.30 a weathered yellow glass (images taken by author)..... | 15 |
| Figure 10: R.38 a colourless glass rim with iridescent weathering (images by author). | 15 |
| Figure 11a: (left) R.28 a thick weathered green glass, b: R.57 a indiscernible black glass (images taken by author)..... | 16 |
| Figure 12: A biplot of MgO vs K ₂ O in a series of glasses demonstrating the difference between natron glass (pre-9th c.) and plant ash glass (post-9th c. and Sassanian) (Freestone, 2021: 249). | 17 |
| Figure 13: A diagram of a centralised glass production model, Egyptian natron was mixed with sand to produce raw glasses at primary glass factories which were then distributed to workshops located in urban centres to be remelted and worked into artifacts (Freestone, 2021: 246)..... | 22 |
| Figure 14: A map showing the locations of the sites chosen for case study (image by author created using Tableau). | 31 |
| Figure 15: KNIME workflow demonstrating how to perform a hierarchical clustering analysis (image by author)..... | 36 |
| Figure 16: The addition of the PCA workflow in KNIME (image by author). | 37 |
| Figure 17: An example of a blank Tableau workbook, data visualisations are made by dragging the variables to the columns and rows, dragging one of each will automatically create a scatter plot (image by author). | 38 |
| Figure 18: A map showing the locations of the sites chosen for case study (image by author, created using Tableau). | 40 |
| Figure 19: A beehive shaped furnace Tell Zujaj 8-9th century CE (Henderson, 2003: 111)..... | 43 |

| | |
|---|----|
| Figure 20: Element map of R.57, a black glass demonstrating that the structure is mostly homogenous with three streaks through the structure that is high in silicon and low in sodium, calcium, and aluminium (image from SEM). | 51 |
| Figure 21: Element map of R.54, a black glass demonstrating that the structure is mostly homogenous apart from sodium and an air bubble in the glass matrix and one area high in sodium (image from SEM). | 51 |
| Figure 22: Element map of R.27, a colourless glass showing a uniform glass matrix, the top part of the glass under the microscope has a part that is high in silicon, sodium, aluminium and magnesium (image created in SEM). | 52 |
| Figure 23: Element map of R.33 a colourless glass showing that the microstructure is mostly consistent though there is a layer of aluminium at the edges (image created in SEM). | 52 |
| Figure 24: A plot of the Rayy glass demonstrating that they are all plant ash glasses (image created by author in Tableau). | 55 |
| Figure 25: A dendrogram produced by KNIME analytics software for the Rayy glass (image create by author). | 58 |
| Figure 26a: (top left) Principal component 1 Al_2O_3 vs Na_2O . B: (top right) Principal component 2 Na_2O vs MgO C: (bottom left) Principal component 3 Na_2O vs SiO_2 . D: (bottom right) Principal Component 4 Na_2O vs CaO . E: Key for biplots (below tables) (image created by author using Tableau). | 61 |
| Figure 27a: (above) Biplot of MgO/CaO vs Al_2O_3 by Phelps (2018: 262) demonstrating his glass types. B: (below) The same biplot plotted with instead the glass from Rayy with the cluster number indicated by the key (analysed here). | 63 |
| Figure 28: Biplot of MgO/CaO vs Al_2O_3 comparing the data from Nishapur coloured (Schibille et al., 2022; Wypyski, 2015, Brill 1995), Gorgan (Schibille et al., 2022) and Rayy (analysed here) (image created by author using Tableau). | 65 |
| Figure 29: Biplot of MgO/CaO vs Al_2O_3 comparing Raqqa Type One (Henderson et al., 2004), the Serçe Limani Wreck (Brill, 2009), Tyre (Freestone, 2002) and Rayy (analysed here) (image created by author using Tableau). | 65 |
| Figure 30: Biplot of MgO/CaO vs Al_2O_3 comparing the data from Nishapur colourless (Type A) (Schibille et al., 2022; Wypyski, 2015, Brill 1995), Rayy (analysed by author) and Samarra (Schibille et al., 2018; Henderson et al., 2016) (image created by author using Tableau). | 66 |
| Figure 31a: (top left) biplot comparing the level of SiO_2 with TiO_2 across Clusters 1-4, b: (top right) biplot comparing the level of SiO_2 with Fe_2O_3 across Clusters 1-4, c: (bottom) biplot comparing SiO_2 with Al_2O_3 alumina across Clusters 1-4 (images produced by author using Tableau). | 67 |
| Figure 32: A biplot of MgO/CaO against Al_2O_3 comparing Clusters 1-4 from Rayy (analysed by author) with the Sassanian glass from Veh Ardašir (Mirti, 2009). | 69 |
| Figure 33: R.28, undiscerned type, 4-6.2mm thick (image taken by author). | 70 |

Figure 34a: (left) R.57, a Cluster 3 black glass, b: (right) R.42 curved glass belonging to a small bottle, almost colourless 0.3mm thick (images taken by author).**Error! Bookmark not defined.**

Figure 35: R.46 blue curved sherd belonging to Cluster 2 group (image taken by author). 75

Figure 36a: (left) R.33 a colourless flat rim sherd, 3mm thick, b: R.38 a colourless elevated rim 0.5mm (images taken by author). 77

List of Tables

Table 1: Mean wt% values for each element in each of Phelps’s types, the final two columns are ratios of elements (Phelps, 2018: 260-1)..... 29

Table 2: The mean element oxide wt% value for Schibille and colleagues’ glass types G1a/b, G2-3 and S1/2, the final two columns are ratios of elements (Schibille et al., 2022: 6, Table 1)..... 29

Table 3: Results of the SEM-EDS analysis of the Rayy assemblage giving sample number and colour. Nd denotes not detected (analysed here). 54

Table 4: Mean, median and standard deviation values for each element included in all samples in Table 3, excluding R.28. 55

Table 5: Standard deviation values for each element from each of the case studies calculated from Appendix 2 Rayy Tape Bahram (Agha-Aligol et al., 2022) Rayy Corning (Schibille et al., 2022) Gorgan (Schibille et al., 2022) Nishapur (Wypyski, 2015, Brill, 1995), Siraf, (Swann et al., 2017) Al Raqqa (Henderson et al., 2004), Samarra natron (Schibille et al., 2022), Samarra Plant ash (Schibille et al. 2018, Schibille et al. 2022, Henderson, 2016) (ah denotes analysed here). 57

Table 6: This table gives the cluster number for each glass sample analysed. 59

Table 7: This table gives each of the oxides mean, minimum and maximum and standard deviation value for each cluster. Mean, minimum and maximum are presented as wt% and STD refers to their standard deviation values. 59

Table 8a: The loading values for each element for PC1-PC4 (above). B: The previous table with the insignificant values (below 0.03) removed (below) (by author, data retrieved from KNIME Analytics Platform). 60

Table 9: Average wt% oxide value for each element for all the case study sites: Rayy Tape Bahram (Agha-Aligol et al., 2022) Rayy Corning (Schibille et al., 2022) Gorgan (Schibille et al., 2022) Nishapur (Wypyski, 2015, Brill, 1995), Siraf, (Swann et al., 2017) Al Raqqa (Henderson et al., 2004), Samarra natron (Schibille et al., 2022), Samarra Plant ash (Schibille et al. 2018, Schibille et al. 2022, Henderson, 2016.) Now including Veh Ardashir (Mirti et al. 2009) (ah denotes analysed here). 64

Table 10: Average MgO/CaO and MgO/K₂O levels for each cluster from the Rayy data (analysed here, calculated using Excel). 68

Table 11: Average MgO/K₂O and average MgO/CaO values for G1-3 and S1/2 (Schibille et al., 2022: 6, Table 1). 68

Chapter 1: Introduction

This thesis analyses 35 samples of archaeological glass artifacts, from the ancient city of Rayy in northern Iran, dated to the 10th century, housed in a collection in the Metropolitan Museum of Art. The glasses are investigated using Scanning Electron Microscopy Coupled with Energy Dispersive Spectroscopy to reveal the microstructure and chemical composition of the artifacts. The aim of this work is to group them based on their composition and to gain an understanding of relationships between the elements to make inferences about their recipe or method of production. The composition of major oxides will be compared to data collected from a series of case study sites (*Figure 14*) to make suggestions about provenance and mode of production, these sites were decided based on secondary research. To contextualise this information the first chapter will describe the site Rayy and its historical setting and the second will give a background to glass, its study and specifically the study of Islamic glass. The chapters that follow will present the methodology, results discussion and conclusions reached.

1.1 The Site, Rayy

Rayy is located on the Iranian Plateau at the foot of the Elborz mountain range, to the south of the modern capital Tehran. The northernmost area of the site is halted by the Elborz mountain slopes, and the southernmost part of the site is met by the western branch of the Dast Kawir, the Great Desert of Iran (Rante, 2007: 161). Due to the presence of natural boundaries in the form of mountains and deserts surrounding the site, it is situated on a prime East to West trade route which developed over time. This route, or rather collection of ancient trade routes has been termed “The Silk Roads”. Rayy is situated on the Khurāsān Road that connected Mesopotamia to the Iranian Plateau and on to China (Tor, 2016: 377). Historical references often point to the city’s function as a commercial hub, Ibn al-Fakih records that the city boasted eight bazars that sold silks, wooden items and lustre ware. Al Muqadassi recorded that the fruit market and the library at Rayy were particularly splendid and includes details of a large caravanserai (Minorsky, 1994: 471).



Figure 1: A Map of the Silk Roads across Eurasia (Schibille et al. 2022: 2), indicating the location of Rayy.

1.2 Preservation at the site

It is recorded by al-Istakhri that the original settlement was $1^{1/2}$ by $1^{1/2}$ farsakhs, roughly 8km by 8km, the buildings were made from clay, brick and plaster (Minorsky, 1994: 471).

Occupation at Rayy was not always continuous, the site was abandoned for centuries and then built over, therefore modern construction of the capital has buried many of the ancient remains at the site. Today the town of *Šāh ‘Abd al-‘Azīm* has absorbed all that lay to the west of Rayy, and the cement factory, already functioning at the beginning of the 20th century destroyed all the northern part of *Kuh-e Sorsore* (the citadel). The motorway constructed between this relief and *Bībī Šahrbanū*, at the foothills of the Elborz mountain range, destroyed even more. (Rante, 2015: 31).

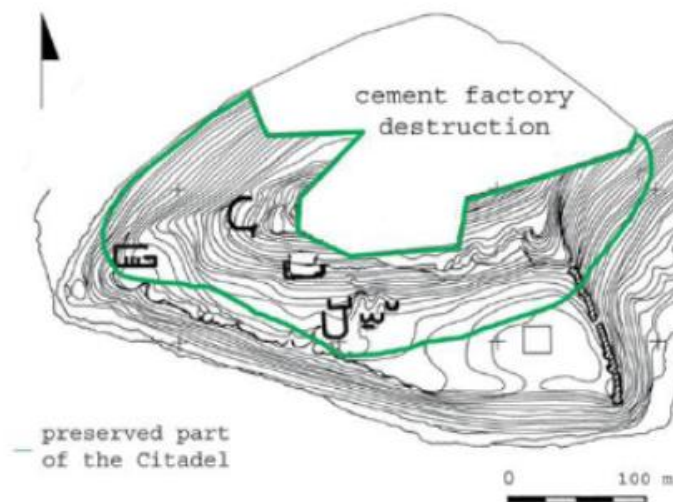


Figure 2: A topographical view of the citadel showing the portion destroyed by the cement factory (Rante, 2015: 39).

1.3 Layout of the city

The ancient city during the Islamic Period (7th-13th centuries) was constituted of three parts, a citadel, a *shahrestan* or government quarter and a suburb where many of the residents lived. According to early excavations, the citadel and the *shahrestan* were built contemporaneously, prior to the Sasanian Period (224-651 CE). The citadel is triangular and extends towards the foothills of the mountain *Bībī Šāhrbānū*, it was split up into two terraces in the north and in the south, the peak of this elevation was encircled by a fortified wall, likely a residence for the governor of the city. Though, nothing of which remains due to modern industrial and agricultural activities. The *shahrestan* sits to the southwest of the citadel's elevation, it is a large area covering approximately 15ha surrounded by a fortified wall which follows the natural geology of the site. However, only the eastern part remains as the majority is buried beneath the town of *Šāh 'Abd al-'Azīm* and a glycerine factory. Schmidt, during his excavations interpreted this space as the government quarter where all economic and administrative personnel lived and carried out their functions. The space gained importance

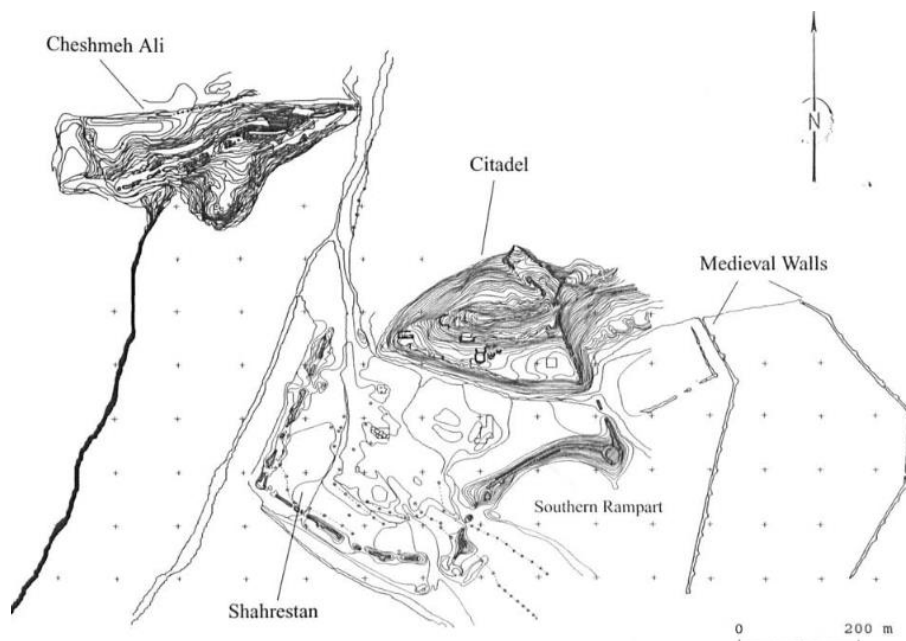


Figure 3: Topographical plan of the site Rayy (Rante, 2008: 191).

and expended during the Seljuk Period (Saadati, 2021: 211). The suburb composed primarily of residential and agricultural areas is situated west of the other two structures, this area was not enclosed by a fortification until the early tenth century under the Buyids when two ramparts were raised as it was deemed that the suburb of the city had become too economically important (Rante, 2008: 192). The part of the site between the *Kuh-e Sorsore*

and *Bībī Šahrībānū* is the oldest Islamic part of the city called *Rey-ye Barin* (upper town) and to the south is *Rey-ye Zirin* (lower town) (Rante, 2015: 35).

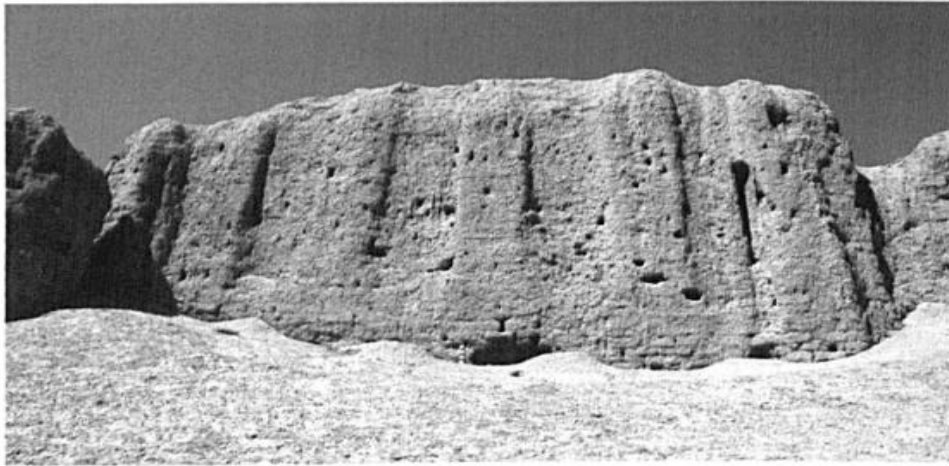


Figure 4: Photograph of the southern rampart (Rante, 2008: 194).

Of the surviving structures at Rayy, the best preserved is the southern rampart, this highlights the defensive character of the city, large ramparts were necessary and standard to other urban settlements in the vicinity such as Merv or Afrasiab to defend against increasingly powerful siege weaponry which was introduced to the area in the Hellenistic Period (Rante, 2008: 196). Moreover, the preliminary analysis of pottery from the rampart and Shahrestan at Rayy indicates that the fortress dates to the Parthian period. An important aspect to consider is the increasing centralisation of the Parthian dynasty. The shift of Parthian power westward, from Nisa to Hekatompylos, Ecbatana, and Seleucia, might have also encompassed Rayy. Therefore, Rayy would be part of the eastern urban and defensive traditions, originating from regions that assimilated and transformed the Hellenistic urban model during the Parthian era (Rante, 2008: 209).

1.4 Previous Excavations

1.4.1 19th Century Survey

Interest soon arose in the site during the 19th century when European explorers were searching for remains of old Raga/Raghae, the name for the ancient Persian city under the Sasanians. Robert Ker Porter drew the first plan of old Rayy in 1821-22, Rocco Rant (2015: 27), however, has pointed out that upon comparison with aerial photography of the site, the orientation is distorted and thus the plan should be treated with caution. The next survey of the site was undertaken by the architect Pascal Coste in 1840, according to aerial

photography this plan appears to be correctly orientated. His rendering of the western elevation of the site is particularly useful because it describes structures that were later destroyed by modern construction. From the left end of the western elevation, a large tower in mud brick and pisé is depicted. The rampart seen descending on the right corresponds to the *Češmeh 'Alī* region, although the connection with the citadel is not evident. In the second plan, the relief of the citadel stands in front of the *Bībī Šahrbanū*. The tower-mausoleum of Naqqāreh Hāneh and the castle of Qal'at Gabr are also visible, followed by the tower-mausoleum of Tuğril Bek. Another large tower marks the right-hand end, likely corresponding to the one near *Šāh 'Abd al-'Azīm* on the plan, Coste likely drew this view from inside the town's western rampart (Rante, 2015: 31).

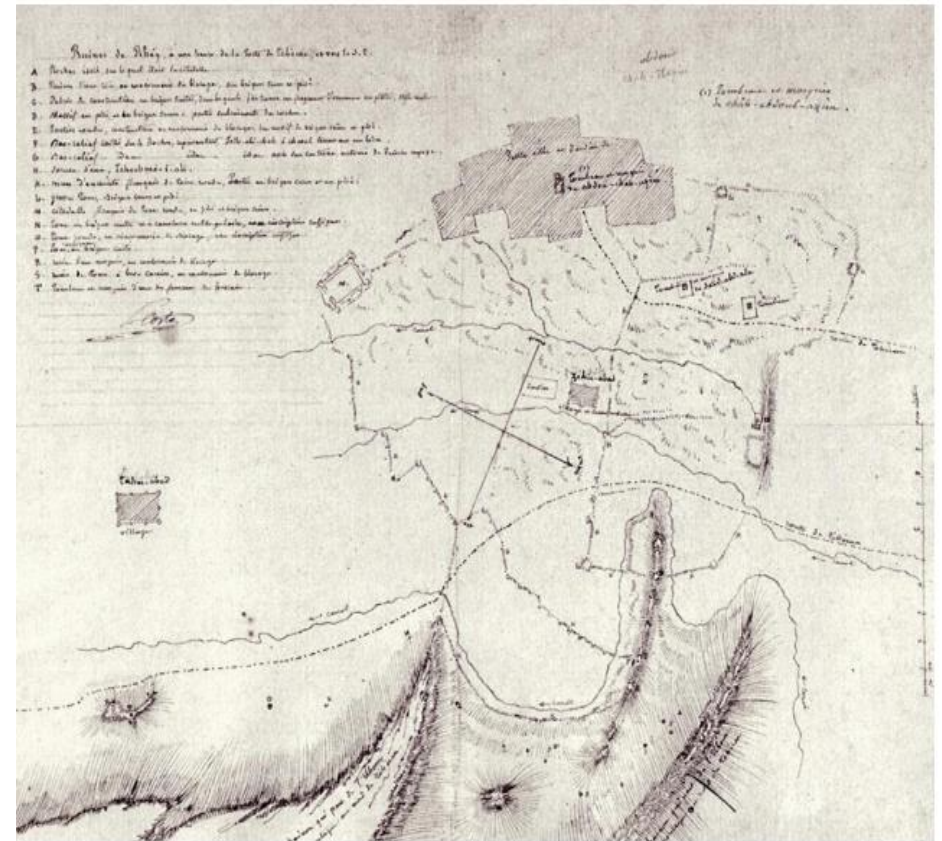
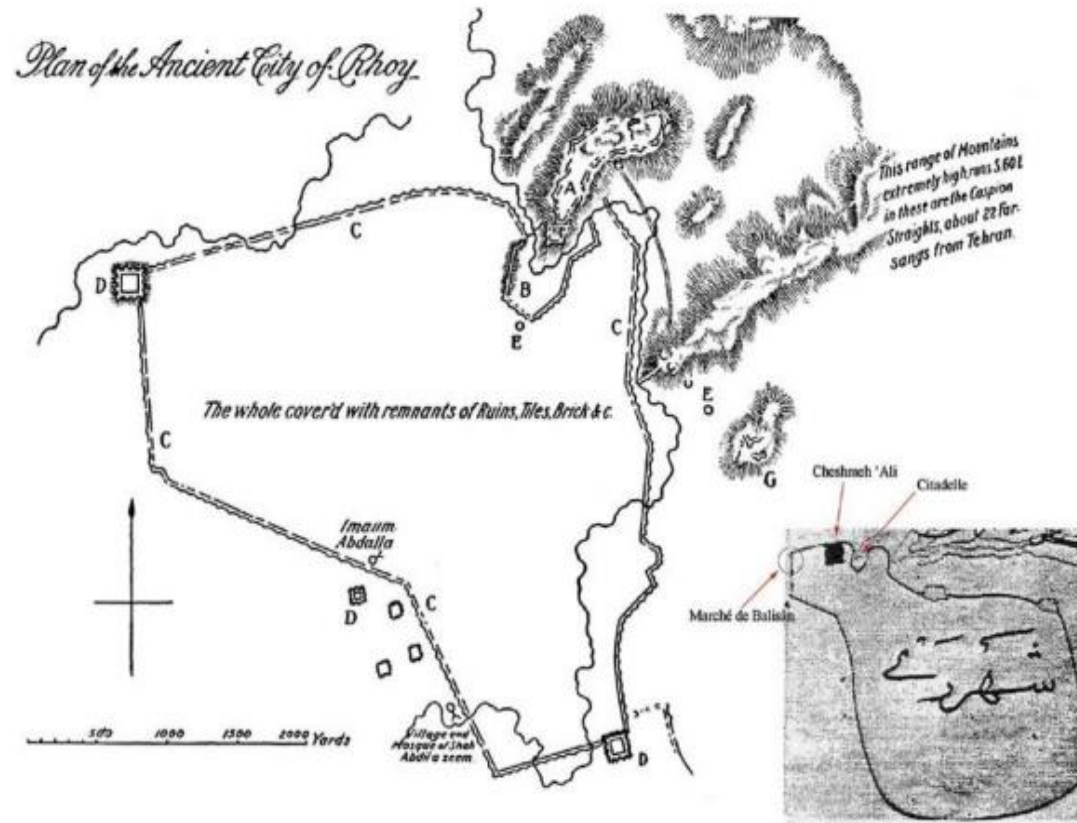


Figure 5a: (left) Plan of Ray by Ker Porter circa 1820 (Rante, 2015: 27). B: (right) Plan of Ray by Pascal Coste circa 1840 (Rante, 2015: 29).

1.4.2 20th Century Excavations

During the 20th century there were two main excavations carried out at the site, the first commencing in 1934 continuing until 1936 under the direction of Erich F. Schmidt (1935) as part of a joint expedition by The Philadelphia Museum of Art and the Boston Museum of Fine Art. During three seasons of excavation the only topographical plan of the site was produced which was never fully completed. At the time of these excavations the northern part of the city had been destroyed and so only the southern part of the city could be excavated. Two plans from the site were produced although any link between the two areas was omitted, furthermore the areas appear to be from different periods further complicating the picture. It is also argued by Rante (2015: 32) that these excavations lacked stratigraphical analysis. Not to mention that the final publication of the excavation was never finished resulting in a huge loss of data about the site.



Figure 6: Topographical map of the Češmeh 'Alī (Rante, 2014: 33).

The second round of excavations during the 1970s was the result of a collaboration between Professor Renata Holod (University of Pennsylvania), Professor E.J. Keall (University of Toronto) and Dr. Chahryar Adle (CNRS, Paris). Adle's publications on the site were concerned with the funerary constructions around the site, and the interior city walls in which he analyses the various construction phases in line with a meticulous study of the ceramic remains and the stratigraphy. Keall (1979) presents an overview of previous archaeological work at Rayy and proposes a project to resume archaeological activities. Summarizing Schmidt's work and addressing associated challenges, Keall outlines a schematic plan of the site, integrating Češmeh 'Alī and the old town of Rayy. He emphasizes the site's complexity,

that its parts were distinct yet interconnected, he further criticises earlier expeditions for misunderstanding the site and lacking archaeological insight.

1.5 The Silk Roads

The term “Silk Road” is a popular one that is used to refer to a corridor or today a series of multiple corridors¹ of land and the later maritime routes that saw the movement of goods including silk, spices, ceramics, metals, slaves and importantly, glass. Today, the shorthand term Silk Road is recognised as a much wider phenomenon of trans-Eurasian exchanges (Hansen, 2012: 56). Components of this interconnected network have occasionally been described using terms focused on a single commodity, such as "the salt route" or "the tea-horse road," or differentiated by geographical features, for example "the desert route." However, these labels fail to fully encompass the intricacy of these exchanges. Such simplistic titles mask the complexity of the commodities, materials, peoples, and their interactions, compartmentalising a multifaceted system of interactions. How can one know when the salt route ends, and the tea-horse roads begins (Williams, 2015: 3). The region of the vast network of routes that makes up the Silk Roads spanned from Japan across central Asia into the Mediterranean world and by the 9th century across to Scandinavia. It is recorded by Ibn Khordādhbeh’s *Kitāb al-Masālik wa l-Mamālik* (Book of Itineraries and Kingdoms), that the Vikings traded furs along the Silk Roads (Romgard, 2016: 238). Furthermore, the 85,000 dirhems discovered in Sweden alone dating particularly between the 9th – 10th centuries demonstrate the connection between Viking and Islamic worlds (Myrdal, 2020: 8). Proto-Silk Roads can be discerned in the archaeological record, the trade of faience beads is particularly elucidating on these early trade routes (Lu et al., 2021: 8). When writing on the Silk Roads however Liu (2010: 62) argues that while the markets of the Han, Kushan, Parthian and Roman empires saw the beginnings of trade between these regions, the Silk Roads were not fully formed until these empires began to collapse in the 3rd century CE.

Trade along the Silk Roads was crucial in enabling the spread of Islamic teachings, papermaking technology brought from China revolutionised the way in which ideas could be transported. Large urban centres became hubs of learning and innovation, The House of Wisdom in Baghdad housed a great library of translated texts (Kaviani et al.2012: 1273). The

¹ It is considered today that the term ‘Silk Road’ coined by Ferdinand Freiherr von Richtofen in 1877 (Waugh, 2007, 2) is misleading, a ‘romantic deception’ propagated by Eurocentric historians attempting to create an East to West transportation corridor and a Chinese dominated understanding of western Asia (Graf, 2018: 444; Whitfield, 2007: 205).

influence of Islamic art and architecture spread as far as Spain, Islamic architectural styles such as a hypostyle prayer hall with horseshoe arches and a *sahn* courtyard can be seen deployed in the Great Mosque of Cordoba, constructed in 785 CE (Dodds, 1992: 11).

1.6 The Historical Setting

1.6.1 The Pre-Islamic Era

Occupation of the Iranian Plateau developed over five millennia from the 8th – 3rd millennium BCE (Helwing, 2012: 501). During the 8th millennium the settlers relied on a broad-spectrum economy based largely on wild resources, the palaeo-osteological record has demonstrated evidence of the development of selective hunting at this time (Helwing, 2012: 505). These earliest phases were constricted to the *Češmeh 'Alī* to the north-west of the site, though these are sparse and further there is extremely little evidence of any major activity during the Bronze Age. Archaeological evidence of floors and rampart segments from the site demonstrates that the next dominant phase of occupation was during Iron Age I-II which overlaps with Parthian occupation, these buildings were reused until the 2nd century BCE (Rante, 2015: 11). Textual sources reveal that under the Sasanians, the longest ruling Persian Imperial dynasty ruling from 224-651 CE, the town was named Raga which was documented to have been the second holy place created by Ahura Mazda (Minorsky, 1994: 471).

1.6.2 The Islamic Era

Typically, the Islamic Period began after the death of the prophet Muhammad in 632 CE, after his death Abu Bakhr was appointed the position of Rashidun. This title refers to an institution or public office that governs a territory in accordance with Islamic law. During this time Arabia became united under Islam, Bakhr and his four successors would form the first Islamic Caliphate, the Rashidun Caliphate. After consolidating power in Iraq, Abu Bakhr began his conquest of Byzantine Syria during which he died, making Umar his successor who completed the Syrian invasion in 637 CE (Madelung 1997: 56-61). Umar further pushed into the remnants of the Sassanian empire capturing Armenia and Egypt by 642 CE. By 643 CE almost the entirety of the Sassanian territory had been brought under Islamic control. In 654 CE Cyprus was taken. The next rulers Uthman and Ali saw the Caliphate fall into fragmentation and the First Islamic Civil War, which led to the overturn of the Rashidun Caliphate and the establishment of the Umayyad Caliphate (Hawting, 2008: 11).

1.6.3 The Umayyad Caliphate

From 661 CE the Caliphate fell into the hands of Muawiya, the governor of Syria. He was the first of a series of rulers who had hereditary rule, they were called the Umayyad Dynasty. In traditional accounts the Umayyads cared much more for territorial expansion than for Islam and Islamic culture (Hawting, 2008: 11). It is therefore not surprising that during this period, glass was sourced heavily from Byzantium suggesting little Umayyad control over the primary production of glass at this time (Henderson, 2013: 259-60). The Umayyads continued to expand Muslim territory by annexing further into Africa taking control of parts of the Maghreb, India, Transoxiana, an area of land comprising modern day eastern Uzbekistan, Western Tajikistan, southern Kazakhstan, parts of Turkmenistan and Southern Kyrgyzstan (Hawting, 2008: 11). Beginning in 711 CE from North Africa, Muslims began to raid land controlled by the Visigoths in Spain and Portugal which ultimately ended in the downfall of the Visigoth kingdom and the beginning of Muslim control over the Iberian Peninsula (Donner, 2008: 43). After Caliph Hisham's death in 743 CE a crisis in succession led to the third civil war of the Islamic Caliphate which paved the way for the Abbasid Dynasty to take power in 750 CE (Kennedy, 2008: 58).

1.6.4 The Abbasid Caliphate

The Abbasid Caliphate is considered by scholars to be The Golden Age of Islam, the focus shifted away from military conquest and the edges of the empire were left to fall into independent kingdoms. Focus shifted inwards towards the Islamic Empire, and Islamic culture thrived. Moreover, there was a geographical shift away from Syria with its strong Byzantine associations towards a universal Muslim identity (Bennison, 2009: 167). While conversely the Umayyad period was the formative period of Islamic art, where even religious monuments set up by Caliphs display a clear mixture of Greco-Roman, Byzantine and Sassanian artistic traditions. Gradually, under the impact of the Muslim faith, these artistic styles began to unify and become uniquely Muslim. This shift is regarded as one of the defining parts of the Abbasid Caliphate and marks it as the period of the fruition of Islamic culture of art, science, literature and poetry. In 762 CE Baghdad was founded as the capital of the Abbasid Dynasty, the city became a centre for science and innovation, much of which took place at The House of Wisdom, a library which inhabited a large collection of scientific works shelved under the names of their donors. It was central to the translation movement where famous works were translated into Arabic (Kaviani et al.2012: 1273). Abbasid art is

possibly best seen at Samarra, here one can observe the use of repetitive geometric forms and pseudo vegetal forms which became intrinsic to the Islamic style. The importance of the Islamic world as a haven for scientific and mathematical innovation is reflected in the use of geometric design (Abdullahi & Rashid Bin Embi, 2013: 245).



Figure 7: Carved stucco from Samara demonstrating the vegetal and geometric designs (Abdullahi & Rashid Bin Embi, 2013: 245).

1.6.5 Persian Resistance and the Buyid Period

Since the Abbasids lost hold over their outer territories, several independent native Iranian dynasties began to emerge across the Iranian Plateau from the 9th-11th century, a period sometimes known as the Iranian Intermezzo (Kraemer, 1986: 33). The first being the Tahirid Dynasty who had previously been governors of Khurāsān Province. Their control presided over the northeastern part of Iran, Afghanistan, Turkmenistan and Uzbekistan, the capital of this state was Nishapur. The relationship between these Iranian kings and the Abbasid Caliphate in Baghdad was complicated, the Tahirid Dynasty (821-873 CE) are described by Hugh Kennedy (2016: 139) as viceroys to the Abbasids, paying taxes in exchange for autonomy over the region.

In 819 CE a new dynasty seized control over the northern Iranian plateau, the Samanids. Although the city Rayy remained de facto under Abbasid control, several coins minted under Samanid authority have been uncovered at Rayy (Rante, 2015: 20). In 926 CE, Caliph al-Muqtadir officially appointed Naṣr b. Aḥmad, a Samanid prince residing in Buhara, as the governor of Rayy, documented by Ibn al-Aṭīr (Rante, 2015: 20). In 943 CE Rayy was captured by the Buyid dynasty and made their capital, yet this only lasted for two years as in 945 CE the capital was moved to Baghdad following the conquest of Iraq, though Rayy held

most of its authority over the Khurāsān region (Tor, 2016: 377). The Buyids consistently revived symbols and customs of the Sassanian empire using the title *Shahanshah* meaning king of kings. The Buyids commissioned many inscriptions at the site of Persepolis which they revered as being built by the legendary Iranian king Jamshid (Herzig & Stewart, 2011: 154). The Buyid dynasty reached its pinnacle under Panah Khusraw, who was renowned for his tolerance and construction projects such as the *Band-e Amir* dam near Shiraz. In 957-958 CE, Rayy endured severe earthquakes, resulting in significant casualties and damage to buildings including the collapse of a potential mosque in the *shahrestan* (Rante, 2015: 22). It was during this period that one of Rayy's most famous inhabitants lived, Al Razi who authored more than two-hundred works on medicine natural science, chemistry, mathematics, optics, astronomy, theology and philosophy (Zaimeche, 2005: 3).

The Buyid lands formed a federation rather than an empire, its major principalities located in Fars, Shiraz, Rayy Baghdad and Basra. (Kennedy, 2016: 188). After the death of the Buyid ruler Rukn al-Dawla's in 976 CE, his sons Asud al-Dawla, Mu'ayyid al-Dawla, and Fakhr al-Dawla divided the Buyid kingdom accordingly. Asud al-Dawla took control of the declining Abbasid centre, Mu'ayyid al-Dawla governed Isfahan and its province (central Iran), and Fakhr al-Dawla ruled over Hamadan and the Gibal provinces (northwest). Rayy was assimilated into the province of the plateau, emerging as its principal town. Between 976 CE and 983 CE control of Rayy and the Gibal region was taken by Mu'ayyid al-Dawla. Following his death in 983 CE, Fakhr al-Dawla regained control over Rayy and the entire Gibal province. After Fakhr al-Dawla's death in 996–997 CE, his young son Abu Talib Rustam ascended the throne, with his mother Sayyida acting as regent on his behalf. Internal struggles among the claimants to the throne weakened the political stability, leading to Rayy's conquest by the Gaznawids in 1029 CE (Rante, 2015: 22).

Following the city's conquest, King Mahmud of Gazna returned to his capital Khurāsān, leaving his son Masud as governor of Rayy and its surrounding regions, which at the time extended as far north as Armenia. Masud further expanded Gaznawid influence by capturing Isfahan from Ala al-Dawla. He furthermore engaged in military campaigns in the west of Iran, for control over Qazwīn, Zangan, Abhar, and adjacent areas. During this period, Rayy rose to prominence as one of the most politically significant cities in the Iranian world. However, in 1040 CE through military force a new dynasty established control of the city, the Seljuk dynasty. During the initial years of their rule, they assigned Rayy as the capital of their domain which encompassed territories stretching from Anatolia, Iran in the west and further

eastward into modern Afghanistan. The southern extent of their territory reached Iraq and parts of the Levant (Kennedy, 2016: 295-7).

Despite political change, the archaeological evidence indicates a continuity in ceramics, albeit with a slight decline in quantity, possibly suggesting a gradual abandonment of the urban centre. Conversely, excavations in the city's periphery revealed a significant increase in ceramic artifacts, suggesting a shift in population dynamics (Rante, 2015: 25). Moreover, the numismatic study by Miles (1938) supports this interpretation, due to a decline in coinage quality during later Seljuk rule. While Rayy retained its economic importance, particularly demonstrated through Schmidt's excavations on the outskirts of the city, recent findings in the urban centre showed a decrease in the abundance of material culture. Throughout the 12th century, Rayy experienced turmoil amidst the degeneration of the Seljuk Empire, marked by civil wars and shifts in regional control. Despite this, artisanal production, especially ceramics, flourished, reflecting local prosperity (Rante, 2015: 25; Rante & Di Pasquale, 2016: 417). Ultimately, Rayy faced devastation during the Mongol invasion in 1220 CE which brought the Islamic Period to an end.

1.7 The Glass Samples R.01-R.57

The glass artifacts under study were kindly sent for analysis by the Metropolitan Museum of Art in New York. It must be stated here that only the glass fragments themselves and a vague date of the 11th century was given for analysis. No contextual information was given alongside the glass fragments, it is assumed that because they are all labelled as being from Rayy that they were uncovered during one of the excavations at the site conducted by the museum. Although this cannot be assumed for certain as they may also come from a private collection donated to the museum. In any case there is no contextual information to complement this study, it is not clear which area of the site they are from or their exact date, though they are labelled as being 11th century.

The glass survives as broken fragments which have been separated into bags and given numbers in order which range from R.01-R.57. However, there are 44 total bags of glass, meaning that there are 13 bags missing from the original collection, this is if there were originally 57 bags of material. The numbers that are missing from the original collection are R.03, R.06, R.07, R.08, R.14, R.21, R.23, R.24, R.29, R.31, R.36, R.40 and R.52, this points to an issue with museum collections which is that items can become lost. Though, they may also have been lost in the field and never reached the museum. The samples represent a range

of colours of glass and a range of shape and sizes, suggesting differences in function. The types of fragments also differ, some are thin vessel bodies and others are thick rims, R42. is separated into two bags, one with an elongated rim and the other with glass from the body of the vessel, possibly it functioned a small bottle used for perfume or cosmetics. Some samples are severely weathered with very little surviving, there is no discernible decoration on the glass, no cuts or lustre applied to the surface.

There is a clear majority in the number of aqua/colourless glasses in the collection, however four of these clear glasses exhibit very little erosion or iridescence in comparison to the others² which are heavily eroded and show much iridescence³. The rest are green⁴, blue⁵ and two are yellow⁶, three examples are black⁷. Red glass is rare in Iran in the Islamic Period, and we find none of it here. Blue and green glasses are common while colourless is also very common in Islamic glass assemblages therefore this collection of glass samples is not out of the ordinary for its time and place of deposition. The majority of the glass finds are thin >1mm thick fragments likely from small bottles, some are however thicker almost 5mm and were possibly used as table ware such as plates or bowls which needed to be thicker in order to be durable enough to eat from. A well in Nishapur revealed a large set of undecorated coloured glass tableware (Kroger, 1995: 31). Other sherds are cylindrical and may be handles for glass cups or drinking vessels, unfortunately however the others are too broken to tell.

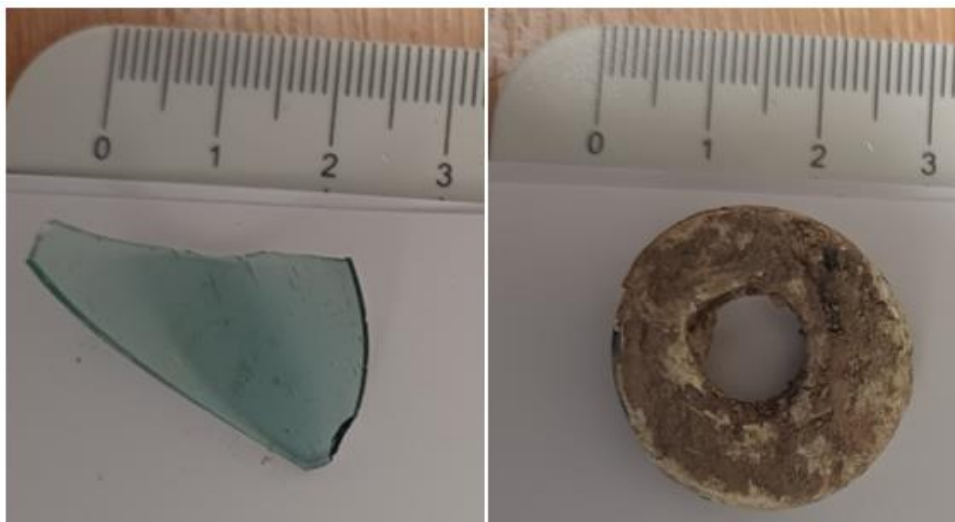


Figure 8: R.42.1/R.41.2, an aqua coloured glass vessel (image taken by author).

² R.02, R.33, R.42, R.51 and R.47.

³ R.04, R.10, R.12, R.13, R.15, R.17, R.18, R.19, R.22, R.25, R.27, R.28, R.32, R.38 and R.56

⁴ R.01, R.34, R.35, R.48, R.50.

⁵ R.09, R.16, R.20, R.26, R.39, R.41, R.45, R.46, R.49, R.55?

⁶ R.30 and R.37.

⁷ R.53, R.54, R.57.

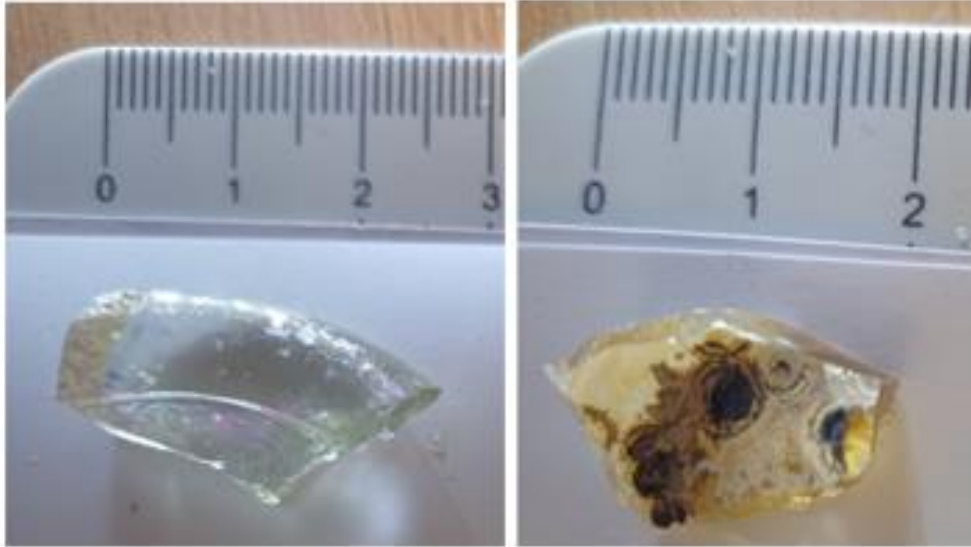


Figure 9a: (left) R.33 a colourless glass rim, b: (right) R.30 a weathered yellow glass (images taken by author).

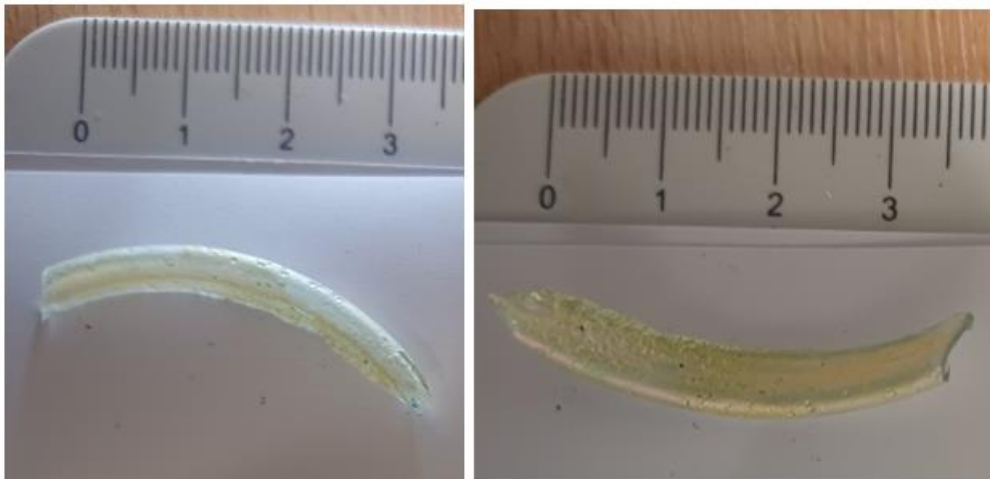


Figure 10: R.38 a colourless glass rim with iridescent weathering (images by author).



Figure 11a: (left) R.28 a thick weathered green glass, b: R.57 a indiscernible black glass (images taken by author).

Chapter 2: Glass

2.1 Glass Composition

Glass is composed of three essential ingredients, silica (SiO_2) the network former, this is the major constitutional material in glass production and can be sourced from crushing quartz pebbles or from sand. In the ancient world the mixture of an alkali was required as this reduced the melting temperature of silica from 1700°C to temperatures achievable during the late Bronze Age, 1050°C (Shugar & Rehren, 2002: 149). When glass was first produced in Mesopotamia the ashes that were used were halophytic or salt-loving plants of the *Chenopodiaceae* family. These plants grow in semi-desert saline environments often on the outskirts of deserts (Henderson, 2013: 23; Tite et al., 2006: 1284).

After primary glassmaking technology arrived in Egypt, glassmakers made a switch to incorporating natron, a soda rich evaporite which occurs naturally in the Wadi El-Natron. A resource that Egyptians had been using for at least a millennium to create faience, a partially vitreous precursor to glass, its microstructure consists of silica crystals encased in a glassy matrix (Shortland et al., 2006: 521; Nicholson, 2009: 1). Early plant ash glass could not be worked and re-melted in the same way as natron glass, high levels of K_2O causes the viscosity of the melt to increase which therein reduces the workability of the glass (Scott et al., 2017: 16). Due to its improved workability natron glass became widespread, and natron was exported and used across the Greco Roman world and even reached as far as China (Lu

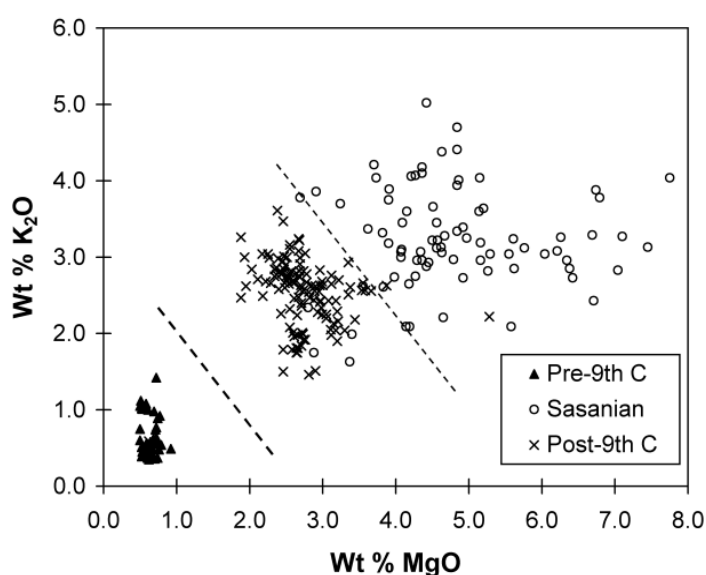


Figure 12: A biplot of MgO vs K_2O in a series of glasses demonstrating the difference between natron glass (pre-9th c.) and plant ash glass (post-9th c. and Sassanian) (Freestone, 2021: 249).

et al., 2021: 9) and Japan (Tamura & Oga, 2016: 7). The difference between natron and plant ash glass can be discerned by the levels of K_2O and MgO , as mentioned previously plant ash glass contains more potassium. Natron glasses contain typically less than 1.5%wt of both magnesium and potassium oxides, whereas Bronze Age Venetian and Islamic plant ash glasses contain more than 1.5wt%. Thus, the two can be distinguished on the basis of the presence of these elements in such quantities (Shortland, 2006: 522; Brill, 2009: 460).

Colour was created in glass by the addition of transition metal ions such as Cr^{2+} , Mn^{2+} , Mn^{3+} , Fe^{2+} , Fe^{3+} , Co^{2+} , Cu^+ , Cu^{2+} . These chemical colourants cause the glass to absorb some wavelengths of light in the spectrum while allowing others to pass through and be reflected onto the eye (Henderson, 2013: 65). The factors that affect the colouration of glass are as follows: the strength of the absorption of the colourant, their concentration and the environment in the furnace i.e. whether there is an oxidising atmosphere or a reducing atmosphere where carbon monoxide is present. In the case of iron, in a reducing atmosphere the colour will be blue and in an oxidising one it will result in a green colour. The most powerful of these transition metals is cobalt, as little as 0.002wt% can create a strong blue colour (Henderson, 2013: 69). Another metal used in glass production is lead, this is known from the Tang Dynasty in China. These glasses contain up to 70wt% lead oxide, this makes the glass soft and workable for longer periods, it produces a green colour that is thought to have resembled jade (Liu et al., 2012: 2129).

Glass can also be decolorised to be transparent, this was primarily done with manganese (MnO), which has been referred to as 'glass makers soap'. Glass could also be made to be opaque, in this form the wavelengths of light are reflected away from the glass as opposed to passing through it by the presence of crystals throughout the glass matrix. Calcium antimonate could produce an opaque white and lead antimonate an opaque yellow, these were early opacifiers. However, from the 2nd century BCE tin oxide (cassiterite) was used to produce opaque white glass and lead tin oxide for yellow, while a mix of cuprous oxide (Cu_2O) and iron produced an opaque red coloured glass (Henderson, 2013: 77).

Understanding colour chemistry is a particularly difficult challenge for researchers of ancient glass.

When analysing plant ash glass, the most common elements can be categorised into two groups: SiO_2 , TiO_2 , Al_2O_3 and Fe_2O_3 are generally linked to the silica source, though traces can be incorporated by the plant ash. Purer silica sources will be higher in SiO_2 and lower in

the other elements, sands with the presence of feldspars and kaolinite used in high quantities will result in increased levels of alumina (Fernández-Navarro & Villegas, 2013: 30). K_2O , MgO , and CaO , on the other hand are primarily associated with the plant ash used, it is important to note that plant ash is a highly variable component, with variations potentially arising from differences in plant parts, ash preparation methods, or the season when the plants were collected (Barkoudah and Henderson, 2006: 320-1). Therefore, although the quantities of these elements indicate which plants were more likely used it is not possible to draw definitive conclusions about exactly which plants were used in each glass recipe. Moreover, in the case of glasses that are highly recycled, it is likely that there are multiple answers to this question.

2.2 The Scientific Analysis of Glass

Analytical methods such as X-ray Fluorescence (XRF) or Scanning Electron Microscopy (SEM) have provided researchers with quantitative information of major and minor elemental components of archaeological glass. The introduction of Laser Ablation Inductively Coupled Mass Spectrometry (LA-ICP-MS), into archaeology in the mid-1900s has enabled the detection of elements at sub parts per million (ppm) levels (Gratuze, 2013: 201). The method of investigation that will be used here is Scanning Electron Microscopy, SEM is a powerful tool for studying ancient glass, it allows for the investigation of the microstructure, composition and surface structure of a glass sample. The technique does this using a focused beam of electrons which scans the surface of the sample generating high resolution images. In conjunction with SEM two main types of detectors are used, EDS and WDS. In EDS when the electron beam interacts with a sample it causes the ejection of inner shell electrons from the atoms in the material, electrons from outer shells then transition to fill the vacancy and emit X-Rays in the process. X-Rays emitted from the sample when the surface of a material is excited are detected by a detector, the detector records the energy and intensity of the X-Rays emitted over a range of energies. Each peak in the spectrum corresponds to a specific element in the sample with the peak's position indicating the energy of the X-Ray and its intensity corresponding to the element's abundance (Herrington, 1985: 472; Fraham, 2014: 6488-9).

This technique offers fast data acquisition and can provide insights into the distribution of elements within a sample and can produce elemental maps useful for understanding the homogeneity of a glass or the identification of frit. Other features that can be detected are

bubbles, crystalline phases or surface defects which can give an indication of processing history such as annealing conditions, melting temperatures or cooling rates. Furthermore, the technique is invaluable in the study of weathering or degradation of glass, the surface morphology and elemental composition of glass allows researchers to determine the reasons for weathering i.e. chemical leaching, surface erosion, microcracking (Janssens, 2013: 148). However, EDS detection has limitations in terms of spatial resolution and detection sensitivity compared to wavelength dispersive spectroscopy (WDS).

In WDS X-Rays emitted from a sample are dispersed by a crystal monochromator based on their wavelengths. The monochromator selects specific wavelengths corresponding to the characteristic emission lines of elements of interest. These selected X-Rays are then identified by a detector positioned at fixed angles corresponding to the desired wavelengths. As the crystal monochromator scans through the range of wavelengths the detector records the intensity of X-Rays at each wavelength. Each peak in the resulting spectrum represents a specific element. Thus, both methods are similar though they are differentiated by the fact that EDS is concerned with the energy distribution of X-Rays and WDS on wavelength selection. While WDS is more sensitive and can provide a better level of detection to lower elements especially cobalt, cobalt is important because as is mentioned earlier as little as 0.002wt% of cobalt could be used to produce a blue glass, this would not be detectable using EDS. WDS has a longer acquisition time meaning that it takes longer to procure the results (Kristiansen, 2008: 121).

2.3 Islamic Glass

2.3.1 Flux Agent

In the beginning of the Islamic Period the process of glass manufacture was adopted from the preceding Roman tradition. The importation and reuse of foreign glass is highly attested during the early Islamic Period from historical sources, especially Byzantine glass. Byzantine glass was extremely highly regarded in the Islamic Period, it is recorded by the tenth-century geographer al-Muqaddasi, that the Caliph al-Walid gathered artisans from Byzantium as well as India, Persia and the Maghreb for the construction of the great Umayyad Mosque in Damascus. Al-Walid is even recorded to have threatened the emperor of Byzantium with the destruction of Christian churches on Muslim lands if materials were not sent (Henderson, 2013: 251-256). Despite political tensions between the Islamic caliphate and the Byzantines

this occurrence of Byzantine glass in early Islamic architecture suggests that trade was still flowing between the two.

The ninth century, along with the development of the Islamic style saw a drastic change in the way that glass was produced in the Islamic world. Glass prior to this time was produced using natron, the main source of which came from the Wadi el-Natrum in Egypt. After the ninth century, however, glass began to be produced using plant or wood ash (*Figure 12*) to provide the alkali flux needed for the glass formation process (Rehren, 2024: 550). This change was dated by Sayre and Smith (1974) to c. 850 CE by analysing dated glass weights from Egypt. Different plant ashes made better glasses than others, historical sources reveal that the white ash produced in Syria produced particularly good glass and was sought after across the world. Much work has been done on using trace element analysis to attempt to identify the kinds of ashes that were used by glassmakers (Tite, et al., 2006; Barkoudah & Henderson, 2006).

The reason for this change is still unknown, it is possibly due to the decline in the availability of natron due to changes in the environment such as an increase in rainfall or a cold period. Although, as Shortland et al. (2006: 524) have shown there were other sources for natron such as the al-Jabbul salt lakes in northern Syria. Another possibility is the disruption of trade routes in Egypt due to political upheaval in the Delta, during the 7th century the Wadi Natrun region was increasingly besieged by Bedouin incursions from the desert and in the 8th century political upheaval between Christian and Muslim groups (815 – 832 CE). In 864/5 CE after a period of restoration in Wadi Natrun, the prefect Ahmad ibn Tulun took control of Egypt this upheaval in 867/8 CE met with disaster and resulted in severe destruction of the Wadi Natrun, an account of which is recorded in the *History of Patriarchs of Egypt*, and is confirmed by burnt layers at Abu Mina in the vicinity of the Wadi Natrun (Shortland et al., 2006, 528). The change to plant ash glasses was likely caused by a mixture of environmental and political factors which meant that the demand for glass was higher than the supply of natron could meet and therefore glassworkers were forced to search for alternative sources of alkali.

2.3.2 Production Model

The arrival of the Islamic Period witnessed another change in the production of glass, prior to the Islamic period the primary production of glass was centralised. This entails that primary glass working sites were located away from urban centres and the glass exported out in blocks to secondary glassmaking workshops, much further from where it was originally made (Freestone, 2021: 246) Glass was also heavily recycled throughout its history and was traded

as scrap to be reused. The long-distance trade of raw glass in this early period is attested by the cargo found on the wreck of the Uluburun ship dated to the 14th century (Shortland, 2009: 1). Primary production sites have been uncovered in Egypt (Nenna, 2015) and Israel (Gorin Rosen, 2015; Freestone, Gorin-Rosen & Hughes, 2000). In the Islamic period, by the 9th century, plant ash glasses begin to be produced across a wider area, on industrial estates near urban centres, this is referred to a decentralised production model. After glasses from Islamic sites began to be analysed it was noticed that their composition is more varied and many glasses appeared to be unrelated, indicating that there was much more primary production occurring.

The decentralised model of primary production for Islamic glass was purported by Henderson and colleagues (2016: 23) in a paper comparing a large amount of trace element data acquired through LA-ICP-MS for sites across the Silk Roads: Samarra (9th c. Iraq), Nishapur (9th-10th c. Iran), Beirut (9th c. Lebanon), Damascus (11th-12th c. Syria), Al Raqqa (9th c. Syria), Ctesiphon (9th-10th c. Iraq) and Cairo (14-15th c. Egypt). Through this analysis of trace elements, the authors were able to identify regional and sub regional production zones. The most poignant example being the glasses from Samarra and Ctesiphon being chemically

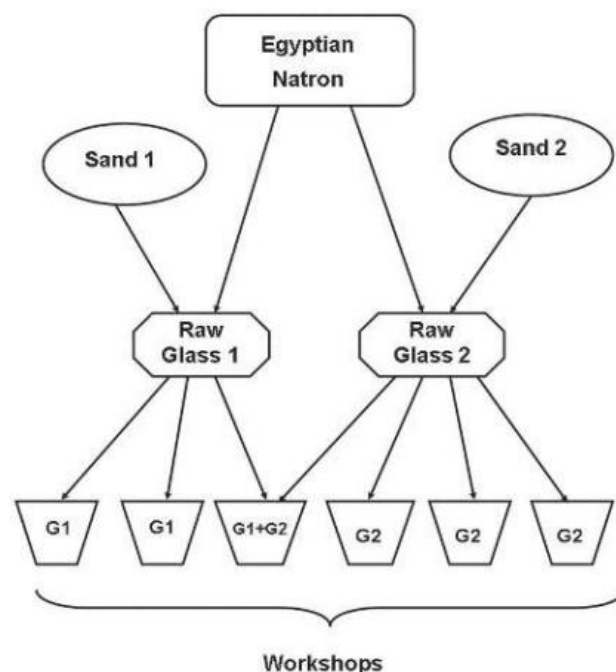


Figure 13: A diagram of a centralised glass production model, Egyptian natron was mixed with sand to produce raw glasses at primary glass factories which were then distributed to workshops located in urban centres to be remelted and worked into artifacts (Freestone, 2021: 246).

distinct despite the two sites only being 84 miles apart (Henderson et al., 2016: 23). Moreover, these regional areas appear to exhibit their own technological specialisation. At Nishapur, although this glass is also argued to have originated from Samarra (Schibille et al., 2022: 7), colourless glass was produced to an outstanding quality. Additionally, the glassworkers at Ctesiphon specialised in producing pale green wheel cut faceted glass vessels (Henderson et al., 2016: 23).

Aside from the chemical data, there is little archaeological evidence for primary glass production at these sites though, primary production at Al Raqqa has been confirmed through the discovery of frit, partially fused raw materials. The industrial complex here is situated close to the site itself and to the palatial complexes to the north, well within the urban landscape. Furthermore, experimentation with glass recipes has been shown to have happened at the site (Henderson et al., 2004: 545), which suggests that there was a centralised control over the production of glass. This model of localised production can also be seen at Siraf, a port city in the south of Iran where glass was produced in a glass factory near the site (Swann et al., 2017: 103), these examples will be discussed further in Chapter 4. By the 11th century compositional variation in glass declines (Henderson, 2013: 100), this could suggest that the raw materials in glass making became more standardised, likely suggesting a decline in experimentation or that the glass making industry began to be standardised.

Despite the existence of regional types, glass vessels were clearly still traded between the centres (Henderson et al., 2016: 22). Furthermore, there is evidence that the trade of raw glass chunks over long distances persisted. Significantly, two tonnes of raw glass chunks were discovered on the Serçe Limani shipwreck, which sank in the 11th century, believed to have been sailing from the Levant. (Henderson, Ma, Evans, 2020: 2). Furthermore, at the medieval part of the ancient city of Tyre there are within the city walls the remains of four glass furnaces, these were built around and over a fallen granite column as part of a Roman colonnade which fell during an earthquake in 551 CE (Aldsworth et al, 2002: 49). The furnaces therefore can be safely assumed to be older than this date. There is little pottery or coinage from a reliable context at the site however written evidence demonstrates that glass production at Tyre was conducted between 985-1227 CE, within the Islamic Period (Carboni et al. 2003: 139-149). At the glass working area in Tyre there is no evidence of fritting at the site, this would provide strong evidence that the fusion of primary materials occurred on site and therefore the occurrence of primary glass production. Isotopic evidence, however, specifically the wide variation in neodymium (Nd) signatures demonstrates that Levantine

sand from different strata were used in the production of the glass showing that the primary materials were taken from close to the site, giving weight to the interpretation that the furnaces at Tyre were used in the primary production of glass (Freestone et al., 2009: 38).

Furnace 1 is the largest of the tank furnaces, the melting chamber was mortar lined and is slightly concave with rounded corners measuring 6.40-3.90 meters (Aldsworth et al, 2002:53). Ethnographic data reveals that it would have taken at least 30 days at 900°C to complete a full melt in a tank furnace (Sode & Kock 2001: 115). This scale of production appears to be much larger than necessary for only localised production, therefore it is likely that the glass was exported to other centres. Furthermore, in contrast to the evidence at Al Raqqa and Siraf the fact that there are no finished vessels that have been discovered at the site, only raw glass chunks, therefore it is more likely that glass was exported from the site in raw blocks to be sent to be purchased by secondary glass working facilities. The quality of the glass from Tyre is attested by Benjamin of Tudela a Spanish traveller who wrote c. 1167 CE that “there (Tyre) the Jews produce the fine glass called glass of Tyre which is prized in all countries” (Carboni et al. 2003: 145-6). This evidence highlights that while the general model of production did become decentralised, that centralised production of prestige raw glass such as from Tyre, and possibly other parts of the Levant, did still occur.

Many glass vessels were blown, particularly mould blown to produce decoration. There is little evidence of these moulds found at glass-working sites, although one example survives in The Corning Museum of Glass. It is 11.4cm high and has a diameter of 8.8cm, it is covered internally in lozenge shaped bosses which produced bottles with a honeycomb pattern. The object is a copper alloy and has an inscription in Arabic on its front reading “Uthman b. Abu Nasr, glassmaker” (von Folsach, 1993: 152). The processes of Islamic glassmaking are described by the Iranian Islamic early scientist or alchemist Jabir ibn Hayyan, possibly court alchemist for Caliph Harun al-Rashid, regarded as one of the fathers of chemistry. His treatises discuss in detail production techniques, colouration techniques and the application of lustre decoration. These descriptions are comprised within chapters four and five of his *Bayan al-Sanat*, a book that functioned to explain crafts (Holakooei, 2016: 95).

2.4 Sasanian Glass

Sasanian glass is unique because in this area natron was never used as the main flux agent in glass production, instead a plant ash flux was always used likely in continuation from the beginnings of glass working in Mesopotamia. (Schibille, 2022: 125; Mirti et al., 2009: 1061)

Sasanian glass is severely understudied in comparison with other glasses, much evidence is lacking on the connection between Islamic and Sasanian glass this is due to the lack of data particularly of analysed data from Sasanian sites. Many Sasanian glasses are samples from museum collections simply labelled as Sasanian with no contextual data to support this or give more detail. Mirti et al. (2009: 1061) state that the samples from Veh Ardašir are the only Sasanian glass samples analysed that are from known archaeological contexts and span the entire period from the mid-third century to the seventh century CE. Veh Ardašir was founded by the first Sasanian king Ardašir facing the capital Ctesiphon on the Tigris River. It was constructed as an administrative centre for the capital to which it was linked by bridges, thus some consider it to be an extension of Ctesiphon (Simpson & Curtis, 2000: 60).

Sasanian glass from Veh Ardašir has been chemically analysed by Mirti and colleagues (2008, 2009), the glass is split into two groups Sasanian 1 which displays lower MgO values averaging between 3-5wt% and Sasanian 2 which averages between 6-8wt% and has lower phosphorus contents. This confirms the use of two different plant ashes or possibly the differential treatment of one plant ash. The exact stratigraphical context reveals that Sasanian 1 was used in the third century and Sasanian 2 appears in the fourth century. Moreover, some glasses with intermediate values during the 5th and 6th centuries may be the product of glassworkers experimenting with mixing the two recipes together (Mirti et al., 2009: 1062). The silica source also appears to change over time, as during the 3rd century a mixture of impure sand and quartz pebbles was used, but at some point, in the 4th century, with increasing occurrence until the end of the occupation, a more homogenous silica source begins to emerge. This is suspected to be a purer sand in the aim of producing a better-quality glass without the labour involved in crushing quartz pebble (Mirti et al., 2009: 1067).

2.5 Regional Fingerprints

In the last decade or so, studies aiming to differentiate various plant ash glasses of Western Asia have observed broad compositional variations in major and minor elements (e.g. potash, magnesium, lime, and alumina) moving in an East-West direction across the region. Plant ash glass from sites in Mesopotamia and Persia tends to have higher magnesia levels than does glass from sites in Syria-Palestine (Freestone 2006: 204-205, Figure 2) as well as an overall higher magnesia-lime ratio, while glasses in Iraq and Iran also tend to have amongst the lowest lime levels (Henderson et al. 2016: 138, Figure 3).

For the past few decades, a lot of work on the topic of Islamic glass has centred around understanding how to determine where a glass is from regionally based on its elemental composition, this includes isotopic data (Lu et al., 2023; Ganio et al., 2012) and both major and minor elements (Henderson et al. 2016; Phelps 2018; Schibille 2022; De Juan Ares, 2018). Much of the discovered data has been based on minor elemental analysis gathered using LA-ICP-MS determining trace elements associated with the primary glass making raw materials to reveal the chemical fingerprint of regional and sub regional glass recipes. Since only major elements are available here as SEM-EDS cannot provide this data, this paper is going to focus on what information can be gathered from major elements.

In 2018 Matt Phelps, building on previous work (Phelps, 2017) formally divided the glasses that he had been studying into four different glass types (*Table 1*). The first is a Syrian type which is not considered here. Next, the Eastern Mediterranean type, this type comprises glass samples from Tyre, Al Raqqa Type 1, Baniyas (Israel) and Fustat (Egypt). The group exhibits a high lime content averaging at 9wt%, relatively high P₂O₅ at 0.3% and low MgO averaging at 2.9wt%, this type has a high lime to magnesia ratio indicating that a plant ash with a high lime content was added into the mix. In terms of the silica related elements, this type has a relatively high level of Al₂O₃ averaging at 1.91wt%, though this is the highest in Egypt, at 2.24wt%. Both titanium oxide (0.09wt%) and iron oxide values (0.52wt%) are low suggesting low silica related impurities (Phelps, 2018: 262).

Mesopotamian Type 2 comprises the colourless glass from Nishapur, the glass from Samarra and the Sasanian Type 2 glass from Veh Ardašir. This group overall exhibits high levels of magnesia (4.95wt% on average), relatively high K₂O (2.51wt%), low P₂O₅ (0.10wt%) and low CaO (6.24wt%). This results in a high ratio of MgO to CaO averaging at 0.79wt% and a K₂O to P₂O₅ ratio of 24.42wt%. When looking at the silica related elements, the group is better defined, it has distinctly low levels of alumina (1wt%), iron oxide (0.27wt%) and titanium oxide (0.04wt%), these low concentrations indicate that for this glass a particularly pure silica source was used. The Nishapur colourless correlates to Wypyski's (2015) Type A which is in turn associated with the glass from Samarra. Turning the discussion to Mesopotamian Type 1, this is a lower quality glass comprising the coloured glass from Nishapur and the Type 1a and 1b Sasanian glass from Veh Ardašir. These display lower average levels of MgO (3.76wt%) and low CaO (7.07wt%) the average ratio of these two elements being 0.4 and of P₂O₅ and K₂O being 8.67wt%. It is likely that these are lower

quality glasses since this type exhibits high average levels of alumina at 2.27wt% and titanium oxide at 0.15wt% indicating more sand/low quality silica was used in the mix.

Nadine Schibille (2022: 127) has criticised this determination of provenance based upon the content of lime and cites two examples, the first being Al Raqqa Type 4, Al Raqqa Type 4 glass contain high CaO levels therefore it fits into the Eastern Mediterranean type although the glass has been shown to have been made on site. However, the Al Raqqa Type 4 glass contains calcium inclusions visible in the SEM thought to have been bone ash (Henderson, 2003: 112), therefore Phelp's designations are still useful. Next, the glass from Siraf fits into the Eastern Mediterranean type while the trace elements present suggest that the glass was manufactured locally (*see pages 47-8*). However, the trace elements referenced (Cr and Zr) are related to the silica source and therefore demonstrate that the silica source was gathered locally, other ingredients in the glassmaking recipe could have come from the Mediterranean especially considering Siraf's location on the maritime Silk Road. For these reasons, Phelp's provenance designations should be treated with caution though understood to help categorise the glasses under study here.

A 2022 study by Schibille, Lankton and Gratuze included glass samples from Rayy, Gorgan, Qom, Hamadan, Samarra and Nishapur (*Table 2*). From the data of the analysed Iranian samples, two primary categories are discerned firstly, a predominant group which exhibits moderate levels of magnesium, potassium, phosphorus, and calcium, comprising 75% of the samples (Groups G1, G2, G3/M). The second category accounts for the remaining 25% (Groups S1, S2), which are distinguished by a significantly higher magnesium content <4wt%, and markedly lower phosphorus >0.15 wt% and, to a lesser extent, lower potassium levels. This variation manifests in elevated ratios of MgO/CaO, MgO/K₂O, and K₂O/P₂O₅, with MgO/K₂O around 2 versus about 1; MgO/CaO around 1 versus approximately 0.5; and K₂O/P₂O₅ around 20 compared to about 10. Additional distinctions within these groups are possible. For instance, the subgroup referred to as the silica group G2 typically shows lower magnesium to potassium ratios (MgO/K₂O <1) and reduced calcium levels. Similarly, a specific subset of 7 samples from the group with high MgO and low P₂O₅ levels exhibited slightly increased levels of Na₂O and K₂O and decreased CaO levels. However, CaO levels in the other groups are relatively consistent, generally ranging between 6wt% and 7wt%. S1 and S2 appear to be strongly associated with the Samarra 1 and Nishapur Type A glass supporting the idea of a higher quality prestigious glass remaining to be traded on a centralised model from a large urban centre such as Samarra.

| Location | Type | Date | Na ₂ O | MgO | Al ₂ O ₃ | SiO ₂ | P ₂ O ₅ | K ₂ O | CaO | TiO ₂ | MnO | Fe ₂ O ₃ | MgO/CaO | K ₂ O/P ₂ O ₅ |
|------------------------------|--------------------------|-----------|-------------------|------|--------------------------------|------------------|-------------------------------|------------------|-------|------------------|------|--------------------------------|---------|--|
| Eastern Mediterranean | | | | | | | | | | | | | | |
| Tyre, Lebanon | Tyre Type | 10th–11th | 12.85 | 3.61 | 1.81 | 65.06 | 0.33 | 2.26 | 11.21 | 0.09 | 1.33 | 0.54 | 0.32 | 6.85 |
| Banias, Israel | | 11th–13th | 11.98 | 2.4 | 1.21 | 71.65 | 0.24 | 1.52 | 8.59 | 0.12 | 0.83 | 0.48 | 0.28 | 6.33 |
| Al Raqqa, Syria | Al-Raqqa Type 1 | 8th– 11th | 12.93 | 3.43 | 1.2 | 67.49 | 0.28 | 2.52 | 9.31 | 0.07 | 1.14 | 0.56 | 0.37 | 9.00 |
| Fustat, Egypt | Egypt Group 3 (A) | 10th–11th | 14 | 2.83 | 2.24 | 66.17 | n/a | 2.26 | 9.17 | 0.17 | 1.2 | 0.85 | 0.31 | |
| Mesopotamian Type 1 | | | | | | | | | | | | | | |
| Veh Ardašir, Iraq | Sasanian 1a | 3rd– 7th | 16.01 | 4.05 | 2.28 | 60.02 | 0.31 | 3.32 | 6.7 | 0.18 | 0.15 | 1.09 | 0.60 | 10.71 |
| | Sasanian 1b | 3rd– 7th | 16.02 | 4.1 | 2.19 | 60.49 | 0.27 | 3.41 | 6.74 | 0.13 | 0.12 | 0.91 | 0.61 | 12.63 |
| Nishapur, Iran | Nishapur Coloured | 9th– 10th | 15.86 | 3.76 | 3.05 | 64.68 | 0.32 | 2.91 | 6.78 | 0.15 | 0.39 | 1.12 | 0.55 | 9.09 |
| Mesopotamian Type 2 | | | | | | | | | | | | | | |
| Veh Ardašir, Iraq | Sasanian 2 | 3rd– 7th | 17.43 | 7.13 | 1.62 | 58.63 | 0.13 | 2.8 | 5.55 | 0.09 | 0.18 | 0.6 | 1.28 | 21.54 |

| | | | | | | | | | | | | | | |
|-----------------------|----------------------------|-----------|-------|------|------|-------|------|------|------|------|------|------|------|-------|
| Nishapur, Iran | Nishapur Colourless | 9th– 10th | 12.53 | 4.69 | 1.17 | 71.18 | 0.12 | 2.45 | 6.27 | 0.05 | 0.4 | 0.37 | 0.75 | 20.42 |
| Samarra, Iraq | | 9th– 10th | 14.52 | 6.66 | 0.94 | 67.92 | 0.08 | 2.45 | 5.09 | 0.06 | 0.85 | 0.4 | 1.37 | 34.08 |

Table 1: Mean wt% values for each element in each of Phelps's types, the final two columns are ratios of elements (Phelps, 2018: 260-1).

| | Na₂O | MgO | Al₂O₃ | SiO₂ | K₂O | CaO | TiO₂ | MnO | Fe₂O₃ | MgO/CaO | MgO/K₂O |
|-------------|------------------------|------------|------------------------------------|------------------------|-----------------------|------------|------------------------|------------|------------------------------------|----------------|---------------------------|
| G1a | 16.0 | 3.38 | 2.27 | 65 | 3.11 | 6.48 | 0.15 | 0.78 | 1.14 | 0.52 | 1.09 |
| G1b | 16.3 | 3.18 | 4.18 | 62.2 | 3.14 | 6.48 | 0.9 | 0.27 | 1.57 | 0.49 | 1.01 |
| G2 | 15.6 | 2.64 | 3.09 | 66.0 | 3.33 | 5.36 | 0.20 | 1.09 | 1.17 | 0.49 | 0.79 |
| G3/M | 15.5 | 3.86 | 2.42 | 65.2 | 2.79 | 6.80 | 0.12 | 0.71 | 1.17 | 0.57 | 1.39 |
| S1 | 12.2 | 4.75 | 1.02 | 71.8 | 2.38 | 6.32 | 0.04 | 0.36 | 0.29 | 0.75 | 2.00 |
| S2 | 14.9 | 5.53 | 1.21 | 68.7 | 2.87 | 4.67 | 0.06 | 0.80 | 0.35 | 1.18 | 1.92 |

Table 2: The mean element oxide wt% value for Schibille and colleagues' glass types G1a/b, G2-3 and S1/2, the final two columns are ratios of elements (Schibille et al., 2022: 6, Table 1).

Chapter 3: Methodology

This thesis aims to investigate the glass assemblage from Rayy and understand it within the wider concept of Islamic glassmaking. Due to a lack of information regarding the assemblage this study will attempt to reveal as much information as possible while it is not detrimental to the survival of the glass fragments as further in the future more advanced techniques may be used to study the assemblage. The samples were analysed using scanning electron microscopy coupled with energy-dispersive spectroscopy. A JEOL IT-200 SEM was used in the Nano and Microscale Research Centre at the University of Nottingham to obtain a view of the microstructure of the glass and the elemental composition for each glass artifact. The assemblage was firstly compared against itself and then to data from sites across the Silk Road that have analysed glass assemblages, including from other studies of glass from Rayy (Agha-Aligol, et al. 2022; Schibille et al. 2022). Through secondary research which was conducted prior to the analysis, a data table was produced with compositional data of glass from select sites in the region.

The case studies used here for comparison (the locations of which are indicated in *Figure 14* below) were selected based on secondary research but also, the availability of compositional data. For example, to complete a statistical analysis a sizable number of analysed samples close to the amount for all the other case study sites, at least 30. Schibille et al. 2022 in their published results give both 17 analysed samples for Hamadan and Qom, therefore these were not included. The sites chosen for comparison with the Rayy data are Nishapur, this is an obvious choice as it is a large site in Iran that has produced much evidence of high-quality glass vessels, though little evidence of production (Wypyski, 2015; Brill 1995). Analysis has been conducted on glass artefacts from Gorgan (Schibille et al., 2022) located between Rayy and Nishapur, which will therefore be included in this study.

Siraf is the largest archaeological site in Iran and there is evidence there for localised primary glass production (Swann et al., 2017: 113), there is also evidence for localised production at Al Raqqa and of experimentation with glass recipes by glassworkers (Henderson, 2013, Henderson, 2004, Henderson, 2005), therefore the glass from this site has also been included. Another important site for Islamic glass studies is the Serçe Limani shipwreck off the coast of Turkey, the cargo revealed a huge amount of glass cullet, chemical analysis of the glass by

Robert Brill (2009: 479) has shown that most of the cullet had come from one area. Finally, the architectural glass from Samarra will offer a valuable comparison as it is known that Byzantine glass was repurposed in its decoration (Schibille, et al., 2018: 11) and because there is evidence that there was a local industry of high quality colourless glass possibly produced from raw materials that took place here and was traded to Nishapur (Wypyski, 2015) and far as Egypt and Japan (Schibille et al., 2022: 8).



Figure 14: A map showing the locations of the sites chosen for case study (image by author created using Tableau).

3.1 Sample Preparation

The analysis began by first visually inspecting the 44 bags of glass using a tabletop microscope, from this a table was constructed to document each of the samples, their colour, shape, thickness, possible function and state of preservation. This could then be used as a reference point after the analysis to be used when making interpretations. All the samples are small broken fragments, some already in several pieces inside their sample bag. Those that were thicker all exhibited thick crusts of weathering therefore they could be sampled destructively without changing them in any way and without there being any loss of information about the sample. R.56 however it was decided was too fragile for sampling, this is a small translucent cylindrical fragment of glass possibly a handle for a miniature vessel, since sampling may have destroyed the sample, it was decided to leave the sample alone. In total seven samples were excluded from the analysis, R.11, R.12, R.17, R.19, R.43, R.55 and R.56 because they are too heavily weathered to produce any good results and they are too

thin, even if they were subsampled, the broken edge would be far too thin and not suitable for mounting in resin. R.56, as mentioned above was excluded because sampling was too dangerous and posed a threat to the sample itself, subsampling should only occur where there is no risk of losing the entire sample.

For most of the sample bags there is a main piece of glass inside with some smaller pieces the smaller pieces were however usually quite weathered. For this reason, clamps were used to fracture off small new pieces at the edge of the main glass pieces in the bag. For thin blown samples sharp edges were carefully removed by applying pressure, when dealing with thicker samples the area with the most weathering, and therefore the weakest part, could be fractured off. The fractured edge will reveal glass that was not previously exposed and therefore is not weathered, additionally this edge will be flat, ideal for SEM study. These sub-samples could then be placed anticlockwise inside the circular mould, they were stuck in order of their R. sample number for example R.01 is followed by R.02, this way one can count along and be able to identify which sample belongs to which glass. Once each mould was full of sampled glass, an Epofix brand resin mixed with hardener was poured over them and left to dry. The moulds while drying were placed inside a vacuum oven to expel as many air bubbles from the resin as possible as this would be detrimental to analysis.

Once cured, the moulds were polished using following a five-step recipe firstly using two coarse polishing mats for a total of 3 minutes and 10 seconds with water and then a series of three increasingly fine polishing mats and Diapro diamond pastes down to one micron for a total of 7 minutes on each block. This will ensure a smooth and even layer and will provide the best results in the SEM, this system does however run the risk that samples could be lost if over polished, if this was to occur then samples would need to be retaken making the process even more destructive. The moulds were documented with photographs and a reference map was drawn, labelling each of the subsamples and the starting point and direction are noted so that one can always know which way up to put the mould in the SEM. The next step in preparing the samples was to coat the top with a carbon coater and use a conductive tape around the resin block as this ensures that a conducting path exists. When the sample is bombarded with electrons during the analysis it is possible for some materials to become electrically charged which would distort the image produced by the backscatter detector, by applying conductive tape a pathway is created for the charges to escape.

3.2 Analysis

The researcher was assured by the SEM technician in the Nano and Microscale Research Centre that calibration using a glass standard before and after each session was not necessary. This is because the JEOL IT 200 SEM-EDS machine is calibrated against Corning Glass Standards A and B in the factory where it was made, these are then recorded onto the machine, weekly the detector is calibrated against a Ni standard to calculate if the detector is in error and maintenance required prior to analysis. Once in the SEM the montage feature was used to create a reference image which was used in conjunction with the map to ensure accuracy of which sample in the mould is being analysed so that the correct data would be assigned to the correct glass. From this, the data could be collected, the analysis began with R.01, moving along numerically. Firstly, SEM can be used to look at the morphology of the glass samples particularly their porosity. In back scatter electron mode changes in the shade of the surface will indicate changes in the composition of the glass, glasses that have no change in shade across its surface are likely quite homogenous. To test this further, an elemental map was made over the glass sample's surface based on the appearance of changes on its surface, the elements included were Na, Mg, Al, Si, K, and Ca. A homogenous glass indicates a high-quality glass, a lack of homogeneity will result in defects such as phase separations, inclusions or regions with various refractive indices having an adverse effect on the properties of the glass such as strength and transparency.

From here, a point analysis was carried out to obtain a result of the glass composition that was collated into a data table, the elements detected in the glasses were converted into oxides, the oxides detected were: Na₂O, MgO, Al₂O₃, SiO₂, K₂O, CaO, TiO₂, MnO, FeO₃, CuO and PbO. The presence of different elements will give information about some glass samples straight away, for example, MgO or K₂O levels of less than 1.5 wt% can be interpreted as a natron glass (Shortland, 2006: 522, Brill 2009: 460). Furthermore, the presence of low concentrations of Sb₂O₅ in the Rayy glass would point to evidence of the inclusion of recycling Roman glass cullet within the glass mix as antimony was used by the Romans to decolourise glass (Freestone, 2015: 30).

3.3 Analysis of The Data

3.3.1 Data Cleaning

After collecting all the data, it was necessary to clean it to make it suitable for analysis, firstly where an element was not detected in one sample it was recorded as 'nd' not detected. An analytics software, however, will require that all the data be numerical and will not understand the abbreviation *nd*, therefore this raw data was amended and changed to 0. Additionally, outliers will skew the results of the data analysis and therefore were removed for example, lead glass will exhibit low silica values that will skew the average value in the data set for that element therefore, outliers were removed and placed at the end of the table. The columns or elements must be standardised and only include the most important elements that can be gathered across all the studies including the analysis here using EDS. The elements included in the table are, Na₂O, MgO, Al₂O₃, SiO₂, K₂O, CaO, TiO₂, MnO, Fe₂O₃, PbO, the element ratios that are compared the most in the literature that are available here are MgO/CaO and MgO/K₂O, these were therefore calculated and added into the table.

3.3.2 Standard Deviation

To investigate the variability and consistency of the chemical compositions, the standard deviation of the results for each element in the data. Standard deviation provides a statistical measure to quantify variability within the composition data. Mathematically, the standard deviation is calculated by comparing each data point to the mean and expressing the difference as a percentage of the reference value. The relative deviation will be calculated using statistical software for the elements analysed. These calculations can be done in Microsoft Excel using the following formulae: Mean: =AVERAGE(cell range), Median: =MEDIAN(cell range), Standard Deviation: =STDEV.P(cell range). The higher the value for standard deviation the higher the variance in the data.

This was also performed on the results from the table that includes secondary research to see how much variation there is for the Rayy assemblage compared with the case study sites, of particular interest are Siraf, Nishapur, and Al Raqqa since Nishapur is known to have variance within its glass compositions, Al Raqqa is known to be a site of recipe experimentation and therefore will provide an anchor for having a particularly high variance. Siraf on the other hand represents a localised glass production used on site suspected to have been made using raw materials and therefore should exhibit low values of standard deviation,

similarly Brill argued that the glass from the Serçe Limani wreck was all produced in the same factory and will also exhibit low standard deviation values. The natron glass from Samarra conversely is recorded to have been brought from various locations across the Byzantine Empire upon being set up as a Caliphal residence and should provide an anchor value for very high variance. If there is a particularly low variance between all of the samples then it is likely that they were produced in a factory at Rayy, possibly from primary materials which supports the decentralised model of Islamic glass production put forward by Henderson et al. (2016: 23).

3.3.3 Cluster Analysis

Next, to find how many groups or clusters the glass can be split up into a cluster analysis was performed. The chosen cluster analysis algorithm employed here is hierarchical clustering. This algorithm begins by taking the first data row or R. sample and finding the most similar data point to it and grouping them into one cluster, this is then repeated for each of the rows in the table to group them into clusters. The distance measure used here is Euclidean distance which calculates the straight-line distance between points on a graph, lower or closer distances indicate that the two data points should be clustered. From this it will produce a cluster tree or dendrogram which visually represents the structure of the data and how it clusters. Furthermore, it is particularly flexible, it can identify clusters of any shape and size. Hierarchical clustering is not sensitive to initial groups or seed points in the data, unlike for example K-Means clustering, which can produce different results depending on those initial seed points (Reddy & Vinzamuri, 2018: 102). Thus, hierarchical clustering can be considered reliable, particularly when dealing with noisy or high-dimensional datasets.

This analysis will be completed using KNIME the Konstanz Information Miner, an open-source data analytics, reporting, and integration platform. The analysis is performed by downloading the data onto a file reader and attaching it to 'nodes' that produce the results. The platform has been used in pharmaceutical research for many years and is named as a leader for Data Science and machine learning platforms by Gartner's Magic Quadrant, a

series of market reports by the IT consultancy Gartner. Therefore, the results gathered from this platform can be considered trustworthy and scientific.

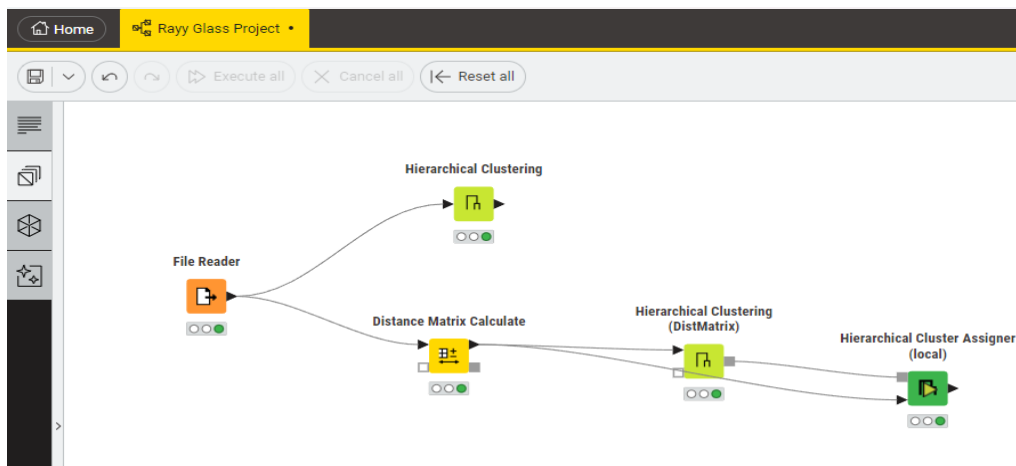


Figure 15: KNIME workflow demonstrating how to perform a hierarchical clustering analysis (image by author).

The figure above shows the workflow that was used to produce a hierarchical cluster in KNIME, firstly a file reader node was added and configured by adding the Excel spreadsheet of the analysed data from Rayy which must be uploaded as a CSV file to be read by the software. From this, the hierarchical clustering mode produced the dendrogram which visually splits the data giving the researcher an idea of how many clusters will be produced. From there, a separate flow was used to calculate the distance between the data points, then a cluster assigner was used to assign each of the rows to a cluster based on the distance between them. This distance can be altered based on the results as, for example, in KNIME it is common for the cluster assigner to produce a large number of clusters which contain only one example. It is possible that the program does not know how to alter the distance for each data set or that it reverts to a standardised distance when first assigning the clusters. To correct this error, it was decided that the distance must be manually increased until each cluster included a minimum of 2-3 samples.

3.3.4 Principal Component Analysis

To further investigate the variance in the dataset a principal component analysis was run, demonstrated in *Figure 16*. This was performed in KNIME analytics also by using the PCA node, a PCA analysis works to standardise the data and plot it three dimensionally, these 3 dimensional axes or eigenvectors represent the direction of maximum variance the data can be placed on these axes based on their covariance matrix to give the eigenvalue, eigenvalues below 0.3 will be discarded as being statistically irrelevant (after Brill 2009: 478) which will leave only the elements that are statistically important for each principle component. From this the principles components of the dataset can be described and investigated using biplots.

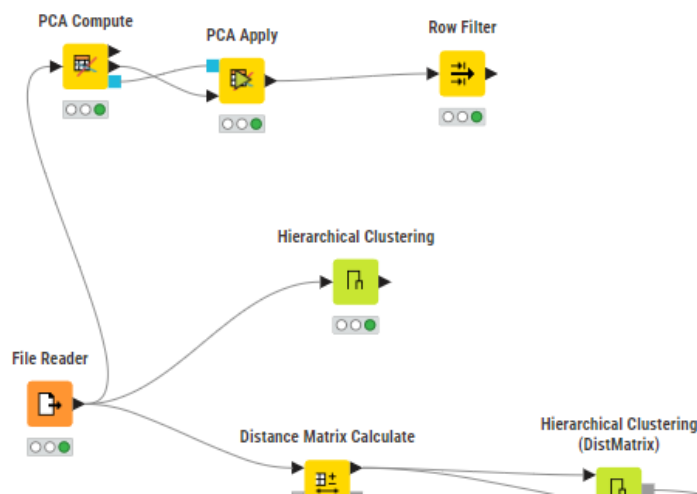


Figure 16: The addition of the PCA workflow in KNIME (image by author).

3.3.5 Data Visualisation

To visualise these clusters so that they may be better described was completed using a data visualisation software. The software chosen here is Tableau, it is recognised as an academic resource and a desktop version of the software is offered by the University of Nottingham. Biplots will be used to visualise the relationship between two variables, these will be distinguished by colour, each point on the biplot represents a analysed glass sample discovered on The Silk Roads. The elements that will be plotted against one another were firstly MgO and K₂O to determine if the glass is plant ash glass or if there is any natron glass in the assemblage. The next plots were created based on the principal relationships between the element oxides that were uncovered by the results of the PCA analysis.

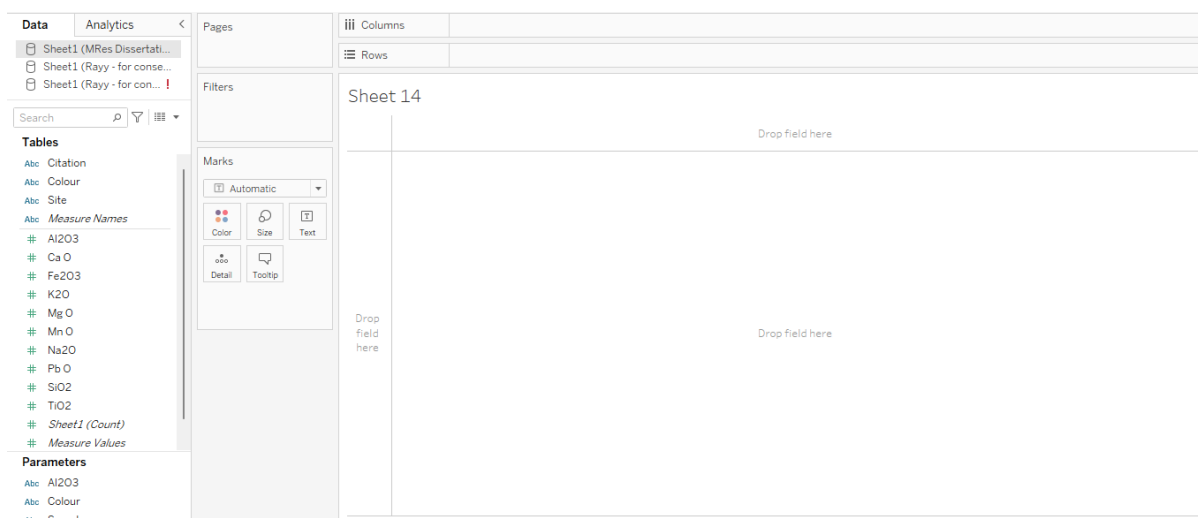


Figure 17: An example of a blank Tableau workbook, data visualisations are made by dragging the variables to the columns and rows, dragging one of each will automatically create a scatter plot (image by author).

3.4 Regional Comparison

This part of the methodology concerns placing the glass from Rayy within the wider tradition of Islamic Glass Studies. By using biplots it was tested if the glass analysed here fit with general regional trends that scholars have noted, for example that glasses from Mesopotamia exhibit higher levels of MgO than those further west sites in Iraq and Syria (Henderson et al. 2016: 13, Figure 3), as well as a higher MgO/CaO ratio (Phelps 2018, Schibille et al., 2022). A biplot was constructed plotting the quantity of Al₂O₃ against the ratio of MgO to CaO. This could then be compared to the provenance categorisations produced by Phelps (2018: 262 Figure 11.5). If the ratio of MgO/CaO is between 0.8 and 1.8 and the level of Al₂O₃ between 0-2.5wt% then it can be considered Mesopotamian Type 2 (*Table 1*). By comparing the data analysed here from Rayy it can be discerned which of Phelp's categories they should be fitted into. From here the glass analysed here can then be plotted against the glasses from the corresponding locations i.e. the glass that fits into Mesopotamian Type 2 glasses will be compared against the glass from Samarra and the colourless glass from Nishapur collected during the secondary research phase.

Schibille et al. in 2022 also categorised the glass types on the Islamic Silk Road into S1 and S2 the smaller group of high-quality glasses that were thought to be associated with the high-quality colourless glass from Samarra and Nishapur. Next the second group of G1, G2 and G3/M, lower quality glasses of which G3 can be described as Mesopotamian based on Cr/La ratios. Although this comparison could not be done, the amount of silica associated impurities

TiO₂, Fe₂O₃, and Al₂O₃ plotted against SiO₂ gave an indication of whether the Rayy glass clusters could be characterised as part of the S1/S2 type or the larger G1/G2/G3M type.

3.5 Limitations of The Study

Limitations of the study include the limitations of SEM, only eight elements could be gathered for all the samples. Furthermore, the automatic polisher was broken and so the blocks had to be polished by hand which meant that they were not polished as well, and many samples were not fully exposed, making analysis more difficult. The main limitation is, as discussed above, the lack of archaeological context for the artifacts. No information was given about which excavation they were from, whether the samples were from the same trench or from different parts of the site. Also, there is no stratigraphical data that could be considered, so it is not clear if all the types were used at the same time or if one type became more popular over time. Moreover, there is a general lack of secure dating in the glass across the sites as many come from museum collections and from poorly conducted 20th century excavations, without a securely dated context when cross comparing the glass, changes over time cannot be accounted for.

Chapter 4: Comparative Data, The Case Studies

This work aims to place the glass finds from Rayy under study here within the context of glass along the Silk Roads, here will be a survey of the evidence of glass production at the sites which were chosen as case studies, beginning with Rayy itself.



Figure 18: A map showing the locations of the sites chosen for case study (image by author, created using Tableau).

4.1 Rayy

As far as can be found here, there are only two studies which have published chemical data of glass from Rayy. Firstly, a 2022 regional study by Schibille et al. of glass at several sites across the Eastern Silk Road of which Rayy is included, this study utilised LA-ICP-MS to obtain both minor and major elements, nineteen samples from the site were analysed from The Corning Museum of Glass. The second (Agha-Aligol et al. 2022), is a paper that specifically looks at an assemblage excavated from the Tape Bahram, a site within the area which is thought to have functioned as a government citadel during the Al-I Buyeh Period (10th-11th century). This analysis was conducted using Micro-PIXIE, Micro Particle Induced X-Ray Emission to obtain minor and major elemental compositions of thirty-six glass samples which were excavated from the area in 2019 by Mehdi Mousavina. All the samples are undecorated fragments of broken vessels of which the form is not known and are all green in colour, ranging from light to dark with varying translucence.

In terms of the elemental compositions that were gathered by the two papers, the glasses are similar, Na₂O averaging at 16.78wt% at Tape Bahram and 16.12wt% in the Corning

assemblage. The average level of MgO from Tape Bahram is higher at 3.67wt% while the assemblage from the Corning Museum of Glass averages at 3.44wt%, the Tape Bahram assemblage also has lower lime levels averaging at 5.34wt% while the other averages at 6.47wt%, in terms of manganese oxide the level for the Tape Bahram glass and from the Corning assemblage are 0.76wt% and 0.47wt% respectively. One more difference is the level of iron oxide in the assemblage from the museum is on average 0.40wt% higher. Schibille et al. divide up the glass into categories which are discussed below, for Rayy the majority of the assemblage is made up of G1, G1 is a silica group with high silica related impurities such as aluminium, titanium, zirconium and cerium. G2 is a compositionally similar group which exhibit higher levels of heavy element impurities zirconium and titanium as well as a lower MgO/K₂O ratio but is underrepresented at Rayy. There are also some higher quality luxury glasses from the Rayy assemblage which exhibit high levels of magnesia and are thought to be imports from Samarra designated as S1/S2 type.

The group from Tape Bahram can be divided into three groups, Group 1 is the largest group, its MgO content varies between 3.62wt% and 4.26wt%, the level of K₂O varies between 2.56wt% and 2.93wt%, it has high concentrations of soda averaging at 16.82wt% and low levels of lime, 5.34wt% on average. Group 2 has a lower average value of MgO (3.12wt%) and slightly higher K₂O (2.89wt%). The main deviation from Group 1 appears to be a higher level of alumina which may suggest a different silica source. Group 3 is the smallest, it represents only four samples which have a constant MgO level of around 2.5wt% but extremely high Na₂O with an average value of 18.76wt%, the iron level in this group is also high (1.38wt%). All the glasses investigated were coloured using iron and copper.

4.2 The Serçe Limani Shipwreck

The Serçe Limani shipwreck is a uniquely useful source of information when looking at Islamic glass as it is preserved in its original context, undisturbed. Shipwrecks can be described as a time capsule providing a snapshot into the past. In 1977 an excavation took place in Serçe Limani, a natural harbour on the southern Turkish coast, the wreck was located around 75m from the shore. It was uncovered during a survey four years prior and was chosen for excavation firstly because of its glass cargo but also because it appeared to be from the 12th century, a critical time in the study of ship hull evolution (Bass & Van Doorninck: 1978: 119). The ship and its cargo have been dated to circa 1025 CE based on Byzantine coins of Basil II and the typology of Fatimid glass weights (Bass 1984: 64). The

ship contained raw glass blocks and around three metric tons of glass cullet, broken vessels sorted into different colours, these were found stowed at the back of the ship, this confirms that this type of glass was traded over long distances for reuse. Recycling adds another layer of complication since a glass vessel that survives today could be made up of several glasses which all have a different provenance. Wear on these broken vessels is indicative of their usage, some appear to have had a long life before ending up as cullet for recycling. This is revealing of a practice that still occurs today, dealers travelling door to door purchasing broken glass for reuse in factories (Bass 1984: 67). There were also over eighty intact glass vessels found across the bow and stern of the ship likely used by merchants on the ship, these were in bottles for storing liquids and vessels for drinking from, one particularly splendid example is decorated with the image of a lion (Bass, 1984: 65).

Chemical analysis of the glass finds reveals that they can be separated into two groups typical of Islamic glass, natron glass and soda rich plant ash glass (Brill 2009: 460). The clear majority is the plant ash glass, in a study of one-hundred and three samples selected on the basis of being representative of the glass from the wreck only four could be described as natron glass (Brill, 2009: 463). Four examples analysed represent another type of glass, lead glass, their PbO contents range between 61.2wt% - 65.4wt%. The rest of the glass samples apart from two that were discarded were made using soda rich plant ash confirmed by the values from K₂O and MgO content which are for all above 2wt%. After performing statistical analysis including standard deviation of element oxides and comparing them to sites across the Eastern Silk Road it indicated that the samples were highly confirmative. Three multivariate statistical calculations were undertaken with the data principal component analysis, cluster analysis and discriminate analysis all indicate that the plant ash glass from the Serçe Limani wreck were made in one workshop or at least in a series of closely related workshops over a short time frame (Brill, 2009: 480).

4.3 Al Raqqa

Located in north central Syria, Al Raqqa was briefly capital of the Abbasid empire between 796 and 808 CE, Harun al Rashid founded a new city here Al Rafika where he constructed several palatial complexes and added a huge industrial complex running 3km in length, Al Raqqa (Henderson, 2003: 109). Across Al Raqqa three production sites have been excavated, one particularly good example is the workshop at Tell Zujaj built into an early Islamic hypocaust, excavation has shown that glass was produced in single chambered tank furnaces and beehive shaped triple chambered glass furnaces (Henderson et al., 2005: 136). The base of the structure would function as a firing chamber and the first set of shelves would have been laid with crucibles to remelt the glass. The top of the structure would function as an annealing chamber in order for finished glass products to cool slowly ensuring they are durable and not brittle. During the 11th-12th century, however, the beehive structures disappear and are replaced by tank furnaces, though they may not have completely fallen out of use (Henderson, 2003: 110).

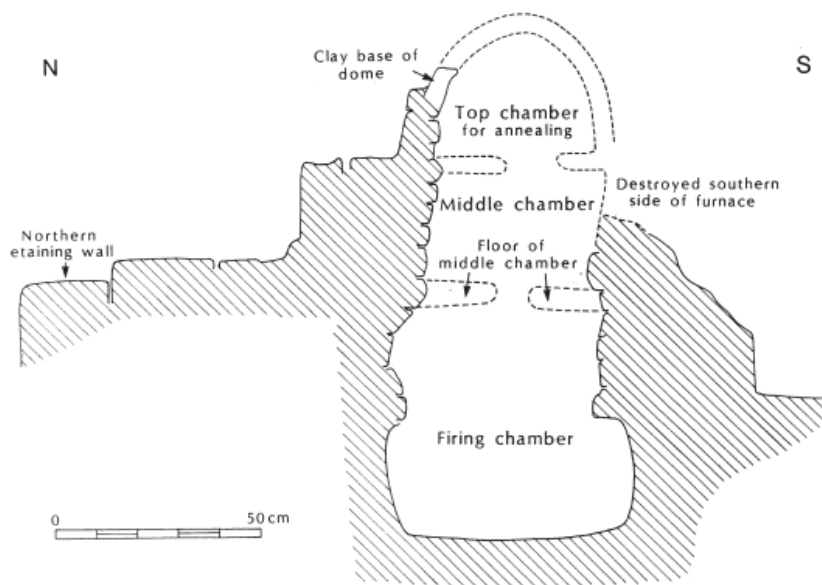


Figure 19: A beehive shaped furnace Tell Zujaj 8-9th century CE (Henderson, 2003: 111).

The discovery of fritted glass at the site is confirmation that primary glass production was taking place at Al Raqqa, likely in the tank furnaces. Dumped at Tell Zujaj was five imperial tonnes of broken glass up to 1m in length, the range of colours included green, purple, brown, blue and colourless as well as working waste such as glass rods, pulls, dribbles and drops. The activity at the site can be placed within a period of 30 years somewhere in the late 8th -

early 9th century, based on typological and numanistic dating methods (Henderson et al. 2004: 441-443).

From analysis conducted on glass samples at the site by Henderson (2004; 1999) four different compositional groups can be discerned. Type 1 is the largest group and represents a soda rich plant ash glass, the high magnesia content points to plants such as *salicornia* or *salsola* although this is speculation. Low alumina levels suggest a particularly pure silica source for this glass, quartz pebbles or possibly even chert (Henderson et al., 2004: 454). Type 3 is a natron glass following a late Roman recipe demonstrating that the move away from Byzantine glass was a gradual one. It is suggested that these glasses were made with sands from the Belus River Israel which gives an aluminium impurity of about 3-4wt% while having low magnesia levels 0.5-1wt% characteristic of natron glasses (Henderson et al., 2004: 455).

The composition of Type 4 differs because its composition is much more scattered than the other types, seen through standard deviation values. Little variation in the composition across types represents a specific glass making recipe, in contrast, the large variation across Type 4 is therefore representative of experimentation with raw materials and the subsequent recycling of cullet from this experimentation (Henderson et al. 2004: 545, Henderson 1999: 238). Henderson and colleagues argue that this provides evidence that the plant ash glass was perfected at sites like Al Raqqa, which is not at all surprising considering its importance. Furthermore, bone inclusions can be seen in the microstructure of the frit demonstrating that the glassworkers were experimenting with materials such as bone to add calcium inadvertently improving the lime content and working properties of the glass (Henderson et al., 2004: 459).

Type 1 and Type 3 appear to be compositionally quite distinct possibly demonstrating that there was a reluctance to mix these two types of glass, furthermore the high reproducibility of the types of glass at Al Raqqa indicates controlled recipes and practices (Henderson et al., 2004: 457). Finally, Type 2 is a much smaller category with negatively correlated distribution linking Type 1 and Type 3, these are high soda, low calcium and relatively low potassium oxide (Henderson et al., 2004: 460). The chemical results that are compared here are from the site Tell Zujaj where the analysis of moils has confirmed that three types of glass recipes were being produced here, types 1, 2 and 4 (Henderson et al., 2004: 451).

4.4 Samarra

Although little survives of Baghdad, the Abbasid capital and virtually nothing of the round city there is another site that has yielded much archaeological evidence. Samarra, north of Baghdad was briefly the Abbasid capital from 836-892 CE, it functioned as a palace city and was known as *Dar al – Khilafa*. Al-Ya ‘qubi in his *Kitab al – Buldan* wrote a contemporary description of the site of Samarra, and he can be cited that the caliph brought from al – Basra ‘people who make glass’ (Northedge, 2007). The use of glass for architectural accentuation was prolific at the site particularly in the throne room such as mosaics, inlays and millefiori tiles. Much of the compositional variety is in line with object type at this site, almost all traditionally shaped tesserae could be denoted as natron glasses. This group of mosaic tesserae, however, are not compositionally homogenous, they exhibit much variation in aluminium, calcium and heavy element concentrations. This reflects a multitude of different silica sources and indicated that the glass was not taken from one place but was taken from a range of sources likely across Egypt, the Levantine coast and recycled Roman glass possibly scavenged from buildings and imported to Samarra (Schibille et al., 2018: 6). Samarra Group 1 is comprised of almost all colourless glasses and are of a high quality, particularly the diamond wall inlays and some examples of highly decorated drinking wares. One particularly exquisite example is decorated with palmette and animal motifs (Berlin Sam 018). These colourless glasses have low manganese content only 0.3% as well as low silica impurities suggesting a particularly pure source of silica was included in the raw materials and that these were probably created directly from primary glass and are not the result of the inclusion of cullet.

Group 2, the largest of types, is a less high-quality glass and comprises a few colourless and aqua vessels, all scratch engraved wares, lamps and windows belong to this type, the silica source for these glasses was less pure as shown by rare earth element impurities. Group 1 and 2 are compositionally similar and based on their magnesia and potash levels both groups are both from a Mesopotamian origin. This indicates the existence of deliberate production strategies in the Abbasid Caliphate. The last group is made up of a group of 23 cobalt blue flasks which are technologically distinct from groups 1 and 2, their moderate potassium and magnesium levels are indicative of a Syrio-Palestinian or Egyptian origin through the chemistry of the cobalt ore used is reminiscent of the Eastern Mediterranean and the furnace at Tyre. The bottles necks are sawn off and appear mass produced they likely were used as containers for some kind of cosmetic product as a they were densely located at the south of

the palatial structure near the so called 'harim' where the concubines of the Caliph were housed (Schibille et al. 2018: 10).

4.5 Gorgan

Gorgan is situated 300km northeast of Rayy along the route to Nishapur. The Gorgan plain is a large area in northeastern Iran, the city of Gorgan was a provincial capital of the Sassanian Empire, its location is particularly strategic as it acts as a corridor between lush Mazandaran and the arid steppes of Dehestan and the Qara Qum Desert (Wilkinson et al, 2013: 28).

Islamic geographers recorded it as being a particularly fertile area which was famous for the production of silk that was exported as far as Lebanon. Arab rule was established under Sa' id b. 'Aṣ in the 8th century who founded the city making it the capital of the province of Gorgan and used it as a defensive frontier against threats from inner Asia. The city is most famous for its great wall a 170km defensive wall built during the Sassanian Period to protect the city from nomadic Turkic invaders, much of the excavation of the site has been concerned with this wall as it was mistakenly originally thought to have been constructed by Alexander the Great. Leadership of the city changed hands throughout its history, first being encompassed by the Saffarid and the Ziyarid Dynasties, the Samanid Empire and the Buyid Dynasty until its destruction by the Mongols in the 13th century (Bosworth, 2012: 154).

During excavations at the site led by Mohammad Kiani from 1970 to 1977, large quantities of glass were uncovered as well as two glass furnaces in the vicinity of the site's industrial workshops. The archaeological evidence shows that these furnaces belong to the 11th–12th centuries (Salehvand et al. 2020, 2). Five of the samples analysed from the site by Schibille (et al, 2022: 2) are glass working waste confirming local secondary or possibly primary glass production as opposed to exclusively finished glass from Rayy or Nishapur. Analysis shows that the 26 of the 30 samples analysed by Schibille can be put into the same compositional group indicating the presence of a local or regional production of glass vessels at this site. Many of the samples contain high concentrations of copper and/or lead, above the natural level indicating the inclusion of colourants or coloured glass cullet into the melt. Most of the fragments from the assemblage analysed by Schibille (2022) and colleagues are strongly coloured either green or blue.

4.6 Siraf

Siraf is the largest archaeological site in Iran, which attests to its importance, it functioned as a port city with a harbour on the Arabian Sea. Literary sources describe the city's prosperity during the Islamic Period, around 950 CE the medieval geographer Istakhiri wrote of the city and accounts that such items as precious stones, ambergris, pearls, ivory and a variety of spices passed through the city. It is also attested that the merchants who resided in the city lived in large multi storey houses. Siraf is located on a barren stretch of the southern Iranian coast, Istakhiri also wrote that vegetables were not grown at the site but imported in from other cities (Whitehouse, 2002: 35). By the 10th century a series of events pushed the city into decline, Muqadassi an Arabian traveller who recorded the lands of Islam wrote that an earthquake hit the city in 977 CE, after the fall of the Buyid dynasty in 1055 CE and most importantly the growth of Qais as a rival port caused the city to fall into ruin (Whitehouse, 2002: 36).

Site D, a suburb area at Siraf turned up evidence of an industrial area, the excavator recorded that a group of kilns was found. Although the majority of these kilns were used for firing ceramics, one of the kilns contained broken glass vessels and the byproducts of glass working such as drops, trails and slag, indicating that it was used for secondary glass production. Furthermore, similar material was uncovered from an adjacent waste heap (Swann et al., 2017: 16). The material from the kiln and waste heap match compositionally the glass objects from around the site in Siraf confirming that the glass was being produced for local use. There is no evidence for primary glass production at the site, implying that the raw glass was made elsewhere. A 1973 survey of the territory surrounding Siraf, a glass factory was identified in the Jamm Valley 16km to the north at *Bid-i Kahr*; just south of a large mound, *Tul-i Shisheh*, "mound of glass" was a 100m² area covered with glass slag and debris, though there has not been any detailed excavation of the area to date (Swann et al., 2017: 103). Furthermore, the glass from the site aside from just two samples do not show any indication through elevated levels of base metals of recycling indicating that they were made from raw glass rather than glass cullet (Swann et al., 2017: 113). Therefore, it is suggested that the glass at the site was reworked from locally produced raw glass, possibly a factory at *Tul-i Shisheh*.

101 samples from The Corning Museum of Glass collected by Robert Brill and David Whitehouse from excavations at the site were analysed by Swann et al. (2017: 106-9). The

glass can be split into three groups, the largest Main Group consists of 64 samples and can be subdivided into Groups A and B based on their Zr and Cr content, Group B having a slightly lower but still elevated Zr and Cr level. While this means that there is a compositional distinction between the two types, this likely represents the difference in minerals from the silica source. This main group is the glass that the excavators believed to be the local type. The second group is characterised by having lower Zr values, these two groups can also be discerned on the basis of other oxide elements. Both main groups have lower alumina and lower lime than the low Zr group. The Main Group has similar levels of K₂O and Na₂O to the Low Zr Group but lower levels MgO. The eight bangles have notably different glass compositions, with some of the lowest silica as well as highest soda and potash levels within the entire assemblage. The most noticeable characteristics of the bangles are their extremely low manganese and high soda contents (Swann, 2017: 105-10).

4.7 Nishapur

Nishapur was the capital of the Tahirid Dynasty in the ninth century, medieval writers attest to Nishapur's function as a flourishing centre for trade and the production of artefacts (Kroger 1995: ix). Much commercial digging took place at the site between 1945-1979, many glass artefacts were placed into private and museum collections from which numerous articles and catalogues were produced. The most numerous and important glass finds at Nishapur come specifically from the site of Tepe Madrasedh, the glass fragments discovered in the rooms here date to between the 9th-10th centuries. The finds from the rooms here generally present wheel cut decoration, faceted or in various slant cut styles. Several different vessel types were uncovered, various bowl and bottle shapes, alembics and possibly lamps (Kroger, 1995: 31).

From 1930-1947 Nishapur was excavated by the Metropolitan Museum of Art's Persian Expedition, renamed the Iranian Expedition. The excavations revealed over 2000 artifacts including architectural elements, ceramics, ivory, metalwork and glass, all dated between the 9th-10th centuries. Prior to these excavations little was known about Iranian glass of the Islamic Period, much of the glass from the region was thought to have Persian influence based on typological differences since the majority of glass finds prior to the excavations were acquired on the art market. Now, more vessels are thought to have originated from Iran than any other Islamic country (Wypyski, 2015: 121). The finds are split between the MET and what is now The National Museum of Iran, among the finds are many simple blown

vessels including bowls, plates, beakers, jugs and various types of bottles, over half of which are mould blown (Wypyski, 2015: 122).

Robert Brill (1995) first categorized the glass from Nishapur into two types, coloured and colourless (water white). A later study by Mark Wypyski (2015) has further categorised the glass finds from Nishapur into three types based on differences in their chemical composition, namely their levels of magnesia, aluminium and potassium. Five of the glasses under study are opaque and opacified with white crystalline tin oxide. A group of the glasses are lead-silica glasses of around 70% PbO although others had a much lower percentage but still incredibly high at 30% suggesting the mixing of lead glass with silica plant ash glasses (Wypyski, 2015: 125). Soda content in the glasses vary from 11wt% - >20wt% and lime contents ranging from 4wt% - 10wt%. All the examples contain high levels of magnesia, as was also observed by Brill (1995: 212).

Type A is classified as having a high ratio of magnesia to potash with a difference of around 2-1% This type also has low alumina levels averaging at 1wt% suggesting a pure source of silica was used, possibly quartz pebbles mixed with the sand, further there is also trace 0.04% of titanium oxide, high levels of this element can indicate low quality silica sources, this group is mainly colourless and translucent (Wypyski, 2015: 126). Both Brill (1995: 37) and Wypyski have noted this type's compositional similarity to the glass from Samarra suggesting that this glass was imported into the city.

Type B comprises one third of the assemblage which exhibit slightly lower levels of magnesia and higher potash with a difference of around 2-1wt%. The level of alumina is slightly higher averaging at 2.6wt% suggesting the use of a less pure source of silica than in Type A, titanium and phosphate levels are also higher indicating this further. This type comprises relatively simple bowls, plates, beakers, bottles and jars, further this includes all the examples with stamped decoration (Wypyski, 2015: 127). Type C represents a smaller group of glass which appear to be defined by higher amounts of potash with an average magnesia to potash ratio of less than 1, the alumina level of this group is particularly high averaging at 3.6wt%.

Nadine Schibille and colleagues (2022: 9) have argued that though it has been previously understood that local glass production did occur at Nishapur (Brill, 1995; Phelps 2018, Henderson, 2016), and Wypyski (2015: 135) specifically suggested that Type B was locally produced, that the evidence makes this picture increasingly less likely. They found that 70%

of Nishapur glass is compositionally linked to Mesopotamian glass through elevated Cr/La ratios and argue that the other 30% were also imported, though this cannot be proven. Schibille and colleagues (2022) have shown that there are many factors surrounding the identification of a Mesopotamian origin for glass but the most important and the one cited the most is the ratio of Cr/La (Shortland et al., 2007: 788). Nadine Schibille (2022: 132) in her book on Islamic glass states “if plant ash glasses have elevated Cr/La the chances are they have been produced from a Mesopotamia silica source”.

Chapter 5: Results

5.1 Element Maps

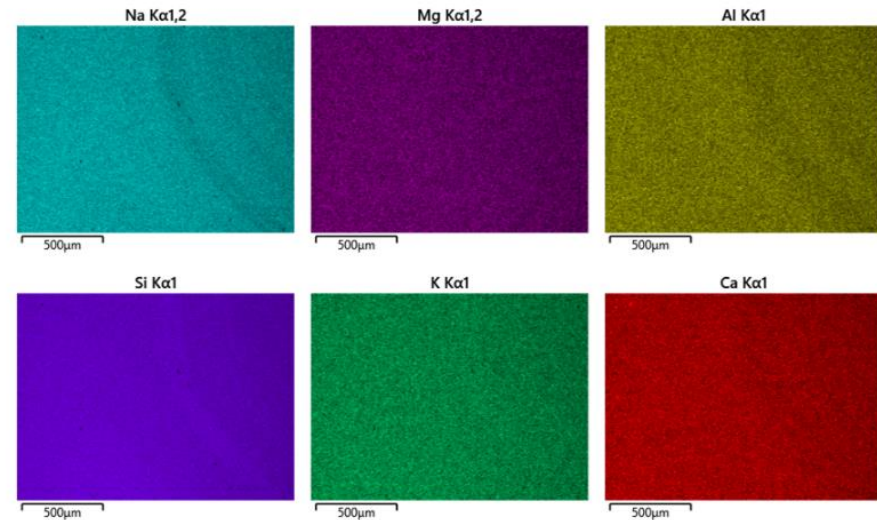


Figure 20: Element map of R.57, a black glass demonstrating that the structure is mostly homogenous with three streaks through the structure that is high in silicon and low in sodium, calcium, and aluminium (image from SEM).

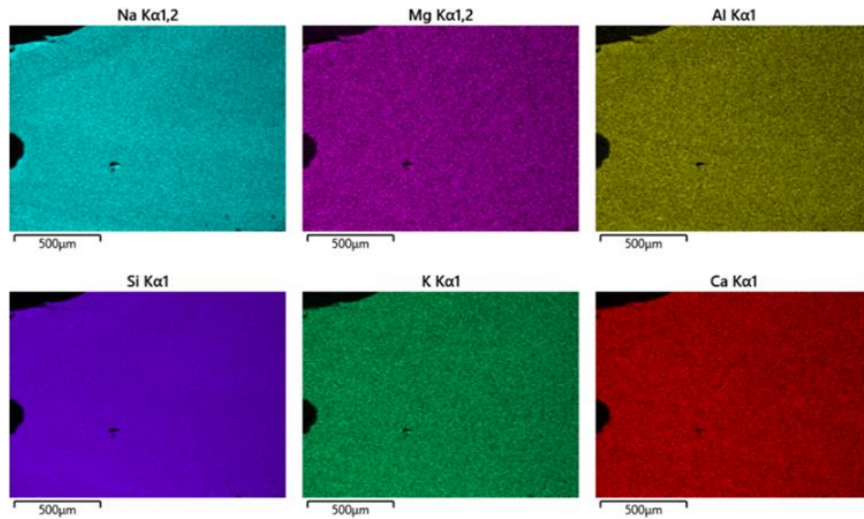


Figure 21: Element map of R.54, a black glass demonstrating that the structure is mostly homogenous apart from sodium and an air bubble in the glass matrix and one area high in sodium (image from SEM).

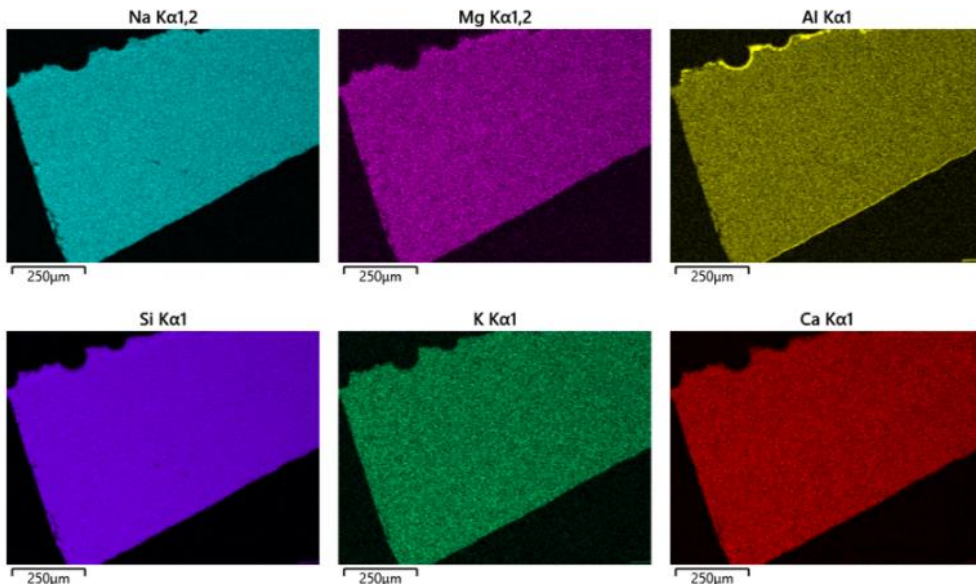


Figure 23: Element map of R.33 a colourless glass showing that the microstructure is mostly consistent though there is a layer of aluminium at the edges (image created in SEM).

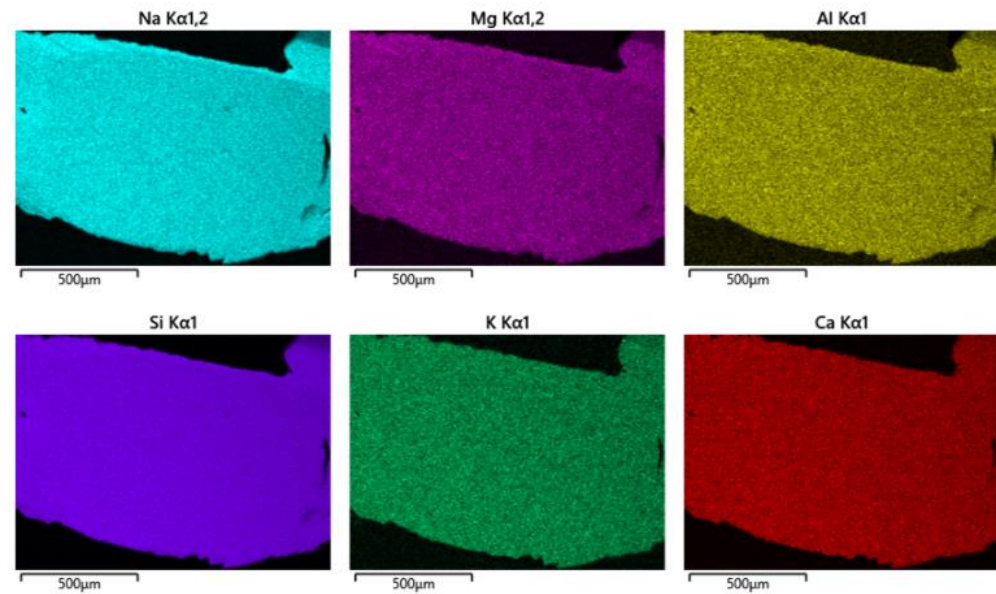


Figure 22: Element map of R.27, a colourless glass showing a uniform glass matrix, the top part of the glass under the microscope has a part that is high in silicon, sodium, aluminium and magnesium (image created in SEM).

These element maps were chosen to be included in the report of the analysis because they represent a clear difference exhibited in many of the glasses. The first two examples, which are black glasses appear to be less homogenous. This means that the raw materials are not as well fused possibly due to lower less stable temperatures which could in turn indicate less specialist production techniques. It can also be indicative of a glass that is highly recycled using glass cullet. The first two are thick black coloured glasses that were likely lower status objects while the second two examples are colourless glasses which appear to have a more consistent microstructure, these would have been produced using more specialist production techniques.

5.2 SEM-EDS Analysis Results

| Sample | Colour | Na ₂ O | MgO | Al ₂ O ₃ | SiO ₂ | K ₂ O | CaO | TiO ₂ | MnO | Fe ₂ O ₃ | CuO | PbO |
|--------|--------------------|-------------------|------|--------------------------------|------------------|------------------|------|------------------|------|--------------------------------|------|-------|
| R.01 | Green | 15.08 | 3.49 | 2.8 | 63.16 | 3.05 | 6.47 | 0.23 | 1.17 | 1.15 | 1.86 | nd |
| R.02 | Colourless | 15.33 | 2.49 | 4.13 | 65.37 | 3.2 | 6.47 | 0.28 | 0.1 | 1.55 | 0.03 | nd |
| R.04 | Black/Grey | 14.32 | 4.43 | 2.07 | 65.51 | 3.04 | 6.56 | 0.2 | 1.75 | 0.99 | nd | nd |
| R.05 | Colourless | 16.13 | 3.89 | 3.03 | 64.54 | 3.09 | 5.94 | 0.23 | 1.02 | 1.06 | 0.11 | nd |
| R.09 | Blue | 14.18 | 2.94 | 2.17 | 67.08 | 2.13 | 6.29 | 0.18 | 0.33 | 2.64 | 0.39 | nd |
| R.10 | Translucent/yellow | 14.7 | 6.24 | 1.32 | 66.55 | 3.07 | 5.27 | 0.12 | 1.31 | 0.3 | 0.05 | nd |
| R.11 | Colourless | 15.68 | 3.9 | 3.11 | 64.5 | 3.09 | 5.94 | 0.23 | 1.02 | 1.06 | nd | nd |
| R.12 | Colourless | 14.08 | 5.49 | 1.63 | 68.21 | 2.23 | 4.44 | 0.12 | 2.22 | 0.57 | 0.05 | nd |
| R.17 | Colourless | 13.19 | 2.65 | 1.75 | 66.97 | 1.94 | 8.35 | 0.06 | 0.46 | 2.69 | 0.39 | nd |
| R.18 | Colourless | 17.12 | 2.95 | 4.03 | 63.5 | 2.53 | 5.95 | 0.34 | 0.78 | 1.12 | nd | nd |
| R.19 | Colourless | 15.5 | 4.03 | 3.05 | 64.88 | 2.97 | 6 | 0.29 | 0.84 | 1.1 | 0.16 | nd |
| R.20 | Aqua | 14.22 | 5.55 | 1.53 | 68.48 | 2.26 | 4.44 | 0.14 | 2.12 | 0.46 | 0.03 | nd |
| R.25 | Colourless | 13.94 | 5.44 | 1.55 | 68.79 | 2.34 | 4.43 | 0.05 | 1.98 | 0.51 | 0.06 | nd |
| R.26 | Blue | 16.48 | 3.08 | 2.53 | 63.98 | 3.68 | 5.71 | 0.15 | 0.84 | 0.82 | 1.17 | nd |
| R.27 | Blue | 15.29 | 3.23 | 2.48 | 63.15 | 2.49 | 8.98 | 0.28 | 2.29 | 0.94 | nd | nd |
| R.28 | Green | nd | nd | nd | 26.09 | nd | nd | nd | nd | nd | 0.59 | 73.32 |
| R.30 | Yellow | 13.06 | 5.27 | 1.05 | 69.39 | 2.56 | 7.26 | 0.07 | 0.44 | 0.23 | 0.1 | nd |
| R.32 | Green | 17.37 | 3.07 | 2.56 | 63.93 | 3.48 | 5.9 | 0.29 | 1.02 | 0.88 | 0.66 | nd |
| R.33 | Colourless | 12.91 | 5.28 | 1.02 | 69.49 | 2.71 | 7.19 | nd | 0.31 | 0.41 | nd | nd |
| R.34 | Blue | 13.04 | 5.28 | 1.05 | 69.58 | 2.57 | 7.3 | nd | 0.44 | 0 | nd | nd |
| R.37 | Translucent/yellow | 15.97 | 4.02 | 3.22 | 64.58 | 3.09 | 6.15 | 0.35 | 0.83 | 1.06 | nd | nd |
| R.38 | Colourless | 14.05 | 7.1 | 1.13 | 67.94 | 3.65 | 4.92 | 0.2 | 0.29 | 0.19 | nd | nd |
| R.39 | Translucent/blue | 16.13 | 3.46 | 3.19 | 63.54 | 3.53 | 7.08 | 0.4 | 0.15 | 1.34 | nd | nd |
| R.41 | Translucent/blue | 16.46 | 3.25 | 3.33 | 63.62 | 3.81 | 7.13 | 0.31 | 0.25 | 1.12 | nd | nd |
| R.42 | Aqua | 16.44 | 3.43 | 3.4 | 63.67 | 3.79 | 6.98 | 0.21 | 0.23 | 1.19 | nd | nd |
| R.45 | Blue | 15.04 | 2.8 | 1.44 | 65.69 | 1.98 | 8.6 | nd | 0.27 | 2.9 | 0.55 | nd |
| R.46 | Blue | 14.21 | 3.01 | 1.67 | 67.13 | 2.6 | 6.8 | 0.12 | 0.84 | 2.27 | 0.5 | nd |
| R.47 | Aqua | 15.91 | 3.62 | 3.22 | 65.33 | 2.9 | 5.99 | 0.17 | 0.84 | 1.24 | nd | nd |
| R.48 | Green | 17.75 | 3.27 | 4.82 | 61.07 | 2.97 | 5.4 | 0.32 | 0.07 | 2.2 | 2.07 | nd |

| | | | | | | | | | | | | |
|-------------|-------|-------|------|------|-------|------|------|------|------|------|------|----|
| R.49 | Blue | 18.37 | 2.99 | 3.43 | 63.25 | 3.45 | 5.81 | 0.2 | 0.43 | 1.4 | 0.25 | nd |
| R.50 | Green | 16.74 | 3.65 | 3.44 | 64.41 | 3.35 | 6.28 | 0.26 | 0.34 | 1.07 | 0.04 | nd |
| R.51 | Aqua | 18.01 | 3.36 | 3.57 | 64.42 | 2.53 | 6.14 | 0.22 | 0.07 | 1.37 | 0.14 | nd |
| R.53 | Black | 18.16 | 3.76 | 2.8 | 63.45 | 3.21 | 6.8 | 0.17 | 0.06 | 0.91 | 0.23 | nd |
| R.54 | Black | 17.3 | 2.66 | 4.11 | 61.51 | 5.78 | 6.7 | 0.21 | 0.11 | 1.08 | 0.03 | nd |
| R.57 | Black | 17.67 | 2.67 | 4.22 | 60.85 | 5.78 | 6.7 | 0.21 | 0.12 | 1.1 | 0.04 | nd |

Table 3: Results of the SEM-EDS analysis of the Rayy assemblage giving sample number and colour. Nd denotes not detected (analysed here).

The compositional results from the analysis are displayed in the table above. Alongside this analysis a larger table of compositional data for the case study sites was collated through secondary research, this can be found in Appendix 2.

5.3 R.28

The most obvious outlier in the assemblage is R.28 a chunk of weathered dark green glass, this is a lead glass yielding 73.32wt% PbO. Lead glass was first produced in China, and it is unknown whether it was also produced in the Islamic world or if it was always traded in. Unfortunately, the assemblage under study here lacks the context to make any inferences about whether it was worked at Rayy (i.e. being discovered in a pile of working waste) or if it was traded or brought in as a finished object. One other lead glass object that was found during the secondary research stage of this study was discovered at Nishapur analysed by Wypyski (2015: 125) it is 70.7wt% PbO. Brill (2009: 463) also noted the existence of lead glass vessels that were uncovered from the cargo of the Serçe Limani shipwreck that ranged between 61-65% PbO. Large quantities of lead glasses have also been found at Aqaba, Jordan (Meyer & Dussibieux, 2022: 94).

Further research further outside the geographical region of this study has found that 13 examples of lead glass beads have been uncovered in Al Basra, Morocco with values ranging between 67.1% and 86.6% (Robertshaw et al., 2010: 365, *Table 2*). The lead glass from Eastern Asia however is associated with elevated levels of Barium. In China, high lead silicate glasses vary between <5% Na₂O/K₂O and SiO₂ 35-75% and 35-75% PbO. This puts R.28 at the highest end of the high lead silicate glasses with particularly low levels of SiO₂. The earliest glasses containing PbO were unearthed in Central China which correlates with the accessibility to lead sources abundant in the area (Gan, 2021: 33). Since as more and more glass assemblages from sites along the Silk Roads are analysed and discovered to contain lead glass, there is increasing weight for the suggestion that there was a market for lead silicate glasses along the Silk Roads into Central Asia.

5.4 Standard Deviation

After removing the outlier, the mean, median and standard deviation was calculated for nine oxides that were found in all analysed samples, Na₂O, MgO, Al₂O₃, SiO₂, K₂O, CaO, TiO₂, MnO and Fe₂O₃.

| Element | Mean | Median | Standard Deviation |
|--------------------------------|-------|--------|--------------------|
| Na ₂ O | 15.58 | 15.59 | 1.6 |
| MgO | 3.88 | 3.48 | 1.16 |
| Al ₂ O ₃ | 2.64 | 2.8 | 1.06 |
| SiO ₂ | 65.22 | 64.56 | 2.39 |
| K ₂ O | 3.08 | 3.05 | 0.86 |
| CaO | 6.36 | 6.29 | 1.01 |
| TiO ₂ | 0.19 | 0.21 | 0.1 |
| MnO | 0.75 | 0.45 | 0.66 |
| Fe ₂ O ₃ | 1.14 | 1.08 | 0.7 |

Table 4: Mean, median and standard deviation values for each element included in all samples in Table 3, excluding R.28.

When comparing the standard deviation of the major oxides there is much variance in the content of silica, it is the only oxide that has a value of above 2, this reflects its function as the network former and the different silica sources used across different recipes. Importantly this gives the first indication that all the glasses in the assemblage are distinct in terms of base ingredients. There is also a high SD value for alumina which may reflect that there were not only different silica sources in the glass recipes, but silica sources of differing qualities were used. This could indicate that in some recipes much sand was included and in others across

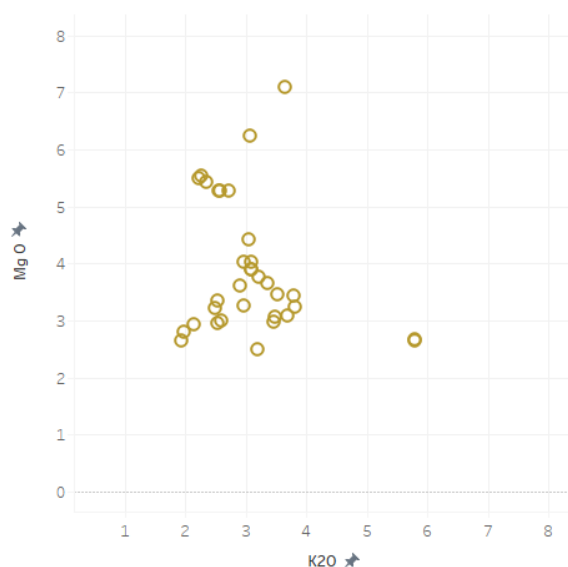


Figure 24: A plot of the Rayy glass demonstrating that they are all plant ash glasses (image created by author in Tableau).

the assemblage there were glasses that employed purer quartz pebbles. This interpretation seems favourable because of the difference between the glasses in their colour, state of preservation and the results of the element maps where some appear to have been made with more specialist techniques. The next oxide with a relatively high standard deviation is soda which likely reflects the use of different plant ashes included in the recipes across the samples. Another oxide with much variance is magnesia, this indicates that some glasses have very high levels of magnesia while others have very low levels of magnesia.

5.4.1 Regional Comparison

The group with the lowest standard deviation values comes from the Serçe Limani shipwreck, followed by the glass from Siraf, next the assemblage from Tepe Bahram at Rayy, closely followed by the glass from Gorgan and then the plant ash glass from Samarra, the glass from Nishapur, the Rayy glass analysed in this paper, the glass from Al Raqqa and finally the Roman/Byzantine natron glass from Samarra.

| Element | Rayy (<i>ah</i>) | Rayy (Corning) | Rayy, Tape Bahram | Gorgan | Nishapur |
|--------------------------------|--------------------|----------------|-------------------|---------------------|--------------|
| Na ₂ O | 1.6 | 1.4 | 1.12 | 1.37 | 1.78 |
| MgO | 1.16 | 0.82 | 0.65 | 0.7 | 1.08 |
| Al ₂ O ₃ | 1.06 | 1.43 | 0.56 | 0.64 | 0.9 |
| SiO ₂ | 2.39 | 3.31 | 1.67 | 2.35 | 2.98 |
| K ₂ O | 0.86 | 0.68 | 0.6 | 0.53 | 0.7 |
| CaO | 1.01 | 1.31 | 0.48 | 0.98 | 1.33 |
| TiO ₂ | 0.1 | 0.07 | 0.04 | 0.04 | 0.05 |
| MnO | 0.66 | 0.63 | 0.46 | 0.75 | 0.62 |
| Fe ₂ O ₃ | 0.7 | 0.74 | 0.28 | 0.52 | 0.51 |
| Average STD DEV | 1.06 | 1.15 | 0.65 | 0.88 | 1.11 |
| Element | Siraf | Al Raqqa | Samarra (Natron) | Samarra (Plant ash) | Serçe Limani |
| Na ₂ O | 0.76 | 1.63 | 2.36 | 1.22 | 0.9 |
| MgO | 0.33 | 1.42 | 0.85 | 0.61 | 0.33 |
| Al ₂ O ₃ | 0.24 | 1.01 | 0.6 | 0.25 | 0.3 |
| SiO ₂ | 1.17 | 2.32 | 4.95 | 2.96 | 1.18 |
| K ₂ O | 0.39 | 0.79 | 0.54 | 0.39 | 0.34 |
| CaO | 0.62 | 1.72 | 2.39 | 0.63 | 1.06 |
| TiO ₂ | 0.02 | 0.06 | 0.05 | 0.02 | 0.03 |
| MnO | 0.64 | 1.62 | 0.7 | 0.73 | 0.4 |
| Fe ₂ O ₃ | 0.56 | 0.51 | 1.13 | 0.54 | 0.18 |

| | | | | | |
|----------------------------|-------------|-------------|-------------|-------------|-------------|
| Average STD DEV | 0.53 | 1.23 | 1.51 | 0.82 | 0.52 |
|----------------------------|-------------|-------------|-------------|-------------|-------------|

Table 5: Standard deviation values for each element from each of the case studies calculated from Appendix 2 Rayy Tape Bahram (Agha-Aligol et al., 2022) Rayy Corning (Schibille et al., 2022) Gorgan (Schibille et al., 2022) Nishapur (Wypyski, 2015, Brill, 1995), Siraf (Swann et al., 2017) Al Raqqa (Henderson et al., 2004), Samarra natron (Schibille et al., 2022), Samarra Plant ash (Schibille et al. 2018, Schibille et al. 2022, Henderson, 2016) (ah denotes analysed here).

The data in Table 5 shows that the samples analysed here (Rayy *ah*), have a similar variance compared with Nishapur. The standard deviation value of silica across the glass from Nishapur and Samarra (plant ash) compares with the low value for the glass from the Serçe Limani wreck, where Brill (2009: 479) has argued that the primary glass came from the same factory or closely linked workshops. The second lowest variance was found at Siraf where there is evidence of a localised glass production possibly from local raw materials, therefore, low variation can be taken to indicate the presence of primary production whereas higher values suggest the contrary. Al Raqqa is different, here the production of glass from raw materials, glass cullet and experimental recipes was taking place together (Henderson et al., 2004: 451), therefore a high variance across the dataset is expected. Furthermore, the high variance of material from Samarra is expected because it is highly recycled material mostly from different natron Roman glasses recycled from other sites. The data from Rayy (*ah*) is closer to the data from Nishapur suggesting that it is unlikely that there was a big localised primary glass production going on at Rayy as has been discovered at Siraf. The study by Agha-Aligol and colleagues (2022) of the glass from Tape Bahram at Rayy, on the other hand, is much lower.

5.5 Cluster Analysis

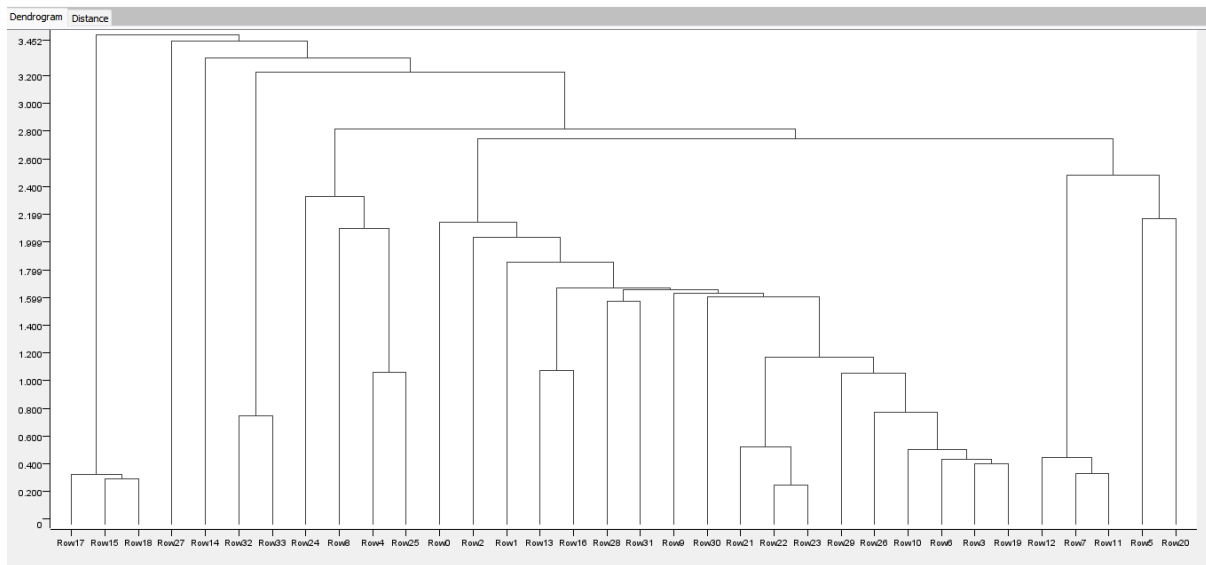


Figure 25: A dendrogram produced by KNIME analytics software for the Rayy glass (image create by author).

The figure above shows the dendrogram that was created for the Rayy data by the KNIME software, it indicates that the cluster assigner node will produce around 8 clusters. When looking at the data, at first the node only produced clusters that were made up of just one sample. This is thought to be the result of a technical problem with the node to combat this, the distance between the data points was reduced manually until all clusters contained multiple samples. At this point the analysis gave 4 clusters, the smallest, Cluster 3 comprising only three samples.

| Sample | Cluster Number | Sample | Cluster Number |
|-------------|----------------|-------------|----------------|
| R.01 | 1 | R.53 | 1 |
| R.02 | 1 | R.04 | 2 |
| R.05 | 1 | R.09 | 2 |
| R.11 | 1 | R.17 | 2 |
| R.18 | 1 | R.45 | 2 |
| R.19 | 1 | R.46 | 2 |
| R.26 | 1 | R.48 | 3 |
| R.27 | 1 | R.54 | 3 |
| R.32 | 1 | R.57 | 3 |
| R.37 | 1 | R.10 | 4 |
| R.39 | 1 | R.12 | 4 |
| R.41 | 1 | R.20 | 4 |

| | | | |
|-------------|---|-------------|---|
| R.42 | 1 | R.25 | 4 |
| R.47 | 1 | R.30 | 4 |
| R.49 | 1 | R.33 | 4 |
| R.50 | 1 | R.34 | 4 |
| R.51 | 1 | R.38 | 4 |

Table 6: This table gives the cluster number for each glass sample analysed.

| Cluster 1 | Na₂O | MgO | Al₂O₃ | SiO₂ | K₂O | CaO | TiO₂ | MnO | Fe₂O₃ | CuO |
|------------------|------------------------|------------|------------------------------------|------------------------|-----------------------|------------|------------------------|------------|------------------------------------|------------|
| Mean | 16.45 | 3.43 | 3.18 | 64.07 | 3.18 | 6.43 | 0.26 | 0.68 | 1.13 | 0.28 |
| STD | 0.98 | 0.41 | 0.45 | 0.69 | 0.4 | 0.76 | 0.07 | 0.54 | 0.19 | 0.49 |
| Min | 15.08 | 2.49 | 2.48 | 63.15 | 2.49 | 5.71 | 0.2 | 0.06 | 0.82 | 0.03 |
| Max | 18.16 | 4.03 | 4.13 | 65.33 | 3.81 | 8.98 | 0.4 | 2.29 | 1.55 | 1.86 |
| Cluster 2 | | | | | | | | | | |
| Mean | 14.19 | 3.17 | 1.82 | 66.48 | 2.34 | 7.32 | 0.11 | 0.73 | 2.3 | 0.37 |
| STD | 0.59 | 0.64 | 0.27 | 0.72 | 0.42 | 0.96 | 0.07 | 0.55 | 0.68 | 0.19 |
| Min | 13.19 | 2.65 | 1.44 | 65.51 | 1.94 | 6.29 | 0.12 | 0.27 | 0.99 | 0.39 |
| Max | 15.04 | 4.43 | 2.17 | 67.13 | 3.04 | 8.35 | 0.2 | 1.75 | 2.69 | 0.55 |
| Cluster 3 | | | | | | | | | | |
| Mean | 17.57 | 2.87 | 4.38 | 61.14 | 4.84 | 6.27 | 0.25 | 0.1 | 1.46 | 0.71 |
| STD | 0.2 | 0.29 | 0.31 | 0.27 | 1.32 | 0.61 | 0.05 | 0.02 | 0.52 | 0.96 |
| Min | 17.3 | 2.66 | 4.11 | 60.85 | 2.97 | 5.4 | 0.21 | 0.07 | 1.08 | 0.03 |
| Max | 17.75 | 3.27 | 4.82 | 61.51 | 5.78 | 6.7 | 0.32 | 0.12 | 2.2 | 2.07 |
| Cluster 4 | | | | | | | | | | |
| Mean | 13.75 | 5.71 | 1.29 | 68.55 | 2.67 | 5.66 | 0.09 | 1.14 | 0.33 | 0.03 |
| STD | 0.62 | 0.6 | 0.24 | 0.95 | 0.45 | 1.26 | 0.07 | 0.81 | 0.18 | 0.03 |
| Min | 12.91 | 5.27 | 1.02 | 66.55 | 2.23 | 4.43 | 0.05 | 0.29 | 0.19 | 0.03 |
| Max | 14.7 | 7.1 | 1.63 | 69.38 | 3.65 | 7.3 | 0.14 | 2.22 | 0.51 | 0.06 |

Table 7: This table gives each of the oxides mean, minimum and maximum and standard deviation value for each cluster. Mean, minimum and maximum are presented as wt% and STD refers to their standard deviation values.

5.6 Principal Component Analysis

From the PCA analysis, a table of values was produced by the KNIME workflow based on the eigenvalues produced by the PCA node. There were ten given by the software, though six were discarded due to having eigenvalues less than 0.03 after Brill (2009: 478). From this data more values could be struck off until only the relevant variables or elements were left.

| Element | PC1 | PC2 | PC3 | PC4 |
|------------------------------------|-------|-------|-------|--------|
| Na₂O | 0.47 | 0.3 | 0.42 | 0.6 |
| MgO | -0.27 | 0.49 | -0.13 | 0.18 |
| Al₂O₃ | 0.31 | 0.07 | 0.16 | -0.31 |
| SiO₂ | -0.75 | 0.02 | 0.47 | 0.04 |
| K₂O | 0.17 | 0.18 | 0.2 | -0.48 |
| CaO | 0.04 | -0.71 | 0.002 | 0.39 |
| TiO₂ | 0.02 | 0.02 | -0.02 | -0.007 |
| MnO | -0.08 | 0.13 | -0.68 | 0.21 |
| Fe₂O₃ | 0.08 | -0.35 | 0.04 | -0.23 |
| CuO | 0.05 | -0.03 | -0.24 | -0.2 |

| Element | PC1 | PC2 | PC3 | PC4 |
|------------------------------------|------|------|------|------|
| Na₂O | 0.47 | 0.3 | 0.42 | 0.6 |
| MgO | | 0.49 | | |
| Al₂O₃ | 0.31 | | | |
| SiO₂ | | | 0.47 | |
| K₂O | | | | |
| CaO | | | | 0.39 |
| TiO₂ | | | | |
| MnO | | | | |
| Fe₂O₃ | | | | |
| CuO | | | | |

Table 8a: The loading values for each element for PC1-PC4 (above). B: The previous table with the insignificant values (below 0.03) removed (below) (by author; data retrieved from KNIME Analytics Platform).

Principal Component 1: The first principal component appears to be the relationship between levels of soda and levels of alumina.

Principal Component 2: The second principal component involves the relationship between soda and magnesia.

Principal Component 3: The third principal component comprises the relationship between soda and silica.

Principal Component 4: The fourth principal component relates to the relationship between the level of soda and lime in the glass samples.



Figure 26a: (top left) Principal component 1 Al_2O_3 vs Na_2O . B: (top right) Principal component 2 Na_2O vs MgO C: (bottom left) Principal component 3 Na_2O vs SiO_2 . D: (bottom right) Principal Component 4 Na_2O vs CaO . E: Key for biplots (below tables) (image created by author using Tableau).

Figure 26a, demonstrating the first principal component, exhibits a clear trend line, as the level of Na_2O increases so does the level of Al_2O_3 , the glass in Cluster 4 having the least amount of each element followed closely by Cluster 2, the glass in Cluster 1 is less uniform to the trend particularly in the level of soda, however this may be expected as it is the largest cluster. Cluster 3 is particularly high in alumina and soda. Figure 26b shows that while there is clear clustering on this graph, there does not appear to be as clear a trend line that is uniform among the clusters. Cluster 4 is extremely high in MgO and is low in Na_2O , though Cluster 2 also has low levels of Na_2O yet has low levels of MgO . Clusters 1 and 3 overlap, they both exhibit high Na_2O and low MgO <4wt%. Figure 26c, the third relationship, between the level of soda and the level of silica clearly reveals that as the wt% of Na_2O

decreases, the level of SiO₂ increases. Cluster 3 has the highest levels of soda and the lowest levels of silica with no overlap and is followed by Cluster 1. There is some overlap between Clusters 2 and 4, though Cluster 4 clearly has the highest wt% values for SiO₂. Finally, *Figure 26d* plots the fourth principal component, this relationship does not appear to follow any trend line, however, Clusters 4 and 2 are lower in soda than Clusters 1 and 3. Since soda is derived from the plant ash flux, this could represent two distinct plant ashes or a different ash treatment process. Since PC1 demonstrates that as soda decreases as does alumina, this could represent that glasses that are better made i.e. Clusters 4 and 2 used both a higher quality silica source as well as a higher quality plant ash alkali which was lower in soda and in the case of the Cluster 4 glass, richer in magnesia. In the case of Cluster 2 however the alkali source is more ambiguous and could instead point to alternative processes such as soda leaching. These ingredients would be specially selected for each glass type. Furthermore, the graphs show a clear separation between the glass types in PC1 of Clusters 2 and 4 and Clusters 3 and 1 which indicates a reluctance to mix these glass types.

5.7 Regional Comparison

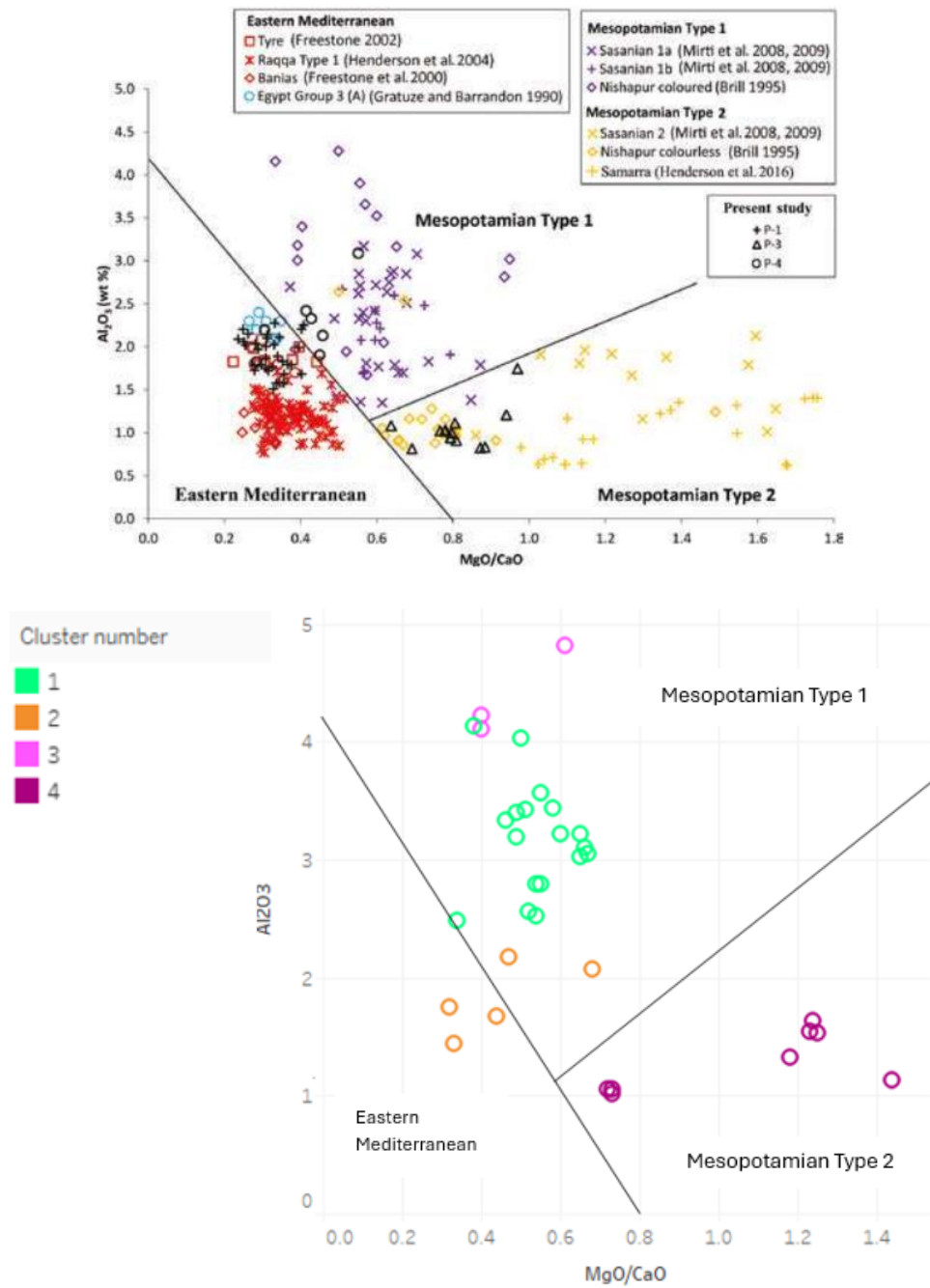


Figure 27a: (above) Biplot of MgO/CaO vs Al_2O_3 by Phelps (2018: 262) demonstrating his glass types. B: (below) The same biplot plotted with instead the glass from Ray with the cluster number indicated by the key (analysed here).

| Element | Rayy <i>ah</i> | Rayy (Corning) | Rayy, Tape Bahram | Gorgan | Nishapur |
|--------------------------------|-------------------|---------------------|------------------------|-----------------|-------------|
| Na ₂ O | 15.14 | 16.12 | 16.78 | 15.2 | 14.87 |
| MgO | 3.96 | 3.44 | 3.67 | 3.28 | 3.84 |
| Al ₂ O ₃ | 2.57 | 3.21 | 3.03 | 2.54 | 2.19 |
| SiO ₂ | 64.1 | 63.92 | 64.11 | 65.93 | 66.54 |
| K ₂ O | 3 | 2.91 | 2.99 | 3.17 | 2.68 |
| CaO | 6.18 | 6.47 | 5.34 | 5.77 | 6.5 |
| TiO ₂ | 0.19 | 0.15 | 0.15 | 0.16 | 0.13 |
| MnO | 0.72 | 0.47 | 0.76 | 0.87 | 0.63 |
| Fe ₂ O ₃ | 1.11 | 1.49 | 1.09 | 0.98 | 1.05 |
| Siraf | Al - Raqqa | Samarra (natron) | Samarra (plant ash) | Serçe Limani | Veh Ardašir |
| 13.88 | 13.83 | 14.81 | 14.35 | 13.06 | 15.75 |
| 2.85 | 2.94 | 0.58 | 4.98 | 2.63 | 4.39 |
| 1.75 | 2.4 | 2.28 | 1.34 | 1.89 | 2.08 |
| 66.93 | 68.33 | 61.74 | 67.35 | 69.68 | 61.48 |
| 2.76 | 1.96 | 0.54 | 2.82 | 2.69 | 2.87 |
| 7.84 | 7.58 | 5.78 | 5.89 | 9.34 | 6.37 |
| 0.13 | 0.07 | 0.14 | 0.07 | 0.13 | 0.13 |
| 1.28 | 0.74 | 0.21 | 0.93 | 1.26 | 0.24 |
| 1 | 0.68 | 0.99 | 0.73 | 0.71 | 0.88 |

Table 9: Average wt% oxide value for each element for all the case study sites: Rayy Tape Bahram (Agha-Aligol et al., 2022) Rayy Corning (Schibille et al., 2022) Gorgan (Schibille et al., 2022) Nishapur (Wypyski, 2015, Brill, 1995), Siraf. (Swann et al., 2017) Al Raqqa (Henderson et al., 2004), Samarra natron (Schibille et al., 2022), Samarra Plant ash (Schibille et al. 2018, Schibille et al. 2022, Henderson, 2016.) Now including Veh Ardashir (Mirti et al. 2009) (*ah* denotes analysed here).

Figure 27 demonstrates that all three of Phelp's types are present in the glass under study here from Rayy. Cluster 2 fits partially into the Eastern Mediterranean Type and will therefore be compared with Al Raqqa Type 1 and the glass from Tyre and the Serçe Limani wreck. Clusters 1 and 3 are firmly rooted in the Mesopotamian Type 1 category and can be compared with Nishapur coloured glass and the glass from Gorgan and Siraf. Finally, Cluster 4 is clearly of the Mesopotamian Type 2 and further clusters into two types, a high and a low MgO which will be compared to the glass from Samarra and the Nishapur colourless glass.

5.7.1 Cluster 1-3

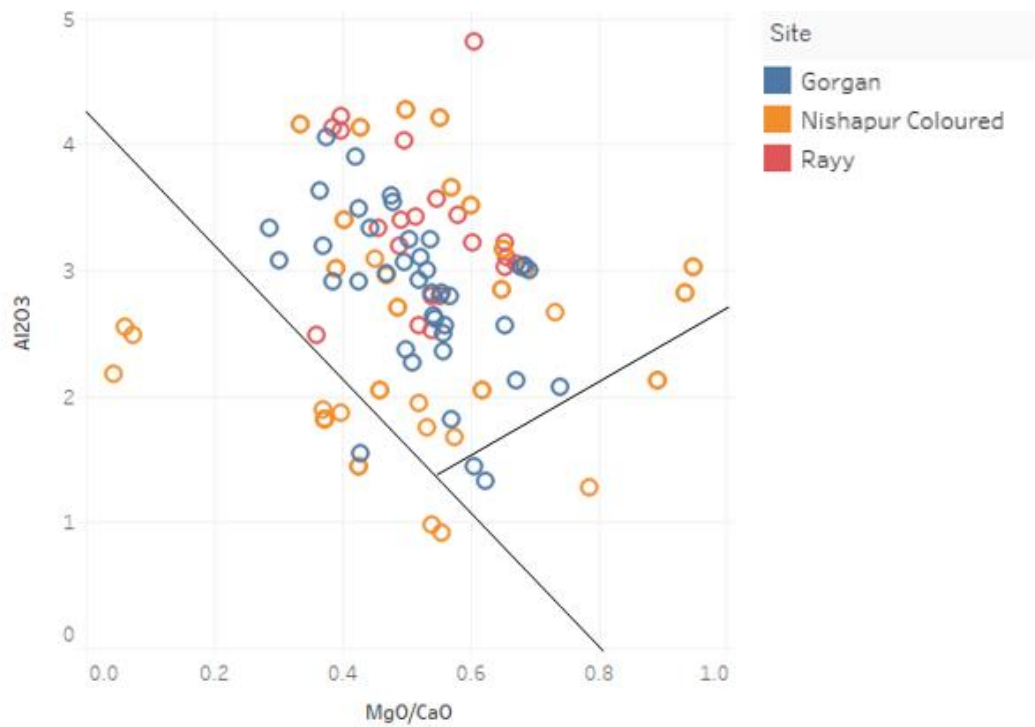


Figure 28: Biplot of MgO/CaO vs Al₂O₃ comparing the data from Nishapur coloured (Schibille et al., 2022; Wypyski, 2015, Brill 1995), Gorgan (Schibille et al., 2022) and Rayy (analysed here) (image created by author using Tableau).

5.7.2 Cluster 2

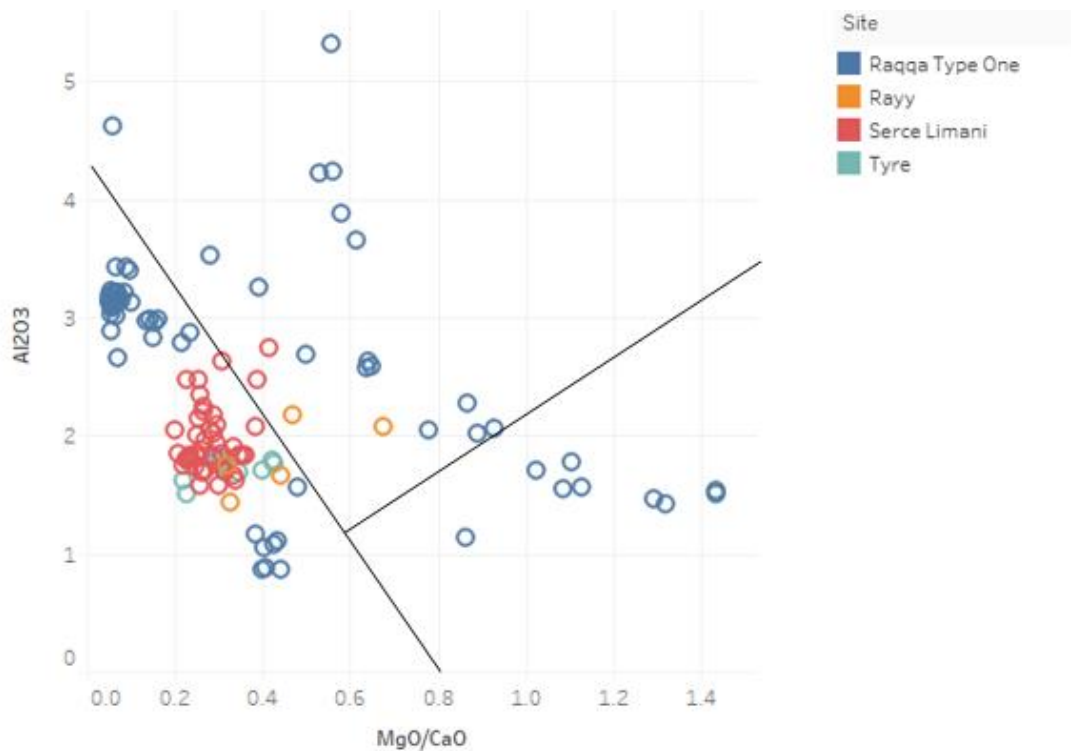


Figure 29: Biplot of MgO/CaO vs Al₂O₃ comparing Raqqa Type One (Henderson et al., 2004), the Serçe Limani Wreck (Brill, 2009), Tyre (Freestone, 2002) and Rayy (analysed here) (image created by author using Tableau).

5.7.3 Cluster 4

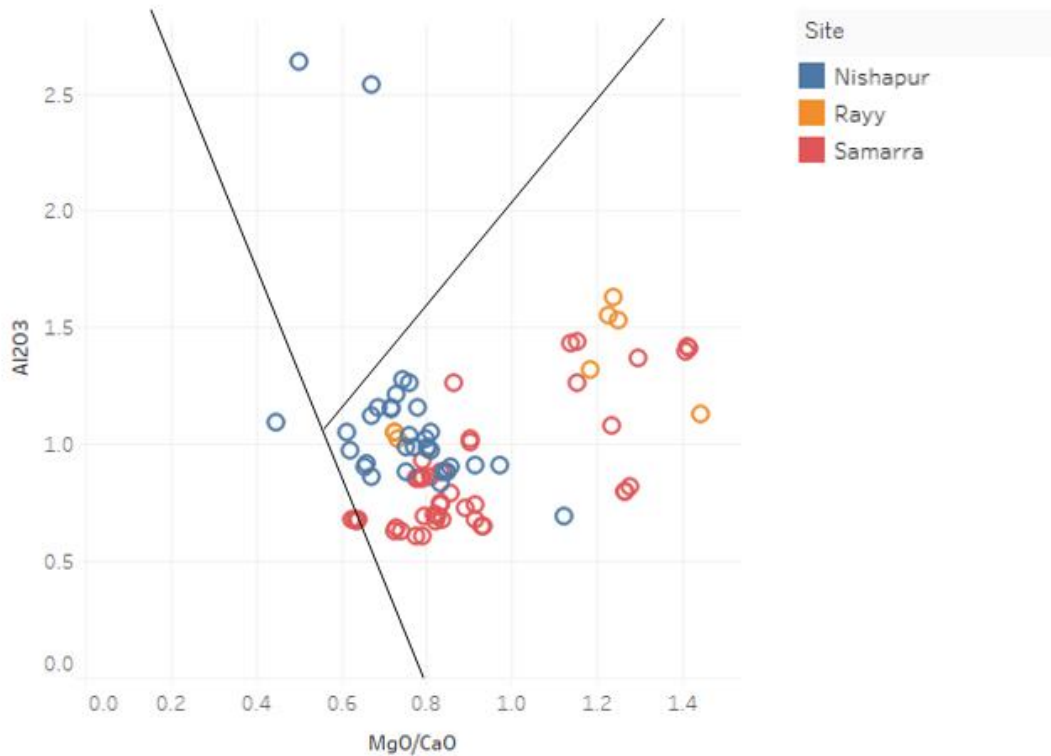


Figure 30: Biplot of MgO/CaO vs Al₂O₃ comparing the data from Nishapur colourless (Type A) (Schibille et al., 2022; Wypyski, 2015, Brill 1995), Rayy (analysed by author) and Samarra (Schibille et al., 2018; Henderson et al., 2016) (image created by author using Tableau).

5.8 Schibille et al. 2022 S1/S2

This glass type is argued to be related to Samarra and Nishapur Type A, it can be distinguished based on high MgO levels and a quartz rich silica source low in mineral impurities. From the analysis it can be deduced that the Cluster 4 Rayy glass belongs to this type. According to Schibille and colleagues, the average MgO/CaO ratio for the S1/S2 glass types are respectively 0.75 and 1.18. The mean value for MgO in Cluster 4 is 1.01 (Table 7), the average ratio of MgO/CaO for Cluster 4 fits nicely inside these two values. In terms of silica impurities, it can be seen from this graph that the Cluster 4 glass type at Rayy does have high levels of silica and low levels of silica related elements.



Figure 31a: (top left) biplot comparing the level of SiO₂ with TiO₂ across Clusters 1-4, b: (top right) biplot comparing the level of SiO₂ with Fe₂O₃ across Clusters 1-4, c: (bottom) biplot comparing SiO₂ with Al₂O₃ alumina across Clusters 1-4 (images produced by author using Tableau).

These biplots show that Cluster 4 has the highest levels of silica averaging at 68.55wt% reaching as high as 68.79wt%, the average SiO₂ value for S1/S2 being 71.8wt% and 68.7wt% respectively. Furthermore, along with Cluster 2, this group exhibits the lowest levels of Al₂O₃ and TiO₂, the average level of Al₂O₃ for Rayy Cluster 4 being 1.29wt%. In comparison with Schibille et al.'s type S1/S2 which sit at 1.02 and 1.21wt%, this is higher but not by any significant amount as the lowest average level of Al₂O₃ for Schibille et al.'s other types are 2.42wt% (Group3/M). Therefore, the Rayy Cluster 4 glass should still be categorised under

S1/S2 in terms of level of alumina. For TiO₂ the average level for Type S1/S2 is 0.04 and 0.06, the average amount of TiO₂ in the Rayy Cluster 4 glass is 0.09wt%, again on the higher side but still within the category. This all suggests that for Clusters 2 and 4 a particularly pure source of silica was used in these glass recipes. Cluster 2 however cannot be considered eligible to be classified under the S1/S2 type because of its low level of MgO detailed above. Moreover, Cluster 2 however has high levels of Fe₂O₃, though this may represent its use as a colourant (*Table 7*).

5.9 Schibille et al. 2022 Group 3/Mesopotamian

| MgO/K₂O | | MgO/CaO | |
|---------------------------|------|------------------|------|
| Cluster 1 | 1.1 | Cluster 1 | 0.54 |
| | | | |
| Cluster 2 | 1.36 | Cluster 2 | 0.45 |
| | | | |
| Cluster 3 | 0.67 | Cluster 3 | 0.47 |
| | | | |
| Cluster 4 | 2.16 | Cluster 4 | 1.07 |

Table 10: Average MgO/CaO and MgO/K₂O levels for each cluster from the Rayy data (analysed here, calculated using Excel).

| MgO/K₂O | | MgO/CaO | |
|---------------------------|------|----------------|------|
| G1a | 1.09 | G1a | 0.52 |
| G1b | 1.01 | G1b | 0.49 |
| G2 | 0.79 | G2 | 0.49 |
| G3/M | 1.39 | G3/M | 0.57 |
| S1 | 2 | S1 | 0.75 |
| S2 | 1.92 | S2 | 1.18 |

Table 11: Average MgO/K₂O and average MgO/CaO values for G1-3 and S1/2 (Schibille et al., 2022: 6, Table 1).

Although this type is most strongly associated with Cr/La ratios which cannot be compared to the data gathered here, it is also associated with specific MgO/K₂O ratios linked to the geochemistry of the Euphrates and Tigris rivers (Schibille et al., 2022: 6). The average MgO/K₂O ratio for G3/M is 1.39, Cluster 1 from the Rayy glass group falls below this number at 1.10, closer to the average value for MgO/K₂O ratio for G1a (1.09). The ratio of

the average levels of MgO and K₂O for Cluster 3 is even lower, at 0.67 and for Cluster 4 this is much higher at 2.16. Cluster 2 however, does fall close to the MgO/K₂O ratio for G3 Mesopotamian glass ranging averaging at 1.36. However, based on Phelp's work however Cluster 2 fits into the Mediterranean Type and appears to be more closely related to the glass from Tyre, the Serçe Limani Wreck and Raqqa Type 1 (*Figure 29*). Though in terms of Phelp's type P1 it exhibits high CaO, at 9wt% while the CaO level of Cluster 2 averages at 7.32wt%, closer to Schibille et al.'s G3/M type averaging at 6.8wt%. Phelp's P1 type also requires low MgO, his type averaging at 2.9wt%, Cluster 2 has an average MgO level of 3.17wt% which is closer to Mediterranean than Mesopotamian as the average MgO level for G3/M is 3.86wt%. Thus, the Rayy glass group Cluster 2 cannot be said to originate from either the Mediterranean or Mesopotamia based on these elements, further investigation into trace elements is required.

Moreover, Schibille et al. state that G3/M is closely related to Sassanian glass, specifically Type 1a, they postulate that this is due to a continuation of traditional glassmaking and raw materials used in Mesopotamia. From this, it would be useful to compare the Cluster 1-3 glass groups from Rayy with the glass from Veh Ardašir. Upon acquiring a dataset for Sasanian glass (Mirti et al. 2009: 1064) and comparing plotting it against the data from Rayy analysed here, there is little overlap. This could indicate that only a small number of the glass under study here has a Mesopotamian origin.

Cluster 1-4 vs Veh Ardašir

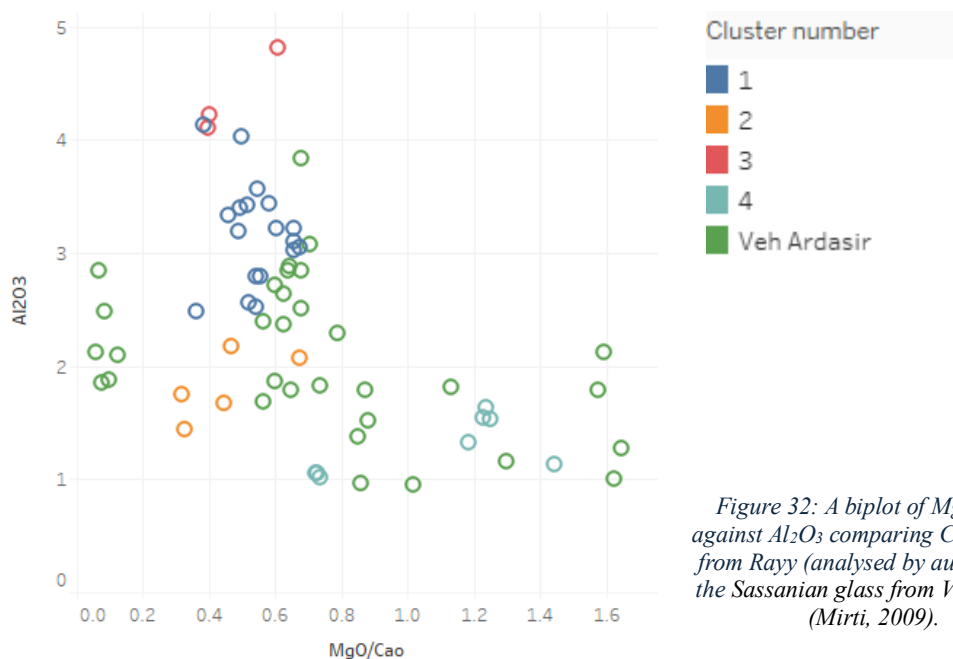


Figure 32: A biplot of MgO/CaO against Al₂O₃ comparing Clusters 1-4 from Rayy (analysed by author) with the Sassanian glass from Veh Ardašir (Mirti, 2009).

Chapter 6: Discussion and Conclusions

6.1 Materials Composition

Aside from a single exception, R.28, a fragment of lead glass likely traded in from China, along the Silk Roads, all the glass analysed, exhibit MgO and K₂O levels standard of plant ash glass. This includes the other glass assemblages from Rayy (Schibille et al. 2022; Agha-Aligol et al. 2022), as shown in *Figure 24*. This places them well within the tradition of Islamic glass making, the lowest values being 2.49wt% and 1.94wt% for MgO and K₂O respectively (*Table 7*). Despite the lack of archaeological remains at Rayy, this hints at the existence of long-distance trade networks such as are described in historical sources (Minorsky, 1994: 471). The lack of natron glass at the site, such as is present at Samarra and Al Raqqa highlights the break from Byzantine styles/traditions in favour of a continuation of a growing culturally Islamic technology and style.



Figure 33: R.28, undiscerned type, 4-6.2mm thick (image taken by author).

Due to the general lack of inclusions and general uniformity of the majority of glass compositions, it can be deduced that the mixing and fusion processes during the production of the glasses under study here, particularly the coloured and colourless glasses were thorough and effective. Though more importantly, that they were well controlled, indicating specialist knowledge and equipment capable of making such quality glass. There is however a stark difference where the black glasses are less homogenous than the colourless ones. Black glasses contain different colourants that are not completely mixed which suggests that these glasses may have been produced from cullet that was not separated into one specific colour but a mixture of different scrap glasses. From this it can be suggested that the black coloured glasses in the assemblage were lower quality, likely also produced in lower quality

furnaces incapable of achieving high stable temperatures which perhaps had other primary functions (*Figure 20; Figure 21*).

6.2 Technological Variance

When comparing the standard deviation values for the elements related to the silica source (*Table 5*); the glass from Rayy has a particularly high variance for Fe_2O_3 , the second highest among the compared assemblages. However, there are some black coloured glasses within Cluster 3 which have very high contents of iron likely due to its use as a colourant. When comparing the value for silica for the glass analysed here (2.39wt%), it is closest to the value seen in the data from Al Raqqa (2.32wt%). Interestingly, the lowest variation in titanium oxide was observed in Rayy glass, though further analysis of the silica sources is necessary to investigate this.

Overall, the highest variation in silica levels is seen in the natron glass from Samarra, this reflects the fact that much of it has been recycled and brought from various sites across the Roman/Byzantine world, as is recorded by historical sources (Northedge, 2007). The lowest variance in silica levels is seen in the glass from the Serçe Limani wreck, on this basis Robert Brill (2009: 479) has suggested that this glass was all made in the same factory. The glass under discussion here exhibits a higher variance indicating that they were not all produced in the same factory from primary materials. The glass in the assemblage was rather made from different glass recipes, though this does not rule out that they were produced in the same factory. They may have been produced through secondary glass working of glass sourced from primary production centre(s) or from recycled glass cullet similarly to the centralised model detailed in *Figure 13*.

In terms of the plant ash components of the Rayy (*ah*) glass, there is a high average variance in the amount of soda at 1.6, which is most comparable to the average standard deviation value from Raqqa (1.63) and Nishapur (1.78). There is also a particularly high variance in the level of magnesia for the assemblage studied here, second only to Al Raqqa where experimentation with glass recipes is thought to have occurred (Henderson et al. 2004: 545). This contrasts to the variance seen at Siraf which is suggested to represent a localised glass tradition where primary glass production was taking place to create glass objects that were used locally (Swann et al., 2017: 113). The average deviation value at Siraf is lower than from any other site apart from the Serçe Limani wreck which represents glass from the same factory. The plant ash glass from Samarra also has a low variance in its plant ash elements,

however, it has been suggested by Schibille (2018) Gratuze and Lankton (2022) and Brill (1995) that Samarra was producing its own range of prestige plant ash glass. It has been argued also that there was little to no primary glass production at Nishapur, relying instead on secondary workshops (Schibille et al., 2022). Since the standard deviation values for Rayy are most comparable to the glass from Nishapur rather than Siraf or Samarra, it follows that the glass from these assemblages were not produced in a local glass factory from raw ingredients. Rather they may have been manufactured across multiple secondary workshops.

When considering the other glass assemblages analysed from Rayy; the Tape Bahram collection and the collection from Corning, the standard deviation values differ across each of the considered oxides in all three assemblages (*Table 5*). Notably the Tepe Bahram has a much lower variation, the average STDev value being 0.65 at Tape Bahram, 1.06 for the assemblage discussed here and 1.15 for the glass from Corning. The glass at Tape Bahram is much closer to the glass from Siraf at 0.53 where there is local use of primary produced glass. Following Brill's line of argument this would suggest that all the glass from the Tape Bahram assemblage came from the same factory, while the other glass assemblages from Rayy did not. Since the glass from the Tape Bahram assemblage is the only glass to have an archaeological context and is known to have all come from the same excavation, this possibility becomes even more likely. This would lead it to be concluded that there was at least some primary glass production occurring at Rayy, perhaps in just one part of the city. Though a counterargument to this could be made as the assemblage from Tape-Bahram only represents one colour, green. Since ancient glass workers would split up glass cullet based on their colours and be reluctant to mix them, if the glass from the Tape Bahram assemblage was produced from secondary glass cullet this would also account for the lack of variance in the glass.

6.3 Cluster Analysis and Principal Component Findings

Returning to the glass analysed here, this assemblage can be split into four groups or clusters, the largest being Cluster 1 which can be joined with Cluster 3 based on the similarity between these two groups. They both reveal high silica related impurities such as alumina and titanium oxide, as well as iron which may relate to impurities from silica sources but also from colourants where no care was taken by glassmakers to prevent the mixing of different colours of glass cullet. The mixture of black glasses also may have provided a way of reusing

glasses where the colouring was unsuccessful or unfavourable. These factors indicate that Cluster 1/3 represents a generally lower quality glass in comparison with Clusters 2 and 4.

The results of the PCA expose that the most important relationships, visualised in *Figure 26*, are firstly, the relationship between alumina and soda. Across the samples analysed, as the content of soda increases as does the quantity of alumina. As discussed in Chapter 2, some sources of silica have high impurities of aluminium due to the presence of kaolinite and feldspars, these being of a lower quality. Clusters 4 and 2 have low quantities of aluminium suggesting that higher quality silicates were used in these recipes such as purer sands or even crushed quartz pebbles. The break between Clusters 2 and 4 and Cluster 1/3 in the graphs likely represents a reluctance by glassmakers to mix high quality and low-quality glasses.

Principle component three demonstrates that as the content of silica increases that the level of soda drops. This indicates that different plant ashes were used with different quality glasses, for glasses made from relatively impure silica, a soda rich plant ash appears to have been used. Looking at the second principal component, it could be suggested that the plant ash flux favoured for higher quality glasses is a magnesium rich flux. This is not the case for Cluster 2 where the plant ash flux is comparatively low in magnesia and in soda. It also has the lowest mean value for K_2O , at 2.34wt%. This may be the result of an additional ashing technique employed to reduce the level of soda in the plant ash used for higher quality glasses. The reduction of soda content in a plant ash flux was beneficial because the alkali makes soda more soluble therefore making a glass with less soda would make it particularly durable to be used for containing water or compounds such as perfumes. It also increases the hardness of the glass and makes it more scratch resistant.

6.4 Comparative Typology with Mesopotamian and Eastern Mediterranean Glasses

6.4.1 Cluster 1/3 (C1/3)

When comparing the Rayy glass analysed here with Phelp's designation of Mesopotamian Types 1/2 and Eastern Mediterranean by plotting MgO/CaO ratios against Al₂O₃ values, clear-cut categorisations emerge. C1/3 fits securely into the Mesopotamian Type 1, this type is related to the Nishapur coloured glasses and the Sassanian glass types 1a and 1b LMG low magnesia glasses. Cluster 3 specifically has higher alumina levels suggesting the use of a different silica source. C1/3 may represent glass that is locally Iranian, though further analysis is required to give weight to this, especially considering there is no large primary production zone for glass in the area uncovered to date. It is possible that primary glass production occurred at Rayy as is suggested by the standard deviation values for the Tape Bahram assemblage. Though the standard deviation values for the rest of the Rayy glass suggests that they are compositionally distinct, though it may be that they were uncovered from different parts of the site, unfortunately a lack of contextual information makes this a difficult issue to resolve.

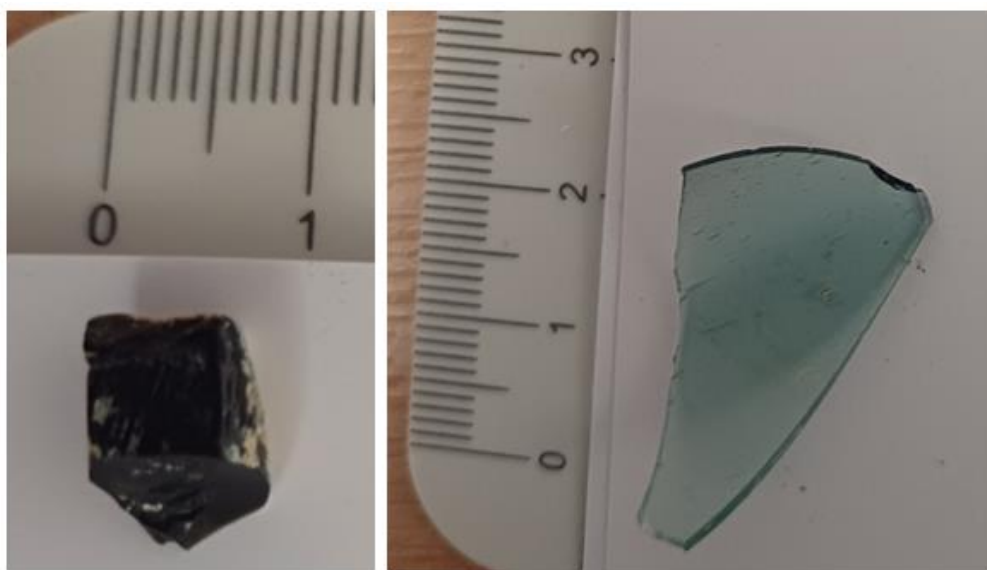


Figure 34a: (left) R.57, a Cluster 3 black glass, b: (right) R.42 curved glass belonging to a small bottle, almost colourless 0.3mm thick (images taken by author).

C1/3 glass overlaps with the glass from Gorgan where two glass furnaces have been uncovered dated to be 11th/12th century (Salehvand et al. 2020, 2). It is possible that a primary producing glass factory on the Iranian plateau served these two sites situated at either one of or somewhere between two, or possibly at Nishapur. This would indicate that the Cluster 1/3 glass was produced on or from glass that was fabricated on the Iranian Plateau.

Further, there are examples of colourless glass in this cluster, the figure above shows a curved body fragment from R.42 which possibly functioned as a cosmetics bottle, it exhibits an aqua tinge due to the presence of iron (1.19wt% Fe₂O₃). However, it is very thin with a uniform thickness of 0.3mm and a few bubbles throughout its composition. This attests to it being a high-quality glass that was made using quality techniques. Clusters 1/3 have the highest variance indicating that these glasses do not have the same provenance and were originally produced from different recipes, without any stratigraphical context it could be argued that this difference reflects that they were made during different glassmaking episodes. It cannot be argued that these glasses were produced on the Iranian Plateau, only further investigation of trace elements using LA-ICP-MS would provide an insight into the provenance of these glasses.

6.4.2 Cluster 2 (C2)

C2 is comprised of five samples one completely weathered, three blue and one aqua glass fragment, the three blue glasses are clearly coloured with iron and the translucent aqua (R.17) decoloured with manganese. In terms of Phelp's glass types (*Figure 27a*), the cluster falls between the edge of Mesopotamian Type 1 and the Eastern Mediterranean Type, falling mostly into the latter, this type comprises glass from Tyre, Al Raqqa Type 1 and Baniyas, Israel, but also the Serçe Limani wreck. Upon comparison with glass from Tyre, Al Raqqa Type 1 and the Serçe Limani wreck, the glass overlaps the most closely with the glass from Tyre and the Serçe Limani wreck. Both glasses from Tyre and the Serçe Limani wreck exhibit high average levels of CaO, 10.52wt% and 9.34wt% respectively. Cluster 2 exhibits the highest levels of CaO in the assemblage (7.32wt%), though not on par with the Mediterranean Type glasses. It is also possible that this group was manufactured using recycled cullet from the Eastern Mediterranean such as was being transported on the Serçe Limani ship and was mixed with some locally made cullet. Another possibility is the



Figure 34: R.46 blue curved sherd belonging to Cluster 2 group (image taken by author).

inclusion of bone ash as is suggested in the Raqqa Type 4 glass (Henderson et al., 2004: 112), a more thorough investigation of the microstructure using element mapping is necessary to investigate this.

6.4.3 Cluster 4 (C4)

C4 is clearly situated within the Mesopotamian Type 2 glass which exhibits both low alumina and high magnesia. This glass is associated with the glass from Samarra, the colourless glass from Nishapur and the high magnesia Sasanian 2 glass. The plant ash used for these glasses is magnesium rich, though due to the complexity of plant ash glass it cannot be deduced which plants were used, although plants growing near the Tigris and Euphrates rivers have been shown to have been high in magnesium (Tite et al., 2006: 1286). When comparing the Rayy Cluster 4 glass with the glass from Veh Ardašir (Mirti et al. 2009), the dataset also used by Phelps (2017, 2018), it becomes evident that Cluster 4 is more closely related to the Samarra/Nishapur colourless glass than to Sassanian glass. Furthermore, Cluster 4 can be placed within Schibille et al.'s S1/S2 type glass because it has high magnesia and low silica related impurities. Schibille and colleagues (2018: 7) suggest that this glass was produced at Samarra primarily for architectural decoration on the banks of the Tigris and was traded over long distances. This indicates that high quality glasses could have been produced using a centralised model from a specialist factory that may have existed at Samarra or within the vicinity. The mean MnO value for Cluster 4 is 1.14wt%, the Nishapur colourless glass, and the colourless glass from Samarra are also high in MnO demonstrating that they were decolourised using manganese. Further research is required to link the Cluster 4 glasses to Samarra.

It is impossible at this stage to define the Samarra glass industry, Schibille and colleagues (2018: 11) suggest that it was primarily producing architectural glass and references the glass palaces such as of King Solomon detailed in the Quran. The C4 glasses, on the other hand, most clearly seen in R.33 and R.38 (Figure 36a/b), are vessels rather than architectural decoration. This could indicate that they were also producing vessels and exporting them over long distances, however, it is also possible that they were exporting raw glass to be worked in secondary glass workshops that produced vessels. Another possibility is that this high quality colourless architectural glass was recognisable to glassmakers, and it was salvaged from collapsed buildings or stolen and reworked to produce vessels for market.



Figure 35a: (left) R.33 a colourless flat rim sherd, 3mm thick, b: R.38 a colourless elevated rim 0.5mm (images taken by author).

The lack of natron glass present in the assemblage suggests that Byzantine glass was no longer considered a more highly sophisticated glass in favour of a high-quality Islamic glass from specialist sites such as Samarra. It is a possibility that a large portion of the glass under study here was fabricated on the Iranian plateau itself, yet it has also been demonstrated that much glass was traded into the city from all directions, China, Mesopotamia and possibly from the maritime Silk Road, highlighting the bidirectional nature of the trade routes. The lack of context for the glasses is particularly disappointing as a spatial analysis would complement this study, for instance concentrations of these high quality/traded glasses could give evidence for high status areas of occupation.

6.5 Conclusions

This study analysed 36 glass artifacts from Rayy, highlighting their composition and implications for Islamic glassmaking and trade. Most glass samples exhibited typical plant ash glass composition, aligning with Islamic/Mesopotamian tradition, a unique lead glass from China underscores Rayy's role as a commercial hub. The uniformity in glass composition, observed through SEM element maps, suggests effective production processes indicative of specialised knowledge and technology. Black glasses, less homogeneous than colourless ones, reflect lower quality and less specialised techniques. The high variance in Fe_2O_3 levels and moderate silica variance, comparable to Al Raqqa, indicate diverse silica sources and distinct glass recipes.

Overall, the analysis of this assemblage of glass from Rayy offers significant insights into the complex trade and production networks of glass in the Islamic world. The elemental analysis

reveals clear distinctions among the clusters, correlating them with Mesopotamian and Eastern Mediterranean glass types, as well as potential local Iranian production. Cluster C1/3, in particular, aligns with Mesopotamian Type 1 and may indicate a local Iranian production, though further trace element analysis is required to substantiate this theory. Meanwhile, Cluster C2 appears linked to Eastern Mediterranean glass, with compositional similarities suggesting either trade or recycling of Mediterranean cullet. Cluster C4, associated with high-magnesium, low-alumina glass, resonates with the architectural glass from Samarra, underscoring the region's influence and the spread of its high-quality glass.

These findings underscore the bidirectional nature of glass trade across the Islamic world, with raw materials and finished glass goods moving between Mesopotamia, the Iranian Plateau, and possibly beyond via Silk Road routes. Although the lack of precise archaeological context limits interpretations that can be made, the compositional analysis advances our understanding of Rayy's glass production and its connections with neighbouring regions.

6.5.1 Proposals for Further Study

Even lacking trace element and isotopic data this study has shown that glass provenance may be indicated. Though conclusions cannot be proven without trace element data, major element oxides do provide a preliminary idea of what rare earth elements and isotopes to look for and provide a method of breaking up the data into groups making it more manageable for further study. LA-ICP-MS is not a commonplace technique and costs a lot of money which is one of its drawbacks, it may be a quick technique when you are performing the analysis, but finding an available facility and the funding to pay for it is not fast, and certainly not easy. An analysis with British Geological Survey can cost upwards of £1000 per day due to the rise in gas prices stimulated by the Ukrainian war (Julian Henderson, 2024: *personal communication*). Doing a preliminary SEM or XRF study of a glass assemblage is beneficial because it can separate the glass of an assemblage into categories. For instance, to answer investigate Iranian/central Asian glass the C1/3 glasses could be selected for analysis. Similarly, if one wanted to investigate the notion of a luxury Samarra glass industry one might isolate the C4 glasses for further analysis. In this way one can create hypotheses prior to LA-ICP-MS to save time and therefore money when performing the analysis.

Further work that should be done on these glasses is an LA-ICP-MS analysis obtain the Cr/La ratios for the C1/3 group to confirm if they are a local Iranian glass type, or more likely how many can be identified as Mesopotamian imports. Next, to compare them with the very understudied Iranian/Central Asian glass from Nishapur, Rayy, Gorgan and other Iranian sites such as Qom and Hamadan to understand if the production model is as decentralised in the east of the Islamic Empire as it is in the west. These findings will have further implications on the control of technological production in the Islamic Empire in the 10th century. It is unlikely that the picture would stay the same for such a large geographical region unless it was tightly controlled by the Islamic government. Therefore, this information carries large implications about the way in which the area was governed by the Caliphate, particularly because the glass crosses the period known as the Iranian Intermezzo. While Rayy was loyal to Baghdad for the majority of the Islamic Period, it would be interesting to see if this control was as tightly held in terms of technological production as it was in Syria and Iraq. In order to answer these questions, however, one would require trace element data from a series of sites across the Islamic Silk Roads with a stratigraphical context that provides secure dating.

Other promising avenues for further study would be to obtain strontium and neodymium isotopes, isotopic baseline signatures of Sr and Nd isotopes along the Silk Road route across Mesopotamia, Iran and Central Asia have been gathered from environmental and bioarchaeological material. The Sr isotopes reflect the bioavailability of the environment where the plants for the ash flux were grown. Neodymium on the other hand relates to the silica source allowing for the raw materials to be provenanced separately (Lu et al., 2023: 1). A study on the C1/3 group would enable the identification of the raw materials and confirm if the glasses are made locally or imported. Furthermore, a comparison of isotopic data between the C4 glasses and the high quality plant ash glass from Samarra would demonstrate whether the Cluster 4 glass was indeed made at Samarra.

Bibliography

Abdullahi, Y., & Embi, M. R. B. (2013). Evolution of Islamic geometric patterns. *Frontiers of Architectural Research*, 2(2), 243-251.

Agha-Aligol, D., Mousavinia, M., & Fathollahi, V. (2022). Micro-PIXE analysis of early Islamic (10th–11th century AD) glass vessels from the Tape-Bahram historical site in Ray, Iran. *Archaeological and Anthropological Sciences*, 15(1), 1-16.

Aldsworth, F., Haggarty, G., Jennings, S., & Whitehouse, D. (2002). Medieval Glassmaking at Tyre, Lebanon. *Journal of Glass Studies*, 44, 49–66.

Ares, J. D. J., Calderón, N. F., López, I. M., Álvarez-Busto, A. G., & Schibille, N. (2018). Islamic soda-ash glasses in the Christian kingdoms of Asturias and León (Spain). *Journal of Archaeological Science: Reports*, 22, 257-263.

Barkoudah, Y., & Henderson, J. (2006). Plant ashes from Syria and the manufacture of ancient glass: ethnographic and scientific aspects. *Journal of glass studies*, 297-321.

Bass, G. F., & Van Doorninck, F. H. (1978). An 11th century shipwreck at Serçe Limani, Turkey. *International Journal of Nautical Archaeology*, 7(2), 119-132.

Bass, G. F. (1984). The nature of the Serçe Limani glass. *Journal of Glass Studies*, 64-69.

Bennison, A. K. (2009). *The Great Caliphs: The Golden Age of the 'Abbasid Empire*. First Edition. Yale University Press.

Biron, I., & Chopinet, M. H. (2013). Colouring, decolouring and opacifying of glass. (in) *Modern methods for analysing archaeological and historical glass, Volume I*, K. Janssens (Ed.), John Wiley & Sons. 49-65.

Brill, R.H. (1995). Appendix 3: Chemical analyses of some glass fragments from Nishapur in the Corning Museum of Art (in) *Nishapur: Glass of the Early Islamic Period*, Metropolitan Museum of Art, Kröger, J. (Ed.), New York. 211-233.

- Brill, R. H. (2009). Part XIII: The Chemistry of the Glass (in). Serçe Limani, *Vol 2: The Glass of an Eleventh-Century Shipwreck*. Bass, G. F., Lledo, B., Matthews, S., Brill, R. H. (Eds.) United States: Texas A&M University Press. 457-497.
- Brill, R.H. & Stapleton, C.P. (2012). *Chemical Analyses of Early Glasses Volume 3*, Corning Museum of Glass, Corning, New York.
- Bosworth, E.C. (2012) Gorgan vi. History From the Rise of Islam To the Beginning Of the Safavid Period, *Encyclopaedia Iranica*, XI/2, 153-154, available online at <http://www.iranicaonline.org/articles/gorgan-vi> (accessed on 02 February 2024).
- Carboni, S., Lacerenza, G., & Whitehouse, D. (2003). Glassmaking in Medieval Tyre: The Written Evidence. *Journal of Glass Studies*, 45, 139–149.
- Dodds, J. D. (1992). *al-Andalus: the art of Islamic Spain*. Metropolitan Museum of Art.
- Donner, F. (2008). Islamic Conquests (in) *A Companion to the History of the Middle East*, Youssef M (Ed.) Choueiri, Wiley. 29-52.
- Fernández-Navarro, J. and Villegas, M. (2013). What is Glass?: An Introduction to the Physics and Chemistry of Silicate Glasses. (in) *Modern methods for analysing archaeological and historical glass, Volume I*, K. Janssens (Ed.), John Wiley & Sons. 1-22.
- Frahm, E. (2014). Scanning electron microscopy (SEM): Applications in archaeology. *Encyclopedia of global archaeology*, 6487-6495.
- Freestone, I. C., & Gorin-Rosen, Y. (1999). The Great Glass Slab at Bet She'arim, Israel: An Early Islamic Glassmaking Experiment? *Journal of Glass Studies*, 41, 105–116.
- Freestone, I. C., Gorin-Rosen, Y., & Hughes, M. J. (2000). Primary glass from Israel and the production of glass in late antiquity and the early Islamic period. *MOM Éditions*, 33(1), 65-83.
- Freestone, I. C. (2002). Composition and Affinities of Glass from the Furnaces on the Island Site, Tyre. *Journal of Glass Studies*, 44, 67–77.
- Freestone, I.C., (2006). Glass production in Late Antiquity and the Early Islamic period. a geochemical perspective, Geological Society, London, Special Publications 257(1), 201–16.

- Freestone, I. C., Wolf, S., & Thirlwall, M. (2009). Isotopic composition of glass from the Levant and south-eastern Mediterranean Region. *Isotopes in vitreous materials, 1*, 31.
- Freestone, I. C. (2015). The Recycling and Reuse of Roman Glass: Analytical Approaches. *Journal of Glass Studies, 57*, 29–40.
- Freestone, I. C. (2021). Glass production in the first millennium CE: A compositional perspective. (in) *Vom Künstlichen Stein zum durchsichtigen Massenprodukt/from Artificial Stone to Translucent Mass-Product*, (Eds.) Klimscha, F., Karlsen H.J., Hansen, S. & Renn, J. 67, 245-263.
- Gan, F. (2021). *Development history of ancient Chinese glass technology* (Vol. 3). World Scientific.
- Ganio, M., Boyen, S., Brems, D., Scott, R., Foy, D., Latruwe, K., ... & Degryse, P. (2012). Trade routes across the Mediterranean: a Sr/Nd isotopic investigation on Roman colourless glass. *Glass Technology-European Journal of Glass Science and Technology Part A, 53*(5), 217-224.
- Gorin-Rosen, Y. (2015). *Ancient Raw Glass Production in Israel: First Century BCE to Eighth Century CE*. PhD Thesis University of Haifa (Israel).
- Graf, D. F. (2018). The Silk Road between Syria and China. (in) *Trade, commerce, and the state in the Roman world*, Wilson, A & Bowman, A (Eds.) Oxford: Oxford University Press. 443-532.
- Gratuze, B. (2013). Glass Characterisation Using Laser Ablation Inductively Coupled Plasma Mass Spectrometry Methods. (in) *Modern methods for analysing archaeological and historical glass* (Vol. 1) Janssens, K. H. (Ed.). John Wiley & Sons. 201-234.
- Hansen, V. (2012). *The Silk Road*. Oxford University Press, USA.
- Hawting, G.R. (2008). The Rise of Islam. (in) *A Companion to the History of the Middle East*, Choueiri, Y.M. (Ed.) Wiley, 9-28.
- Hedenstierna-Jonson, C. (2020). With Asia as Neighbour: Archaeological evidence of contacts between Scandinavia and Central Asia (in) *The Viking Age and the Tang Dynasty*. Bulletin of the Museum of Far Eastern Antiquities, 81, Stockholm. 43-64.

Henderson, J. (1999). Archaeological and Scientific Evidence for the Production of Early Islamic Glass in al-Raqqa, Syria. *Levant (London)*, 31(1), 225–240.

Henderson, J. (2003). Glass trade and chemical analysis: a possible model for Islamic glass production. In *Echanges et commerce du verre dans le monde antique (Actes du colloque de l'AFAV, Aix-en-Provence et Marseille, 7–9 juin 2001)*. 109-123.

Henderson, J., McLoughlin, S. D., & McPhail, D. S. (2004). Radical changes in Islamic glass technology: evidence for conservatism and experimentation with new glass recipes from early and middle Islamic Raqqa, Syria. *Archaeometry*, 46(3), 439-468.

Henderson, J., Challis, K., O'Hara, S. McLoughlin, S. Gardner, A., Priestnall, G. (2005). Experiment and innovation: early Islamic industry at al-Raqqa, Syria. *Antiquity*, 79(303). 130-145.

Henderson, J. (2013). *Ancient Glass: An Interdisciplinary Exploration*. Cambridge University Press.

Henderson, J., Chenery, S., Faber, E., Kröger, J. (2016) 'The Use of Electron Probe Microanalysis and Laser Ablation-Inductively Coupled Plasma-Mass Spectrometry for the Investigation of 8th–14th Century Plant Ash Glasses from the Middle East'. *Microchemical Journal*, 128. 134-152.

Henderson, J., Ma, H., & Evans, J. (2020). Glass Production for the Silk Road? Provenance and Trade of Islamic Glasses Using Isotopic and Chemical Analyses in a Geological Context. *Journal of Archaeological Science*, 119, 105164.

Henderson, J., Chenery, S., Faber, E. W., & Kröger, J. (2021). Political and Technological Changes, glass provenance and a new glass production model along the west Asian Silk Road. (in) *From Artificial Stone to Transparent Mass Product: innovations in glass technology and their social consequences between the Bronze Age and antiquity*. Berlin Studies of the Ancient World (67). Topoi. 119-143

Herrington, C. R. (1985). Quantitative EDS and WDS X-ray microanalysis of semiconductor materials: Principles and comparisons. *Journal of electron microscopy technique*, 2(5), 471-479.

- Herzig, E., & Stewart, S. (2011). *Early Islamic Iran*. Bloomsbury Publishing.
- Helwing, B. (2012). The Iranian Plateau. (in) *A companion to the archaeology of the ancient Near East*, (Ed.) Potts, D.T. Wiley. 501-511.
- Hodgkinson, A. K., Röhrs, S., Müller, K., & Reiche, I. (2019). The use of Cobalt in 18th Dynasty Blue Glass from Amarna: the results from an on-site analysis using portable XRF technology. *STAR: Science & Technology of Archaeological Research*, 5(2), 36-52.
- Holakooei, P. (2016). A Mediaeval Persian Treatise on Coloured and Enamelled Glass: Bayan Al-Sana'at. *Iran*, 54(2), 95-106.
- Janssens, K. H. (2013). Electron Microscopy. (in) *Modern methods for analysing archaeological and historical glass* (Vol. 1) Janssens, K. H. (Ed.). John Wiley & Sons. 129-154.
- Kaviani, R., Salehi, N., Ibrahim, A. Z. B., Nor, M. R. M., Hamid, F. A. F. A., Hamzah, N. H., & Yusof, A. (2012). The Significance of the Bayt al-Hikma (House of Wisdom) in The Early Abbasid Caliphate (132A.H-218A.H). *Middle-East Journal of Scientific Research*, 11(9), 1272-1277.
- Keall, E.J. (1979). The Topography and Architecture of Medieval Rayy, (in) *Akten des VII. Internationalen Kongresses für Iranische Kunst und Archäologie München, 7–10 September 1976* (Archäologische Mitteilungen aus Iran, Ergänzungsband 6), Berlin. 537–543.
- Kennedy, H. (2008). The Caliphate. (in) *A Companion to the History of the Middle East*, (Ed.) Choueiri, Y.M. Wiley, 52-69.
- Kennedy, H. (2016). *The Prophet and the Age of the Caliphates: The Islamic Near East from the 6th to the 11th Century* (Third ed.). Abingdon, Oxon and New York: Routledge.
- Kraemer, J. L. (1986). Setting the Stage: The Early Buyid Era. (in) *Humanism in the Renaissance of Islam* Brill. 31-102.
- Kristiansen, K. (2008). 6 Scanning Electron Microscope with Energy-and Wavelength-Dispersive Spectrometry. (in) *Surface Characterization: A User's Sourcebook*. (Eds.) Brune, D., Harry J., Whitlow, O.H & Ragnar, H. Germany: Wiley. 111-129.
- Kröger, J. (1995). *Nishapur: glass of the early Islamic period*. Metropolitan Museum of Art.
- Liu, X. (2010). *The Silk Road in world history*. Oxford: Oxford University Press.

Liu, S., Li, Q. H., Gan, F., Zhang, P., & Lankton, J. W. (2012). Silk Road Glass in Xinjiang, China: chemical compositional analysis and interpretation using a high-resolution portable XRF spectrometer. *Journal of Archaeological Science*, 39(7), 2128-2142.

Lü, Q. Q., Henderson, J., Wang, Y., & Wang, B. (2021). Natron Glass Beads Reveal Proto-Silk Road Between the Mediterranean and China in the 1st Millennium BCE. *Scientific Reports*, 11(1), 3537.

Lü, Q. Q., Basafa, H., & Henderson, J. (2023). Connected in Diversity: Isotopic analysis refines provenance for Islamic plant-ash glass from the eastern Silk Roads. *Iscience*, 26(12).

Madelung, W. (1997). *The succession to Muḥammad: a study of the early Caliphate*. Cambridge: Cambridge University Press.

Meyer, C., & Dussubieux, L. (2022). Emerald-Green Glass from Aqaba. *Journal of Glass Studies*, 64, 85–104.

Mirti, P. Pace, M, Negro Ponzi, M.M & Aceto, M. (2008). ICP–MS analysis of glass fragments of Parthian and Sasanian epoch from Seleucia and Veh Ardašīr (central Iraq) *Archaeometry*, 50. 429-450.

Mirti, P. Pace, M. Malandrino, M & Negro Ponzi, M. (2009). Sasanian Glass from Veh Ardašīr: new evidences by ICP-MS analysis *Journal of Archaeological Science*, 36. 1061-1069.

Minorsky, V. (1994). ‘Rayy’, in *Encyclopédie de l’Islam*, 2nd ed. 8, Leiden. 487–89.

Miles, G. (1938). *The Numismatic History of Rayy*, New York.

Myrdal, Eva. (2020). Editor’s Preface (in) *Asia and Scandinavia: New perspectives on the Early Medieval Silk Roads*. The Museum of Far Eastern Antiquities Bulletin No 81. Stockholm. 5-23.

- Nenna, M. D. (2015). Primary glass workshops in Graeco-Roman Egypt: preliminary report on the excavations of the site of Beni Salama, Wadi Natrun (2003, 2005-9). (in) *Glass of the Roman World*. (Eds.) Jackson, C., Freestone, I. & Bayley, J. Oxford: Oxbow Books, 1-22.
- Northedge A. (2007). *The Historical Topography of Samarra: Samarra Studies I*. London: British School of Archaeology in Iraq.
- Nicholson, P. T., & Jackson, C. M. (2000). Tell el-Amarna and the Glassmakers' Workshop of the Second Millenium BC. *MOM Éditions*, 33(1), 11-21.
- Nicholson, P.T. (2009). Faience Technology. *UCLA encyclopedia of Egyptology*, 1(1).
- Petrie, W. M. F. (1894). *Tell el-Amarna*. Cambridge University Press.
- Phelps, M. (2017). *An Investigation into Technological Change and Organisational Developments in Glass Production between the Byzantine and Early Islamic Periods (7th–12th Centuries) Focussing on Evidence from Israel*. PhD thesis, University of London.
- Phelps, M. (2018). Glass supply and trade in early Islamic Ramla: an investigation of the plant ash glass. *Things that travelled: Mediterranean glass in the first millennium CE*, 236-282.
- Rante, R. (2007). The Topography of Rayy during the early Islamic period. *Iran*, 45(1), 161-180.
- R. Rante (2008) The Iranian City of Rayy: Urban Model and Military Architecture, *Iran*, 46(1), 189-211.
- Rante, R. (2015). *Rayy: from its Origins to the Mongol Invasion*. Brill.
- Rante, R., & Di Pasquale, C. (2016). The Urbanisation of Rayy in the Seljūq Period. *Der Islam*, 93(2), 413-432.
- Reddy, C. K., & Vinzamuri, B. (2018). A survey of partitional and hierarchical clustering algorithms. In *Data clustering*. (Eds.) Reddy, C.K & Aggarwal, C.C. Chapman and Hall CRC. 87-110
- Rehren, T. (2024). Glass: Primary Production. (in) *Encyclopedia of Archaeology, 2nd edition*, Volume 2. (Eds.) Voyakin, D., Efthymia, N. & Rehren, T. Elsevier, 554-558.

- Robertshaw, P., Benco, N., Wood, M., Dussubieux, L., Melchiorre, E., & Ettahiri, A. (2010). Chemical analysis of glass beads from medieval Al-basra (Morocco). *Archaeometry*, 52(3), 355-379.
- Romgard, J. (2016). Did the Vikings trade with China?: on a controversial passage in Ibn Khordāhbeh's Book of itineraries and kingdoms. *Fornvännen*, 111(4), 229-242.
- Saadati, M., Neyestani, J., Kouphar, S. M. M., & Nobari, A. H. (2021). Review and Analysis of the Spatial Structure of Seljuk Cities in Iran, Case Study: City of Rey. *TUBA-AR: Turkish Academy of Sciences, Journal of Archaeology*, 28(28), 211-224.
- Salehvand, N., Agha-Aligol, D., Shishegar, A., & Racht, M. L. (2020). The Study of Chemical Composition of Persian Glass Vessels of the Early Islamic Centuries (10th– 11th c. AD) by Micro-PIXE; Case Study: Islamic collection in the National Museum of Iran. *Journal of Archaeological Science: Reports*, 29, 102034.
- Sayre, E.V. and Smith, R.W. (1974). Analytical Studies of Ancient Egyptian Glass (in) *Recent Advances in the Science and Technology of Materials vol. 3*. A. Bishay (Ed.), New York. 47–70.
- Schibille, N., Meek, A., Wypyski, M. T., Kröger, J., Rosser-Owen, M., & Wade Haddon, R. (2018). The Glass Walls of Samarra (Iraq): Ninth-century Abbasid glass production and imports. *PLoS One*, 13(8), 1-15.
- Schibille, N., Lankton, J. W., & Gratuze, B. (2022). Compositions of Early Islamic Glass Along the Iranian Silk Road. *Geochemistry*, 82(4), 125903. 1-11.
- Schibille, N. (2022). *Islamic glass in the making: chronological and geographical dimensions*. Leuven University Press.
- Schmidt, E.F. (1935) "The Persian Expedition," *Bulletin of the Museum of Fine Arts* 33, Boston, 56.
- Scott, R. B., Neyt, B., Brems, D., Eekelers, K., Shortland, A. J., & Degryse, P. (2017). Experimental Mixing of Natron and Plant Ash Style Glass: implications for ancient glass recycling. *Glass Technology-European Journal of Glass Science and Technology Part A*, 58(1), 8-16.

- Shortland, A., Schachner, L., Freestone, I., & Tite, M. (2006). Natron as a Flux in the Early Vitreous Materials Industry: sources, beginnings and reasons for decline. *Journal of Archaeological Science*, 33(4), 521-530.
- Shortland, A., Rogers, N., & Eremin, K. (2007). Trace element discriminants between Egyptian and Mesopotamian late Bronze Age glasses. *Journal of Archaeological Science*, 34(5), 781-789.
- Shortland, A. (2009). Glass production. *UCLA Encyclopedia of Egyptology*, 1(1).
- Simpson, S. J., & Curtis, J. (2000). Mesopotamia in the Sasanian Period: Settlement patterns, arts and crafts. *Mesopotamia and Iran in the Parthian and Sasanian periods: rejection and revival c. 238*, (Ed.) Curtis, J. Cambridge University Press. 57-80.
- Shugar, A., & Rehren, T. (2002). Formation and Composition of Glass as a Function of Firing Temperature. *Glass Technology*, 43, 145-150.
- Sode, T., & Kock, J. (2001). Traditional Raw Glass Production in Northern India: the final stage of an ancient technology. *Journal of Glass Studies*, 43, 155-169.
- Swann, C.M. *et al.* (2017) 'Compositional observations for Islamic Glass from Sīrāf, Iran, in the Corning Museum of Glass collection', *Journal of archaeological science, reports*, 16, pp. 102–116.
- Tamura, T., & Oga, K. (2016). Archaeometrical Investigation of Natron Glass Excavated in Japan. *Microchemical Journal*, 126, 7-17.
- Tite, M. S., Shortland, A., Maniatis, Y., Kavoussanaki, D., & Harris, S. A. (2006). The Composition of the Soda-Rich and Mixed Alkali Plant Ashes Used in the Production of Glass. *Journal of Archaeological Science*, 33(9), 1284-1292.
- Tor, D. G. (2016). Rayy and the Religious History of the Seljūq Period. *Der Islam (Berlin)*, 93(2), 374–402.
- von Folsach, K. (1993). Three Islamic Molds. *Journal of Glass Studies*, 35, 149–153.

- Waugh, D. C. (2007). Richthofen's 'Silk Roads': Toward the archaeology of a concept. *The Silk Road*, 5(1), 1-10.
- Whitehouse, D. (2002). *The Houses of Siraf, Iran*. (in) *Patterns of Everyday Life*. (Ed.) Waines, D. United Kingdom: Taylor & Francis. 35-43.
- Whitfield, S. (2007). Was There a Silk Road? *Asian Medicine*, 3(2), 201-213.
- Wilkinson, T. J. Omrani Rekavandi, H., Hopper, K., Priestman, S., Roustaei, K. & Galiatsatos, N. (2013). *Persia's imperial power in late antiquity: the Great Wall of Gorgān and the frontier landscapes of Sasanian Iran; a joint fieldwork project by the Iranian Cultural Heritage, Handcraft and Tourism Organization, the Iranian Center for Archaeological Research and the Universities of Edinburgh and Durham (2005-2009)* *Qudrat-i imparāṭūrī-i Īrān dar awāḥir-i daurān-i bāstān: dīwār-i buzurg-i Gurgān wa čāšm-andāz-i marzī-i Īrān dar दौरā-i sāsānī* (Vol. 2). (Ed.) Sauer, E. W. Oxbow Books.
- Williams, T. (2015). Mapping the Silk Roads. *The Silk Road: interwoven history*, 1.
- Wypyski, M. T. (2015). Chemical Analysis of Early Islamic Glass from Nishapur. *Journal of Glass Studies*, 121-136.
- Zaimeche, S. (2005). Ravy (Rayy). *Foundation for Science Technology and Innovation*. 1-9.

Appendix 1: A Catalogue of the Rayy Glass.

| Sample Number | Date | Type | Colour | Thickness | Image |
|---------------|---------|----------------------|--------------------|-----------|---|
| R01 | 10th C. | Indiscernible | Green | 0.5mm |  |
| R02 | 10th C. | Body fragment | Colourless | 0.3mm |  |
| R04 | 10th C. | Plate rim? | Black/Grey? | 1.3mm |  |
| R05 | 10th C. | Body fragment | Colourless | 0.4mm |  |
| R09 | 10th C. | Body fragment | Cobalt Blue | 0.6mm |  |
| R10 | 10th C. | Plate rim | Translucent Yellow | 2mm |  |
| R11 | 10th C. | Rim | Aqua | 0.4mm |  |
| R12 | 10th C. | Rim | Colourless | 0.2mm |  |
| R13 | 10th C. | Body fragment | Aqua | 0.2mm |  |
| R15 | 10th C. | Body fragment? | Colourless | 0.3mm |  |
| R16 | 10th C. | Body fragment | Blue | 0.5mm |  |
| R17 | 10th C. | Rim | Colourless | 0.8mm |  |
| R18 | 10th C. | Indiscernible | Colourless | 0.5mm |  |
| R19 | 10th C. | Indiscernible | Colourless | 0.7mm |  |
| R20 | 10th C. | Rim | Aqua | 0.4mm |  |
| R22 | 10th C. | Body sherd | Colourless | 0.9mm |  |
| R25 | 10th C. | Indiscernible | Colourless | 0.8-2mm |  |
| R26 | 10th C. | Rim | Blue | 2.4mm |  |
| R27 | 10th C. | Body fragment | Blue | 0.3mm |  |
| R28 | 10th C. | Indiscernible | Green | 4mm |  |
| R30 | 10th C. | Indiscernible | Yellow | 1.9-0.6mm |  |
| R32 | 10th C. | Indiscernible | Green | 0.9mm |  |
| R33 | 10th C. | Rim | Colourless | 3mm |  |
| R34 | 10th C. | Body fragment | Blue | 0.6mm |  |
| R37 | 10th C. | Body fragment | Translucent/yellow | 1.7-1.2mm |  |
| R38 | 10th C. | Rim | Colourless | 0.5mm |  |
| R39 | 10th C. | Rim | Aqua | 0.5mm |  |
| R41 | 10th C. | Body fragment | Aqua | 1.8-1.4mm |  |
| R42 | 10th C. | Body fragment | Aqua | 0.3mm |  |
| R42/2 | 10th C. | Rim | Aqua | 1.6mm |  |
| R43 | 10th C. | Indiscernible | Colourless? | 0.1mm |  |
| R45 | 10th C. | Indiscernible | Blue | 0.4mm |  |
| R46 | 10th C. | Body fragment | Blue | 0.2mm |  |
| R47 | 10th C. | Body fragment | Aqua | 0.5mm |  |
| R48 | 10th C. | Indiscernible | Green | 1.6mm |  |
| R49 | 10th C. | Base sherd? | Blue | 2.1mm |  |
| R50 | 10th C. | Indiscernible | Green | 0.5mm |  |
| R51 | 10th C. | Indiscernible | Aqua | 0.7mm |  |
| R53 | 10th C. | Indiscernible | Black | 2mm |  |
| R54 | 10th C. | Cylindrical fragment | Black | 2.6mm |  |
| R55 | 10th C. | Indiscernible | Aqua? | 1.8mm |  |
| R56 | 10th C. | Cylindrical fragment | Aqua | 1.9mm |  |
| R57 | 10th C. | Indiscernible | Black | 2.3mm |  |

Appendix 2: Table Comprising all Data Considered

| Site | Colour | Na 2O | M g O | Al 2O 3 | Si O 2 | K 2 O | Ca O | Ti O 2 | M n O | Fe 2O 3 | Pb O | Citati on | MgO /CaO | MgO /K2O |
|--------------|------------|---------------|-------------|---------------|---------------|--------------|----------|--------------|-------------|---------------|-----------|--------------|-------------|-------------|
| Rayy | Green Tr | 15 .0 8 | 3. 49 | 2.8 | 63 .1 6 | 3. 0 5 | 6. 47 | 0. 23 | 1. 17 | 1.1 5 | 0 | Auth or | 0.54 | 1.14 |
| Rayy (AH) | Colourless | 15 .3 3 | 2. 49 | 4.1 3 | 65 .3 7 | 3. 2 | 6. 47 | 0. 28 | 0. 1 | 1.5 5 | 0 | Auth or | 0.38 | 0.78 |
| Rayy (AH) | Colourless | 14 .3 2 | 4. 43 | 2.0 7 | 65 .5 1 | 3. 0 4 | 6. 56 | 0. 2 | 1. 75 | 0.9 9 | 0 | Auth or | 0.68 | 1.46 |
| Rayy (AH) | Colourless | 16 .1 3 | 3. 89 | 3.0 3 | 64 .5 4 | 3. 0 9 | 5. 94 | 0. 23 | 1. 02 | 1.0 6 | 0 | Auth or | 0.65 | 1.26 |
| Rayy (AH) | Blue Co | 14 .1 8 | 2. 94 | 2.1 7 | 67 .0 8 | 2. 1 3 | 6. 29 | 0. 18 | 0. 33 | 2.6 4 | 0 | Auth or | 0.47 | 1.38 |
| Rayy (AH) | Colourless | 14 .7 | 6. 24 | 1.3 2 | 66 .5 5 | 3. 0 7 | 5. 27 | 0. 12 | 1. 31 | 0.3 | 0 | Auth or | 1.18 | 2.03 |
| Rayy (AH) | Green Tr | 15 .6 8 | 3. 9 | 3.1 1 | 64 .5 9 | 3. 0 9 | 5. 94 | 0. 23 | 1. 02 | 1.0 6 | 0 | Auth or | 0.66 | 1.26 |
| Rayy (AH) | Colourless | 14 .0 8 | 5. 49 | 1.6 3 | 68 .2 1 | 2. 2 3 | 4. 44 | 0. 12 | 2. 22 | 0.5 7 | 0 | Auth or | 1.24 | 2.46 |
| Rayy (AH) | Green | 13 .1 9 | 2. 65 | 1.7 5 | 66 .9 7 | 1. 9 4 | 8. 35 | 0. 06 | 0. 46 | 2.6 9 | 0 | Auth or | 0.32 | 1.37 |
| Rayy (AH) | Colourless | 17 .1 2 | 2. 95 | 4.0 3 | 63 .5 3 | 2. 5 3 | 5. 95 | 0. 34 | 0. 78 | 1.1 2 | 0 | Auth or | 0.50 | 1.17 |
| Rayy (AH) | Colourless | 15 .5 | 4. 03 | 3.0 5 | 64 .8 8 | 2. 9 7 | 6 | 0. 29 | 0. 84 | 1.1 | 0 | Auth or | 0.67 | 1.36 |
| Rayy (AH) | Blue Co | 14 .2 2 | 5. 55 | 1.5 3 | 68 .4 8 | 2. 2 6 | 4. 44 | 0. 14 | 2. 12 | 0.4 6 | 0 | Auth or | 1.25 | 2.46 |
| Rayy (AH) | Colourless | 13 .9 4 | 5. 44 | 1.5 5 | 68 .7 9 | 2. 3 4 | 4. 43 | 0. 05 | 1. 98 | 0.5 1 | 0 | Auth or | 1.23 | 2.32 |
| Rayy (AH) | Blue Co | 16 .4 8 | 3. 08 | 2.5 3 | 63 .9 8 | 3. 6 8 | 5. 71 | 0. 15 | 0. 84 | 0.8 2 | 0 | Auth or | 0.54 | 0.84 |
| Rayy (AH) | Colourless | 15 .2 9 | 3. 23 | 2.4 8 | 63 .1 5 | 2. 4 9 | 8. 98 | 0. 28 | 2. 29 | 0.9 4 | 0 | Auth or | 0.36 | 1.30 |
| Rayy (AH) | Green Tr | 0 | 0 | 0 | 26 .0 9 | 0 | 0 | 0 | 0 | 0 | 73. 32 | Auth or | 0.00 | 0.00 |
| Rayy (AH) | Yellow | 13 .0 6 | 5. 27 | 1.0 5 | 69 .3 9 | 2. 5 6 | 7. 26 | 0. 07 | 0. 44 | 0.2 3 | 0 | Auth or | 0.73 | 2.06 |
| Rayy (AH) | Green Tr | 17 .3 7 | 3. 07 | 2.5 6 | 63 .9 3 | 3. 4 8 | 5. 9 | 0. 29 | 1. 02 | 0.8 8 | 0 | Auth or | 0.52 | 0.88 |
| Rayy (AH) | Colourless | 12 .9 1 | 5. 28 | 1.0 2 | 69 .4 9 | 2. 7 1 | 7. 19 | 0 | 0. 31 | 0.4 1 | 0 | Auth or | 0.73 | 1.95 |
| Rayy (AH) | Green Tr | 13 .0 4 | 5. 28 | 1.0 5 | 69 .5 8 | 2. 5 7 | 7. 3 | 0 | 0. 44 | 0 | 0 | Auth or | 0.72 | 2.05 |

| | | | | | | | | | | | | | | |
|-----------|------------|-------|------|------|-------|------|------|------|------|------|---|-----------------------|------|------|
| Rayy (AH) | Yellow | 15.97 | 4.02 | 3.22 | 64.58 | 3.09 | 6.15 | 0.35 | 0.83 | 1.06 | 0 | Author | 0.65 | 1.30 |
| Rayy (AH) | Colourless | 14.05 | 7.1 | 1.13 | 67.94 | 3.65 | 4.92 | 0.2 | 0.29 | 0.19 | 0 | Author | 1.44 | 1.95 |
| Rayy (AH) | Blue Co | 16.13 | 3.46 | 3.19 | 63.54 | 3.53 | 7.08 | 0.4 | 0.15 | 1.34 | 0 | Author | 0.49 | 0.98 |
| Rayy (AH) | Blue Co | 16.46 | 3.25 | 3.33 | 63.62 | 3.81 | 7.13 | 0.31 | 0.25 | 1.12 | 0 | Author | 0.46 | 0.85 |
| Rayy (AH) | Colourless | 16.44 | 3.43 | 3.4 | 63.67 | 3.79 | 6.98 | 0.21 | 0.23 | 1.19 | 0 | Author | 0.49 | 0.91 |
| Rayy (AH) | Blue Co | 15.04 | 2.8 | 1.44 | 65.69 | 1.98 | 8.6 | 0 | 0.27 | 2.9 | 0 | Author | 0.33 | 1.41 |
| Rayy (AH) | Blue Co | 14.21 | 3.01 | 1.67 | 67.13 | 2.66 | 6.8 | 0.12 | 0.84 | 2.27 | 0 | Author | 0.44 | 1.16 |
| Rayy (AH) | Colourless | 15.91 | 3.62 | 3.22 | 65.33 | 2.99 | 5.99 | 0.17 | 0.84 | 1.24 | 0 | Author | 0.60 | 1.25 |
| Rayy (AH) | Green Tr | 17.75 | 3.27 | 4.82 | 61.07 | 2.97 | 5.4 | 0.32 | 0.07 | 2.2 | 0 | Author | 0.61 | 1.10 |
| Rayy (AH) | Blue Co | 18.37 | 2.99 | 3.43 | 63.25 | 3.45 | 5.81 | 0.2 | 0.43 | 1.4 | 0 | Author | 0.51 | 0.87 |
| Rayy (AH) | Green Tr | 16.74 | 3.65 | 3.44 | 64.41 | 3.35 | 6.28 | 0.26 | 0.34 | 1.07 | 0 | Author | 0.58 | 1.09 |
| Rayy (AH) | Colourless | 18.01 | 3.36 | 3.57 | 64.42 | 2.53 | 6.14 | 0.22 | 0.07 | 1.37 | 0 | Author | 0.55 | 1.33 |
| Rayy (AH) | Black | 18.16 | 3.76 | 2.8 | 63.45 | 3.21 | 6.8 | 0.17 | 0.06 | 0.91 | 0 | Author | 0.55 | 1.17 |
| Rayy (AH) | Black | 17.3 | 2.66 | 4.11 | 61.51 | 5.78 | 6.7 | 0.21 | 0.11 | 1.08 | 0 | Author | 0.40 | 0.46 |
| Rayy (AH) | Black | 17.67 | 2.67 | 4.22 | 60.85 | 5.78 | 6.7 | 0.21 | 0.12 | 1.1 | 0 | Author | 0.40 | 0.46 |
| Rayy | Blue Co | 16.7 | 3.41 | 2.74 | 64.2 | 3.48 | 6.67 | 0.13 | 0.05 | 1.15 | 0 | Schibille | 0.51 | 0.98 |
| Rayy | Black | 15.5 | 3.8 | 2.11 | 63.6 | 2.56 | 6 | 0.09 | 0.91 | 4.24 | 0 | Schibille | 0.63 | 1.48 |
| Rayy | Black | 17 | 3.49 | 3.23 | 62.2 | 3.96 | 6.99 | 0.15 | 0.18 | 1.25 | 0 | Schibille et al. 2022 | 0.50 | 0.88 |
| Rayy | Green | 17 | 2.99 | 5.15 | 58.6 | 3.12 | 7.4 | 0.23 | 0.11 | 2.16 | 0 | Schibille et al. 2022 | 0.40 | 0.96 |
| Rayy | Green | 16.9 | 3 | 5.45 | 59.4 | 3.07 | 6.53 | 0.24 | 0.1 | 2.16 | 0 | Schibille et al. 2022 | 0.46 | 0.98 |

| | | | | | | | | | | | | | | |
|----------|------------|------|------|------|------|------|------|------|------|------|---|-----------------------|------|------|
| Rayy | Green | 16.5 | 2.99 | 5.46 | 59.7 | 3.09 | 6.72 | 0.24 | 0.01 | 2.23 | 0 | Schibille et al. 2022 | 0.44 | 0.97 |
| Rayy | Green | 17 | 3.02 | 5.43 | 59.3 | 3.08 | 6.63 | 0.24 | 0.09 | 2.18 | 0 | Schibille et al. 2022 | 0.46 | 0.98 |
| Rayy | Blue Tr | 16.2 | 4.23 | 3.77 | 64 | 2.24 | 5.81 | 0.02 | 0.17 | 1.85 | 0 | Schibille et al. 2022 | 0.73 | 1.89 |
| Rayy | Colourless | 17.9 | 2.67 | 3.54 | 64.2 | 3.98 | 4.3 | 0.15 | 0.71 | 1 | 0 | Schibille et al. 2022 | 0.62 | 0.67 |
| Rayy | Green | 16.6 | 2.84 | 5.01 | 60.6 | 3.02 | 6.29 | 0.23 | 0.01 | 2.23 | 0 | Schibille et al. 2022 | 0.45 | 0.94 |
| Rayy | Blue Co | 13.5 | 3.33 | 2.92 | 67.2 | 1.87 | 7.72 | 0.22 | 0.06 | 1.91 | 0 | Schibille et al. 2022 | 0.43 | 1.78 |
| Rayy | Aqua | 15.7 | 3.83 | 2.19 | 64.7 | 3.18 | 7.96 | 0.09 | 0.01 | 0.98 | 0 | Schibille et al. 2022 | 0.48 | 1.20 |
| Rayy | Aqua | 15.3 | 3.88 | 2.3 | 64.5 | 3.22 | 8.26 | 0.01 | 0.09 | 0.99 | 0 | Schibille et al. 2022 | 0.47 | 1.20 |
| Rayy | Yellow | 17.2 | 1.6 | 2.89 | 66.8 | 3.29 | 3.53 | 0.17 | 2.04 | 0.91 | 0 | Schibille et al. 2022 | 0.45 | 0.49 |
| Rayy | Aqua | 15.1 | 3.64 | 2.23 | 66 | 3.07 | 7.62 | 0.09 | 0.01 | 0.97 | 0 | Schibille et al. 2022 | 0.48 | 1.19 |
| Rayy | Aqua | 18.5 | 3.93 | 3.12 | 61.7 | 2.91 | 6.68 | 0.13 | 0.31 | 1.01 | 0 | Schibille et al. 2022 | 0.59 | 1.35 |
| Rayy | Blue Tr | 15 | 3.93 | 3.01 | 64.7 | 2.85 | 7.12 | 0.13 | 0.78 | 1.14 | 0 | Schibille et al. 2022 | 0.55 | 1.38 |
| Rayy | Colourless | 15.4 | 4.95 | 1.49 | 67.8 | 2.58 | 4.68 | 0.07 | 1.72 | 0.38 | 0 | Schibille et al. 2022 | 1.06 | 1.92 |
| Rayy | Colourless | 15.7 | 4.79 | 1.35 | 68 | 2.62 | 4.42 | 0.07 | 1.71 | 0.4 | 0 | Schibille et al. 2022 | 1.08 | 1.83 |
| Rayy | Colourless | 13.7 | 2.51 | 0.86 | 71.3 | 0.99 | 8.03 | 0.07 | 0.03 | 0.59 | 0 | Schibille et al. 2022 | 0.31 | 2.54 |
| Nishapur | Green Tr | 13.1 | 4.79 | 1.67 | 65.1 | 3.73 | 8.34 | 0.06 | 0.91 | 1.07 | 0 | Schibille et al. 2022 | 0.57 | 1.28 |

| | | | | | | | | | | | | | | |
|----------|------------|------|------|------|------|------|------|------|------|------|---|-----------------------|------|------|
| Nishapur | Blue | 16.9 | 2.75 | 1.95 | 66.7 | 2.34 | 5.3 | 0.15 | 1.41 | 0.98 | 0 | Schibille et al. 2022 | 0.52 | 1.18 |
| Nishapur | Aqua | 15.6 | 3.96 | 3.52 | 65.1 | 2.85 | 6.6 | 0.19 | 0.05 | 1.1 | 0 | Schibille et al. 2022 | 0.60 | 1.39 |
| Nishapur | Green | 15.2 | 3.85 | 3.66 | 65.3 | 2.85 | 6.76 | 0.19 | 0.06 | 1.14 | 0 | Schibille et al. 2022 | 0.57 | 1.35 |
| Nishapur | Green/Blue | 15.3 | 3.25 | 3.4 | 64.6 | 2.83 | 8.05 | 0.17 | 0.06 | 0.97 | 0 | Schibille et al. 2022 | 0.40 | 1.15 |
| Nishapur | Blue Co | 17.2 | 3.57 | 4.21 | 59.3 | 3.12 | 6.47 | 0.13 | 0.77 | 1.13 | 0 | Schibille et al. 2022 | 0.55 | 1.14 |
| Nishapur | Green | 16.3 | 1.94 | 4.16 | 64.5 | 4.07 | 5.8 | 0.21 | 0.07 | 1.49 | 0 | Schibille et al. 2022 | 0.33 | 0.48 |
| Nishapur | Yellow | 17.9 | 3.73 | 4.28 | 60.7 | 3.1 | 7.47 | 0.2 | 0.11 | 1.31 | 0 | Schibille et al. 2022 | 0.50 | 1.20 |
| Nishapur | Green | 15.1 | 2.45 | 4.13 | 63.3 | 2.53 | 5.73 | 0.28 | 0.94 | 1.27 | 0 | Schibille et al. 2022 | 0.43 | 0.97 |
| Nishapur | Green | 14.4 | 2.95 | 3.01 | 67.5 | 2.14 | 7.54 | 0.18 | 0.05 | 1.03 | 0 | Schibille et al. 2022 | 0.39 | 1.38 |
| Nishapur | Blue | 17.2 | 1.69 | 2.96 | 66.7 | 4.07 | 3.61 | 0.18 | 0.85 | 1.19 | 0 | Schibille et al. 2022 | 0.47 | 0.42 |
| Nishapur | Blue | 16.1 | 1.7 | 2.7 | 68.3 | 3.9 | 3.5 | 0.18 | 0.86 | 1.2 | 0 | Schibille et al. 2022 | 0.49 | 0.44 |
| Nishapur | Blue Tr | 11.9 | 2.9 | 2.05 | 69.4 | 1.84 | 6.31 | 0.13 | 0.87 | 2.77 | 0 | Schibille et al. 2022 | 0.46 | 1.58 |
| Nishapur | Green Tr | 16.1 | 4.2 | 3.17 | 64.5 | 2.53 | 6.44 | 0.15 | 0.44 | 1.07 | 0 | Schibille et al. 2022 | 0.65 | 1.66 |
| Nishapur | Colourless | 12.1 | 3.86 | 1.05 | 72.9 | 2.11 | 6.28 | 0.06 | 0.36 | 0.35 | 0 | Schibille et al. 2022 | 0.61 | 1.83 |
| Nishapur | Blue | 16.9 | 4.48 | 2.85 | 61.9 | 3.35 | 6.89 | 0.14 | 0.68 | 1.31 | 0 | Schibille et al. 2022 | 0.65 | 1.34 |
| Nishapur | Blue Co | 17.5 | 4.09 | 2.13 | 64.3 | 3.76 | 4.58 | 0.08 | 0.69 | 1.21 | 0 | Schibille et al. 2022 | 0.89 | 1.09 |

| | | | | | | | | | | | | | | |
|----------|------------|----------|----------|----------|----------|--------------|----------|----------|----------|----------|---|---------------------------------|------|------|
| Nishapur | Blue Co | 14 .1 | 2. 84 | 1.4 4 | 68 | 2. 2 1 | 6. 65 | 0. 08 | 0. 17 | 2.5 6 | 0 | Schib ille et al. 2022 | 0.43 | 1.29 |
| Nishapur | Blue Co | 13 .7 | 3 | 1.8 1 | 64 .9 | 1. 9 6 | 8. 05 | 0. 09 | 2. 62 | 2.0 5 | 0 | Schib ille et al. 2022 | 0.37 | 1.53 |
| Nishapur | Blue Co | 13 .8 | 3. 08 | 1.8 2 | 64 .4 | 1. 9 4 | 8. 28 | 0. 1 | 2. 63 | 2.1 2 | 0 | Schib ille et al. 2022 | 0.37 | 1.59 |
| Nishapur | Colourless | 12 .7 | 4 | 2.6 4 | 67 .1 | 2. 3 | 8. 01 | 0. 14 | 1. 08 | 0.7 5 | 0 | Schib ille et al. 2022 | 0.50 | 1.74 |
| Nishapur | Colourless | 17 .4 | 4. 25 | 2.5 4 | 62 .4 | 3. 6 1 | 6. 33 | 0. 13 | 0. 68 | 1.2 6 | 0 | Schib ille et al. 2022 | 0.67 | 1.18 |
| Nishapur | Green Tr | 17 .2 | 6. 15 | 2.8 2 | 61 .2 | 2. 6 6 | 6. 58 | 0. 12 | 0. 73 | 1.2 5 | 0 | Schib ille et al. 2022 | 0.93 | 2.31 |
| Nishapur | Green Tr | 17 .6 | 6. 14 | 3.0 2 | 60 .5 | 2. 7 6 | 6. 47 | 0. 13 | 0. 75 | 1.3 1 | 0 | Schib ille et al. 2022 | 0.95 | 2.22 |
| Nishapur | Green/Blue | 18 .4 | 3. 13 | 2.0 5 | 65 .7 | 2. 7 2 | 5. 06 | 0. 14 | 0. 04 | 1.0 7 | 0 | Schib ille et al. 2022 | 0.62 | 1.15 |
| Nishapur | Aqua | 15 .6 | 3. 96 | 3.5 2 | 65 .1 | 2. 8 5 | 6. 6 | 0. 19 | 0. 05 | 1.1 | 0 | Schib ille et al. 2022 | 0.60 | 1.39 |
| Nishapur | Green | 15 .2 | 3. 85 | 3.6 6 | 65 .3 | 2. 8 5 | 6. 76 | 0. 19 | 0. 06 | 1.1 4 | 0 | Schib ille et al. 2022 | 0.57 | 1.35 |
| Nishapur | Green/Blue | 15 .3 | 3. 25 | 3.4 | 64 .6 | 2. 8 3 | 8. 05 | 0. 17 | 0. 06 | 0.9 7 | 0 | Schib ille et al. 2022 | 0.40 | 1.15 |
| Nishapur | Blue Co | 17 .2 | 3. 57 | 4.2 1 | 59 .3 | 3. 1 2 | 6. 47 | 0. 13 | 0. 77 | 1.1 3 | 0 | Schib ille et al. 2022 | 0.55 | 1.14 |
| Nishapur | Green | 16 .3 | 1. 94 | 4.1 6 | 64 .5 | 4. 0 7 | 5. 8 | 0. 21 | 0. 07 | 1.4 9 | 0 | Schib ille et al. 2022 | 0.33 | 0.48 |
| Nishapur | Yellow Tr | 17 .9 | 3. 73 | 4.2 8 | 60 .7 | 3. 1 | 7. 47 | 0. 2 | 0. 11 | 1.3 1 | 0 | Schib ille et al. 2022 | 0.50 | 1.20 |
| Nishapur | Green Tr | 15 .1 | 2. 45 | 4.1 3 | 63 .3 | 2. 5 3 | 5. 73 | 0. 28 | 0. 94 | 1.2 7 | 0 | Schib ille et al. 2022 | 0.43 | 0.97 |
| Nishapur | Green | 14 .4 | 2. 95 | 3.0 1 | 67 .5 | 2. 1 4 | 7. 54 | 0. 18 | 0. 05 | 1.0 3 | 0 | Schib ille et al. 2022 | 0.39 | 1.38 |

| | | | | | | | | | | | | | | |
|----------|------------|------|------|------|------|------|------|------|------|------|---|-----------------------|------|------|
| Nishapur | Blue | 17.2 | 1.69 | 2.96 | 66.7 | 4.07 | 3.61 | 0.18 | 0.85 | 1.19 | 0 | Schibille et al. 2022 | 0.47 | 0.42 |
| Nishapur | Blue | 16.1 | 1.7 | 2.7 | 68.3 | 3.9 | 3.5 | 0.18 | 0.86 | 1.2 | 0 | Schibille et al. 2022 | 0.49 | 0.44 |
| Nishapur | Blue Tr | 11.9 | 2.9 | 2.05 | 69.4 | 1.84 | 6.31 | 0.13 | 0.87 | 2.77 | 0 | Schibille et al. 2022 | 0.46 | 1.58 |
| Nishapur | Green Tr | 16.1 | 4.2 | 3.17 | 64.5 | 2.53 | 6.44 | 0.15 | 0.44 | 1.07 | 0 | Schibille et al. 2022 | 0.65 | 1.66 |
| Nishapur | Colourless | 12.1 | 3.86 | 1.05 | 72.9 | 2.11 | 6.28 | 0.06 | 0.36 | 0.35 | 0 | Schibille et al. 2022 | 0.61 | 1.83 |
| Nishapur | Blue | 16.9 | 4.48 | 2.85 | 61.9 | 3.35 | 6.89 | 0.14 | 0.68 | 1.31 | 0 | Schibille et al. 2022 | 0.65 | 1.34 |
| Nishapur | Blue Co | 17.5 | 4.09 | 2.13 | 64.3 | 3.76 | 4.58 | 0.08 | 0.69 | 1.21 | 0 | Schibille et al. 2022 | 0.89 | 1.09 |
| Nishapur | Blue Co | 14.1 | 2.84 | 1.44 | 68 | 2.21 | 6.65 | 0.08 | 0.17 | 2.56 | 0 | Schibille et al. 2022 | 0.43 | 1.29 |
| Nishapur | Blue Co | 13.7 | 3 | 1.81 | 64.9 | 1.96 | 8.05 | 0.09 | 2.62 | 2.05 | 0 | Schibille et al. 2022 | 0.37 | 1.53 |
| Nishapur | Blue Co | 13.8 | 3.08 | 1.82 | 64.4 | 1.94 | 8.28 | 0.1 | 2.63 | 2.12 | 0 | Schibille et al. 2022 | 0.37 | 1.59 |
| Nishapur | Colourless | 12.7 | 4 | 2.64 | 67.1 | 2.3 | 8.01 | 0.14 | 1.08 | 0.75 | 0 | Schibille et al. 2022 | 0.50 | 1.74 |
| Nishapur | Colourless | 17.4 | 4.25 | 2.54 | 62.4 | 3.61 | 6.33 | 0.13 | 0.68 | 1.26 | 0 | Schibille et al. 2022 | 0.67 | 1.18 |
| Nishapur | Blue Tr | 17.2 | 6.15 | 2.82 | 61.2 | 2.66 | 6.58 | 0.12 | 0.73 | 1.25 | 0 | Schibille et al. 2022 | 0.93 | 2.31 |
| Nishapur | Green Tr | 17.6 | 6.14 | 3.02 | 60.5 | 2.76 | 6.47 | 0.13 | 0.75 | 1.31 | 0 | Schibille et al. 2022 | 0.95 | 2.22 |
| Nishapur | Green/Blue | 18.4 | 3.13 | 2.05 | 65.7 | 2.72 | 5.06 | 0.14 | 0.04 | 1.07 | 0 | Schibille et al. 2022 | 0.62 | 1.15 |
| Nishapur | Colourless | 11.7 | 4.67 | 0.99 | 73.1 | 2.25 | 5.83 | 0.03 | 0.37 | 0.29 | 0 | Schibille et al. 2022 | 0.80 | 2.08 |

| | | | | | | | | | | | | | | |
|----------|------------|------|------|------|------|------|------|------|------|------|---|-----------------------|------|------|
| Nishapur | Colourless | 13.5 | 5.39 | 0.91 | 70.2 | 2.73 | 5.91 | 0.03 | 0.25 | 0.23 | 0 | Schibille et al. 2022 | 0.91 | 1.97 |
| Nishapur | Colourless | 11.2 | 4.29 | 1.16 | 73.8 | 1.83 | 5.97 | 0.06 | 0.48 | 0.41 | 0 | Schibille et al. 2022 | 0.72 | 2.34 |
| Nishapur | Colourless | 12.9 | 4.74 | 1.04 | 70.9 | 2.36 | 6.23 | 0.05 | 0.42 | 0.38 | 0 | Schibille et al. 2022 | 0.76 | 2.01 |
| Nishapur | Colourless | 11.3 | 4.94 | 1.16 | 71.6 | 2.4 | 7.21 | 0.05 | 0.25 | 0.35 | 0 | Schibille et al. 2022 | 0.69 | 2.06 |
| Nishapur | Colourless | 13 | 4.88 | 1.02 | 71.2 | 2.38 | 6.1 | 0.04 | 0.24 | 0.26 | 0 | Schibille et al. 2022 | 0.80 | 2.05 |
| Nishapur | Colourless | 12.7 | 4.64 | 0.97 | 72.1 | 2.47 | 5.74 | 0.04 | 0.24 | 0.26 | 0 | Schibille et al. 2022 | 0.81 | 1.88 |
| Nishapur | Colourless | 13 | 4.45 | 1.28 | 71 | 2.07 | 5.97 | 0.06 | 0.63 | 0.48 | 0 | Schibille et al. 2022 | 0.75 | 2.15 |
| Nishapur | Colourless | 10.9 | 4.89 | 0.99 | 73.5 | 2.11 | 6.33 | 0.04 | 0.24 | 0.28 | 0 | Schibille et al. 2022 | 0.77 | 2.32 |
| Nishapur | Colourless | 12.1 | 5.13 | 0.88 | 71.2 | 2.6 | 6.82 | 0.03 | 0.3 | 0.22 | 0 | Schibille et al. 2022 | 0.75 | 1.97 |
| Nishapur | Colourless | 11.2 | 4.58 | 1.16 | 73.3 | 2.11 | 5.87 | 0.04 | 0.54 | 0.38 | 0 | Schibille et al. 2022 | 0.78 | 2.17 |
| Nishapur | Colourless | 13.4 | 5.31 | 1.05 | 69.5 | 2.63 | 6.55 | 0.04 | 0.27 | 0.32 | 0 | Schibille et al. 2022 | 0.81 | 2.02 |
| Nishapur | Colourless | 12.4 | 4.26 | 0.86 | 71.6 | 2.86 | 6.36 | 0.04 | 0.45 | 0.27 | 0 | Schibille et al. 2022 | 0.67 | 1.49 |
| Nishapur | Colourless | 11.6 | 4.19 | 0.9 | 72.7 | 2.75 | 6.39 | 0.04 | 0.43 | 0.26 | 0 | Schibille et al. 2022 | 0.66 | 1.52 |
| Nishapur | Colourless | 11.2 | 4.23 | 0.97 | 72.5 | 2.72 | 6.8 | 0.04 | 0.43 | 0.26 | 0 | Schibille et al. 2022 | 0.62 | 1.56 |
| Nishapur | Colourless | 11.8 | 4.24 | 0.92 | 72.3 | 2.75 | 6.43 | 0.04 | 0.43 | 0.26 | 0 | Schibille et al. 2022 | 0.66 | 1.54 |
| Nishapur | Colourless | 13.2 | 4.8 | 0.98 | 71.1 | 2.44 | 5.99 | 0.04 | 0.24 | 0.26 | 0 | Schibille et al. 2022 | 0.80 | 1.97 |
| Nishapur | Blue Co | 14.6 | 4.02 | 3.01 | 64.7 | 3.4 | 5.86 | 0.12 | 1.56 | 1.21 | 0 | Schibille et | 0.69 | 1.18 |

| | | | | | | | | | | | | | | |
|----------|--------------|----------|----------|----------|----------|--------------|----------|----------|----------|----------|---|---------------------------------|------|------|
| | | | | | | | | | | | | al. 2022 | | |
| Nishapur | Blue Co | 12 .7 | 3. 81 | 1.7 5 | 68 .4 | 2. 3 8 | 7. 17 | 0. 09 | 0. 91 | 1.5 2 | 0 | Schib ille et al. 2022 | 0.53 | 1.60 |
| Nishapur | White | 13 .2 | 4. 21 | 2.6 6 | 61 | 2. 9 5 | 5. 74 | 0. 09 | 1. 17 | 0.5 5 | 0 | Schib ille et al. 2022 | 0.73 | 1.43 |
| Nishapur | Black | 15 | 2. 81 | 3.0 9 | 63 | 3. 3 5 | 6. 21 | 0. 2 | 0. 62 | 4.3 5 | 0 | Schib ille et al. 2022 | 0.45 | 0.84 |
| Nishapur | Yellow Tr | 11 | 4. 84 | 1.2 8 | 72 .3 | 2. 2 3 | 6. 15 | 0. 06 | 0. 74 | 0.5 6 | 0 | Schib ille et al. 2022 | 0.79 | 2.17 |
| Nishapur | Red opaque | 16 .4 | 2. 64 | 0.9 8 | 67 .2 | 3. 7 6 | 4. 89 | 0. 05 | 0. 05 | 0.5 1 | 0 | Schib ille et al. 2022 | 0.54 | 0.70 |
| Nishapur | Black | 19 .2 | 2. 04 | 1.8 9 | 66 .6 | 1. 1 7 | 5. 5 | 0. 17 | 0. 31 | 0.9 3 | 0 | Schib ille et al. 2022 | 0.37 | 1.74 |
| Nishapur | Red opaque | 15 .8 | 2. 37 | 0.9 2 | 68 .6 | 3. 9 5 | 4. 27 | 0. 05 | 0. 04 | 0.5 7 | 0 | Schib ille et al. 2022 | 0.56 | 0.60 |
| Nishapur | Black | 19 .3 | 2. 06 | 1.8 7 | 66 .7 | 1. 1 2 | 5. 18 | 0. 17 | 0. 32 | 0.8 6 | 0 | Schib ille et al. 2022 | 0.40 | 1.84 |
| Nishapur | Colourless | 17 .7 | 0. 44 | 2.1 7 | 65 .2 | 0. 3 1 | 10 .3 | 0. 24 | 1. 17 | 0.9 5 | 0 | Schib ille et al. 2022 | 0.04 | 1.42 |
| Nishapur | Blue Co | 14 .5 | 0. 66 | 2.5 5 | 67 .4 | 0. 3 7 | 10 .8 | 0. 27 | 0. 12 | 1.4 9 | 0 | Schib ille et al. 2022 | 0.06 | 1.78 |
| Nishapur | Blue | 14 .5 | 0. 68 | 2.4 9 | 67 | 0. 9 | 9. 35 | 0. 26 | 0. 13 | 2.0 4 | 0 | Schib ille et al. 2022 | 0.07 | 0.76 |
| Nishapur | Colourless | 12 .6 | 5. 4 | 0.8 8 | 71 | 2. 5 | 5. 9 | 0. 02 | 0. 35 | 0.2 | 0 | Schib ille et al. 2022 | 0.92 | 2.16 |
| Nishapur | Blue | 15 .3 | 6. 4 | 1.3 | 65 .7 | 2. 8 | 4. 6 | 0. 05 | 1. 3 | 1.2 | 0 | Wypy ski 2015 | 1.39 | 2.29 |
| Nishapur | Colourless | 18 .3 | 4. 2 | 2.5 | 64 | 2. 8 | 5. 4 | 0. 16 | 0. 32 | 0.8 4 | 0 | Wypy ski 2015 | 0.78 | 1.50 |
| Nishapur | Yellow-Green | 15 .7 | 4. 6 | 4 | 59 .8 | 5. 3 | 7. 6 | 0. 08 | 0. 79 | 0.7 7 | 0 | Wypy ski 2015 | 0.61 | 0.87 |
| Nishapur | Greenish | 12 .8 | 3. 4 | 2.3 | 66 .2 | 3. 3 | 7. 9 | 0. 1 | 1. 6 | 0.6 9 | 0 | Wypy ski 2015 | 0.43 | 1.03 |
| Nishapur | Dark Blue | 18 .4 | 0. 8 | 2.2 | 64 | 0. 6 2 | 8. 7 | 0. 12 | 0. 62 | 1.8 | 0 | Wypy ski 2015 | 0.09 | 1.29 |

| | | | | | | | | | | | | | | |
|----------|-----------------------|------|------|------|------|------|------|------|-------|------|------|--------------|------|------|
| Nishapur | Opaque White | 12.9 | 3 | 3.8 | 58.8 | 5.2 | 6.6 | 0.07 | 0.03 | 0.47 | 3.8 | Wypyski 2015 | 0.45 | 0.58 |
| Nishapur | Opaque Yellow | 14.4 | 5.7 | 1.1 | 53.7 | 2.5 | 4.4 | 0.07 | 0.86 | 0.41 | 14 | Wypyski 2015 | 1.30 | 2.28 |
| Nishapur | Blue | 13.6 | 3.34 | 1.84 | 67.2 | 2.01 | 6.25 | 0.2 | 0.59 | 3.69 | 0.05 | Brill 1995 | 0.53 | 1.66 |
| Nishapur | Dark Green | 17.6 | 3.13 | 3.19 | 61.6 | 2.69 | 5.6 | 0.35 | 0.61 | 1.14 | 0.09 | Brill 1995 | 0.56 | 1.16 |
| Nishapur | Greenish Aqua | 16.7 | 4.7 | 3.19 | 63.2 | 3.09 | 6.91 | 0.2 | 0.06 | 1.14 | 0 | Brill 1995 | 0.68 | 1.52 |
| Nishapur | Strong Aqua | 15.7 | 3.07 | 2.98 | 67.3 | 2.17 | 7.38 | 0.25 | 0.052 | 0.97 | 0 | Brill 1995 | 0.42 | 1.41 |
| Nishapur | Bluish Aqua | 14.6 | 2.77 | 3.54 | 68.4 | 3.15 | 5.91 | 0.2 | 0.54 | 0.78 | 0 | Brill 1995 | 0.47 | 0.88 |
| Nishapur | Yellow/Green | 16.5 | 4.24 | 3.57 | 60.4 | 2.77 | 7.26 | 0.2 | 1.15 | 0.71 | 0 | Brill 1995 | 0.58 | 1.53 |
| Nishapur | Green Tr | 15.2 | 4.67 | 1.58 | 64.4 | 3.9 | 8.01 | 0.2 | 0.9 | 1 | 0 | Brill 1995 | 0.58 | 1.20 |
| Nishapur | Bluish Green | 17.3 | 2.77 | 1.91 | 67.7 | 2.31 | 5.47 | 0.2 | 1.34 | 0.86 | 0 | Brill 1995 | 0.51 | 1.20 |
| Nishapur | Colourless | 17.6 | 3.75 | 1.51 | 66.2 | 2.95 | 6.66 | 0.2 | 0.35 | 0.66 | 0 | Brill 1995 | 0.56 | 1.27 |
| Nishapur | Blue | 19.3 | 4.53 | 2.49 | 61.1 | 3.58 | 6.74 | 0.2 | 0.63 | 1.8 | 0 | Brill 1995 | 0.67 | 1.27 |
| Nishapur | Blue | 18.2 | 4.27 | 1.9 | 64.8 | 3.78 | 4.78 | 0.15 | 0.63 | 1.15 | 0 | Brill 1995 | 0.89 | 1.13 |
| Nishapur | Blue | 14.4 | 3.02 | 1.43 | 67.9 | 2.15 | 7.58 | 0.15 | 0.18 | 2.47 | 0 | Brill 1995 | 0.40 | 1.40 |
| Nishapur | Blue | 17.1 | 1.74 | 2.85 | 68 | 3.84 | 4.07 | 0.25 | 0.82 | 1.07 | 0 | Brill 1995 | 0.43 | 0.45 |
| Nishapur | Blue Co | 14.1 | 2.97 | 1.64 | 65.7 | 1.88 | 8.22 | 0.15 | 2.65 | 1.88 | 0 | Brill 1995 | 0.36 | 1.58 |
| Nishapur | Blue Co | 14.5 | 2.97 | 1.69 | 65.5 | 1.88 | 8.22 | 0.15 | 2.48 | 1.88 | 0 | Brill 1995 | 0.36 | 1.58 |
| Nishapur | Blue/Green | 18.2 | 3.8 | 3.77 | 59.9 | 3.32 | 6.82 | 0.2 | 0.72 | 1.03 | 0.02 | Brill 1995 | 0.56 | 1.14 |
| Nishapur | Blue and Opaque white | 14.9 | 4.44 | 3.11 | 63.6 | 3.33 | 6.33 | 0.08 | 1.57 | 2.19 | 0.05 | Brill 1995 | 0.70 | 1.33 |
| Nishapur | Dark Green | 21.6 | 4.69 | 3.86 | 57.2 | 1.78 | 8.05 | 0.2 | 0.06 | 1.07 | 0 | Brill 1995 | 0.58 | 2.63 |
| Nishapur | Colourless | 13.6 | 6.11 | 0.91 | 69.6 | 2.29 | 6.28 | 0.05 | 0.24 | 0.33 | 0 | Brill 1995 | 0.97 | 2.78 |
| Nishapur | Colourless | 12.9 | 7.39 | 0.69 | 68.6 | 2.78 | 6.58 | 0.03 | 0.17 | 0.24 | 0 | Brill 1995 | 1.12 | 2.66 |

| | | | | | | | | | | | | | | |
|----------|----------------------------|---------------|----------|----------|---------------|--------------|---------------|----------|----------|----------|----------|------------------------|------|------|
| Nishapur | Colourless | 11 .4 5 | 5. 63 | 0.9 | 71 .6 8 | 1. 8 | 6. 58 | 0. 06 | 0. 33 | 0.7 8 | 0 | Brill 1995 | 0.86 | 3.13 |
| Nishapur | Colourless | 11 .9 | 4. 75 | 1.1 5 | 71 .8 8 | 2. 7 6 | 6. 64 | 0. 2 | 0. 25 | 0.2 8 | 0.7 | Brill 1995 | 0.72 | 1.72 |
| Nishapur | Colourless | 11 .8 | 4. 91 | 1.1 2 | 71 .9 4 | 2. 3 4 | 7. 33 | 0. 1 | 0. 24 | 0.1 2 | 0 | Brill 1995 | 0.67 | 2.10 |
| Nishapur | Colourless | 15 .2 | 5. 34 | 0.8 3 | 68 .5 4 | 3. 1 3 | 6. 42 | 0. 05 | 0. 2 | 0.1 9 | 0 | Brill 1995 | 0.83 | 1.71 |
| Nishapur | Colourless | 13 .1 | 4. 8 | 1.2 6 | 71 .6 5 | 1. 8 9 | 6. 33 | 0. 1 | 0. 4 | 0.3 7 | 0 | Brill 1995 | 0.76 | 2.54 |
| Nishapur | Colourless | 13 .6 | 5. 32 | 0.8 8 | 70 .9 | 2. 4 | 6. 27 | 0. 1 | 0. 23 | 0.2 4 | 0.0 1 | Brill 1995 | 0.85 | 2.22 |
| Nishapur | Colourless | 13 .2 | 5. 21 | 0.8 8 | 71 .4 8 | 2. 3 7 | 6. 19 | 0. 1 | 0. 23 | 0.2 4 | 0 | Brill 1995 | 0.84 | 2.20 |
| Nishapur | Colourless | 12 .4 | 4. 88 | 1.2 1 | 71 .5 2 | 1. 9 6 | 6. 71 | 0. 15 | 0. 63 | 0.4 4 | 0 | Brill 1995 | 0.73 | 2.49 |
| Nishapur | Colourless | 10 .2 | 3. 43 | 1.0 9 | 74 .0 6 | 2. 2 6 | 7. 65 | 0. 1 | 0. 77 | 0.3 4 | 0 | Brill 1995 | 0.45 | 1.52 |
| Nishapur | Colourless | 13 | 5. 13 | 0.9 9 | 70 .8 1 | 2. 5 6 | 6. 82 | 0. 05 | 0. 28 | 0.2 6 | 0 | Brill 1995 | 0.75 | 2.00 |
| Siraf | light green- colourless | 13 .5 | 2. 07 | 0.8 | 68 .8 | 2. 8 8 | 7 | 0. 1 | 2. 98 | 0.4 4 | 0 | Swan et al. 2017 | 0.30 | 0.72 |
| Siraf | naturally aqua | 13 .9 | 2. 02 | 1.6 7 | 65 .5 | 2. 6 5 | 9 | 0. 13 | 0. 45 | 2.7 1 | 0 | Swan et al. 2017 | 0.22 | 0.76 |
| Siraf | naturally aqua | 14 | 2. 43 | 1.4 9 | 66 .3 | 3. 2 6 | 9. 51 | 0. 13 | 1. 27 | 0.4 4 | 0 | Swan et al. 2017 | 0.26 | 0.75 |
| Siraf | light green | 13 .7 | 2. 29 | 1.3 2 | 66 .8 | 2. 8 7 | 8. 74 | 0. 17 | 0. 55 | 2.1 7 | 0 | Swan et al. 2017 | 0.26 | 0.80 |
| Siraf | light green | 14 .5 | 2. 3 | 1.0 5 | 64 .8 | 2. 3 3 | 9. 9 | 0. 18 | 2. 8 | 0.5 8 | 0 | Swan et al. 2017 | 0.23 | 0.99 |
| Siraf | naturally aqua | 12 .8 | 2. 74 | 1.2 8 | 68 .1 | 2. 2 8 | 8. 62 | 0. 14 | 1. 88 | 0.8 3 | 0 | Swan et al. 2017 | 0.32 | 1.20 |
| Siraf | yellow-green | 12 .6 | 2. 48 | 1.3 | 67 | 2. 4 6 | 10 .1 2 | 0. 18 | 1. 62 | 0.7 4 | 0 | Swan et al. 2017 | 0.25 | 1.01 |
| Siraf | naturally aqua | 13 .6 | 2. 49 | 1.1 2 | 68 .6 | 2. 3 6 | 8. 83 | 0. 17 | 0. 35 | 1.0 4 | 0 | Swan et al. 2017 | 0.28 | 1.06 |
| Siraf | naturally aqua | 13 .6 | 2. 89 | 1.5 | 66 .7 | 2. 5 6 | 8. 07 | 0. 14 | 2. 22 | 0.9 | 0 | Swan et al. 2017 | 0.36 | 1.13 |
| Siraf | naturally aqua | 14 .1 | 2. 56 | 1 | 67 | 2. 4 7 | 8. 9 | 0. 16 | 1. 3 | 0.9 4 | 0 | Swan et al. 2017 | 0.29 | 1.04 |
| Siraf | light green | 12 .2 | 2. 34 | 1.7 5 | 68 .4 | 2. 7 5 | 8. 68 | 0. 16 | 0. 6 | 1.7 | 0 | Swan et al. 2017 | 0.27 | 0.85 |
| Siraf | green | 12 .6 | 3. 07 | 1.5 9 | 66 .8 | 2. 0 8 | 8. 9 | 0. 16 | 2. 38 | 0.7 7 | 0 | Swan et al. 2017 | 0.34 | 1.48 |

| | | | | | | | | | | | | | | |
|-------|------------------|------|------|------|------|------|------|------|------|------|---|------------------|------|------|
| Siraf | light green-aqua | 12.3 | 3.09 | 1.74 | 66.8 | 2.02 | 9.19 | 0.17 | 2.42 | 0.78 | 0 | Swan et al. 2017 | 0.34 | 1.53 |
| Siraf | green | 13.6 | 2.09 | 1.65 | 66.8 | 3.09 | 8.39 | 0.17 | 2.07 | 0.62 | 0 | Swan et al. 2017 | 0.25 | 0.68 |
| Siraf | green | 12.3 | 2.98 | 1.55 | 67.5 | 2.04 | 8.89 | 0.16 | 2.4 | 0.66 | 0 | Swan et al. 2017 | 0.34 | 1.46 |
| Siraf | light green-aqua | 12.4 | 2.97 | 1.47 | 67.5 | 2.05 | 8.93 | 0.16 | 2.33 | 0.67 | 0 | Swan et al. 2017 | 0.33 | 1.45 |
| Siraf | green | 12.2 | 3 | 1.5 | 67.7 | 2.03 | 8.9 | 0.16 | 2.27 | 0.62 | 0 | Swan et al. 2017 | 0.34 | 1.48 |
| Siraf | light green | 12.1 | 2.84 | 1.4 | 68.2 | 2.06 | 8.65 | 0.16 | 2.29 | 0.66 | 0 | Swan et al. 2017 | 0.33 | 1.38 |
| Siraf | light green | 12.3 | 2.77 | 1.38 | 68.7 | 2.11 | 8.53 | 0.16 | 1.81 | 0.66 | 0 | Swan et al. 2017 | 0.32 | 1.31 |
| Siraf | light green | 13.8 | 2.21 | 1.66 | 66.1 | 2.09 | 9.11 | 0.18 | 1.72 | 0.85 | 0 | Swan et al. 2017 | 0.24 | 0.74 |
| Siraf | yellow-green | 11.5 | 1.99 | 1.17 | 70.3 | 2.05 | 7.75 | 0.18 | 2.09 | 1.18 | 0 | Swan et al. 2017 | 0.26 | 0.78 |
| Siraf | light green | 13.9 | 2.25 | 1.68 | 65.7 | 2.09 | 9.18 | 0.18 | 1.84 | 0.85 | 0 | Swan et al. 2017 | 0.25 | 0.75 |
| Siraf | naturally aqua | 13.9 | 2.22 | 1.67 | 66 | 2.09 | 9.13 | 0.18 | 1.59 | 0.83 | 0 | Swan et al. 2017 | 0.24 | 0.75 |
| Siraf | light green | 13.8 | 2.22 | 1.67 | 66.2 | 2.09 | 9.3 | 0.18 | 1.56 | 0.84 | 0 | Swan et al. 2017 | 0.24 | 0.75 |
| Siraf | light green | 13.8 | 2.21 | 1.66 | 66 | 2.09 | 9.19 | 0.18 | 1.79 | 0.88 | 0 | Swan et al. 2017 | 0.24 | 0.75 |
| Siraf | naturally aqua | 13.9 | 2.23 | 1.68 | 66.2 | 2.09 | 9.14 | 0.18 | 1.51 | 0.85 | 0 | Swan et al. 2017 | 0.24 | 0.76 |
| Siraf | indeterminate | 14 | 2.21 | 1.64 | 66 | 3 | 9.09 | 0.18 | 1.58 | 0.8 | 0 | Swan et al. 2017 | 0.24 | 0.74 |
| Siraf | light green | 13.9 | 2.21 | 1.63 | 66.1 | 2.09 | 9.06 | 0.19 | 1.7 | 0.77 | 0 | Swan et al. 2017 | 0.24 | 0.74 |
| Siraf | light green | 13.4 | 2.2 | 1.24 | 68.2 | 2.11 | 7.14 | 0.25 | 0.51 | 3.08 | 0 | Swan et al. 2017 | 0.31 | 1.04 |
| Siraf | naturally aqua | 13.8 | 2.23 | 1.66 | 66.3 | 2.09 | 9.18 | 0.18 | 1.48 | 0.82 | 0 | Swan et al. 2017 | 0.24 | 0.75 |
| Siraf | green | 14 | 2.24 | 1.65 | 66.1 | 3.01 | 9.27 | 0.18 | 1.42 | 0.82 | 0 | Swan et al. 2017 | 0.24 | 0.74 |
| Siraf | green | 14 | 2.3 | 1.83 | 65.9 | 3.03 | 9.42 | 0.19 | 1.07 | 0.88 | 0 | Swan et al. 2017 | 0.24 | 0.76 |
| Siraf | light green | 14.1 | 2.33 | 1.71 | 65.4 | 2.09 | 9.55 | 0.19 | 1.51 | 0.86 | 0 | Swan et al. 2017 | 0.24 | 0.78 |

| | | | | | | | | | | | | | | |
|-------|----------------|------|------|------|------|------|-------|------|------|------|---|------------------|------|------|
| Siraf | green | 13.8 | 2.23 | 1.67 | 66.1 | 2.99 | 9.2 | 0.19 | 1.52 | 0.85 | 0 | Swan et al. 2017 | 0.24 | 0.75 |
| Siraf | green | 13.8 | 2.22 | 1.65 | 66.3 | 2.98 | 9.08 | 0.19 | 1.44 | 0.81 | 0 | Swan et al. 2017 | 0.24 | 0.74 |
| Siraf | light green | 13.6 | 2.21 | 1.68 | 66.1 | 2.93 | 9.24 | 0.18 | 1.79 | 0.83 | 0 | Swan et al. 2017 | 0.24 | 0.75 |
| Siraf | naturally aqua | 13.8 | 2.92 | 1.36 | 66.2 | 2.51 | 8.69 | 0.16 | 2.05 | 0.94 | 0 | Swan et al. 2017 | 0.34 | 1.16 |
| Siraf | naturally aqua | 12.7 | 2.46 | 1.14 | 67.7 | 2.45 | 9.1 | 0.17 | 1.39 | 1.42 | 0 | Swan et al. 2017 | 0.27 | 1.00 |
| Siraf | light green | 13.5 | 2.27 | 1.71 | 66.3 | 2.96 | 9.39 | 0.19 | 1.56 | 0.93 | 0 | Swan et al. 2017 | 0.24 | 0.77 |
| Siraf | light green | 13.7 | 2.26 | 1.71 | 65.8 | 2.98 | 9.55 | 0.18 | 1.6 | 0.84 | 0 | Swan et al. 2017 | 0.24 | 0.76 |
| Siraf | light green | 13.7 | 2.25 | 1.69 | 65.5 | 2.95 | 9.65 | 0.18 | 1.73 | 0.86 | 0 | Swan et al. 2017 | 0.23 | 0.76 |
| Siraf | light green | 15 | 2.51 | 1.46 | 63.3 | 3.03 | 10.92 | 0.19 | 0.74 | 1.57 | 0 | Swan et al. 2017 | 0.23 | 0.83 |
| Siraf | green | 13.3 | 2.45 | 1.64 | 64.7 | 2.88 | 10.4 | 0.18 | 2.12 | 0.94 | 0 | Swan et al. 2017 | 0.24 | 0.88 |
| Siraf | light green | 13.2 | 2.18 | 1.48 | 65.9 | 2.87 | 9.81 | 0.2 | 0.93 | 1.8 | 0 | Swan et al. 2017 | 0.22 | 0.76 |
| Siraf | light blue | 12.3 | 2.03 | 1.32 | 68 | 2.46 | 8.94 | 0.2 | 0.46 | 2.45 | 0 | Swan et al. 2017 | 0.23 | 0.83 |
| Siraf | dark blue | 12.5 | 2.22 | 1.16 | 66.6 | 2.83 | 8.33 | 0.2 | 2.28 | 2.13 | 0 | Swan et al. 2017 | 0.27 | 0.78 |
| Siraf | light green | 14 | 2.49 | 1.02 | 67.7 | 1.77 | 8.14 | 0.17 | 2.43 | 0.6 | 0 | Swan et al. 2017 | 0.31 | 1.41 |
| Siraf | light green | 12.8 | 1.82 | 1.25 | 68.4 | 2.68 | 8.66 | 0.18 | 1.75 | 1.06 | 0 | Swan et al. 2017 | 0.21 | 0.68 |
| Siraf | light green | 13.1 | 1.74 | 1.03 | 69 | 3.27 | 8.17 | 0.2 | 0.33 | 1.7 | 0 | Swan et al. 2017 | 0.21 | 0.53 |
| Siraf | light green | 14.8 | 2.57 | 0.79 | 69.3 | 1.69 | 7.38 | 0.08 | 1.62 | 0.5 | 0 | Swan et al. 2017 | 0.35 | 1.52 |
| Siraf | colourless | 14.8 | 3.01 | 0.95 | 66.1 | 2.11 | 9.17 | 0.1 | 1.83 | 0.61 | 0 | Swan et al. 2017 | 0.33 | 1.43 |
| Siraf | naturally aqua | 12.1 | 2.57 | 1.04 | 70.1 | 2.6 | 9.01 | 0.1 | 0.44 | 0.76 | 0 | Swan et al. 2017 | 0.29 | 0.99 |
| Siraf | yellow-brown | 12.6 | 3.08 | 1.35 | 68 | 2.68 | 8.09 | 0.1 | 2.29 | 0.68 | 0 | Swan et al. 2017 | 0.38 | 1.15 |
| Siraf | light green | 13.4 | 2.15 | 1.49 | 70 | 2.33 | 6.5 | 0.11 | 0.93 | 1.69 | 0 | Swan et al. 2017 | 0.33 | 0.92 |

| | | | | | | | | | | | | | | |
|-------|-----------------------------|----------|----------|----------|----------|--------------|----------|----------|----------|----------|---|------------------------|------|------|
| Siraf | yellow-green | 13 .7 | 2. 41 | 0.6 4 | 69 .8 | 1. 8 3 | 6. 59 | 0. 09 | 2. 72 | 0.9 3 | 0 | Swan et al. 2017 | 0.37 | 1.32 |
| Siraf | light green | 14 | 2. 81 | 0.8 4 | 67 .9 | 2. 0 3 | 7. 85 | 0. 1 | 1. 45 | 1.6 6 | 0 | Swan et al. 2017 | 0.36 | 1.38 |
| Siraf | colourless- light green? | 14 .5 | 2. 58 | 0.6 9 | 69 .6 | 1. 9 8 | 6. 56 | 0. 1 | 2. 26 | 0.4 3 | 0 | Swan et al. 2017 | 0.39 | 1.30 |
| Siraf | naturally aqua | 14 .1 | 2. 55 | 0.6 8 | 69 .9 | 1. 9 8 | 6. 69 | 0. 11 | 2. 27 | 0.4 3 | 0 | Swan et al. 2017 | 0.38 | 1.29 |
| Siraf | colourless | 14 .2 | 2. 31 | 0.6 4 | 71 .9 | 1. 7 2 | 4. 93 | 0. 1 | 2. 55 | 0.3 4 | 0 | Swan et al. 2017 | 0.47 | 1.34 |
| Siraf | naturally aqua | 12 .5 | 2. 71 | 1.3 2 | 70 .7 | 2. 0 6 | 6. 95 | 0. 19 | 1. 21 | 0.7 4 | 0 | Swan et al. 2017 | 0.39 | 1.32 |
| Siraf | aqua-light green | 14 .6 | 2. 29 | 0.8 3 | 67 .7 | 2. 3 4 | 9. 34 | 0. 16 | 1. 03 | 0.4 5 | 0 | Swan et al. 2017 | 0.25 | 0.98 |
| Siraf | naturally aqua | 13 .3 | 3. 09 | 1.2 7 | 68 .3 | 2. 3 1 | 8 | 0. 11 | 1. 53 | 0.9 1 | 0 | Swan et al. 2017 | 0.39 | 1.34 |
| Siraf | light green | 13 .2 | 2. 06 | 1.2 8 | 68 | 2. 1 9 | 9. 39 | 0. 15 | 0. 54 | 1.7 1 | 0 | Swan et al. 2017 | 0.22 | 0.94 |
| Siraf | naturally aqua | 13 .1 | 3. 18 | 1.2 6 | 67 .7 | 2. 4 9 | 8. 39 | 0. 11 | 1. 69 | 0.8 6 | 0 | Swan et al. 2017 | 0.38 | 1.28 |
| Siraf | blue | 14 .2 | 4. 83 | 1.2 | 66 .8 | 3. 2 3 | 6. 81 | 0. 03 | 0. 47 | 0.4 5 | 0 | Swan et al. 2017 | 0.71 | 1.50 |
| Siraf | colourless | 11 .8 | 4. 75 | 1.2 9 | 72 .1 | 2. 1 | 6. 69 | 0. 03 | 0. 26 | 0.3 4 | 0 | Swan et al. 2017 | 0.71 | 2.26 |
| Siraf | naturally aqua | 11 .3 | 4. 51 | 1.0 6 | 72 .7 | 2. 4 2 | 6. 38 | 0. 03 | 0. 39 | 0.3 7 | 0 | Swan et al. 2017 | 0.71 | 1.86 |
| Siraf | aqua-light blue | 12 | 5. 05 | 1.4 3 | 70 .4 | 2. 2 4 | 6. 85 | 0. 03 | 0. 63 | 0.5 1 | 0 | Swan et al. 2017 | 0.74 | 2.25 |
| Siraf | colourless | 11 .7 | 3. 3 | 1.8 3 | 71 .3 | 3. 0 9 | 6. 89 | 0. 05 | 0. 3 | 0.6 2 | 0 | Swan et al. 2017 | 0.48 | 1.07 |
| Siraf | colourless- light yellow | 13 .9 | 3. 78 | 2.2 1 | 67 .8 | 3. 3 4 | 6. 65 | 0. 04 | 1. 02 | 0.3 4 | 0 | Swan et al. 2017 | 0.57 | 1.13 |
| Siraf | colourless- light green | 13 .8 | 3. 64 | 2.1 5 | 68 .2 | 3. 3 7 | 6. 58 | 0. 04 | 0. 99 | 0.3 3 | 0 | Swan et al. 2017 | 0.55 | 1.08 |
| Siraf | colourless- light green? | 12 .8 | 4. 88 | 1.2 | 70 .2 | 2. 3 1 | 6. 75 | 0. 04 | 0. 47 | 0.3 9 | 0 | Swan et al. 2017 | 0.72 | 2.11 |
| Siraf | naturally aqua | 14 | 3. 86 | 2.7 3 | 69 .2 | 3. 1 6 | 4. 71 | 0. 05 | 0. 9 | 0.4 3 | 0 | Swan et al. 2017 | 0.82 | 1.22 |
| Siraf | colourless | 12 .3 | 3. 4 | 2.3 8 | 70 .9 | 2. 9 7 | 5. 46 | 0. 05 | 1. 02 | 0.4 8 | 0 | Swan et al. 2017 | 0.62 | 1.14 |
| Siraf | green? | 15 .5 | 4. 65 | 2.4 5 | 65 .2 | 3. 2 | 6. 4 | 0. 05 | 0. 84 | 0.5 1 | 0 | Swan et al. 2017 | 0.73 | 1.45 |

| | | | | | | | | | | | | | | |
|-------|-------------------------|------|------|------|------|------|------|------|------|------|---|------------------|------|------|
| Siraf | colourless-light yellow | 14.5 | 4.21 | 2.65 | 67.9 | 2.86 | 5.55 | 0.06 | 0.96 | 0.45 | 0 | Swan et al. 2017 | 0.76 | 1.47 |
| Siraf | light green | 14.3 | 4.22 | 2.68 | 68 | 2.85 | 5.49 | 0.06 | 1 | 0.45 | 0 | Swan et al. 2017 | 0.77 | 1.48 |
| Siraf | colourless | 15.2 | 3.19 | 2.62 | 65.1 | 3.24 | 7.24 | 0.07 | 1.36 | 0.77 | 0 | Swan et al. 2017 | 0.44 | 0.98 |
| Siraf | colourless | 15 | 3.14 | 2.55 | 65.5 | 3.28 | 7.14 | 0.07 | 1.35 | 0.77 | 0 | Swan et al. 2017 | 0.44 | 0.96 |
| Siraf | colourless | 14.8 | 3.15 | 2.56 | 65.7 | 3.26 | 7.16 | 0.07 | 1.35 | 0.76 | 0 | Swan et al. 2017 | 0.44 | 0.97 |
| Siraf | yellowish-colourless | 13.4 | 3.14 | 3.25 | 67.1 | 3.22 | 7.03 | 0.07 | 1.04 | 0.71 | 0 | Swan et al. 2017 | 0.45 | 0.98 |
| Siraf | dark blue | 12.8 | 2.37 | 2.12 | 69.3 | 2.18 | 5.62 | 0.08 | 0.5 | 2.84 | 0 | Swan et al. 2017 | 0.42 | 1.09 |
| Siraf | black (very dark blue) | 13.1 | 2.39 | 1.79 | 67.7 | 1.71 | 5.92 | 0.07 | 1.54 | 3.17 | 0 | Swan et al. 2017 | 0.40 | 1.40 |
| Siraf | dark blue | 14.3 | 3.99 | 2.55 | 64 | 2.55 | 7.72 | 0.09 | 1.61 | 1.26 | 0 | Swan et al. 2017 | 0.52 | 1.56 |
| Siraf | indeterminate | 14 | 3.93 | 2.67 | 67 | 3.1 | 5.77 | 0.12 | 1.49 | 0.71 | 0 | Swan et al. 2017 | 0.68 | 1.27 |
| Siraf | light green | 14.2 | 3.27 | 2.29 | 66.5 | 2.92 | 6.62 | 0.09 | 2.05 | 0.78 | 0 | Swan et al. 2017 | 0.49 | 1.12 |
| Siraf | naturally aqua | 14.9 | 4.11 | 2.04 | 65.6 | 2.84 | 6.72 | 0.07 | 1.84 | 0.71 | 0 | Swan et al. 2017 | 0.61 | 1.45 |
| Siraf | indeterminate | 14.3 | 3.35 | 2.28 | 66 | 2.94 | 6.76 | 0.09 | 2.19 | 0.77 | 0 | Swan et al. 2017 | 0.50 | 1.14 |
| Siraf | yellow | 18.3 | 3.58 | 1.52 | 52.4 | 2.66 | 5.43 | 0.05 | 0.04 | 0.77 | 0 | Swan et al. 2017 | 0.66 | 1.35 |
| Siraf | blue | 17 | 2.4 | 0.82 | 68.5 | 2.87 | 5.5 | 0.03 | 0.18 | 0.76 | 0 | Swan et al. 2017 | 0.44 | 0.84 |
| Siraf | blue | 19.2 | 3.78 | 1.62 | 64 | 2.78 | 5.36 | 0.05 | 0.05 | 1.33 | 0 | Swan et al. 2017 | 0.71 | 1.36 |
| Siraf | indeterminate (blue?) | 15.5 | 4.03 | 2.14 | 63.3 | 3.93 | 8.58 | 0.08 | 0.07 | 0.91 | 0 | Swan et al. 2017 | 0.47 | 1.03 |
| Siraf | blue | 17 | 3.21 | 1.66 | 64.2 | 3.61 | 6.85 | 0.09 | 0.06 | 1.56 | 0 | Swan et al. 2017 | 0.47 | 0.89 |
| Siraf | light blue-turquoise | 19.4 | 2.14 | 0.53 | 66.4 | 3.62 | 4.33 | 0.19 | 0.03 | 0.31 | 0 | Swan et al. 2017 | 0.49 | 0.59 |
| Siraf | indeterminate (blue?) | 13.1 | 1.92 | 0.51 | 72 | 3.28 | 5.21 | 0.31 | 0.02 | 1.95 | 0 | Swan et al. 2017 | 0.37 | 0.59 |
| Siraf | light green | 14.2 | 2.89 | 7.58 | 56.8 | 7.92 | 7.15 | 0.19 | 0.03 | 1.83 | 0 | Swan et al. 2017 | 0.40 | 0.36 |

| | | | | | | | | | | | | | | |
|--------|------------------------------|------|------|------|------|------|------|------|------|------|---|-----------------------|------|------|
| Siraf | indeterminate (light green?) | 12.2 | 2.74 | 8.06 | 57.8 | 7.17 | 8.28 | 0.21 | 0.03 | 2 | 0 | Swan et al. 2017 | 0.33 | 0.38 |
| Siraf | dark aqua | 20.5 | 1.52 | 4.73 | 64.1 | 0.76 | 2.84 | 0.28 | 0.06 | 1.42 | 0 | Swan et al. 2017 | 0.54 | 2.00 |
| Siraf | naturally aqua | 14.3 | 3.22 | 2.17 | 67.3 | 2.03 | 8.44 | 0.07 | 0.04 | 0.86 | 0 | Swan et al. 2017 | 0.38 | 1.59 |
| Siraf | light green | 15.5 | 4.9 | 3.23 | 63.5 | 3.33 | 7.11 | 0.08 | 0.04 | 1.06 | 0 | Swan et al. 2017 | 0.69 | 1.48 |
| Siraf | aqua-light green | 16.4 | 4.72 | 3.63 | 61.6 | 2.88 | 8.46 | 0.1 | 0.04 | 0.86 | 0 | Swan et al. 2017 | 0.56 | 1.64 |
| Siraf | light green | 14.9 | 2.1 | 0.87 | 67.3 | 3.12 | 5.8 | 0.31 | 0.04 | 3.65 | 0 | Swan et al. 2017 | 0.36 | 0.67 |
| Gorgan | yellowish transparent | 12.7 | 2.38 | 2.91 | 69.2 | 2.06 | 6.16 | 0.24 | 1.41 | 1.38 | 0 | Schibille et al. 2022 | 0.39 | 1.16 |
| Gorgan | blue | 13.8 | 3.99 | 1.81 | 64.6 | 3.44 | 6.98 | 0.14 | 0.19 | 0.73 | 0 | Schibille et al. 2022 | 0.57 | 1.16 |
| Gorgan | green | 16.2 | 4.31 | 1.44 | 64.3 | 3.54 | 7.12 | 0.11 | 0.91 | 0.52 | 0 | Schibille et al. 2022 | 0.61 | 1.22 |
| Gorgan | green pale transparent | 17.9 | 4.26 | 1.33 | 63.2 | 3.65 | 6.84 | 0.1 | 0.94 | 0.39 | 0 | Schibille et al. 2022 | 0.62 | 1.17 |
| Gorgan | colourless | 13.4 | 3.91 | 1.55 | 65.5 | 4.64 | 9.11 | 0.09 | 0.04 | 0.74 | 0 | Schibille et al. 2022 | 0.43 | 0.84 |
| Gorgan | green | 15.6 | 3.4 | 2.64 | 65 | 3 | 6.26 | 0.19 | 1.47 | 1.06 | 0 | Schibille et al. 2022 | 0.54 | 1.13 |
| Gorgan | colourless | 15.8 | 3.12 | 2.36 | 66.2 | 3.04 | 5.59 | 0.17 | 1.39 | 1.05 | 0 | Schibille et al. 2022 | 0.56 | 1.03 |
| Gorgan | blue greenish | 15.6 | 2.83 | 2.37 | 66.4 | 3.12 | 5.67 | 0.16 | 0.85 | 1.46 | 0 | Schibille et al. 2022 | 0.50 | 0.91 |
| Gorgan | green pale transparent | 15.8 | 3.4 | 2.56 | 65.1 | 3.07 | 6.08 | 0.19 | 1.47 | 1.06 | 0 | Schibille et al. 2022 | 0.56 | 1.11 |
| Gorgan | green pale transparent | 15.6 | 3.39 | 2.62 | 65.2 | 2.99 | 6.21 | 0.19 | 1.48 | 1.07 | 0 | Schibille et al. 2022 | 0.55 | 1.13 |
| Gorgan | colourless | 16 | 3.27 | 2.5 | 65.4 | 3.08 | 5.86 | 0.17 | 1.43 | 1.04 | 0 | Schibille et al. 2022 | 0.56 | 1.06 |
| Gorgan | blue | 14.7 | 2.67 | 4.06 | 62.9 | 3.32 | 7.1 | 0.19 | 0.39 | 2.73 | 0 | Schibille et | 0.38 | 0.80 |

| | | | | | | | | | | | | | | |
|--------|-------------------------------|------|------|------|------|------|------|------|------|------|---|-----------------------|------|------|
| | | | | | | | | | | | | al. 2022 | | |
| Gorgan | white | 15 | 2.54 | 3.49 | 58.1 | 3.02 | 5.97 | 0.17 | 0.71 | 1.08 | 0 | Schibille et al. 2022 | 0.43 | 0.84 |
| Gorgan | green | 13.8 | 1.8 | 3.34 | 67.5 | 3.4 | 6.29 | 0.22 | 1.38 | 1.2 | 0 | Schibille et al. 2022 | 0.29 | 0.53 |
| Gorgan | red opaque ? | 14 | 2.66 | 2.27 | 66.8 | 2.81 | 5.23 | 0.2 | 3.42 | 1.09 | 0 | Schibille et al. 2022 | 0.51 | 0.95 |
| Gorgan | green to green bluish | 13.5 | 1.82 | 3.63 | 68.4 | 3.7 | 4.99 | 0.24 | 1.39 | 1.26 | 0 | Schibille et al. 2022 | 0.36 | 0.49 |
| Gorgan | green bluish | 13.2 | 2.16 | 3.9 | 67.6 | 4.24 | 5.12 | 0.24 | 1.03 | 1.46 | 0 | Schibille et al. 2022 | 0.42 | 0.51 |
| Gorgan | green transparent | 15.7 | 2.85 | 2.98 | 64.5 | 3.64 | 6.07 | 0.19 | 1.35 | 1.55 | 0 | Schibille et al. 2022 | 0.47 | 0.78 |
| Gorgan | aqua | 15.1 | 3.19 | 3.02 | 68.4 | 3.8 | 4.7 | 0.12 | 0.11 | 0.47 | 0 | Schibille et al. 2022 | 0.68 | 0.84 |
| Gorgan | aqua | 15.5 | 3.2 | 3.04 | 67.8 | 3.93 | 4.68 | 0.12 | 0.11 | 0.51 | 0 | Schibille et al. 2022 | 0.68 | 0.81 |
| Gorgan | green pale transparent | 13.1 | 1.86 | 3.19 | 69.7 | 3.14 | 5.02 | 0.21 | 1.3 | 1.26 | 0 | Schibille et al. 2022 | 0.37 | 0.59 |
| Gorgan | blue Co pale | 17.1 | 2.48 | 2.82 | 65.4 | 3.38 | 4.59 | 0.21 | 0.8 | 1.57 | 0 | Schibille et al. 2022 | 0.54 | 0.73 |
| Gorgan | green pale transparent | 15.6 | 3.26 | 3 | 67.7 | 3.86 | 4.71 | 0.11 | 0.06 | 0.45 | 0 | Schibille et al. 2022 | 0.69 | 0.84 |
| Gorgan | blue Co pale | 17.2 | 2.46 | 2.92 | 64.9 | 3.56 | 4.74 | 0.22 | 0.79 | 1.59 | 0 | Schibille et al. 2022 | 0.52 | 0.69 |
| Gorgan | black with red trailed design | 16.4 | 2.86 | 3.54 | 62.4 | 3.19 | 5.96 | 0.25 | 1.53 | 2.54 | 0 | Schibille et al. 2022 | 0.48 | 0.90 |
| Gorgan | yellowish transparent | 16.7 | 2.94 | 3 | 67 | 2.83 | 5.53 | 0.15 | 0.02 | 0.49 | 0 | Schibille et al. 2022 | 0.53 | 1.04 |
| Gorgan | amber transparent | 15.8 | 3.02 | 3.11 | 67.6 | 2.74 | 5.78 | 0.16 | 0.02 | 0.51 | 0 | Schibille et al. 2022 | 0.52 | 1.10 |
| Gorgan | yellowish pale | 16.2 | 3.85 | 2.56 | 64.1 | 3.14 | 5.88 | 0.15 | 1.6 | 1.2 | 0 | Schibille et al. 2022 | 0.65 | 1.23 |

| | | | | | | | | | | | | | | |
|--------|-----------------------------|------|------|------|------|------|------|------|------|------|---|-----------------------|------|------|
| Gorgan | green pale transparent | 17.4 | 2.82 | 2.82 | 65.3 | 3.28 | 5.07 | 0.2 | 0.65 | 0.95 | 0 | Schibille et al. 2022 | 0.56 | 0.86 |
| Gorgan | green pale transparent | 16.6 | 3.09 | 3.25 | 64.9 | 3.16 | 5.76 | 0.2 | 0.67 | 0.98 | 0 | Schibille et al. 2022 | 0.54 | 0.98 |
| Gorgan | colourless | 17.3 | 3.44 | 2.07 | 65.8 | 3.02 | 4.65 | 0.18 | 1.16 | 0.78 | 0 | Schibille et al. 2022 | 0.74 | 1.14 |
| Gorgan | blue pale transparent | 16.5 | 2.78 | 2.79 | 65.7 | 3.13 | 4.89 | 0.19 | 0.93 | 1.51 | 0 | Schibille et al. 2022 | 0.57 | 0.89 |
| Gorgan | yellowish transparent | 16.5 | 1.21 | 3.08 | 67.9 | 3.04 | 4.4 | 0.23 | 1.4 | 0.8 | 0 | Schibille et al. 2022 | 0.30 | 0.40 |
| Gorgan | green pale transparent | 17.2 | 1.83 | 2.91 | 66.3 | 3.24 | 4.3 | 0.2 | 1.22 | 1.02 | 0 | Schibille et al. 2022 | 0.43 | 0.56 |
| Gorgan | blue pale transparent | 15.9 | 2.69 | 3.07 | 65.2 | 3.37 | 5.4 | 0.19 | 0.92 | 1.61 | 0 | Schibille et al. 2022 | 0.50 | 0.80 |
| Gorgan | green translucent | 17.2 | 2.67 | 3.34 | 60 | 5.07 | 6.03 | 0.22 | 3.24 | 0.78 | 0 | Schibille et al. 2022 | 0.44 | 0.53 |
| Gorgan | blue pale transparent | 15.2 | 3.07 | 3.59 | 63.7 | 3.45 | 6.44 | 0.21 | 1.57 | 1.51 | 0 | Schibille et al. 2022 | 0.48 | 0.89 |
| Gorgan | green translucent | 14.7 | 3.17 | 3.24 | 64.9 | 3.28 | 6.27 | 0.19 | 1.53 | 1.51 | 0 | Schibille et al. 2022 | 0.51 | 0.97 |
| Gorgan | green translucent | 17.6 | 3 | 2.12 | 65.8 | 3.2 | 4.47 | 0.14 | 1.52 | 0.7 | 0 | Schibille et al. 2022 | 0.67 | 0.94 |
| Gorgan | blue dark | 17 | 4.11 | 3.15 | 63.1 | 3.53 | 5.91 | 0.24 | 0.04 | 1.55 | 0 | Schibille et al. 2022 | 0.70 | 1.16 |
| Gorgan | green pale transparent | 15.8 | 3.13 | 2.88 | 67.9 | 3.94 | 4.54 | 0.11 | 0.08 | 0.48 | 0 | Schibille et al. 2022 | 0.69 | 0.79 |
| Gorgan | aqua | 16.1 | 2.91 | 2.77 | 66.1 | 3.65 | 4.81 | 0.17 | 0.98 | 1.09 | 0 | Schibille et al. 2022 | 0.60 | 0.80 |
| Gorgan | aqua | 17.3 | 4.39 | 3.19 | 63.7 | 3.44 | 4.79 | 0.26 | 0.46 | 1.09 | 0 | Schibille et al. 2022 | 0.92 | 1.28 |
| Gorgan | green yellowish transparent | 17.7 | 4.07 | 2.87 | 62.4 | 3.11 | 6.2 | 0.14 | 0.82 | 1.31 | 0 | Schibille et al. 2022 | 0.66 | 1.31 |

| | | | | | | | | | | | | | | |
|----------|-----------------------------|-------|------|------|-------|------|------|------|------|------|------|-----------------------|------|------|
| Gorgan | green yellowish transparent | 19.6 | 4.03 | 2.9 | 61.7 | 3.29 | 5.98 | 0.12 | 0.14 | 0.71 | 0 | Schibille et al. 2022 | 0.67 | 1.22 |
| Gorgan | green translucent | 16.7 | 4.44 | 2.95 | 64.4 | 2.99 | 5.54 | 0.23 | 0.31 | 1.22 | 0 | Schibille et al. 2022 | 0.80 | 1.48 |
| Gorgan | colourless | 11.7 | 5.06 | 1.18 | 71.5 | 1.98 | 6.99 | 0.04 | 0.43 | 0.35 | 0 | Schibille et al. 2022 | 0.72 | 2.56 |
| Gorgan | colourless | 12.6 | 4.91 | 1.04 | 71.7 | 2.29 | 5.9 | 0.03 | 0.42 | 0.27 | 0 | Schibille et al. 2022 | 0.83 | 2.14 |
| Gorgan | colourless | 11 | 5.02 | 1.14 | 71.3 | 2.35 | 7.64 | 0.03 | 0.45 | 0.23 | 0 | Schibille et al. 2022 | 0.66 | 2.14 |
| Gorgan | colourless | 11.1 | 4.99 | 1.05 | 72.7 | 2.28 | 6.52 | 0.03 | 0.34 | 0.23 | 0 | Schibille et al. 2022 | 0.77 | 2.19 |
| Gorgan | colourless | 12 | 5.18 | 0.87 | 72.1 | 2.55 | 5.97 | 0.03 | 0.32 | 0.22 | 0 | Schibille et al. 2022 | 0.87 | 2.03 |
| Gorgan | colourless | 12 | 4.29 | 1.02 | 72.3 | 2.42 | 6.58 | 0.04 | 0.42 | 0.35 | 0 | Schibille et al. 2022 | 0.65 | 1.77 |
| Gorgan | colourless | 15.1 | 6.29 | 1.15 | 68 | 3.2 | 4.78 | 0.06 | 0.36 | 0.28 | 0 | Schibille et al. 2022 | 1.32 | 1.97 |
| Gorgan | blue greenish opaque | 10.2 | 1.3 | 0.81 | 49.4 | 1.48 | 3.29 | 0.03 | 0.04 | 0.47 | 0 | Schibille et al. 2022 | 0.40 | 0.88 |
| Gorgan | aqua | 11.2 | 2.89 | 0.73 | 71.7 | 1.49 | 10.6 | 0.05 | 0.07 | 0.26 | 0 | Schibille et al. 2022 | 0.27 | 1.94 |
| Al Raqqa | C/BR | 11.77 | 2.71 | 3.46 | 66.83 | 1.42 | 6 | 0.27 | 3.76 | 2.32 | 0.08 | Henderson et al. 2004 | 0.45 | 1.91 |
| Al Raqqa | C/P | 14.27 | 3.95 | 1 | 67.84 | 2.39 | 8.26 | 0.06 | 0.41 | 0.47 | 0 | Henderson et al. 2004 | 0.48 | 1.65 |
| Al Raqqa | G | 10.85 | 3.74 | 1.32 | 69.33 | 2.26 | 9.38 | 0.09 | 1.07 | 0.63 | 0.08 | Henderson et al. 2004 | 0.40 | 1.65 |
| Al Raqqa | pG | 13.35 | 3.94 | 1.02 | 68.57 | 2.45 | 8.13 | 0.07 | 0.44 | 0.42 | 0.21 | Henderson et al. 2004 | 0.48 | 1.61 |
| Al Raqqa | aG | 15.89 | 2.77 | 2.35 | 63.83 | 3.4 | 6.72 | 0.11 | 2.42 | 1.04 | 0 | Henderson et al. 2004 | 0.41 | 0.81 |

| | | | | | | | | | | | | | | |
|----------|----|---------------|----------|----------|---------------|--------------|---------------|----------|----------|----------|---|---------------------------------|------|------|
| Al Raqqa | P | 11 .4 3 | 3. 62 | 1.1 8 | 68 .2 1 | 2. 2 5 | 10 .4 | 0. 06 | 0. 86 | 0.5 1 | 0 | Hend erson et al. 2004 | 0.35 | 1.61 |
| Al Raqqa | G | 13 .0 7 | 0. 52 | 3.3 2 | 69 .8 9 | 0. 5 1 | 11 .0 3 | 0. 06 | 0 | 0.4 3 | 0 | Hend erson et al. 2004 | 0.05 | 1.02 |
| Al Raqqa | C | 15 .0 2 | 4. 04 | 1.1 3 | 66 .3 4 | 2. 4 2 | 8. 83 | 0. 06 | 0. 36 | 0.5 0 | 0 | Hend erson et al. 2004 | 0.46 | 1.67 |
| Al Raqqa | GR | 11 | 6 | 0.5 8 | 69 .5 6 | 1. 4 8 | 7. 36 | 0 | 0 | 0.5 2 | 0 | Hend erson et al. 2004 | 0.82 | 4.05 |
| Al Raqqa | G | 13 .1 | 6. 3 | 1 | 67 .6 4 | 3 | 6. 9 | 0 | 0. 53 | 0.2 6 | 0 | Hend erson et al. 2004 | 0.91 | 2.10 |
| Al Raqqa | G | 12 .5 | 6 | 0.9 | 70 .3 3 | 2. 3 | 5. 9 | 0 | 0. 55 | 0.2 7 | 0 | Hend erson et al. 2004 | 1.02 | 2.61 |
| Al Raqqa | dG | 15 .4 | 3. 4 | 3.5 | 61 .6 2 | 2. 6 | 8. 8 | 0 | 2 | 1.1 | 0 | Hend erson et al. 2004 | 0.39 | 1.31 |
| Al Raqqa | B | 15 .7 3 | 3. 65 | 1.1 3 | 65 .2 8 | 2. 6 6 | 8. 23 | 0. 07 | 0. 86 | 0.7 2 | 0 | Hend erson et al. 2004 | 0.44 | 1.37 |
| Al Raqqa | BR | 14 .9 4 | 4. 18 | 0.9 7 | 66 .1 | 2. 4 1 | 9. 3 | 0 | 0 | 0.3 4 | 0 | Hend erson et al. 2004 | 0.45 | 1.73 |
| Al Raqqa | P | 12 .6 8 | 4. 21 | 1.2 9 | 68 .2 5 | 2. 5 2 | 8. 7 | 0. 07 | 0. 8 | 0.5 8 | 0 | Hend erson et al. 2004 | 0.48 | 1.67 |
| Al Raqqa | P | 11 .8 6 | 3. 36 | 1.1 | 71 .3 4 | 2. 3 | 7. 17 | 0. 06 | 1. 43 | 0.4 7 | 0 | Hend erson et al. 2004 | 0.47 | 1.46 |
| Al Raqqa | P | 8. 76 | 2. 38 | 4.1 4 | 63 .3 9 | 3. 0 7 | 6. 34 | 0. 22 | 8. 54 | 2.2 9 | 0 | Hend erson et al. 2004 | 0.38 | 0.78 |
| Al Raqqa | C | 12 .6 1 | 2. 34 | 4.3 3 | 64 .4 3 | 4. 9 9 | 4. 94 | 0. 22 | 3. 11 | 1.4 5 | 0 | Hend erson et al. 2004 | 0.47 | 0.47 |
| Al Raqqa | B | 14 .4 9 | 3. 87 | 1.1 3 | 65 .5 4 | 2. 4 9 | 8. 66 | 0. 07 | 0. 99 | 1.2 5 | 0 | Hend erson et al. 2004 | 0.45 | 1.55 |
| Al Raqqa | OR | 13 .9 1 | 3. 74 | 2.3 7 | 64 .7 | 2. 5 7 | 8. 45 | 0. 11 | 1. 11 | 1.2 8 | 0 | Hend erson et al. 2004 | 0.44 | 1.46 |
| Al Raqqa | P | 13 .1 6 | 3. 35 | 1.1 6 | 68 .0 2 | 2. 2 3 | 7. 36 | 0. 06 | 2. 75 | 0.4 2 | 0 | Hend erson et al. 2004 | 0.46 | 1.50 |

| | | | | | | | | | | | | | | |
|----------|----|---------------|----------|----------|---------------|--------------|---------------|----------|----------|----------|----------|-----------------------|------|------|
| Al Raqqa | G | 11 .6 8 | 2. 67 | 2.0 2 | 69 .8 8 | 1. 5 5 | 4. 21 | 0. 22 | 4. 88 | 1.7 2 | 0 | Henderson et al. 2004 | 0.63 | 1.72 |
| Al Raqqa | A | 13 .9 8 | 3. 56 | 1.3 1 | 66 .6 8 | 2. 4 1 | 8. 87 | 0. 07 | 1. 06 | 0.5 8 | 0 | Henderson et al. 2004 | 0.40 | 1.48 |
| Al Raqqa | pG | 13 .4 2 | 6. 86 | 1.3 7 | 66 .7 1 | 3. 4 1 | 5. 25 | 0. 06 | 1. 43 | 0.4 2 | 0 | Henderson et al. 2004 | 1.31 | 2.01 |
| Al Raqqa | pG | 14 .3 2 | 3. 34 | 1.3 2 | 66 .7 5 | 2. 5 5 | 8. 15 | 0. 07 | 1. 45 | 0.5 3 | 0 | Henderson et al. 2004 | 0.41 | 1.31 |
| Al Raqqa | B | 15 .3 6 | 3. 72 | 1.2 7 | 63 .5 2 | 2. 7 1 | 10 .7 3 | 0. 06 | 0. 25 | 0.7 1 | 0 | Henderson et al. 2004 | 0.35 | 1.37 |
| Al Raqqa | G | 15 .9 1 | 2. 52 | 2.0 7 | 67 .4 9 | 2. 2 5 | 5. 04 | 0. 13 | 2. 13 | 0.9 1 | 0 | Henderson et al. 2004 | 0.50 | 1.12 |
| Al Raqqa | C | 13 .1 1 | 1. 24 | 3.1 8 | 70 .1 6 | 0. 9 2 | 9. 69 | 0. 06 | 0. 12 | 0.5 8 | 0 | Henderson et al. 2004 | 0.13 | 1.35 |
| Al Raqqa | pG | 13 .7 5 | 0. 54 | 3.4 9 | 71 .1 | 0. 5 1 | 9 | 0 | 0 | 0.4 3 | 0 | Henderson et al. 2004 | 0.06 | 1.06 |
| Al Raqqa | G | 14 .4 1 | 2. 96 | 1.5 | 66 .4 7 | 2. 9 8 | 7. 1 | 0. 09 | 2. 16 | 0.7 4 | 0 | Henderson et al. 2004 | 0.42 | 0.99 |
| Al Raqqa | pG | 15 .8 2 | 4. 88 | 2.3 6 | 63 .1 9 | 2. 8 2 | 7. 89 | 0. 07 | 0. 86 | 0.6 9 | 0 | Henderson et al. 2004 | 0.62 | 1.73 |
| Al Raqqa | pG | 15 .5 1 | 6. 33 | 1.4 8 | 66 .5 4 | 2. 6 2 | 4. 54 | 0. 06 | 1. 44 | 0.4 3 | 0 | Henderson et al. 2004 | 1.39 | 2.42 |
| Al Raqqa | pG | 13 .2 3 | 3. 39 | 1.3 1 | 68 .5 1 | 2. 4 | 7. 33 | 0. 07 | 1. 91 | 0.4 5 | 0 | Henderson et al. 2004 | 0.46 | 1.41 |
| Al Raqqa | C | 13 .5 3 | 3. 78 | 1.1 2 | 67 .6 5 | 2. 5 6 | 8. 65 | 0. 06 | 0. 66 | 0.3 7 | 0 | Henderson et al. 2004 | 0.44 | 1.48 |
| Al Raqqa | C | 13 .7 3 | 3. 62 | 1.1 1 | 67 .2 3 | 2. 4 8 | 8. 36 | 0. 06 | 1. 53 | 0.3 6 | 0.0 9 | Henderson et al. 2004 | 0.43 | 1.46 |
| Al Raqqa | P | 15 .1 8 | 2. 47 | 1.9 | 67 .8 7 | 2. 1 2 | 5. 37 | 0. 09 | 2. 65 | 0.8 5 | 0 | Henderson et al. 2004 | 0.46 | 1.17 |
| Al Raqqa | pG | 13 .5 5 | 3. 57 | 1.1 2 | 67 .4 7 | 2. 5 1 | 8. 23 | 0. 06 | 1. 62 | 0.3 4 | 0.0 5 | Henderson et al. 2004 | 0.43 | 1.42 |

| | | | | | | | | | | | | | | |
|----------|-----|---------------|----------|----------|---------------|--------------|----------|----------|----------|----------|----------|-----------------------|------|------|
| Al Raqqa | pG | 15 .6 1 | 2. 49 | 1.6 2 | 68 .8 6 | 2. 2 2 | 5. 24 | 0. 07 | 1. 88 | 0.5 8 | 0 | Henderson et al. 2004 | 0.48 | 1.12 |
| Al Raqqa | pG | 15 .8 1 | 2. 5 | 1.5 8 | 68 .1 4 | 2. 3 1 | 5. 35 | 0. 09 | 1. 93 | 0.6 2 | 0.0 5 | Henderson et al. 2004 | 0.47 | 1.08 |
| Al Raqqa | P | 13 .3 8 | 3. 45 | 1.1 3 | 67 .4 1 | 2. 4 3 | 9. 04 | 0. 06 | 1. 29 | 0.3 7 | 0 | Henderson et al. 2004 | 0.38 | 1.42 |
| Al Raqqa | Y/G | 13 .8 2 | 3. 23 | 1.0 1 | 66 .0 7 | 2. 5 8 | 9. 42 | 0. 06 | 1. 92 | 0.4 3 | 0.0 5 | Henderson et al. 2004 | 0.34 | 1.25 |
| Al Raqqa | C | 13 .5 5 | 3. 59 | 1.1 4 | 67 .7 7 | 2. 5 2 | 8. 1 | 0. 06 | 0. 87 | 0.9 7 | 0 | Henderson et al. 2004 | 0.44 | 1.42 |
| Al Raqqa | G | 13 .3 6 | 4. 22 | 1.9 7 | 64 .8 2 | 2. 3 4 | 9. 29 | 0. 12 | 1. 6 | 0.9 | 0.0 9 | Henderson et al. 2004 | 0.45 | 1.80 |
| Al Raqqa | A | 14 .5 4 | 0. 57 | 3.2 4 | 70 | 0. 5 2 | 9. 49 | 0. 05 | 0 | 0.3 7 | 0.0 7 | Henderson et al. 2004 | 0.06 | 1.10 |
| Al Raqqa | T | 14 .8 2 | 1. 06 | 2.3 9 | 69 .2 9 | 1. 0 4 | 7. 62 | 0. 07 | 0. 15 | 0.5 6 | 0.1 8 | Henderson et al. 2004 | 0.14 | 1.02 |
| Al Raqqa | G | 12 .7 7 | 4. 75 | 3.4 7 | 63 .3 4 | 2. 9 7 | 8. 79 | 0. 18 | 0. 75 | 1.6 9 | 0 | Henderson et al. 2004 | 0.54 | 1.60 |
| Al Raqqa | pG | 14 .7 7 | 4. 53 | 3.0 3 | 62 .3 4 | 1. 8 7 | 8. 27 | 0. 13 | 2. 34 | 1.1 7 | 0 | Henderson et al. 2004 | 0.55 | 2.42 |
| Al Raqqa | A | 12 .7 5 | 0. 74 | 3.1 9 | 72 .4 6 | 0. 5 8 | 8. 68 | 0. 06 | 0 | 0.4 4 | 0 | Henderson et al. 2004 | 0.09 | 1.28 |
| Al Raqqa | C | 12 .8 5 | 5. 32 | 1.0 6 | 70 .9 2 | 2. 1 1 | 6. 05 | 0 | 0. 24 | 0.2 6 | 0.0 6 | Henderson et al. 2004 | 0.88 | 2.52 |
| Al Raqqa | pG | 13 .1 6 | 6. 33 | 1.2 6 | 69 .5 1 | 3. 0 3 | 4. 7 | 0. 05 | 0. 59 | 0.3 3 | 0 | Henderson et al. 2004 | 1.35 | 2.09 |
| Al Raqqa | A | 13 .9 6 | 0. 6 | 3.2 6 | 70 .7 4 | 0. 5 9 | 9. 36 | 0. 06 | 0 | 0.3 5 | 0 | Henderson et al. 2004 | 0.06 | 1.02 |
| Al Raqqa | B | 14 .6 1 | 8. 05 | 1.3 1 | 65 .1 | 3. 1 2 | 5. 88 | 0. 07 | 0. 27 | 0.4 2 | 0.0 7 | Henderson et al. 2004 | 1.37 | 2.58 |
| Al Raqqa | pG | 17 .1 | 7. 57 | 1.0 9 | 64 .0 2 | 3. 3 1 | 4. 46 | 0 | 0. 88 | 0.3 4 | 0 | Henderson et al. 2004 | 1.70 | 2.29 |

| | | | | | | | | | | | | | | |
|----------|----|---------------|----------|----------|---------------|--------------|---------------|----------|----------|----------|----------|---------------------------------|------|------|
| Al Raqqa | pG | 13 .7 4 | 0. 57 | 3.3 8 | 68 .8 1 | 0. 5 | 11 .3 2 | 0. 07 | 0 | 0.3 2 | 0 | Hend erson et al. 2004 | 0.05 | 1.14 |
| Al Raqqa | pG | 14 .6 3 | 4. 29 | 2.7 8 | 64 .5 | 2. 6 3 | 7. 75 | 0. 13 | 0. 89 | 0.9 5 | 0.1 1 | Hend erson et al. 2004 | 0.55 | 1.63 |
| Al Raqqa | pG | 13 .6 6 | 4. 41 | 2.9 6 | 65 .1 9 | 3. 9 9 | 6. 79 | 0. 13 | 0. 3 | 1.1 6 | 0 | Hend erson et al. 2004 | 0.65 | 1.11 |
| Al Raqqa | G | 13 .7 2 | 4. 1 | 2.3 9 | 67 .4 4 | 4. 2 | 5. 89 | 0. 11 | 0 | 0.8 8 | 0.0 8 | Hend erson et al. 2004 | 0.70 | 0.98 |
| Al Raqqa | pG | 13 .3 8 | 4. 5 | 2.0 8 | 69 .1 | 3. 2 | 5. 65 | 0. 1 | 0 | 0.8 5 | 0.0 6 | Hend erson et al. 2004 | 0.80 | 1.41 |
| Al Raqqa | pG | 13 .4 1 | 4. 54 | 2.0 8 | 69 .0 4 | 3. 2 5 | 5. 61 | 0. 07 | 0. 05 | 0.7 9 | 0.0 6 | Hend erson et al. 2004 | 0.81 | 1.40 |
| Al Raqqa | pG | 13 .1 6 | 5. 75 | 2.2 1 | 68 .3 | 2. 7 5 | 5. 73 | 0. 13 | 0 | 0.9 1 | 0 | Hend erson et al. 2004 | 1.00 | 2.09 |
| Al Raqqa | A | 13 .6 4 | 0. 52 | 3.2 2 | 70 .6 6 | 0. 4 7 | 9. 86 | 0. 05 | 0 | 0.3 7 | 0 | Hend erson et al. 2004 | 0.05 | 1.11 |
| Al Raqqa | pG | 13 .4 | 0. 47 | 3.0 9 | 72 .9 7 | 0. 4 5 | 8. 18 | 0. 06 | 0 | 0.2 9 | 0 | Hend erson et al. 2004 | 0.06 | 1.04 |
| Al Raqqa | A | 12 .5 7 | 0. 5 | 3.1 4 | 72 .0 4 | 0. 4 8 | 9. 75 | 0. 05 | 0 | 0.3 8 | 0.0 8 | Hend erson et al. 2004 | 0.05 | 1.04 |
| Al Raqqa | pG | 12 .7 4 | 5. 1 | 1.5 7 | 70 .8 7 | 3. 4 2 | 4. 52 | 0. 06 | 0. 29 | 0.5 1 | 0.0 5 | Hend erson et al. 2004 | 1.13 | 1.49 |
| Al Raqqa | BR | 15 .0 5 | 0. 97 | 3.4 2 | 67 .1 9 | 0. 7 3 | 10 .9 | 0. 07 | 0 | 0.4 7 | 0.0 5 | Hend erson et al. 2004 | 0.09 | 1.33 |
| Al Raqqa | pG | 14 .1 7 | 1. 98 | 2.8 7 | 69 .5 6 | 1. 2 8 | 8. 51 | 0. 05 | 0. 09 | 0.4 8 | 0.0 9 | Hend erson et al. 2004 | 0.23 | 1.55 |
| Al Raqqa | pG | 14 .7 3 | 6. 2 | 1.5 1 | 68 .6 | 2. 8 2 | 4. 32 | 0. 07 | 0. 18 | 0.4 7 | 0 | Hend erson et al. 2004 | 1.44 | 2.20 |
| Al Raqqa | pG | 14 .5 1 | 6. 24 | 1.5 3 | 68 .7 8 | 2. 7 5 | 4. 35 | 0. 07 | 0. 21 | 0.4 9 | 0.0 6 | Hend erson et al. 2004 | 1.43 | 2.27 |
| Al Raqqa | pG | 13 .1 6 | 0. 5 | 3.1 4 | 71 .7 6 | 0. 4 6 | 9. 49 | 0 | 0 | 0.3 3 | 0 | Hend erson et al. 2004 | 0.05 | 1.09 |

| | | | | | | | | | | | | | | |
|----------|----|---------------|----------|----------|---------------|--------------|----------|----------|----------|----------|----------|---------------------------------|------|------|
| Al Raqqa | pG | 13 .9 6 | 4. 52 | 1.7 | 69 .1 5 | 3. 0 9 | 4. 41 | 0. 07 | 1. 3 | 0.6 | 0.0 7 | Hend erson et al. 2004 | 1.02 | 1.46 |
| Al Raqqa | pG | 12 .9 2 | 0. 44 | 3.0 3 | 73 .6 3 | 0. 4 4 | 8. 16 | 0. 05 | 0 | 0.3 1 | 0 | Hend erson et al. 2004 | 0.05 | 1.00 |
| Al Raqqa | oG | 14 .6 2 | 4. 75 | 2.5 8 | 64 .0 6 | 2. 5 9 | 7. 31 | 0. 11 | 1. 97 | 0.8 9 | 0 | Hend erson et al. 2004 | 0.65 | 1.83 |
| Al Raqqa | pG | 12 .7 6 | 0. 68 | 3.2 1 | 73 .1 6 | 0. 5 8 | 8. 17 | 0. 05 | 0 | 0.4 | 0 | Hend erson et al. 2004 | 0.08 | 1.17 |
| Al Raqqa | pG | 14 .2 7 | 4. 07 | 2.5 7 | 66 .3 7 | 3. 5 3 | 6. 35 | 0. 11 | 0. 4 | 1.1 1 | 0 | Hend erson et al. 2004 | 0.64 | 1.15 |
| Al Raqqa | pG | 13 .3 5 | 0. 78 | 3.5 1 | 72 .9 6 | 0. 5 2 | 7. 12 | 0. 07 | 0 | 0.4 5 | 0.1 3 | Hend erson et al. 2004 | 0.11 | 1.50 |
| Al Raqqa | oG | 15 .7 2 | 3. 74 | 3.6 4 | 64 .7 8 | 3. 1 3 | 6. 74 | 0. 11 | 0 | 0.9 5 | 0 | Hend erson et al. 2004 | 0.55 | 1.19 |
| Al Raqqa | G | 14 .4 7 | 3. 4 | 1.4 | 68 .2 2 | 2. 3 5 | 6. 62 | 0. 08 | 1. 36 | 0.7 6 | 0 | Hend erson et al. 2004 | 0.51 | 1.45 |
| Al Raqqa | pG | 14 .7 7 | 4. 15 | 1.9 2 | 68 .0 6 | 3. 8 2 | 5 | 0. 07 | 0. 21 | 0.7 7 | 0 | Hend erson et al. 2004 | 0.83 | 1.09 |
| Al Raqqa | dB | 12 .8 | 3. 11 | 1.8 5 | 69 .5 9 | 1. 5 9 | 5. 11 | 0. 05 | 1. 1 | 2.9 5 | 0 | Hend erson et al. 2004 | 0.61 | 1.96 |
| Al Raqqa | pG | 14 .1 6 | 4. 33 | 1.8 1 | 69 .2 8 | 3. 6 5 | 4. 88 | 0. 07 | 0. 05 | 0.6 7 | 0.0 5 | Hend erson et al. 2004 | 0.89 | 1.19 |
| Al Raqqa | pG | 13 .3 4 | 5. 03 | 2.7 3 | 67 .0 9 | 3. 1 5 | 6. 27 | 0. 13 | 0. 1 | 1.0 4 | 0 | Hend erson et al. 2004 | 0.80 | 1.60 |
| Al Raqqa | pG | 15 .0 8 | 0. 65 | 3.2 9 | 69 .7 | 0. 4 7 | 9. 45 | 0. 06 | 0 | 0.3 2 | 0 | Hend erson et al. 2004 | 0.07 | 1.38 |
| Al Raqqa | pG | 13 .1 3 | 3. 51 | 2.5 7 | 69 .7 | 3. 1 3 | 5. 52 | 0. 13 | 0. 14 | 1.0 6 | 0 | Hend erson et al. 2004 | 0.64 | 1.12 |
| Al Raqqa | pG | 12 .6 7 | 5. 48 | 1.4 2 | 71 .7 7 | 2. 6 | 4. 15 | 0. 06 | 0. 53 | 0.4 5 | 0 | Hend erson et al. 2004 | 1.32 | 2.11 |
| Al Raqqa | oG | 14 .6 4 | 3. 75 | 3.8 8 | 65 .2 7 | 3. 1 2 | 6. 47 | 0. 15 | 0. 15 | 1.4 2 | 0 | Hend erson et al. 2004 | 0.58 | 1.20 |

| | | | | | | | | | | | | | | |
|----------|----|-------|------|------|-------|------|-------|------|------|------|------|-----------------------|------|------|
| Al Raqqa | pG | 15.3 | 0.58 | 3.17 | 71.1 | 0.51 | 7.77 | 0.06 | 0 | 0.32 | 0 | Henderson et al. 2004 | 0.07 | 1.14 |
| Al Raqqa | pG | 13.07 | 4.16 | 2.06 | 70.72 | 2.2 | 4.49 | 0.08 | 1.04 | 0.87 | 0.07 | Henderson et al. 2004 | 0.93 | 1.89 |
| Al Raqqa | pG | 14.53 | 6.53 | 1.47 | 67.53 | 2.92 | 5.05 | 0 | 0.54 | 0.45 | 0 | Henderson et al. 2004 | 1.29 | 2.24 |
| Al Raqqa | pG | 14.74 | 0.91 | 3.39 | 69.34 | 0.73 | 9.51 | 0.07 | 0 | 0.55 | 0 | Henderson et al. 2004 | 0.10 | 1.25 |
| Al Raqqa | pG | 13.76 | 5.32 | 2.27 | 67.32 | 2.83 | 6.14 | 0.11 | 0.23 | 0.91 | 0 | Henderson et al. 2004 | 0.87 | 1.88 |
| Al Raqqa | C | 13.51 | 3 | 1.05 | 69.02 | 2.49 | 7.48 | 0.05 | 1.75 | 0.3 | 0 | Henderson et al. 2004 | 0.40 | 1.20 |
| Al Raqqa | pB | 12.7 | 3.24 | 2.86 | 68.62 | 1.81 | 6.23 | 0.12 | 0.63 | 2.19 | 0.1 | Henderson et al. 2004 | 0.52 | 1.79 |
| Al Raqqa | dB | 12.54 | 3.04 | 1.87 | 69.56 | 1.59 | 5.18 | 0.07 | 1.05 | 3.07 | 0.18 | Henderson et al. 2004 | 0.59 | 1.91 |
| Al Raqqa | B | 13.62 | 3.04 | 3.21 | 66.91 | 2.55 | 6.6 | 0.09 | 0.09 | 1.91 | 0 | Henderson et al. 2004 | 0.46 | 1.19 |
| Al Raqqa | dG | 13.55 | 4.6 | 2.77 | 65.68 | 2.65 | 5.84 | 0.08 | 2.59 | 0.99 | 0 | Henderson et al. 2004 | 0.79 | 1.74 |
| Al Raqqa | pG | 14.76 | 4.22 | 2.69 | 64.4 | 2.52 | 8.45 | 0.1 | 0.84 | 0.98 | 0.08 | Henderson et al. 2004 | 0.50 | 1.67 |
| Al Raqqa | C | 14.08 | 3.69 | 0.87 | 67.52 | 2.4 | 8.4 | 0 | 1.34 | 0.28 | 0 | Henderson et al. 2004 | 0.44 | 1.54 |
| Al Raqqa | pG | 14.24 | 4.61 | 5.32 | 59.53 | 3.35 | 8.27 | 0.2 | 0.83 | 2.29 | 0 | Henderson et al. 2004 | 0.56 | 1.38 |
| Al Raqqa | pG | 14.46 | 0.59 | 3.11 | 69.75 | 0.57 | 10.04 | 0 | 0 | 0.37 | 0 | Henderson et al. 2004 | 0.06 | 1.04 |
| Al Raqqa | A | 13.66 | 0.49 | 3.02 | 73.06 | 0.42 | 7.73 | 0.05 | 0 | 0.34 | 0.12 | Henderson et al. 2004 | 0.06 | 1.17 |
| Al Raqqa | pG | 15.43 | 0.45 | 2.88 | 71.13 | 0.44 | 8.32 | 0 | 0 | 0.25 | 0 | Henderson et al. 2004 | 0.05 | 1.02 |

| | | | | | | | | | | | | | | |
|----------|----|-------|------|------|-------|------|-------|------|------|------|------|-----------------------|------|------|
| Al Raqqa | pG | 14.3 | 4.19 | 2.63 | 65.72 | 3.66 | 6.56 | 0.13 | 0.44 | 1.14 | 0.05 | Henderson et al. 2004 | 0.64 | 1.14 |
| Al Raqqa | pG | 12.11 | 3.04 | 1.16 | 69.76 | 2.33 | 7.94 | 0.06 | 2.07 | 0.43 | 0 | Henderson et al. 2004 | 0.38 | 1.32 |
| Al Raqqa | pG | 14.92 | 3.11 | 1.56 | 67.48 | 3 | 6.47 | 0.09 | 1.41 | 0.69 | 0 | Henderson et al. 2004 | 0.48 | 1.04 |
| Al Raqqa | pG | 12.43 | 0.77 | 3.13 | 73.66 | 0.55 | 7.87 | 0.05 | 0 | 0.4 | 0.06 | Henderson et al. 2004 | 0.10 | 1.40 |
| Al Raqqa | C | 15.25 | 0.53 | 3.12 | 71.17 | 0.52 | 7.86 | 0 | 0 | 0.33 | 0 | Henderson et al. 2004 | 0.07 | 1.02 |
| Al Raqqa | A | 13.7 | 0.51 | 3.08 | 71.12 | 0.47 | 9.68 | 0 | 0 | 0.29 | 0 | Henderson et al. 2004 | 0.05 | 1.09 |
| Al Raqqa | pP | 13.32 | 3.3 | 0.88 | 68.78 | 2.54 | 8.12 | 0.06 | 1.43 | 0.31 | 0 | Henderson et al. 2004 | 0.41 | 1.30 |
| Al Raqqa | pG | 12.91 | 0.54 | 3.15 | 72.58 | 0.56 | 8.81 | 0.08 | 0 | 0.53 | 0 | Henderson et al. 2004 | 0.06 | 0.96 |
| Al Raqqa | C | 12.88 | 0.48 | 3.12 | 71.84 | 0.46 | 9.71 | 0 | 0 | 0.31 | 0.07 | Henderson et al. 2004 | 0.05 | 1.04 |
| Al Raqqa | pG | 13.86 | 0.54 | 2.66 | 73.23 | 0.47 | 7.75 | 0.05 | 0 | 0.43 | 0 | Henderson et al. 2004 | 0.07 | 1.15 |
| Al Raqqa | pG | 13.11 | 4.58 | 1.55 | 71.02 | 2.97 | 4.22 | 0.07 | 0.75 | 0.5 | 0.06 | Henderson et al. 2004 | 1.09 | 1.54 |
| Al Raqqa | pG | 13.45 | 1.43 | 2.95 | 70.06 | 1.06 | 9.31 | 0.06 | 0.17 | 0.6 | 0 | Henderson et al. 2004 | 0.15 | 1.35 |
| Al Raqqa | C | 13.95 | 5.03 | 1.77 | 68.21 | 2.99 | 4.55 | 0.09 | 1.62 | 0.63 | 0 | Henderson et al. 2004 | 1.11 | 1.68 |
| Al Raqqa | pG | 13.6 | 1.41 | 2.99 | 70.46 | 0.97 | 8.83 | 0.07 | 0.17 | 0.53 | 0.07 | Henderson et al. 2004 | 0.16 | 1.45 |
| Al Raqqa | pG | 12.67 | 4.46 | 2.02 | 70.82 | 2.88 | 5.01 | 0.09 | 0.21 | 0.86 | 0 | Henderson et al. 2004 | 0.89 | 1.59 |
| Al Raqqa | C | 14.43 | 0.69 | 3.2 | 68.23 | 0.52 | 11.44 | 0 | 0 | 0.44 | 0.08 | Henderson et al. 2004 | 0.06 | 1.33 |

| | | | | | | | | | | | | | | |
|----------|----|---------------|----------|----------|---------------|--------------|----------|----------|----------|----------|----------|-----------------------|------|------|
| Al Raqqa | A | 13 .2 1 | 0. 48 | 3.1 8 | 71 .9 2 | 0. 4 9 | 9. 32 | 0 | 0 | 0.3 3 | 0 | Henderson et al. 2004 | 0.05 | 0.98 |
| Al Raqqa | pG | 15 .9 1 | 0. 61 | 3.1 4 | 70 .1 3 | 0. 5 4 | 7. 97 | 0. 05 | 0 | 0.3 7 | 0.1 | Henderson et al. 2004 | 0.08 | 1.13 |
| Al Raqqa | A | 12 .5 5 | 0. 47 | 3.1 | 73 .6 1 | 0. 4 | 8. 41 | 0 | 0 | 0.2 6 | 0 | Henderson et al. 2004 | 0.06 | 1.18 |
| Al Raqqa | pG | 14 .5 4 | 0. 61 | 3.2 1 | 70 .4 8 | 0. 6 1 | 8. 84 | 0 | 0 | 0.4 3 | 0.1 1 | Henderson et al. 2004 | 0.07 | 1.00 |
| Al Raqqa | pG | 13 .2 | 0. 53 | 3.2 1 | 72 .1 | 0. 4 9 | 8. 89 | 0 | 0 | 0.3 5 | 0 | Henderson et al. 2004 | 0.06 | 1.08 |
| Al Raqqa | A | 13 .9 4 | 1. 86 | 2.7 9 | 70 .2 | 1. 0 3 | 8. 6 | 0. 06 | 0. 12 | 0.4 3 | 0.0 5 | Henderson et al. 2004 | 0.22 | 1.81 |
| Al Raqqa | pG | 13 .7 4 | 1. 23 | 2.9 8 | 70 .6 6 | 0. 8 6 | 8. 77 | 0. 07 | 0. 15 | 0.6 5 | 0 | Henderson et al. 2004 | 0.14 | 1.43 |
| Al Raqqa | pG | 13 .2 5 | 3. 23 | 0.8 6 | 69 .0 1 | 2. 5 1 | 8. 08 | 0. 06 | 1. 41 | 0.2 6 | 0 | Henderson et al. 2004 | 0.40 | 1.29 |
| Al Raqqa | pG | 13 .3 2 | 3. 87 | 2.0 4 | 68 .5 3 | 3. 3 5 | 4. 96 | 0. 1 | 1. 8 | 0.8 6 | 0.0 8 | Henderson et al. 2004 | 0.78 | 1.16 |
| Al Raqqa | A | 13 .4 5 | 1. 34 | 2.8 3 | 71 .1 1 | 0. 8 4 | 8. 9 | 0. 07 | 0. 07 | 0.4 2 | 0.1 1 | Henderson et al. 2004 | 0.15 | 1.60 |
| Al Raqqa | pG | 13 .4 | 1. 32 | 2.9 7 | 69 .9 4 | 0. 8 8 | 9. 79 | 0. 07 | 0. 15 | 0.5 2 | 0.2 1 | Henderson et al. 2004 | 0.13 | 1.50 |
| Al Raqqa | oG | 13 .7 3 | 2. 32 | 3.5 3 | 67 .3 1 | 2. 3 | 8. 27 | 0. 12 | 0. 13 | 1.2 1 | 0.1 2 | Henderson et al. 2004 | 0.28 | 1.01 |
| Al Raqqa | A | 14 .2 6 | 0. 52 | 4.6 2 | 69 .9 1 | 0. 4 8 | 8. 75 | 0 | 0. 05 | 0.2 1 | 0 | Henderson et al. 2004 | 0.06 | 1.08 |
| Al Raqqa | oG | 15 .0 1 | 4. 28 | 4.2 4 | 62 .0 3 | 3. 3 8 | 7. 63 | 0. 19 | 0. 19 | 1.7 1 | 0 | Henderson et al. 2004 | 0.56 | 1.27 |
| Al Raqqa | pG | 12 .8 6 | 3. 83 | 1.0 8 | 67 .3 9 | 2. 5 8 | 8. 98 | 0. 06 | 1. 49 | 0.4 | 0 | Henderson et al. 2004 | 0.43 | 1.48 |
| Al Raqqa | oG | 14 .7 3 | 3. 72 | 4.2 2 | 63 .8 4 | 3. 4 1 | 7. 01 | 0. 16 | 0. 06 | 1.5 4 | 0.0 5 | Henderson et al. 2004 | 0.53 | 1.09 |

| | | | | | | | | | | | | | | |
|----------|----|---------------|----------|----------|---------------|--------------|---------------|----------|----------|----------|---|-----------------------|------|------|
| Al Raqqa | oG | 14 .6 4 | 4. 63 | 3.6 5 | 63 .6 6 | 2. 6 4 | 7. 54 | 0. 15 | 0. 51 | 1.2 9 | 0 | Henderson et al. 2004 | 0.61 | 1.75 |
| Al Raqqa | pG | 15 .7 4 | 3. 08 | 3.2 6 | 62 .9 3 | 2. 4 9 | 7. 85 | 0. 12 | 1. 8 | 1.0 2 | 0 | Henderson et al. 2004 | 0.39 | 1.24 |
| Al Raqqa | oG | 14 .3 3 | 0. 69 | 3.4 2 | 69 .1 3 | 0. 5 5 | 10 .4 3 | 0. 05 | 0 | 0.4 1 | 0 | Henderson et al. 2004 | 0.07 | 1.25 |
| Al Raqqa | C | 12 .8 3 | 5. 51 | 1.1 4 | 70 .4 | 2. 0 4 | 6. 4 | 0 | 0. 27 | 0.3 | 0 | Henderson et al. 2004 | 0.86 | 2.70 |
| Al Raqqa | pB | 12 .9 2 | 0. 41 | 3.2 1 | 74 .9 3 | 0. 5 | 6. 59 | 0. 05 | 0 | 0.3 2 | 0 | Henderson et al. 2004 | 0.06 | 0.82 |
| Al Raqqa | pG | 13 .3 7 | 1 | 3.1 1 | 73 .2 5 | 0. 7 3 | 6. 98 | 0. 07 | 0. 09 | 0.4 1 | 0 | Henderson et al. 2004 | 0.14 | 1.37 |
| Al Raqqa | pG | 13 .2 8 | 0. 48 | 3.3 7 | 72 .1 4 | 0. 5 | 8. 65 | 0. 07 | 0 | 0.3 2 | 0 | Henderson et al. 2004 | 0.06 | 0.96 |
| Al Raqqa | C | 14 .9 6 | 0. 49 | 3.0 9 | 70 .2 3 | 0. 4 8 | 9. 36 | 0. 05 | 0 | 0.3 2 | 0 | Henderson et al. 2004 | 0.05 | 1.02 |
| Al Raqqa | pG | 13 .4 1 | 0. 68 | 3.4 5 | 71 .5 8 | 0. 5 3 | 8. 77 | 0. 05 | 0 | 0.3 9 | 0 | Henderson et al. 2004 | 0.08 | 1.28 |
| Al Raqqa | pG | 15 .8 2 | 3. 72 | 1.0 8 | 64 .3 | 2. 4 8 | 9. 98 | 0. 05 | 0. 64 | 0.3 5 | 0 | Henderson et al. 2004 | 0.37 | 1.50 |
| Al Raqqa | A | 12 .3 8 | 0. 48 | 3.2 8 | 73 .3 9 | 0. 5 8 | 8. 54 | 0 | 0 | 0.2 8 | 0 | Henderson et al. 2004 | 0.06 | 0.83 |
| Al Raqqa | A | 13 .3 3 | 0. 45 | 2.9 8 | 72 .9 7 | 1. 0 4 | 7. 71 | 0. 05 | 0 | 0.3 6 | 0 | Henderson et al. 2004 | 0.06 | 0.43 |
| Al Raqqa | A | 15 .7 2 | 0. 61 | 3.3 8 | 68 .5 8 | 0. 5 1 | 9. 57 | 0. 05 | 0 | 0.3 8 | 0 | Henderson et al. 2004 | 0.06 | 1.20 |
| Al Raqqa | pG | 14 .6 7 | 6. 06 | 1.6 9 | 67 .4 1 | 3. 3 7 | 3. 79 | 0. 09 | 1. 21 | 0.5 3 | 0 | Henderson et al. 2004 | 1.60 | 1.80 |
| Al Raqqa | C | 14 .2 4 | 5. 56 | 1.7 6 | 67 .0 4 | 3 | 4. 86 | 0. 08 | 1. 76 | 0.6 1 | 0 | Henderson et al. 2004 | 1.14 | 1.85 |
| Al Raqqa | pG | 12 .5 5 | 2. 83 | 1.3 9 | 70 .9 5 | 4. 4 5 | 5. 72 | 0. 06 | 0 | 0.4 3 | 0 | Henderson et al. 2004 | 0.49 | 0.64 |

| | | | | | | | | | | | | | | |
|-------------------|------------|---------------|----------|----------|---------------|--------------|---------------|----------|----------|----------|----------|---------------------------------|------|------|
| Al Raqqa | dBR | 20 .6 3 | 4. 69 | 5.7 3 | 59 .9 7 | 2. 2 3 | 4. 22 | 0. 18 | 0 | 1.2 1 | 0 | Hend erson et al. 2004 | 1.11 | 2.10 |
| Al Raqqa | A | 12 .9 5 | 0. 5 | 3.1 6 | 70 .7 | 0. 4 2 | 10 .8 9 | 0. 06 | 0 | 0.3 7 | 0 | Hend erson et al. 2004 | 0.05 | 1.19 |
| Al Raqqa | G | 12 .7 2 | 2. 9 | 1.5 1 | 68 .0 5 | 2. 1 5 | 10 .3 8 | 0. 07 | 0. 11 | 0.9 7 | 0.7 | Hend erson et al. 2004 | 0.28 | 1.35 |
| Al Raqqa | pG | 14 .6 8 | 5. 3 | 2.2 4 | 65 .3 3 | 3. 0 6 | 5. 94 | 0. 09 | 1. 35 | 0.7 9 | 0 | Hend erson et al. 2004 | 0.89 | 1.73 |
| Al Raqqa | pG | 14 .2 8 | 5. 06 | 1.6 5 | 67 .8 3 | 1. 5 2 | 5. 1 | 0. 06 | 2. 66 | 0.5 | 0 | Hend erson et al. 2004 | 0.99 | 3.33 |
| Al Raqqa | A | 12 .9 3 | 0. 51 | 3.1 8 | 71 .1 6 | 0. 4 5 | 10 .3 | 0 | 0 | 0.3 5 | 0 | Hend erson et al. 2004 | 0.05 | 1.13 |
| Al Raqqa | pG | 13 .3 6 | 3. 54 | 1.2 3 | 67 .4 4 | 2. 4 7 | 8. 28 | 0. 07 | 1. 77 | 0.3 7 | 0 | Hend erson et al. 2004 | 0.43 | 1.43 |
| Al Raqqa | pG | 13 .7 4 | 3. 58 | 1.1 7 | 67 .3 3 | 2. 1 2 | 8. 46 | 0. 07 | 1. 58 | 0.5 7 | 0 | Hend erson et al. 2004 | 0.42 | 1.69 |
| Al Raqqa | A | 13 .1 8 | 0. 61 | 3.2 4 | 71 .0 7 | 0. 5 9 | 9. 57 | 0. 07 | 0 | 0.3 9 | 0 | Hend erson et al. 2004 | 0.06 | 1.03 |
| Al Raqqa | A | 13 .1 5 | 0. 47 | 3.1 8 | 72 .6 1 | 0. 4 3 | 8. 73 | 0 | 0 | 0.3 2 | 0 | Hend erson et al. 2004 | 0.05 | 1.09 |
| Al Raqqa | pG | 14 .3 | 0. 53 | 3.2 | 70 .7 3 | 0. 5 8 | 9. 19 | 0. 05 | 0 | 0.3 5 | 0 | Hend erson et al. 2004 | 0.06 | 0.91 |
| Al Raqqa | A | 12 .8 9 | 0. 76 | 3.4 5 | 71 .8 7 | 0. 5 5 | 8. 97 | 0 | 0 | 0.3 9 | 0 | Hend erson et al. 2004 | 0.08 | 1.38 |
| Samarra Natron | Green | 18 .4 | 0. 36 | 2.5 | 67 .5 | 0. 4 1 | 2. 15 | 0. 14 | 0. 03 | 0.7 2 | 4.8 | Schib ille et al. 2018 | 0.17 | 0.88 |
| Samarra Natron | Green | 13 .5 | 0. 64 | 2.9 9 | 64 .6 | 0. 7 1 | 8. 82 | 0. 08 | 0. 03 | 0.4 7 | 5.4 | Schib ille et al. 2018 | 0.07 | 0.90 |
| Samarra Natron | Yellow | 14 .8 | 0. 86 | 2 | 54 .4 | 0. 5 1 | 7. 13 | 0. 12 | 1. 13 | 0.7 6 | 15. 7 | Schib ille et al. 2018 | 0.12 | 1.69 |
| Samarra Natron | Colourless | 18 .2 | 0. 37 | 2.0 7 | 69 .4 | 0. 6 8 | 7. 17 | 0. 06 | 0. 04 | 0.3 5 | 0.0 1 | Schib ille et al. 2018 | 0.05 | 0.54 |

| | | | | | | | | | | | | | | |
|----------------|------------|------|------|------|------|------|-------|------|------|------|------|-----------------------|------|------|
| Samarra Natron | Green | 15.7 | 0.53 | 3.23 | 62 | 0.53 | 2.73 | 0.24 | 0.04 | 1.01 | 10.8 | Schibille et al. 2018 | 0.19 | 1.00 |
| Samarra Natron | Blue | 15.1 | 0.61 | 3.15 | 69.2 | 0.93 | 8.56 | 0.09 | 0.21 | 0.82 | 0.04 | Schibille et al. 2018 | 0.07 | 0.66 |
| Samarra Natron | Green | 14.3 | 0.74 | 3.2 | 66.7 | 0.83 | 10.23 | 0.09 | 2.25 | 0.66 | 0.01 | Schibille et al. 2018 | 0.07 | 0.89 |
| Samarra Natron | Gold leaf | 17.5 | 0.78 | 2.3 | 69.9 | 0.34 | 5.59 | 0.1 | 1.4 | 0.68 | 0 | Schibille et al. 2018 | 0.14 | 2.29 |
| Samarra Natron | Gold leaf | 18 | 0.82 | 2.44 | 69.4 | 0.35 | 5.63 | 0.14 | 0.89 | 0.84 | 0 | Schibille et al. 2018 | 0.15 | 2.34 |
| Samarra Natron | Gold leaf | 17.8 | 1.05 | 2.71 | 66 | 0.66 | 7.99 | 0.14 | 1.48 | 0.99 | 0.01 | Schibille et al. 2018 | 0.13 | 1.59 |
| Samarra Natron | Gold leaf | 17.7 | 1.04 | 2.74 | 66.1 | 0.67 | 7.98 | 0.13 | 1.4 | 0.97 | 0.01 | Schibille et al. 2018 | 0.13 | 1.55 |
| Samarra Natron | Gold leaf | 16.9 | 1.23 | 2.82 | 64.7 | 0.93 | 7.11 | 0.15 | 1.29 | 3.5 | 0.01 | Schibille et al. 2018 | 0.17 | 1.32 |
| Samarra Natron | Gold leaf | 17.5 | 1.36 | 3.04 | 64.1 | 0.87 | 7.74 | 0.17 | 1.26 | 2.65 | 0.01 | Schibille et al. 2018 | 0.18 | 1.56 |
| Samarra Natron | Gold leaf | 14.2 | 0.65 | 3.18 | 67.3 | 0.79 | 9.28 | 0.09 | 2.91 | 0.63 | 0.01 | Schibille et al. 2018 | 0.07 | 0.82 |
| Samarra Natron | Blue | 16.3 | 0.63 | 3.13 | 67.5 | 0.74 | 8.4 | 0.09 | 0.34 | 0.56 | 0.09 | Schibille et al. 2018 | 0.08 | 0.85 |
| Samarra Natron | Blue | 14.9 | 0.59 | 3.43 | 68.7 | 0.9 | 8.49 | 0.07 | 0.08 | 0.48 | 0.11 | Schibille et al. 2018 | 0.07 | 0.66 |
| Samarra Natron | Blue | 18.8 | 0.74 | 2.1 | 66.7 | 0.31 | 8.03 | 0.1 | 0.03 | 0.54 | 0.02 | Schibille et al. 2018 | 0.09 | 2.39 |
| Samarra Natron | Green/Blue | 18.1 | 0.47 | 2.92 | 66.4 | 0.42 | 2.31 | 0.22 | 0.06 | 0.97 | 5.1 | Schibille et al. 2018 | 0.20 | 1.12 |
| Samarra Natron | Green/Blue | 12.7 | 0.57 | 2.48 | 57.9 | 0.69 | 8.2 | 0.07 | 0.04 | 0.5 | 13.6 | Schibille et al. 2018 | 0.07 | 0.83 |
| Samarra Natron | Green/Blue | 18.7 | 0.74 | 1.87 | 67.2 | 0.32 | 7.69 | 0.1 | 0.03 | 0.56 | 0.03 | Schibille et al. 2018 | 0.10 | 2.31 |

| | | | | | | | | | | | | | | |
|----------------|------------|------|------|------|------|------|------|------|------|------|------|-----------------------|------|------|
| Samarra Natron | Green | 12.1 | 0.62 | 2.84 | 57.2 | 0.54 | 8.92 | 0.07 | 0.04 | 0.46 | 13.7 | Schibille et al. 2018 | 0.07 | 1.15 |
| Samarra Natron | Green | 15.8 | 0.34 | 1.54 | 64.3 | 0.34 | 3.97 | 0.21 | 0.04 | 0.71 | 9.16 | Schibille et al. 2018 | 0.09 | 1.00 |
| Samarra Natron | Green | 12.5 | 0.56 | 2.68 | 59.4 | 0.6 | 6.9 | 0.07 | 0.02 | 0.39 | 12.7 | Schibille et al. 2018 | 0.08 | 0.93 |
| Samarra Natron | Yellow | 13.7 | 0.68 | 2.93 | 61 | 1.09 | 8.89 | 0.08 | 0.17 | 0.53 | 8 | Schibille et al. 2018 | 0.08 | 0.62 |
| Samarra Natron | Yellow | 19.9 | 0.39 | 2.25 | 64.9 | 0.29 | 1.85 | 0.21 | 0.02 | 0.73 | 6.55 | Schibille et al. 2018 | 0.21 | 1.34 |
| Samarra Natron | Yellow | 9.9 | 0.85 | 1.6 | 50.5 | 0.84 | 5.77 | 0.07 | 0.08 | 0.41 | 26.6 | Schibille et al. 2018 | 0.15 | 1.01 |
| Samarra Natron | Yellow | 12.7 | 0.34 | 1.4 | 54.3 | 0.43 | 3.77 | 0.21 | 0.32 | 0.75 | 21.8 | Schibille et al. 2018 | 0.09 | 0.79 |
| Samarra Natron | Yellow | 13.2 | 0.67 | 1.96 | 57 | 0.35 | 3.53 | 0.23 | 0.07 | 0.84 | 17.5 | Schibille et al. 2018 | 0.19 | 1.91 |
| Samarra Natron | Yellow | 13.7 | 0.28 | 1.22 | 56.9 | 0.25 | 3.36 | 0.18 | 0.26 | 0.59 | 19.1 | Schibille et al. 2018 | 0.08 | 1.12 |
| Samarra Natron | Aqua | 15.1 | 0.69 | 3.05 | 68.1 | 0.9 | 9.37 | 0.09 | 0.26 | 0.63 | 0.14 | Schibille et al. 2018 | 0.07 | 0.77 |
| Samarra Natron | Black | 12.9 | 0.75 | 2.89 | 68.3 | 0.68 | 7.84 | 0.07 | 0.09 | 5.4 | 0.06 | Schibille et al. 2018 | 0.10 | 1.10 |
| Samarra Natron | Blue | 17.5 | 0.87 | 2.48 | 66.1 | 0.56 | 7.98 | 0.14 | 1.17 | 1.67 | 0.03 | Schibille et al. 2018 | 0.11 | 1.55 |
| Samarra Natron | Blue/Green | 18.6 | 0.39 | 2.39 | 68.3 | 0.35 | 2.19 | 0.16 | 0.03 | 0.74 | 3.05 | Schibille et al. 2018 | 0.18 | 1.11 |
| Samarra | Blue Co | 13.8 | 2.64 | 1.89 | 67.6 | 2.31 | 6.3 | 0.11 | 0.38 | 3.06 | 0.01 | Schibille et al. 2018 | 0.42 | 1.14 |
| Samarra | Blue Co | 13.7 | 3.02 | 2.22 | 65.6 | 2.16 | 6.81 | 0.12 | 0.63 | 3.46 | 0.01 | Schibille et al. 2018 | 0.44 | 1.40 |
| Samarra | Blue Co | 14.7 | 4.19 | 1.35 | 65.4 | 1.86 | 8.59 | 0.08 | 0.14 | 2.22 | 0.02 | Schibille et al. 2018 | 0.49 | 2.25 |

| | | | | | | | | | | | | | | |
|---------|---------|------|------|------|------|------|------|------|------|------|------|-----------------------|------|------|
| Samarra | Blue Co | 14.8 | 2.86 | 2.02 | 65.6 | 2.27 | 6.84 | 0.12 | 1.13 | 2.68 | 0.03 | Schibille et al. 2018 | 0.42 | 1.26 |
| Samarra | Blue Co | 13.1 | 3.4 | 2.11 | 67.6 | 1.56 | 6.66 | 0.13 | 0.61 | 2.71 | 0.01 | Schibille et al. 2018 | 0.51 | 2.18 |
| Samarra | Blue Co | 14 | 2.39 | 2.17 | 68.2 | 2.07 | 5.64 | 0.13 | 0.38 | 3.06 | 0.02 | Schibille et al. 2018 | 0.42 | 1.15 |
| Samarra | Blue Co | 14.2 | 2.78 | 2.61 | 66.8 | 2.56 | 6.43 | 0.14 | 0.28 | 2.36 | 0.03 | Schibille et al. 2018 | 0.43 | 1.09 |
| Samarra | Blue Co | 14.7 | 2.65 | 1.82 | 65.5 | 2.1 | 7.77 | 0.11 | 0.82 | 2.79 | 0.02 | Schibille et al. 2018 | 0.34 | 1.26 |
| Samarra | Blue Co | 14.9 | 2.78 | 2.23 | 67.1 | 2.31 | 6.48 | 0.13 | 0.64 | 1.9 | 0.01 | Schibille et al. 2018 | 0.43 | 1.20 |
| Samarra | Blue Co | 14 | 2.82 | 2.21 | 66.5 | 2.63 | 6.26 | 0.13 | 0.66 | 2.85 | 0.02 | Schibille et al. 2018 | 0.45 | 1.07 |
| Samarra | Blue Co | 13.6 | 2.88 | 2.18 | 66.5 | 2.51 | 6.14 | 0.13 | 0.62 | 3.42 | 0.01 | Schibille et al. 2018 | 0.47 | 1.15 |
| Samarra | Blue Co | 14.2 | 2.71 | 2.3 | 67.2 | 2.56 | 6.05 | 0.14 | 0.4 | 2.65 | 0.02 | Schibille et al. 2018 | 0.45 | 1.06 |
| Samarra | Blue Co | 13.8 | 2.41 | 2.21 | 68.6 | 2.34 | 5.89 | 0.14 | 0.33 | 2.45 | 0.02 | Schibille et al. 2018 | 0.41 | 1.03 |
| Samarra | Blue Co | 13.8 | 2.68 | 1.62 | 67.5 | 1.82 | 7.89 | 0.11 | 0.1 | 2.88 | 0 | Schibille et al. 2018 | 0.34 | 1.47 |
| Samarra | Blue Co | 14.1 | 2.48 | 1.74 | 68.9 | 2.05 | 6.3 | 0.11 | 0.84 | 1.82 | 0.01 | Schibille et al. 2018 | 0.39 | 1.21 |
| Samarra | Blue Co | 15.5 | 2.99 | 2.2 | 64.4 | 2.28 | 7.2 | 0.13 | 0.99 | 2.68 | 0.02 | Schibille et al. 2018 | 0.42 | 1.31 |
| Samarra | Blue Co | 15 | 2.87 | 2.37 | 65.6 | 2.42 | 6.57 | 0.15 | 0.96 | 2.45 | 0.01 | Schibille et al. 2018 | 0.44 | 1.19 |
| Samarra | Blue Co | 14.8 | 2.73 | 2.08 | 66.6 | 2.4 | 6.93 | 0.12 | 0.54 | 2.18 | 0.01 | Schibille et al. 2018 | 0.39 | 1.14 |
| Samarra | Blue Co | 14 | 2.68 | 2.19 | 67 | 2.28 | 6.65 | 0.14 | 0.76 | 2.51 | 0.01 | Schibille et al. 2018 | 0.40 | 1.18 |

| | | | | | | | | | | | | | | |
|---------|------------|------|------|------|------|------|------|------|------|------|------|-----------------------|------|------|
| Samarra | Blue Co | 14.3 | 2.52 | 2.01 | 69.7 | 2.23 | 5.88 | 0.13 | 0.21 | 1.51 | 0 | Schibille et al. 2018 | 0.43 | 1.13 |
| Samarra | Blue Co | 13.9 | 2.35 | 2.13 | 68.5 | 2.1 | 5.6 | 0.13 | 0.35 | 2.95 | 0.02 | Schibille et al. 2018 | 0.42 | 1.12 |
| Samarra | Blue Co | 13.5 | 2.82 | 2.13 | 68.5 | 2.49 | 6.22 | 0.13 | 0.99 | 1.72 | 0.01 | Schibille et al. 2018 | 0.45 | 1.13 |
| Samarra | Blue Co | 14.5 | 2.8 | 2.1 | 67 | 2.32 | 6.74 | 0.12 | 0.78 | 2.1 | 0.01 | Schibille et al. 2018 | 0.42 | 1.21 |
| Samarra | Colourless | 13.2 | 5.58 | 0.83 | 69.7 | 2.95 | 6.26 | 0.02 | 0.31 | 0.17 | 0 | Schibille et al. 2018 | 0.89 | 1.89 |
| Samarra | White | 12.6 | 4.79 | 0.66 | 68.1 | 3.41 | 6.02 | 0.03 | 0.27 | 0.18 | 0.91 | Schibille et al. 2018 | 0.80 | 1.40 |
| Samarra | White | 12.6 | 5.01 | 0.67 | 68.3 | 3.15 | 5.84 | 0.02 | 0.21 | 0.17 | 1.4 | Schibille et al. 2018 | 0.86 | 1.59 |
| Samarra | Colourless | 13.6 | 5.5 | 0.88 | 68.3 | 3.58 | 6.93 | 0.03 | 0.18 | 0.24 | 0 | Schibille et al. 2018 | 0.79 | 1.54 |
| Samarra | Colourless | 12.1 | 5.19 | 1.08 | 70.2 | 2.97 | 7 | 0.04 | 0.39 | 0.29 | 0 | Schibille et al. 2018 | 0.74 | 1.75 |
| Samarra | Colourless | 14.4 | 5.2 | 1 | 69.9 | 1.97 | 6.08 | 0.05 | 0.27 | 0.3 | 0 | Schibille et al. 2018 | 0.86 | 2.64 |
| Samarra | Colourless | 13.6 | 4.99 | 0.68 | 69.6 | 3.45 | 6.3 | 0.03 | 0.2 | 0.17 | 0 | Schibille et al. 2018 | 0.79 | 1.45 |
| Samarra | Colourless | 13.1 | 5.52 | 0.7 | 69.7 | 3.01 | 6.33 | 0.02 | 0.41 | 0.19 | 0 | Schibille et al. 2018 | 0.87 | 1.83 |
| Samarra | Blue | 12.8 | 5.49 | 1 | 71.7 | 3.15 | 3.82 | 0.04 | 0.15 | 0.69 | 0 | Schibille et al. 2018 | 1.44 | 1.74 |
| Samarra | Colourless | 10.9 | 4.61 | 0.97 | 73.2 | 2.42 | 6.39 | 0.04 | 0.4 | 0.26 | 0 | Schibille et al. 2018 | 0.72 | 1.90 |
| Samarra | Colourless | 13.6 | 5.15 | 1.17 | 69.3 | 2.23 | 6.71 | 0.05 | 0.58 | 0.41 | 0 | Schibille et al. 2018 | 0.77 | 2.31 |
| Samarra | Colourless | 12.7 | 5.59 | 0.97 | 69.3 | 2.81 | 7.09 | 0.03 | 0.38 | 0.29 | 0 | Schibille et al. 2018 | 0.79 | 1.99 |

| | | | | | | | | | | | | | | |
|---------|------------|------|------|------|------|------|------|------|------|------|---|-----------------------|------|------|
| Samarra | Colourless | 13.2 | 5.06 | 1.05 | 70.8 | 2.18 | 6.19 | 0.05 | 0.28 | 0.33 | 0 | Schibille et al. 2018 | 0.82 | 2.32 |
| Samarra | Colourless | 12.3 | 4.95 | 0.7 | 71.6 | 2.77 | 6.11 | 0.03 | 0.4 | 0.2 | 0 | Schibille et al. 2018 | 0.81 | 1.79 |
| Samarra | Colourless | 12.3 | 5.36 | 0.85 | 71.3 | 2.46 | 6.03 | 0.03 | 0.47 | 0.22 | 0 | Schibille et al. 2018 | 0.89 | 2.18 |
| Samarra | Colourless | 13.3 | 5.41 | 1.03 | 69.4 | 3.02 | 6.58 | 0.04 | 0.19 | 0.29 | 0 | Schibille et al. 2018 | 0.82 | 1.79 |
| Samarra | Colourless | 11.8 | 5.3 | 1.05 | 71.4 | 2.45 | 6.66 | 0.04 | 0.23 | 0.31 | 0 | Schibille et al. 2018 | 0.80 | 2.16 |
| Samarra | Colourless | 12.6 | 5.51 | 0.97 | 69.6 | 2.81 | 7.02 | 0.03 | 0.25 | 0.27 | 0 | Schibille et al. 2018 | 0.78 | 1.96 |
| Samarra | Colourless | 12.8 | 5.48 | 0.8 | 69.9 | 2.99 | 6.68 | 0.03 | 0.23 | 0.21 | 0 | Schibille et al. 2018 | 0.82 | 1.83 |
| Samarra | Colourless | 12.8 | 5 | 0.72 | 70.8 | 2.88 | 6.42 | 0.02 | 0.3 | 0.2 | 0 | Schibille et al. 2018 | 0.78 | 1.79 |
| Samarra | Colourless | 11.9 | 5.01 | 0.72 | 71.6 | 2.88 | 6.13 | 0.03 | 0.45 | 0.22 | 0 | Schibille et al. 2018 | 0.82 | 1.74 |
| Samarra | Green | 13.9 | 5.28 | 0.83 | 68.6 | 3.24 | 6.84 | 0.03 | 0.04 | 0.24 | 0 | Schibille et al. 2018 | 0.77 | 1.63 |
| Samarra | Colourless | 13.4 | 5.59 | 0.71 | 69.5 | 2.81 | 6.47 | 0.02 | 0.33 | 0.17 | 0 | Schibille et al. 2018 | 0.86 | 1.99 |
| Samarra | Colourless | 14.4 | 5.22 | 1.02 | 69.7 | 1.99 | 6.15 | 0.05 | 0.27 | 0.31 | 0 | Schibille et al. 2018 | 0.85 | 2.62 |
| Samarra | Colourless | 14.4 | 5.27 | 1.11 | 67.8 | 2.66 | 7.18 | 0.05 | 0.27 | 0.34 | 0 | Schibille et al. 2018 | 0.73 | 1.98 |
| Samarra | Green | 13.2 | 5.76 | 0.7 | 69.2 | 3.09 | 6.57 | 0.02 | 0.32 | 0.19 | 0 | Schibille et al. 2018 | 0.88 | 1.86 |
| Samarra | colourless | 13.3 | 5.34 | 0.74 | 68.9 | 3.84 | 6.54 | 0.02 | 0.22 | 0.16 | 0 | Schibille et al. 2018 | 0.82 | 1.39 |
| Samarra | colourless | 12.9 | 4.16 | 0.65 | 70.7 | 3.66 | 6.7 | 0.03 | 0.23 | 0.19 | 0 | Schibille et al. 2018 | 0.62 | 1.14 |

| | | | | | | | | | | | | | | |
|---------|------------|------|------|------|------|------|------|------|------|------|---|-----------------------|------|------|
| Samarra | colourless | 12.9 | 5.23 | 0.8 | 69.4 | 3.66 | 6.57 | 0.03 | 0.31 | 0.24 | 0 | Schibille et al. 2018 | 0.80 | 1.43 |
| Samarra | colourless | 12.7 | 5.08 | 0.85 | 70.2 | 3.23 | 6.5 | 0.03 | 0.35 | 0.25 | 0 | Schibille et al. 2018 | 0.78 | 1.57 |
| Samarra | colourless | 12.9 | 4.26 | 0.68 | 70.5 | 3.63 | 6.83 | 0.03 | 0.2 | 0.19 | 0 | Schibille et al. 2018 | 0.62 | 1.17 |
| Samarra | colourless | 12.7 | 5.09 | 0.86 | 70.3 | 3.21 | 6.48 | 0.03 | 0.35 | 0.25 | 0 | Schibille et al. 2018 | 0.79 | 1.59 |
| Samarra | colourless | 14.8 | 5.83 | 0.65 | 67.1 | 3.97 | 6.28 | 0.02 | 0.26 | 0.15 | 0 | Schibille et al. 2018 | 0.93 | 1.47 |
| Samarra | colourless | 13.2 | 4.79 | 0.61 | 70.5 | 3.48 | 6.06 | 0.02 | 0.28 | 0.17 | 0 | Schibille et al. 2018 | 0.79 | 1.38 |
| Samarra | colourless | 12.6 | 5.03 | 0.85 | 70.4 | 3.22 | 6.45 | 0.03 | 0.35 | 0.25 | 0 | Schibille et al. 2018 | 0.78 | 1.56 |
| Samarra | colourless | 12.7 | 5.06 | 0.85 | 70.3 | 3.22 | 6.42 | 0.03 | 0.35 | 0.26 | 0 | Schibille et al. 2018 | 0.79 | 1.57 |
| Samarra | colourless | 13.3 | 4.99 | 0.69 | 69.7 | 3.7 | 6.27 | 0.02 | 0.21 | 0.15 | 0 | Schibille et al. 2018 | 0.80 | 1.35 |
| Samarra | colourless | 13.2 | 4.7 | 0.63 | 70.1 | 3.56 | 6.5 | 0.03 | 0.24 | 0.17 | 0 | Schibille et al. 2018 | 0.72 | 1.32 |
| Samarra | colourless | 12.7 | 5.05 | 0.85 | 70.4 | 3.2 | 6.51 | 0.03 | 0.35 | 0.25 | 0 | Schibille et al. 2018 | 0.78 | 1.58 |
| Samarra | colourless | 13.4 | 5.15 | 0.74 | 70 | 3.25 | 6.19 | 0.02 | 0.2 | 0.17 | 0 | Schibille et al. 2018 | 0.83 | 1.58 |
| Samarra | colourless | 15 | 5.86 | 0.65 | 66.9 | 3.94 | 6.29 | 0.02 | 0.26 | 0.15 | 0 | Schibille et al. 2018 | 0.93 | 1.49 |
| Samarra | colourless | 13.3 | 4.78 | 0.61 | 70.3 | 3.5 | 6.17 | 0.03 | 0.24 | 0.17 | 0 | Schibille et al. 2018 | 0.77 | 1.37 |
| Samarra | colourless | 13.5 | 4.76 | 0.88 | 70 | 3.79 | 5.71 | 0.05 | 0.3 | 0.28 | 0 | Schibille et al. 2018 | 0.83 | 1.26 |
| Samarra | colourless | 13.1 | 4.77 | 0.64 | 70 | 3.54 | 6.55 | 0.03 | 0.24 | 0.18 | 0 | Schibille et al. 2018 | 0.73 | 1.35 |

| | | | | | | | | | | | | | | |
|---------|------------|------|------|------|------|------|------|------|------|------|---|-----------------------|------|------|
| Samarra | colourless | 12.7 | 5.15 | 0.86 | 70.2 | 3.17 | 6.5 | 0.03 | 0.36 | 0.25 | 0 | Schibille et al. 2018 | 0.79 | 1.62 |
| Samarra | colourless | 13.3 | 4.79 | 0.63 | 70 | 3.51 | 6.46 | 0.02 | 0.24 | 0.17 | 0 | Schibille et al. 2018 | 0.74 | 1.36 |
| Samarra | colourless | 12.8 | 5.07 | 0.85 | 70.3 | 3.17 | 6.42 | 0.03 | 0.36 | 0.25 | 0 | Schibille et al. 2018 | 0.79 | 1.60 |
| Samarra | colourless | 13.3 | 5.18 | 0.68 | 69.7 | 3.64 | 6.18 | 0.02 | 0.25 | 0.16 | 0 | Schibille et al. 2018 | 0.84 | 1.42 |
| Samarra | colourless | 13 | 4.32 | 0.68 | 70.3 | 3.57 | 6.82 | 0.03 | 0.21 | 0.19 | 0 | Schibille et al. 2018 | 0.63 | 1.21 |
| Samarra | colourless | 13 | 5.27 | 0.86 | 69.6 | 3.31 | 6.52 | 0.03 | 0.35 | 0.26 | 0 | Schibille et al. 2018 | 0.81 | 1.59 |
| Samarra | colourless | 13 | 4.34 | 0.67 | 70.3 | 3.57 | 6.84 | 0.03 | 0.2 | 0.19 | 0 | Schibille et al. 2018 | 0.63 | 1.22 |
| Samarra | colourless | 13.4 | 5.25 | 0.75 | 69.8 | 3.21 | 6.29 | 0.02 | 0.2 | 0.17 | 0 | Schibille et al. 2018 | 0.83 | 1.64 |
| Samarra | colourless | 13.4 | 5.2 | 0.75 | 70 | 3.22 | 6.23 | 0.02 | 0.2 | 0.17 | 0 | Schibille et al. 2018 | 0.83 | 1.61 |
| Samarra | colourless | 13.3 | 5.14 | 0.7 | 69.7 | 3.59 | 6.25 | 0.02 | 0.26 | 0.16 | 0 | Schibille et al. 2018 | 0.82 | 1.43 |
| Samarra | colourless | 13.4 | 5.19 | 0.69 | 69.5 | 3.64 | 6.29 | 0.02 | 0.26 | 0.16 | 0 | Schibille et al. 2018 | 0.83 | 1.43 |
| Samarra | colourless | 13 | 4.31 | 0.68 | 70.5 | 3.54 | 6.74 | 0.03 | 0.21 | 0.19 | 0 | Schibille et al. 2018 | 0.64 | 1.22 |
| Samarra | colourless | 13.2 | 5.2 | 0.84 | 69.7 | 3.27 | 6.41 | 0.03 | 0.28 | 0.24 | 0 | Schibille et al. 2018 | 0.81 | 1.59 |
| Samarra | colourless | 13.2 | 5.17 | 0.83 | 69.8 | 3.28 | 6.37 | 0.03 | 0.28 | 0.24 | 0 | Schibille et al. 2018 | 0.81 | 1.58 |
| Samarra | colourless | 14.6 | 5.72 | 1.1 | 68.3 | 2.25 | 6.4 | 0.04 | 0.39 | 0.31 | 0 | Schibille et al. 2018 | 0.89 | 2.54 |
| Samarra | colourless | 13.1 | 5.21 | 0.84 | 69.6 | 3.34 | 6.52 | 0.03 | 0.35 | 0.26 | 0 | Schibille et al. 2018 | 0.80 | 1.56 |

| | | | | | | | | | | | | | | |
|---------|------------|----------|----------|----------|----------|--------------|----------|----------|----------|----------|----------|---------------------------------|------|------|
| Samarra | colourless | 13 | 4. 27 | 0.6 6 | 70 .5 | 3. 5 8 | 6. 7 | 0. 03 | 0. 2 | 0.1 9 | 0 | Schib ille et al. 2018 | 0.64 | 1.19 |
| Samarra | colourless | 13 .5 | 5. 21 | 0.8 1 | 69 .3 | 3. 2 9 | 6. 7 | 0. 03 | 0. 18 | 0.2 2 | 0 | Schib ille et al. 2018 | 0.78 | 1.58 |
| Samarra | colourless | 13 .7 | 5. 34 | 0.8 1 | 68 .8 | 3. 4 | 6. 77 | 0. 03 | 0. 18 | 0.2 3 | 0 | Schib ille et al. 2018 | 0.79 | 1.57 |
| Samarra | colourless | 13 .1 | 4. 5 | 0.8 6 | 70 .5 | 3. 8 4 | 5. 61 | 0. 05 | 0. 45 | 0.2 8 | 0 | Schib ille et al. 2018 | 0.80 | 1.17 |
| Samarra | colourless | 12 .9 | 4. 77 | 0.6 2 | 70 .6 | 3. 5 2 | 6. 16 | 0. 02 | 0. 29 | 0.1 7 | 0 | Schib ille et al. 2018 | 0.77 | 1.36 |
| Samarra | colourless | 12 .7 | 4. 25 | 0.6 8 | 70 .6 | 3. 6 5 | 6. 85 | 0. 03 | 0. 21 | 0.2 | 0 | Schib ille et al. 2018 | 0.62 | 1.16 |
| Samarra | colourless | 13 .1 | 4. 46 | 0.8 7 | 70 .6 | 3. 8 7 | 5. 58 | 0. 05 | 0. 44 | 0.2 7 | 0 | Schib ille et al. 2018 | 0.80 | 1.15 |
| Samarra | colourless | 14 .3 | 5. 68 | 1.1 2 | 68 .4 | 2. 3 | 6. 54 | 0. 04 | 0. 4 | 0.3 2 | 0 | Schib ille et al. 2018 | 0.87 | 2.47 |
| Samarra | colourless | 13 .1 | 5. 14 | 0.6 9 | 69 .7 | 3. 6 6 | 6. 42 | 0. 02 | 0. 26 | 0.1 6 | 0 | Schib ille et al. 2018 | 0.80 | 1.40 |
| Samarra | colourless | 13 .2 | 4. 48 | 0.8 6 | 70 .5 | 3. 8 8 | 5. 58 | 0. 05 | 0. 45 | 0.2 7 | 0 | Schib ille et al. 2018 | 0.80 | 1.15 |
| Samarra | colourless | 13 .3 | 5. 14 | 0.7 4 | 70 .1 | 3. 2 6 | 6. 19 | 0. 02 | 0. 2 | 0.1 7 | 0 | Schib ille et al. 2018 | 0.83 | 1.58 |
| Samarra | colourless | 13 | 5. 17 | 0.8 6 | 69 .7 | 3. 3 8 | 6. 48 | 0. 03 | 0. 35 | 0.2 7 | 0 | Schib ille et al. 2018 | 0.80 | 1.53 |
| Samarra | Black | 15 | 5. 62 | 1.2 8 | 65 .1 | 2. 9 8 | 5. 44 | 0. 08 | 3. 07 | 0.4 7 | 0.0 1 | Schib ille et al. 2018 | 1.03 | 1.89 |
| Samarra | Black | 15 .1 | 5. 5 | 1.2 3 | 65 .2 | 3. 0 1 | 5. 32 | 0. 08 | 3. 08 | 0.4 7 | 0.0 1 | Schib ille et al. 2018 | 1.03 | 1.83 |
| Samarra | Black | 14 .8 | 5. 59 | 1.1 9 | 66 .4 | 2. 7 5 | 5. 4 | 0. 08 | 2. 32 | 0.5 1 | 0.0 1 | Schib ille et al. 2018 | 1.04 | 2.03 |
| Samarra | Aqua | 16 .8 | 6. 3 | 1.4 8 | 66 | 2. 9 2 | 4. 75 | 0. 08 | 0. 41 | 0.4 7 | 0 | Schib ille et al. 2018 | 1.33 | 2.16 |

| | | | | | | | | | | | | | | |
|---------|------------|----------|----------|-----------|----------|--------------|----------|----------|----------|----------|----------|---------------------------------|------|------|
| Samarra | Blue/Green | 13 .1 | 5. 05 | 1.3 2 | 66 .6 | 2. 6 8 | 6. 18 | 0. 07 | 0. 72 | 0.6 8 | 0.1 7 | Schib ille et al. 2018 | 0.82 | 1.88 |
| Samarra | Black | 12 .6 | 5. 56 | 0.8 4 | 69 .7 | 3. 1 5 | 5. 08 | 0. 05 | 0. 78 | 0.2 7 | 0.3 2 | Schib ille et al. 2018 | 1.09 | 1.77 |
| Samarra | Yellow | 13 .1 | 5. 04 | 1.2 4 | 59 .3 | 2. 4 9 | 4. 12 | 0. 08 | 0. 76 | 0.4 4 | 10. 9 | Schib ille et al. 2018 | 1.22 | 2.02 |
| Samarra | Blue | 13 .3 | 5. 17 | 1.1 3 | 67 .4 | 3. 1 9 | 5. 88 | 0. 06 | 0. 94 | 1.0 5 | 0.3 | Schib ille et al. 2018 | 0.88 | 1.62 |
| Samarra | Red | 14 .4 | 4. 61 | 1.5 1 | 64 | 2. 8 5 | 5. 74 | 0. 1 | 1. 77 | 1.9 2 | 0.1 1 | Schib ille et al. 2018 | 0.80 | 1.62 |
| Samarra | Yellow | 12 .8 | 4. 72 | 1.2 7 | 63 .5 | 2. 7 3 | 4. 22 | 0. 07 | 0. 95 | 0.3 9 | 7.3 1 | Schib ille et al. 2018 | 1.12 | 1.73 |
| Samarra | Green | 15 .1 | 5. 59 | 1.2 9 | 67 | 2. 8 | 4. 85 | 0. 08 | 0. 37 | 0.4 1 | 0.7 2 | Schib ille et al. 2018 | 1.15 | 2.00 |
| Samarra | Black | 13 .2 | 5. 16 | 1.3 1 | 62 .9 | 2. 5 6 | 5. 66 | 0. 08 | 2. 65 | 0.5 6 | 3.2 8 | Schib ille et al. 2018 | 0.91 | 2.02 |
| Samarra | Red | 13 .9 | 4. 07 | 1.7 .1 | 64 | 2. 7 8 | 6. 06 | 0. 11 | 1. 84 | 2.2 5 | 0.2 2 | Schib ille et al. 2018 | 0.67 | 1.46 |
| Samarra | Yellow | 12 .4 | 4. 54 | 1.1 9 | 61 .4 | 2. 6 2 | 4. 11 | 0. 07 | 0. 92 | 0.3 9 | 9.8 5 | Schib ille et al. 2018 | 1.10 | 1.73 |
| Samarra | Blue Co | 15 | 5. 48 | 1.3 7 | 65 .9 | 2. 8 9 | 5. 32 | 0. 08 | 1. 16 | 1.4 9 | 0.0 1 | Schib ille et al. 2018 | 1.03 | 1.90 |
| Samarra | Red | 14 .1 | 4. 15 | 1.6 6 | 64 .2 | 2. 7 5 | 6. 07 | 0. 11 | 1. 78 | 2.1 4 | 0.1 6 | Schib ille et al. 2018 | 0.68 | 1.51 |
| Samarra | Yellow | 13 .8 | 5. 63 | 1.0 1 | 57 .4 | 2. 5 8 | 4. 95 | 0. 07 | 0. 88 | 0.3 9 | 10. 9 | Schib ille et al. 2018 | 1.14 | 2.18 |
| Samarra | White | 15 .9 | 6. 56 | 1.1 4 | 62 .6 | 2. 7 3 | 5. 31 | 0. 09 | 1. 05 | 0.4 4 | 1.1 8 | Schib ille et al. 2018 | 1.24 | 2.40 |
| Samarra | Blue | 15 .2 | 5. 74 | 1.2 3 | 66 .5 | 2. 9 9 | 4. 94 | 0. 09 | 1. 16 | 0.9 5 | 0 | Schib ille et al. 2018 | 1.16 | 1.92 |
| Samarra | Red | 14 .5 | 4. 55 | 1.5 4 | 63 .6 | 2. 9 4 | 6. 03 | 0. 11 | 1. 75 | 1.8 8 | 0.1 4 | Schib ille et al. 2018 | 0.75 | 1.55 |

| | | | | | | | | | | | | | | |
|---------|------------|----------|----------|----------|----------|--------------|----------|----------|----------|----------|----------|---------------------------------|------|------|
| Samarra | Black | 14 .1 | 5. 38 | 1.5 4 | 67 .2 | 2. 6 5 | 5. 61 | 0. 08 | 1. 89 | 0.6 8 | 0 | Schib ille et al. 2018 | 0.96 | 2.03 |
| Samarra | Gold leaf | 15 .5 | 5. 82 | 1.4 3 | 67 .5 | 2. 1 7 | 5. 14 | 0. 08 | 1. 08 | 0.4 5 | 0 | Schib ille et al. 2018 | 1.13 | 2.68 |
| Samarra | Gold leaf | 15 .5 | 5. 83 | 1.4 1 | 67 .5 | 2. 1 6 | 5. 11 | 0. 07 | 1. 05 | 0.4 4 | 0 | Schib ille et al. 2018 | 1.14 | 2.70 |
| Samarra | Gold leaf | 16 .3 | 6. 25 | 1.5 | 64 .8 | 2. 7 5 | 5. 56 | 0. 08 | 1. 28 | 0.5 2 | 0 | Schib ille et al. 2018 | 1.12 | 2.27 |
| Samarra | Gold leaf | 16 .3 | 6. 34 | 1.4 9 | 64 .6 | 2. 7 3 | 5. 65 | 0. 08 | 1. 34 | 0.5 4 | 0 | Schib ille et al. 2018 | 1.12 | 2.32 |
| Samarra | Aqua | 16 .4 | 5. 77 | 1.4 8 | 66 .8 | 2. 9 | 4. 54 | 0. 07 | 0. 62 | 0.4 2 | 0 | Schib ille et al. 2018 | 1.27 | 1.99 |
| Samarra | Black | 14 .3 | 5. 51 | 1.3 4 | 67 | 2. 6 5 | 5. 38 | 0. 07 | 2. 4 | 0.5 3 | 0.0 1 | Schib ille et al. 2018 | 1.02 | 2.08 |
| Samarra | Blue Co | 14 .6 | 4. 7 | 1.5 4 | 68 .7 | 1. 7 2 | 4. 75 | 0. 08 | 1. 46 | 0.9 5 | 0.0 1 | Schib ille et al. 2018 | 0.99 | 2.73 |
| Samarra | Colourless | 14 .7 | 5. 58 | 1.4 3 | 67 .4 | 3. 0 1 | 5. 06 | 0. 08 | 1. 51 | 0.4 3 | 0 | Schib ille et al. 2018 | 1.10 | 1.85 |
| Samarra | Green | 15 .2 | 5. 92 | 1.4 5 | 66 .5 | 2. 5 9 | 5. 5 | 0. 07 | 1. 37 | 0.4 5 | 0 | Schib ille et al. 2018 | 1.08 | 2.29 |
| Samarra | Aqua | 14 .7 | 5. 59 | 1.5 1 | 66 .3 | 2. 9 1 | 6. 06 | 0. 1 | 1. 14 | 0.6 4 | 0.0 1 | Schib ille et al. 2018 | 0.92 | 1.92 |
| Samarra | Colourless | 16 .1 | 5. 55 | 1.2 | 67 .3 | 2. 5 5 | 4. 51 | 0. 07 | 1. 4 | 0.3 9 | 0 | Schib ille et al. 2018 | 1.23 | 2.18 |
| Samarra | Colourless | 12 .3 | 4. 19 | 1.2 | 71 .9 | 2. 3 4 | 6. 3 | 0. 04 | 0. 51 | 0.3 8 | 0 | Schib ille et al. 2018 | 0.67 | 1.79 |
| Samarra | Colourless | 11 .2 | 4. 22 | 1.2 | 72 .3 | 2. 3 4 | 6. 79 | 0. 05 | 0. 67 | 0.3 8 | 0 | Schib ille et al. 2018 | 0.62 | 1.80 |
| Samarra | Colourless | 14 .8 | 5. 79 | 1.1 9 | 66 .4 | 3. 2 2 | 6. 1 | 0. 08 | 1. 15 | 0.3 9 | 0 | Schib ille et al. 2018 | 0.95 | 1.80 |
| Samarra | Colourless | 16 .2 | 5. 77 | 1.0 4 | 66 .1 | 3. 0 7 | 5. 41 | 0. 07 | 1. 1 | 0.3 3 | 0 | Schib ille et al. 2018 | 1.07 | 1.88 |

| | | | | | | | | | | | | | | |
|---------|------------|----------|----------|----------|----------|--------------|----------|----------|----------|----------|----------|---------------------------------|------|------|
| Samarra | Colourless | 13 .7 | 5. 58 | 1.2 4 | 67 .5 | 2. 5 8 | 6. 99 | 0. 06 | 0. 81 | 0.5 2 | 0.0 2 | Schib ille et al. 2018 | 0.80 | 2.16 |
| Samarra | Green | 13 .3 | 4. 67 | 1.3 4 | 71 .5 | 2. 5 2 | 4. 48 | 0. 07 | 0. 83 | 0.4 2 | 0 | Schib ille et al. 2018 | 1.04 | 1.85 |
| Samarra | Aqua | 13 .9 | 5. 07 | 1.2 5 | 69 .7 | 2. 7 9 | 5. 73 | 0. 06 | 0. 28 | 0.3 7 | 0 | Schib ille et al. 2018 | 0.88 | 1.82 |
| Samarra | Colourless | 12 .8 | 4. 92 | 0.8 2 | 72 .2 | 3. 4 4 | 4. 29 | 0. 07 | 0. 37 | 0.2 4 | 0 | Schib ille et al. 2018 | 1.15 | 1.43 |
| Samarra | Blue | 12 .9 | 5. 56 | 0.7 7 | 71 .6 | 3. 1 7 | 3. 97 | 0. 04 | 0. 15 | 0.7 4 | 0.0 1 | Schib ille et al. 2018 | 1.40 | 1.75 |
| Samarra | Blue | 15 .3 | 5. 23 | 1.2 8 | 67 .9 | 2. 3 3 | 4. 77 | 0. 06 | 1. 11 | 0.9 1 | 0 | Schib ille et al. 2018 | 1.10 | 2.24 |
| Samarra | Blue | 13 .1 | 5. 13 | 1.1 9 | 66 | 2. 8 | 6. 48 | 0. 07 | 0. 73 | 0.7 | 0.1 7 | Schib ille et al. 2018 | 0.79 | 1.83 |
| Samarra | Aqua | 17 .3 | 5. 91 | 1.2 6 | 65 .2 | 3. 2 2 | 5. 03 | 0. 07 | 0. 53 | 0.4 1 | 0 | Schib ille et al. 2018 | 1.17 | 1.84 |
| Samarra | Purple | 14 .1 | 5. 33 | 1.5 | 66 .9 | 2. 6 1 | 5. 84 | 0. 08 | 2. 05 | 0.7 4 | 0 | Schib ille et al. 2018 | 0.91 | 2.04 |
| Samarra | Purple | 14 .3 | 5. 43 | 1.5 | 66 .8 | 2. 6 2 | 5. 87 | 0. 08 | 1. 83 | 0.7 | 0 | Schib ille et al. 2018 | 0.93 | 2.07 |
| Samarra | Purple | 14 .1 | 5. 34 | 1.5 1 | 66 .8 | 2. 6 6 | 5. 84 | 0. 08 | 1. 97 | 0.7 4 | 0 | Schib ille et al. 2018 | 0.91 | 2.01 |
| Samarra | Purple | 13 .3 | 5. 61 | 1.5 4 | 67 .1 | 2. 6 1 | 6. 06 | 0. 08 | 1. 99 | 0.7 8 | 0 | Schib ille et al. 2018 | 0.93 | 2.15 |
| Samarra | Purple | 14 .3 | 5. 35 | 1.4 9 | 66 .6 | 2. 6 8 | 5. 82 | 0. 08 | 2. 04 | 0.7 8 | 0 | Schib ille et al. 2018 | 0.92 | 2.00 |
| Samarra | Purple | 14 .2 | 5. 39 | 1.5 | 66 .9 | 2. 6 5 | 5. 79 | 0. 08 | 1. 91 | 0.7 2 | 0 | Schib ille et al. 2018 | 0.93 | 2.03 |
| Samarra | Purple | 14 .1 | 5. 37 | 1.6 3 | 66 .4 | 2. 6 4 | 5. 88 | 0. 09 | 2. 11 | 0.8 4 | 0 | Schib ille et al. 2018 | 0.91 | 2.03 |
| Samarra | Purple | 14 .4 | 5. 36 | 1.4 8 | 66 .8 | 2. 6 7 | 5. 82 | 0. 08 | 1. 82 | 0.6 9 | 0 | Schib ille et al. 2018 | 0.92 | 2.01 |

| | | | | | | | | | | | | | | |
|---------|--------|----------|----------|----------|----------|--------------|----------|----------|----------|----------|----------|---------------------------------|------|------|
| Samarra | Purple | 14 .4 | 5. 37 | 1.4 7 | 66 .9 | 2. 6 8 | 5. 76 | 0. 08 | 1. 8 | 0.7 | 0 | Schib ille et al. 2018 | 0.93 | 2.00 |
| Samarra | Purple | 14 .2 | 5. 35 | 1.4 8 | 66 .8 | 2. 6 6 | 5. 84 | 0. 08 | 2 | 0.7 6 | 0 | Schib ille et al. 2018 | 0.92 | 2.01 |
| Samarra | Green | 14 .3 | 5. 19 | 1.2 4 | 67 .7 | 2. 5 6 | 4. 98 | 0. 07 | 0. 74 | 0.5 7 | 1.0 1 | Schib ille et al. 2018 | 1.04 | 2.03 |
| Samarra | Green | 14 .4 | 5. 24 | 1.2 5 | 68 .3 | 2. 6 1 | 5 | 0. 08 | 0. 72 | 0.6 | 0.3 4 | Schib ille et al. 2018 | 1.05 | 2.01 |
| Samarra | Green | 16 .2 | 6. 13 | 1.2 6 | 65 .5 | 2. 7 5 | 5. 44 | 0. 07 | 0. 49 | 0.5 1 | 0.3 9 | Schib ille et al. 2018 | 1.13 | 2.23 |
| Samarra | Green | 14 .5 | 5. 27 | 1.2 2 | 68 .2 | 2. 6 3 | 4. 97 | 0. 07 | 0. 67 | 0.5 7 | 0.6 | Schib ille et al. 2018 | 1.06 | 2.00 |
| Samarra | Green | 14 .5 | 5. 29 | 1.2 5 | 68 .1 | 2. 6 3 | 5. 01 | 0. 07 | 0. 69 | 0.5 8 | 0.5 3 | Schib ille et al. 2018 | 1.06 | 2.01 |
| Samarra | Green | 14 .6 | 5. 28 | 1.2 4 | 67 .7 | 2. 6 4 | 5. 07 | 0. 08 | 0. 7 | 0.5 8 | 0.5 4 | Schib ille et al. 2018 | 1.04 | 2.00 |
| Samarra | Green | 13 .6 | 5. 1 | 1.1 8 | 66 .4 | 2. 5 2 | 4. 93 | 0. 07 | 0. 66 | 0.5 5 | 2.7 3 | Schib ille et al. 2018 | 1.03 | 2.02 |
| Samarra | Green | 14 .7 | 4. 82 | 1.3 2 | 68 .4 | 2. 3 5 | 4. 9 | 0. 07 | 0. 74 | 0.5 9 | 0.6 5 | Schib ille et al. 2018 | 0.98 | 2.05 |
| Samarra | Green | 14 .2 | 5. 18 | 1.1 9 | 68 .5 | 2. 6 | 4. 85 | 0. 07 | 0. 7 | 0.5 6 | 0.7 6 | Schib ille et al. 2018 | 1.07 | 1.99 |
| Samarra | Green | 17 .2 | 6. 61 | 1.2 6 | 64 | 2. 8 5 | 5. 8 | 0. 07 | 0. 24 | 0.4 7 | 0.3 1 | Schib ille et al. 2018 | 1.14 | 2.32 |
| Samarra | Green | 16 .7 | 6. 18 | 1.2 8 | 62 .5 | 2. 7 6 | 5. 76 | 0. 08 | 0. 45 | 0.4 8 | 1.7 3 | Schib ille et al. 2018 | 1.07 | 2.24 |
| Samarra | Green | 14 .7 | 5. 24 | 1.1 5 | 67 .1 | 2. 6 7 | 4. 73 | 0. 07 | 0. 66 | 0.5 1 | 1.8 2 | Schib ille et al. 2018 | 1.11 | 1.96 |
| Samarra | Green | 14 .4 | 5. 14 | 1.2 | 68 .1 | 2. 5 9 | 4. 91 | 0. 07 | 0. 71 | 0.5 5 | 0.8 | Schib ille et al. 2018 | 1.05 | 1.98 |
| Samarra | Green | 16 .8 | 6. 4 | 1.2 8 | 62 .7 | 2. 7 9 | 5. 86 | 0. 07 | 0. 38 | 0.4 7 | 1.4 5 | Schib ille et al. 2018 | 1.09 | 2.29 |
| Samarra | Green | 14 .3 | 5. 14 | 1.2 2 | 67 .9 | 2. 6 | 4. 92 | 0. 08 | 0. 73 | 0.5 6 | 0.7 9 | Schib ille et | 1.04 | 1.98 |

| | | | | | | | | | | | | | | |
|---------|--------|------|------|------|------|------|------|------|------|------|------|-----------------------|------|------|
| | | | | | | | | | | | | al. 2018 | | |
| Samarra | Green | 17 | 6.41 | 1.26 | 63.6 | 2.85 | 5.82 | 0.07 | 0.31 | 0.48 | 0.79 | Schibille et al. 2018 | 1.10 | 2.25 |
| Samarra | Green | 16.4 | 6.44 | 1.33 | 63.6 | 2.82 | 5.92 | 0.08 | 0.46 | 0.5 | 0.74 | Schibille et al. 2018 | 1.08 | 2.27 |
| Samarra | Green | 14.4 | 5.23 | 1.24 | 68.3 | 2.63 | 4.97 | 0.07 | 0.7 | 0.59 | 0.47 | Schibille et al. 2018 | 1.05 | 1.99 |
| Samarra | Green | 16.5 | 6.33 | 1.32 | 63.5 | 2.8 | 5.89 | 0.08 | 0.47 | 0.5 | 0.86 | Schibille et al. 2018 | 1.07 | 2.26 |
| Samarra | Green | 14.2 | 5.11 | 1.24 | 67.5 | 2.6 | 4.98 | 0.08 | 0.78 | 0.58 | 1.06 | Schibille et al. 2018 | 1.03 | 1.97 |
| Samarra | Purple | 14.1 | 5.31 | 1.47 | 66.8 | 2.72 | 5.84 | 0.08 | 2.03 | 0.74 | 0 | Schibille et al. 2018 | 0.91 | 1.95 |
| Samarra | Purple | 14.2 | 5.29 | 1.44 | 67 | 2.73 | 5.77 | 0.08 | 1.84 | 0.7 | 0 | Schibille et al. 2018 | 0.92 | 1.94 |
| Samarra | Purple | 14.1 | 5.28 | 1.47 | 67 | 2.7 | 5.85 | 0.08 | 1.96 | 0.75 | 0 | Schibille et al. 2018 | 0.90 | 1.96 |
| Samarra | Purple | 14.2 | 5.32 | 1.46 | 67 | 2.71 | 5.81 | 0.08 | 1.8 | 0.7 | 0 | Schibille et al. 2018 | 0.92 | 1.96 |
| Samarra | Purple | 14.3 | 5.3 | 1.45 | 66.9 | 2.71 | 5.83 | 0.08 | 1.82 | 0.7 | 0.06 | Schibille et al. 2018 | 0.91 | 1.96 |
| Samarra | Purple | 14.3 | 5.32 | 1.44 | 66.8 | 2.7 | 5.8 | 0.08 | 1.92 | 0.73 | 0 | Schibille et al. 2018 | 0.92 | 1.97 |
| Samarra | Purple | 14.2 | 5.35 | 1.47 | 66.8 | 2.69 | 5.86 | 0.08 | 1.97 | 0.74 | 0 | Schibille et al. 2018 | 0.91 | 1.99 |
| Samarra | Purple | 14.3 | 5.29 | 1.46 | 66.8 | 2.69 | 5.8 | 0.08 | 1.98 | 0.74 | 0 | Schibille et al. 2018 | 0.91 | 1.97 |
| Samarra | Purple | 14.3 | 5.36 | 1.44 | 66.9 | 2.71 | 5.79 | 0.08 | 1.79 | 0.69 | 0 | Schibille et al. 2018 | 0.93 | 1.98 |
| Samarra | Purple | 14.2 | 5.27 | 1.45 | 67 | 2.75 | 5.86 | 0.08 | 1.84 | 0.71 | 0 | Schibille et al. 2018 | 0.90 | 1.92 |
| Samarra | Green | 14.6 | 5.35 | 1.24 | 65.1 | 2.76 | 4.93 | 0.07 | 0.47 | 0.41 | 3 | Schibille et al. 2018 | 1.09 | 1.94 |

| | | | | | | | | | | | | | | |
|---------|--------------|------|------|------|------|------|------|------|------|------|------|-----------------------|------|------|
| Samarra | Green | 14 | 5.39 | 1.26 | 65.3 | 2.73 | 5.03 | 0.07 | 0.39 | 0.41 | 3.09 | Schibille et al. 2018 | 1.07 | 1.97 |
| Samarra | Purple | 13.7 | 5.17 | 1.38 | 63.2 | 2.71 | 5.76 | 0.08 | 2.7 | 0.58 | 2.52 | Schibille et al. 2018 | 0.90 | 1.91 |
| Samarra | Purple | 14 | 5.05 | 1.54 | 63.3 | 2.8 | 6.18 | 0.09 | 2.55 | 0.72 | 1.79 | Schibille et al. 2018 | 0.82 | 1.80 |
| Samarra | Purple | 14.1 | 5.12 | 1.54 | 63.5 | 2.79 | 6.15 | 0.09 | 2.36 | 0.71 | 1.77 | Schibille et al. 2018 | 0.83 | 1.84 |
| Samarra | Purple | 15.3 | 5.48 | 1.31 | 65.3 | 3.2 | 6.05 | 0.09 | 1.82 | 0.49 | 0 | Schibille et al. 2018 | 0.91 | 1.71 |
| Samarra | Purple | 14.3 | 5.23 | 1.35 | 69.2 | 2.74 | 4.52 | 0.06 | 1.38 | 0.36 | 0 | Schibille et al. 2018 | 1.16 | 1.91 |
| Samarra | Purple | 17 | 6.76 | 1.3 | 64.3 | 2.85 | 5.32 | 0.09 | 1.09 | 0.46 | 0 | Schibille et al. 2018 | 1.27 | 2.37 |
| Samarra | Purple | 14.2 | 5.23 | 1.35 | 69.2 | 2.75 | 4.57 | 0.06 | 1.4 | 0.36 | 0 | Schibille et al. 2018 | 1.14 | 1.90 |
| Samarra | Purple | 15.1 | 5.11 | 1.58 | 66.2 | 2.67 | 6.03 | 0.09 | 1.68 | 0.64 | 0.01 | Schibille et al. 2018 | 0.85 | 1.91 |
| Samarra | Purple | 15.2 | 5.89 | 1.25 | 66.2 | 3.4 | 5.52 | 0.1 | 1.13 | 0.44 | 0 | Schibille et al. 2018 | 1.07 | 1.73 |
| Samarra | Aqua/Blue Co | 14.9 | 5.15 | 1.47 | 68.8 | 2.49 | 4.87 | 0.08 | 0.58 | 0.71 | 0 | Schibille et al. 2018 | 1.06 | 2.07 |
| Samarra | Blue Co | 14 | 3.75 | 1.42 | 69.5 | 1.95 | 4.3 | 0.07 | 1.64 | 1.75 | 0.01 | Schibille et al. 2018 | 0.87 | 1.92 |
| Samarra | Green | 17.8 | 5.73 | 1.46 | 63.3 | 2.5 | 5.83 | 0.08 | 1.75 | 0.54 | 0 | Schibille et al. 2018 | 0.98 | 2.29 |
| Samarra | Green | 18 | 5.75 | 1.46 | 63.2 | 2.49 | 5.82 | 0.08 | 1.62 | 0.53 | 0 | Schibille et al. 2018 | 0.99 | 2.31 |
| Samarra | Green | 18 | 5.8 | 1.46 | 63.2 | 2.49 | 5.85 | 0.08 | 1.64 | 0.53 | 0 | Schibille et al. 2018 | 0.99 | 2.33 |
| Samarra | Green | 16.7 | 5.56 | 1.51 | 64.6 | 2.5 | 5.55 | 0.09 | 2.08 | 0.51 | 0 | Schibille et al. 2018 | 1.00 | 2.22 |

| | | | | | | | | | | | | | | |
|---------|-------|------|------|------|------|------|------|------|------|------|---|-----------------------|------|------|
| Samarra | Green | 16.8 | 6.15 | 1.4 | 64.5 | 2.75 | 5.53 | 0.08 | 1.36 | 0.49 | 0 | Schibille et al. 2018 | 1.11 | 2.24 |
| Samarra | Green | 15.9 | 5.65 | 1.36 | 67.5 | 2.19 | 5.08 | 0.07 | 1.04 | 0.44 | 0 | Schibille et al. 2018 | 1.11 | 2.58 |
| Samarra | Green | 14.5 | 5.19 | 1.59 | 68.6 | 2 | 5.23 | 0.1 | 1.28 | 0.64 | 0 | Schibille et al. 2018 | 0.99 | 2.60 |
| Samarra | Green | 15 | 5.99 | 1.41 | 66.2 | 2.74 | 5.65 | 0.08 | 1.54 | 0.47 | 0 | Schibille et al. 2018 | 1.06 | 2.19 |
| Samarra | Green | 18 | 5.77 | 1.45 | 63.2 | 2.47 | 5.77 | 0.08 | 1.7 | 0.54 | 0 | Schibille et al. 2018 | 1.00 | 2.34 |
| Samarra | Green | 16.7 | 6.19 | 1.42 | 64.5 | 2.72 | 5.57 | 0.08 | 1.36 | 0.49 | 0 | Schibille et al. 2018 | 1.11 | 2.28 |
| Samarra | Green | 15.9 | 5.87 | 1.36 | 66.2 | 2.57 | 5.11 | 0.08 | 1.31 | 0.62 | 0 | Schibille et al. 2018 | 1.15 | 2.28 |
| Samarra | Green | 14.6 | 5.46 | 1.51 | 68.2 | 2.26 | 5.29 | 0.09 | 1.18 | 0.55 | 0 | Schibille et al. 2018 | 1.03 | 2.42 |
| Samarra | Green | 14.9 | 5.81 | 1.39 | 66.4 | 2.83 | 5.78 | 0.08 | 1.45 | 0.47 | 0 | Schibille et al. 2018 | 1.01 | 2.05 |
| Samarra | Green | 15.5 | 5.55 | 1.37 | 67.7 | 2.25 | 5.2 | 0.08 | 1.06 | 0.44 | 0 | Schibille et al. 2018 | 1.07 | 2.47 |
| Samarra | Green | 17.7 | 5.62 | 1.42 | 63.7 | 2.54 | 5.8 | 0.08 | 1.69 | 0.53 | 0 | Schibille et al. 2018 | 0.97 | 2.21 |
| Samarra | Green | 16.8 | 6.36 | 1.34 | 64 | 3.39 | 5.38 | 0.07 | 1.26 | 0.42 | 0 | Schibille et al. 2018 | 1.18 | 1.88 |
| Samarra | Green | 16 | 5.69 | 1.49 | 66.4 | 2.27 | 5.38 | 0.08 | 1.34 | 0.49 | 0 | Schibille et al. 2018 | 1.06 | 2.51 |
| Samarra | Green | 15.7 | 5.51 | 1.35 | 67.7 | 2.24 | 5.17 | 0.08 | 1.05 | 0.45 | 0 | Schibille et al. 2018 | 1.07 | 2.46 |
| Samarra | Green | 16.6 | 6.27 | 1.28 | 64.8 | 3.26 | 5.06 | 0.07 | 1.35 | 0.41 | 0 | Schibille et al. 2018 | 1.24 | 1.92 |
| Samarra | Green | 17.7 | 5.69 | 1.43 | 63.6 | 2.55 | 5.89 | 0.08 | 1.64 | 0.56 | 0 | Schibille et al. 2018 | 0.97 | 2.23 |

| | | | | | | | | | | | | | | |
|---------|--------------|------|------|------|------|------|------|------|------|------|------|-----------------------|------|------|
| Samarra | Green | 17.9 | 5.67 | 1.43 | 63.3 | 2.54 | 5.8 | 0.08 | 1.72 | 0.54 | 0 | Schibille et al. 2018 | 0.98 | 2.23 |
| Samarra | Green | 16.7 | 6.07 | 1.39 | 64.6 | 2.78 | 5.52 | 0.08 | 1.35 | 0.49 | 0 | Schibille et al. 2018 | 1.10 | 2.18 |
| Samarra | Colourless | 15.3 | 5.77 | 1.07 | 68.8 | 2.34 | 4.63 | 0.07 | 0.74 | 0.41 | 0 | Schibille et al. 2018 | 1.25 | 2.47 |
| Samarra | Colourless | 15.8 | 5.76 | 1.23 | 67.1 | 2.63 | 4.72 | 0.07 | 1.42 | 0.35 | 0 | Schibille et al. 2018 | 1.22 | 2.19 |
| Samarra | Blue Co | 14.9 | 6.04 | 1.3 | 66.6 | 2.68 | 4.82 | 0.07 | 1.25 | 1.26 | 0.01 | Schibille et al. 2018 | 1.25 | 2.25 |
| Samarra | Blue Co | 14.9 | 6.09 | 1.32 | 66.4 | 2.64 | 4.79 | 0.07 | 1.25 | 1.34 | 0.01 | Schibille et al. 2018 | 1.27 | 2.31 |
| Samarra | Aqua/Blue Co | 15.6 | 5.3 | 1.33 | 67.4 | 2.35 | 4.78 | 0.06 | 1.14 | 0.95 | 0 | Schibille et al. 2018 | 1.11 | 2.26 |
| Samarra | Aqua/Blue Co | 15.7 | 5.33 | 1.34 | 67.2 | 2.34 | 4.8 | 0.06 | 1.14 | 0.95 | 0 | Schibille et al. 2018 | 1.11 | 2.28 |
| Samarra | Aqua/Blue Co | 15.6 | 5.31 | 1.34 | 67.3 | 2.36 | 4.81 | 0.06 | 1.15 | 0.97 | 0 | Schibille et al. 2018 | 1.10 | 2.25 |
| Samarra | Blue Co | 14.8 | 6.03 | 1.31 | 66.6 | 2.67 | 4.81 | 0.07 | 1.24 | 1.25 | 0.01 | Schibille et al. 2018 | 1.25 | 2.26 |
| Samarra | Blue Co | 15 | 6.12 | 1.31 | 66.4 | 2.66 | 4.79 | 0.07 | 1.22 | 1.23 | 0.01 | Schibille et al. 2018 | 1.28 | 2.30 |
| Samarra | Aqua | 16 | 5.49 | 1.47 | 66.1 | 2.62 | 5.52 | 0.1 | 1.23 | 0.6 | 0 | Schibille et al. 2018 | 0.99 | 2.10 |
| Samarra | Green | 14.6 | 5.08 | 1.39 | 64 | 2.64 | 5.05 | 0.09 | 1.61 | 0.62 | 2.87 | Schibille et al. 2018 | 1.01 | 1.92 |
| Samarra | Colourless | 15.9 | 5.68 | 1.3 | 67.5 | 2.44 | 4.88 | 0.06 | 1.05 | 0.42 | 0 | Schibille et al. 2018 | 1.16 | 2.33 |
| Samarra | Aqua | 17.7 | 6.94 | 1.12 | 64.7 | 2.86 | 4.51 | 0.06 | 0.87 | 0.31 | 0 | Schibille et al. 2018 | 1.54 | 2.43 |
| Samarra | Aqua | 14.7 | 4.94 | 1.24 | 69.1 | 2.64 | 5.12 | 0.09 | 0.78 | 0.48 | 0 | Schibille et al. 2018 | 0.96 | 1.87 |
| Samarra | Aqua | 17.7 | 6.89 | 1.15 | 64.8 | 2.9 | 4.45 | 0.06 | 0.83 | 0.32 | 0 | Schibille et | 1.55 | 2.38 |

| | | | | | | | | | | | | | | |
|---------|------------|----------|----------|----------|----------|--------------|---------------|----------|----------|----------|----------|---------------------------------|------|------|
| | | | | | | | | | | | | al. 2018 | | |
| Samarra | Aqua | 17 | 5. 96 | 1.2 9 | 66 .6 | 2. 7 9 | 4. 6 | 0. 08 | 0. 39 | 0.4 5 | 0 | Schib ille et al. 2018 | 1.30 | 2.14 |
| Samarra | Blue Co | 14 .6 | 4. 22 | 2.3 1 | 64 .1 | 2. 6 5 | 7. 6 | 0. 14 | 1. 06 | 1.5 3 | 0.0 2 | Schib ille et al. 2018 | 0.56 | 1.59 |
| Samarra | Aqua | 11 .9 | 3. 27 | 1.4 9 | 72 .4 | 3. 5 5 | 5. 42 | 0. 08 | 0. 29 | 0.7 4 | 0 | Schib ille et al. 2018 | 0.60 | 0.92 |
| Samarra | Green | 18 .4 | 3. 59 | 3.2 6 | 61 .1 | 2. 9 7 | 7. 28 | 0. 15 | 0. 71 | 0.9 8 | 0.0 2 | Schib ille et al. 2018 | 0.49 | 1.21 |
| Samarra | Green | 12 .1 | 3. 49 | 0.7 | 69 .3 | 3. 1 2 | 9. 74 | 0. 05 | 0. 03 | 0.3 7 | 0 | Schib ille et al. 2018 | 0.36 | 1.12 |
| Samarra | Colourless | 13 .2 | 3. 19 | 2.5 6 | 69 | 3. 0 3 | 4. 85 | 0. 15 | 2. 2 | 0.8 5 | 0 | Schib ille et al. 2018 | 0.66 | 1.05 |
| Samarra | Purple | 12 .8 | 3. 38 | 2.6 7 | 67 .2 | 2. 8 5 | 5. 55 | 0. 15 | 3. 44 | 0.8 4 | 0 | Schib ille et al. 2018 | 0.61 | 1.19 |
| Samarra | Colourless | 13 .9 | 3. 33 | 0.9 | 71 .4 | 3. 4 2 | 4. 83 | 0. 05 | 0. 67 | 0.5 4 | 0.0 1 | Schib ille et al. 2018 | 0.69 | 0.97 |
| Samarra | Aqua | 15 .1 | 3. 21 | 2.2 4 | 63 .6 | 3. 0 7 | 7. 8 | 0. 14 | 2. 7 | 0.9 7 | 0.0 1 | Schib ille et al. 2018 | 0.41 | 1.05 |
| Samarra | Aqua | 15 | 3. 21 | 2.2 8 | 63 .5 | 3. 0 8 | 7. 98 | 0. 15 | 2. 74 | 0.9 7 | 0.0 1 | Schib ille et al. 2018 | 0.40 | 1.04 |
| Samarra | Aqua | 15 .1 | 3. 25 | 2.2 8 | 63 .4 | 3. 0 2 | 7. 9 | 0. 14 | 2. 69 | 0.9 7 | 0.0 1 | Schib ille et al. 2018 | 0.41 | 1.08 |
| Samarra | Green | 15 .8 | 3. 15 | 6.3 7 | 59 .7 | 3. 3 2 | 7. 69 | 0. 31 | 0. 06 | 2.6 1 | 0 | Schib ille et al. 2018 | 0.41 | 0.95 |
| Samarra | Yellow | 13 .9 | 2. 47 | 1.6 2 | 67 | 1. 9 7 | 10 .4 1 | 0. 13 | 0. 75 | 0.7 1 | 0.0 2 | Schib ille et al. 2018 | 0.24 | 1.25 |
| Samarra | Colourless | 14 .2 | 2. 74 | 2.3 2 | 66 .4 | 2. 7 7 | 6. 62 | 0. 15 | 2. 62 | 1.0 4 | 0 | Schib ille et al. 2018 | 0.41 | 0.99 |
| Samarra | Green | 12 .1 | 2. 72 | 2.7 4 | 67 .4 | 3. 2 3 | 6. 78 | 0. 2 | 2. 37 | 1.2 4 | 0 | Schib ille et al. 2018 | 0.40 | 0.84 |
| Samarra | Aqua | 16 .1 | 3. 66 | 3.3 7 | 64 .2 | 2. 8 9 | 6. 36 | 0. 17 | 0. 77 | 1.2 4 | 0.0 2 | Schib ille et al. 2018 | 0.58 | 1.27 |

| | | | | | | | | | | | | | | |
|--------------|------------|-------|------|------|-------|------|-------|------|------|------|---|-----------------------|------|------|
| Samarra | Yellow | 15.8 | 4.08 | 4.1 | 61.4 | 3.73 | 7.54 | 0.24 | 0.18 | 1.79 | 0 | Schibille et al. 2018 | 0.54 | 1.09 |
| Serce Limani | Not Stated | 12.36 | 1.95 | 2.47 | 71.3 | 2.62 | 8.57 | 0.2 | 0.78 | 0.73 | 0 | Brill, 2009 | 0.23 | 0.74 |
| Serce Limani | Not Stated | 14.06 | 2.46 | 2.75 | 71.85 | 1.79 | 5.94 | 0.15 | 1.6 | 1.14 | 0 | Brill, 2009 | 0.41 | 1.37 |
| Serce Limani | Not Stated | 11.46 | 2.69 | 1.96 | 70.51 | 2.58 | 10.09 | 0.15 | 1.82 | 0.72 | 0 | Brill, 2009 | 0.27 | 1.04 |
| Serce Limani | Not Stated | 13.39 | 3.05 | 1.91 | 69.65 | 2.25 | 9.14 | 0.15 | 1.78 | 0.66 | 0 | Brill, 2009 | 0.33 | 1.39 |
| Serce Limani | Not Stated | 12.16 | 2.58 | 1.85 | 69.81 | 2.68 | 10.32 | 0.15 | 1.75 | 0.6 | 0 | Brill, 2009 | 0.25 | 0.96 |
| Serce Limani | Not Stated | 12.09 | 2.43 | 2.21 | 71.04 | 2.26 | 9.22 | 0.15 | 0.38 | 0.76 | 0 | Brill, 2009 | 0.26 | 1.08 |
| Serce Limani | Not Stated | 13.29 | 3 | 2.63 | 67.83 | 2.63 | 9.76 | 0.15 | 1.56 | 0.87 | 0 | Brill, 2009 | 0.31 | 1.14 |
| Serce Limani | Not Stated | 11.9 | 2.37 | 2 | 70.84 | 2.86 | 9.45 | 0.15 | 1.25 | 0.59 | 0 | Brill, 2009 | 0.25 | 0.83 |
| Serce Limani | Not Stated | 11.92 | 2.25 | 1.83 | 70.72 | 3.04 | 9.68 | 0.15 | 1.48 | 0.55 | 0 | Brill, 2009 | 0.23 | 0.74 |
| Serce Limani | Not Stated | 11.71 | 1.88 | 1.85 | 71.62 | 3.26 | 9.07 | 0.1 | 1.48 | 0.61 | 0 | Brill, 2009 | 0.21 | 0.58 |
| Serce Limani | Not Stated | 13.98 | 2.97 | 1.58 | 68.49 | 2.43 | 9.91 | 0.1 | 0.92 | 0.65 | 0 | Brill, 2009 | 0.30 | 1.22 |
| Serce Limani | Not Stated | 13.26 | 2.48 | 2.02 | 70.38 | 2.66 | 8.59 | 0.15 | 1.24 | 0.67 | 0 | Brill, 2009 | 0.29 | 0.95 |
| Serce Limani | Not Stated | 13.12 | 2.69 | 1.84 | 68.76 | 2.91 | 9.38 | 0.15 | 0.24 | 1.3 | 0 | Brill, 2009 | 0.29 | 0.92 |
| Serce Limani | Not Stated | 13.42 | 2.48 | 1.7 | 69.91 | 2.66 | 9.3 | 0.15 | 1.06 | 0.53 | 0 | Brill, 2009 | 0.27 | 0.93 |
| Serce Limani | Not Stated | 12.35 | 2.55 | 2.05 | 70.93 | 2.32 | 9.08 | 0.15 | 0.81 | 0.72 | 0 | Brill, 2009 | 0.28 | 1.10 |
| Serce Limani | Not Stated | 13.06 | 2.98 | 1.93 | 68.98 | 2.34 | 10.09 | 0.15 | 1.58 | 0.63 | 0 | Brill, 2009 | 0.30 | 1.27 |
| Serce Limani | Not Stated | 12.13 | 2.45 | 2.04 | 67.6 | 2.79 | 12.23 | 0.13 | 1.5 | 0.76 | 0 | Brill, 2009 | 0.20 | 0.88 |
| Serce Limani | Not Stated | 12.06 | 2.11 | 1.75 | 71.22 | 2.71 | 9.6 | 0.1 | 1.1 | 0.55 | 0 | Brill, 2009 | 0.22 | 0.78 |
| Serce Limani | Not Stated | 14.09 | 3.11 | 1.67 | 69.18 | 2.05 | 9.35 | 0.1 | 1.08 | 0.55 | 0 | Brill, 2009 | 0.33 | 1.52 |
| Serce Limani | Not Stated | 13.33 | 2.47 | 2.48 | 68.19 | 3.01 | 9.78 | 0.1 | 1.83 | 0.74 | 0 | Brill, 2009 | 0.25 | 0.82 |

| | | | | | | | | | | | | | | |
|--------------|------------|---------------|----------|----------|---------------|--------------|---------------|----------|----------|----------|---|----------------|------|------|
| Serce Limani | Not Stated | 11 .3 5 | 2. 34 | 1.8 2 | 71 .6 8 | 2. 8 4 | 9. 35 | 0. 1 | 1. 95 | 0.6 2 | 0 | Brill, 2009 | 0.25 | 0.82 |
| Serce Limani | Not Stated | 12 .9 2 | 2. 71 | 1.8 5 | 70 .5 9 | 2. 4 | 8. 84 | 0. 1 | 1. 44 | 0.6 9 | 0 | Brill, 2009 | 0.31 | 1.13 |
| Serce Limani | Not Stated | 13 .4 1 | 2. 68 | 1.6 9 | 68 .5 9 | 2. 8 2 | 10 .2 6 | 0. 1 | 1. 34 | 0.5 4 | 0 | Brill, 2009 | 0.26 | 0.95 |
| Serce Limani | Not Stated | 13 .1 1 | 2. 68 | 1.6 9 | 69 .0 1 | 2. 8 2 | 10 .1 3 | 0. 1 | 1. 34 | 0.5 6 | 0 | Brill, 2009 | 0.26 | 0.95 |
| Serce Limani | Not Stated | 12 .5 7 | 2. 46 | 1.7 9 | 68 .3 7 | 3. 4 7 | 10 .8 5 | 0. 13 | 1. 1 | 0.4 8 | 0 | Brill, 2009 | 0.23 | 0.71 |
| Serce Limani | Not Stated | 14 .3 2 | 3. 05 | 1.6 2 | 69 .2 9 | 2. 2 5 | 9. 01 | 0. 1 | 1. 3 | 0.4 6 | 0 | Brill, 2009 | 0.34 | 1.36 |
| Serce Limani | Not Stated | 12 .8 9 | 2. 78 | 1.8 8 | 68 .3 2 | 2. 7 8 | 10 .6 6 | 0. 1 | 1. 24 | 0.6 9 | 0 | Brill, 2009 | 0.26 | 1.00 |
| Serce Limani | Not Stated | 12 .1 7 | 2. 22 | 1.8 1 | 71 .0 3 | 2. 6 8 | 9. 53 | 0. 1 | 1. 94 | 0.5 7 | 0 | Brill, 2009 | 0.23 | 0.83 |
| Serce Limani | Not Stated | 12 .2 6 | 2. 27 | 1.7 3 | 70 .8 9 | 2. 9 9 | 9. 26 | 0. 1 | 1. 11 | 0.5 9 | 0 | Brill, 2009 | 0.25 | 0.76 |
| Serce Limani | Not Stated | 13 .9 8 | 3. 12 | 1.8 3 | 68 .4 5 | 2. 7 6 | 8. 89 | 0. 1 | 1. 2 | 0.9 7 | 0 | Brill, 2009 | 0.35 | 1.13 |
| Serce Limani | Not Stated | 13 .7 2 | 2. 6 | 1.8 4 | 70 .6 8 | 2. 6 9 | 7. 5 | 0. 1 | 1. 42 | 0.9 6 | 0 | Brill, 2009 | 0.35 | 0.97 |
| Serce Limani | Not Stated | 12 .2 4 | 2. 45 | 1.5 8 | 70 .3 4 | 2. 9 5 | 9. 53 | 0. 1 | 1. 09 | 0.9 1 | 0 | Brill, 2009 | 0.26 | 0.83 |
| Serce Limani | Not Stated | 12 .0 5 | 2. 43 | 1.8 1 | 69 .3 8 | 2. 7 8 | 10 .8 1 | 0. 1 | 1. 65 | 0.7 4 | 0 | Brill, 2009 | 0.22 | 0.87 |
| Serce Limani | Not Stated | 12 .5 3 | 2. 96 | 1.7 9 | 69 .8 7 | 2. 6 3 | 9. 55 | 0. 15 | 1. 07 | 0.7 6 | 0 | Brill, 2009 | 0.31 | 1.13 |
| Serce Limani | Not Stated | 13 .9 2 | 3. 2 | 2.4 7 | 69 .1 | 2. 2 9 | 8. 28 | 0. 08 | 1. 74 | 0.7 5 | 0 | Brill, 2009 | 0.39 | 1.40 |
| Serce Limani | Not Stated | 15 .2 3 | 2. 74 | 1.8 3 | 69 .3 9 | 2. 5 7 | 7. 61 | 0. 1 | 1. 94 | 0.6 3 | 0 | Brill, 2009 | 0.36 | 1.07 |
| Serce Limani | Not Stated | 12 .4 3 | 2. 55 | 2.3 5 | 68 .9 6 | 3. 1 1 | 9. 96 | 0. 1 | 1. 24 | 0.6 4 | 0 | Brill, 2009 | 0.26 | 0.82 |
| Serce Limani | Not Stated | 14 .1 6 | 3. 12 | 2.0 8 | 69 .2 4 | 2. 6 5 | 8. 12 | 0. 1 | 1. 35 | 0.6 3 | 0 | Brill, 2009 | 0.38 | 1.18 |
| Serce Limani | Not Stated | 13 .5 | 2. 49 | 2.1 7 | 69 .5 2 | 2. 8 9 | 8. 71 | 0. 15 | 1. 2 | 0.7 1 | 0 | Brill, 2009 | 0.29 | 0.86 |
| Serce Limani | Not Stated | 12 .9 | 2. 39 | 2.2 5 | 69 .7 1 | 2. 9 8 | 9. 04 | 0. 1 | 1. 78 | 0.7 3 | 0 | Brill, 2009 | 0.26 | 0.80 |
| Serce Limani | Not Stated | 14 .1 9 | 2. 67 | 1.6 9 | 69 .3 3 | 3. 0 8 | 8. 51 | 0. 15 | 1. 06 | 0.5 3 | 0 | Brill, 2009 | 0.31 | 0.87 |

| | | | | | | | | | | | | | | |
|------------------|------------|-------|------|------|-------|------|-------|------|------|------|---|--------------------|------|------|
| Serce Limani | Not Stated | 13.25 | 2.82 | 2.09 | 69.17 | 2.47 | 9.53 | 0.15 | 0.78 | 0.68 | 0 | Brill, 2009 | 0.30 | 1.14 |
| Serce Limani | Not Stated | 12.35 | 2.37 | 2.14 | 70.44 | 2.77 | 9.32 | 0.09 | 0.63 | 0.61 | 0 | Brill, 2009 | 0.25 | 0.86 |
| Serce Limani | Not Stated | 13.81 | 2.78 | 1.95 | 68.83 | 2.67 | 9.11 | 0.1 | 1.16 | 0.84 | 0 | Brill, 2009 | 0.31 | 1.04 |
| Serce Limani | Not Stated | 14.28 | 2.52 | 1.67 | 69.66 | 2.73 | 8.71 | 0.15 | 0.27 | 0.43 | 0 | Brill, 2009 | 0.29 | 0.92 |
| Serce Limani | Not Stated | 13.73 | 2.93 | 0.7 | 69.13 | 2.28 | 10.93 | 0 | 0.04 | 0.3 | 0 | Brill, 2009 | 0.27 | 1.29 |
| Serce Limani | Not Stated | 12.27 | 3.35 | 0.98 | 67.55 | 2.93 | 12.27 | 0.15 | 1.75 | 0.64 | 0 | Brill, 2009 | 0.27 | 1.14 |
| Serce Limani | Not Stated | 12.8 | 2.55 | 1.96 | 68.33 | 3.16 | 10.53 | 0.2 | 2.73 | 0.68 | 0 | Brill, 2009 | 0.24 | 0.81 |
| Serce Limani | Not Stated | 13.68 | 1.88 | 1.92 | 74.16 | 2.47 | 5.21 | 0.13 | 1.7 | 0.68 | 0 | Brill, 2009 | 0.36 | 0.76 |
| Serce Limani | Not Stated | 13.33 | 2.68 | 2.04 | 68.33 | 3.22 | 9.06 | 0.79 | 0.22 | 1.34 | 0 | Brill, 2009 | 0.30 | 0.83 |
| Serce Limani | Not Stated | 15.4 | 3.21 | 0.95 | 67.71 | 2.16 | 8.82 | 0.08 | 0.09 | 1.76 | 0 | Brill, 2009 | 0.36 | 1.49 |
| Rayy Tape Bahram | Green | 16.36 | 3.16 | 4.13 | 65.27 | 2.83 | 4.43 | 0.15 | 0.11 | 1.09 | 0 | Aligol et al. 2022 | 0.71 | 1.12 |
| Rayy Tape Bahram | Green | 16.31 | 3.53 | 2.92 | 64.83 | 3.25 | 5.06 | 0.11 | 0.43 | 1.11 | 0 | Aligol et al. 2022 | 0.70 | 1.09 |
| Rayy Tape Bahram | Green | 17.02 | 4.26 | 3.68 | 63.26 | 2.93 | 5.06 | 0.14 | 0.47 | 1.13 | 0 | Aligol et al. 2022 | 0.84 | 1.45 |
| Rayy Tape Bahram | Green | 15.71 | 2.91 | 3.33 | 65.91 | 2.54 | 5.55 | 0.21 | 0.13 | 1.57 | 0 | Aligol et al. 2022 | 0.52 | 1.15 |
| Rayy Tape Bahram | Green | 17.34 | 3.98 | 2.4 | 64.07 | 2.57 | 5.5 | 0.13 | 1.03 | 0.94 | 0 | Aligol et al. 2022 | 0.72 | 1.47 |
| Rayy Tape Bahram | Green | 17.52 | 3.37 | 3.28 | 61.65 | 3.19 | 5.48 | 0.25 | 1.31 | 1.42 | 0 | Aligol et al. 2022 | 0.61 | 1.06 |
| Rayy Tape Bahram | Green | 17.41 | 3.71 | 3.8 | 60.63 | 2.84 | 5.52 | 0.16 | 0.05 | 1.32 | 0 | Aligol et al. 2022 | 0.67 | 1.31 |
| Rayy Tape Bahram | Green | 13.83 | 3.36 | 2.68 | 64.85 | 5.32 | 5.22 | 0.1 | 0.07 | 1.37 | 0 | Aligol et al. 2022 | 0.64 | 0.63 |
| Rayy Tape Bahram | Green | 16.72 | 4.08 | 2.88 | 64.57 | 2.66 | 5.17 | 0.12 | 1.02 | 0.9 | 0 | Aligol et al. 2022 | 0.79 | 1.53 |
| Rayy Tape Bahram | Green | 14.77 | 2.66 | 2.98 | 65.99 | 2.98 | 5.73 | 0.16 | 1.24 | 1.23 | 0 | Aligol et al. 2022 | 0.46 | 0.89 |
| Rayy Tape Bahram | Green | 16.96 | 4.22 | 2.88 | 63.2 | 2.73 | 5.32 | 0.12 | 0.96 | 0.99 | 0 | Aligol et al. 2022 | 0.79 | 1.55 |

| | | | | | | | | | | | | | | |
|------------------|-------|-------|------|------|-------|------|------|------|------|------|---|--------------------|------|------|
| Rayy Tape Bahram | Green | 17.02 | 3.97 | 2.68 | 63.23 | 2.83 | 5.56 | 0.16 | 1.18 | 1.29 | 0 | Aligol et al. 2022 | 0.71 | 1.40 |
| Rayy Tape Bahram | Green | 16.62 | 3.98 | 3 | 63.82 | 2.72 | 5.56 | 0.14 | 1.21 | 1.09 | 0 | Aligol et al. 2022 | 0.72 | 1.46 |
| Rayy Tape Bahram | Green | 17.09 | 3.96 | 2.99 | 65.33 | 2.66 | 5.19 | 0.13 | 0.86 | 0.83 | 0 | Aligol et al. 2022 | 0.76 | 1.49 |
| Rayy Tape Bahram | Green | 18.11 | 4.11 | 2.91 | 67.17 | 2.92 | 5.66 | 0.12 | 1.05 | 1.04 | 0 | Aligol et al. 2022 | 0.73 | 1.41 |
| Rayy Tape Bahram | Green | 16.99 | 3.78 | 2.43 | 63.64 | 2.73 | 5.7 | 0.15 | 1.12 | 1.08 | 0 | Aligol et al. 2022 | 0.66 | 1.38 |
| Rayy Tape Bahram | Green | 16.31 | 3.97 | 3.08 | 63.61 | 2.72 | 5.69 | 0.15 | 1.26 | 1.27 | 0 | Aligol et al. 2022 | 0.70 | 1.46 |
| Rayy Tape Bahram | Green | 16.07 | 3.91 | 2.78 | 65.98 | 2.56 | 4.95 | 0.12 | 0.9 | 0.78 | 0 | Aligol et al. 2022 | 0.79 | 1.53 |
| Rayy Tape Bahram | Green | 16.41 | 3.85 | 2.35 | 64.73 | 2.65 | 5.3 | 0.16 | 1.13 | 0.95 | 0 | Aligol et al. 2022 | 0.73 | 1.45 |
| Rayy Tape Bahram | Green | 16.24 | 3.93 | 2.93 | 63.88 | 2.61 | 5.16 | 0.14 | 1.11 | 0.89 | 0 | Aligol et al. 2022 | 0.76 | 1.51 |
| Rayy Tape Bahram | Green | 16.7 | 4.04 | 2.78 | 64.28 | 2.77 | 5.36 | 0.14 | 0.93 | 0.85 | 0 | Aligol et al. 2022 | 0.75 | 1.50 |
| Rayy Tape Bahram | Green | 17.42 | 4.02 | 2.69 | 64.51 | 2.66 | 4.88 | 0.13 | 0.99 | 0.77 | 0 | Aligol et al. 2022 | 0.82 | 1.51 |
| Rayy Tape Bahram | Green | 15.27 | 3.64 | 3.79 | 63.32 | 2.66 | 5.12 | 0.14 | 0.98 | 1.78 | 0 | Aligol et al. 2022 | 0.71 | 1.37 |
| Rayy Tape Bahram | Green | 16.81 | 3.7 | 3.06 | 64.13 | 2.77 | 5.33 | 0.15 | 1.03 | 0.91 | 0 | Aligol et al. 2022 | 0.69 | 1.37 |
| Rayy Tape Bahram | Green | 16.05 | 3.98 | 2.66 | 64.31 | 2.77 | 5.66 | 0.16 | 1.17 | 1.02 | 0 | Aligol et al. 2022 | 0.70 | 1.44 |
| Rayy Tape Bahram | Green | 16.53 | 3.68 | 2.63 | 64.17 | 2.78 | 5.66 | 0.16 | 1.29 | 1.19 | 0 | Aligol et al. 2022 | 0.65 | 1.32 |
| Rayy Tape Bahram | Green | 19.02 | 2.57 | 3.41 | 60.8 | 4.26 | 5.93 | 0.13 | 0.05 | 1.4 | 0 | Aligol et al. 2022 | 0.43 | 0.60 |
| Rayy Tape Bahram | Green | 18.65 | 2.41 | 3.47 | 61.49 | 4.28 | 5.93 | 0.21 | 0.05 | 1.24 | 0 | Aligol et al. 2022 | 0.41 | 0.56 |
| Rayy Tape Bahram | Green | 15.23 | 5.98 | 1.67 | 67.88 | 2.97 | 3.93 | 0.05 | 0.13 | 0.31 | 0 | Aligol et al. 2022 | 1.52 | 2.01 |
| Rayy Tape Bahram | Green | 18.59 | 2.6 | 3.68 | 61.03 | 3.96 | 6.47 | 0.21 | 0.07 | 1.45 | 0 | Aligol et al. 2022 | 0.40 | 0.66 |
| Rayy Tape Bahram | Green | 16.7 | 4.12 | 3.29 | 63.61 | 2.73 | 5.37 | 0.13 | 0.97 | 1.08 | 0 | Aligol et al. 2022 | 0.77 | 1.51 |
| Rayy Tape Bahram | Green | 15.75 | 3.06 | 4.65 | 66.19 | 2.55 | 4.34 | 0.09 | 0.1 | 0.82 | 0 | Aligol et al. 2022 | 0.71 | 1.20 |

| | | | | | | | | | | | | | | |
|------------------|-----------------|-------|------|------|-------|------|------|------|------|------|---|-----------------------|------|------|
| Rayy Tape Bahram | Green | 19.05 | 3.76 | 2.32 | 63.56 | 2.81 | 4.54 | 0.07 | 0.04 | 0.68 | 0 | Aligol et al. 2022 | 0.83 | 1.34 |
| Rayy Tape Bahram | Green | 16.58 | 3.71 | 2.78 | 64.99 | 2.77 | 5.58 | 0.14 | 1.01 | 1 | 0 | Aligol et al. 2022 | 0.66 | 1.34 |
| Rayy Tape Bahram | Green | 16.64 | 3.62 | 2.3 | 65.95 | 2.67 | 5.42 | 0.17 | 1.05 | 0.84 | 0 | Aligol et al. 2022 | 0.67 | 1.36 |
| Rayy Tape Bahram | Green | 18.76 | 2.41 | 3.49 | 61.64 | 4.44 | 5.9 | 0.18 | 0.05 | 1.41 | 0 | Aligol et al. 2022 | 0.41 | 0.58 |
| Rayy Tape Bahram | Green | 16.4 | 3.88 | 3.23 | 64.47 | 2.72 | 5.3 | 0.19 | 1.14 | 1.14 | 0 | Aligol et al. 2022 | 0.73 | 1.43 |
| Tyre | Opal | 11.1 | 3.2 | 1.5 | 65.5 | 1.9 | 14.1 | 0.1 | 0.7 | 0.4 | 0 | Frees tone 2002 | 0.23 | 0.86 |
| Tyre | Blue | 12.9 | 3.66 | 1.77 | 62.4 | 2.56 | 11.9 | 0.09 | 1.64 | 0.45 | 0 | Frees tone 2002 | 0.31 | 1.56 |
| Tyre | Yellow-Green | 13.1 | 3.58 | 1.74 | 62.8 | 2.57 | 11.5 | 0.1 | 1.56 | 0.45 | 0 | Frees tone 2002 | 0.31 | 1.26 |
| Tyre | Yellow-Green | 13 | 3.53 | 1.78 | 62.6 | 2.56 | 12.1 | 0.1 | 1.67 | 0.46 | 0 | Frees tone 2002 | 0.29 | 1.24 |
| Tyre | Pale Green/Pink | 10.8 | 3.12 | 1.62 | 64.9 | 1.98 | 14.3 | 0.09 | 0.89 | 0.38 | 0 | Frees tone 2002 | 0.22 | 1.10 |
| Tyre | Colourless | 14.3 | 3.38 | 1.69 | 64.3 | 2.61 | 9.8 | 0.09 | 0.77 | 0.42 | 0 | Frees tone 2002 | 0.34 | 1.08 |
| Tyre | Pale pink | 14.2 | 3.88 | 1.76 | 64.3 | 2.63 | 9.1 | 0.09 | 1.95 | 0.47 | 0 | Frees tone 2002 | 0.43 | 0.95 |
| Tyre | Purple | 13.8 | 3.55 | 1.79 | 64.9 | 2.66 | 8.4 | 0.1 | 2.3 | 0.43 | 0 | Frees tone 2002 | 0.42 | 1.15 |
| Tyre | Green | 10.9 | 2.03 | 1.71 | 74 | 2.84 | 5.1 | 0.1 | 0.54 | 0.3 | 0 | Frees tone 2002 | 0.40 | 0.80 |
| Tyre | Blue | 12.1 | 2.67 | 1.8 | 65.5 | 2.48 | 8.8 | 0.08 | 0.82 | | 0 | Frees tone 2002 | 0.30 | 1.25 |
| Raqqa Type One | | 13.73 | 3.62 | 1.1 | 67.23 | 2.48 | 8.36 | 0.06 | 1.53 | 0.36 | 0 | Henderson et al. 2004 | 0.43 | 3.37 |
| Raqqa Type One | | 13.64 | 0.52 | 3.22 | 70.66 | 0.47 | 9.86 | 0.05 | 0 | 0.37 | 0 | Henderson et al. 2004 | 0.05 | 3.50 |
| Raqqa Type One | | 13.4 | 0.47 | 3.09 | 72.97 | 0.45 | 8.18 | 0.06 | 0 | 0.29 | 0 | Henderson et al. 2004 | 0.06 | 7.28 |
| Raqqa Type One | | 12.57 | 0.5 | 3.14 | 72.04 | 0.48 | 9.75 | 0.05 | 0 | 0.38 | 0 | Henderson et al. 2004 | 0.05 | 4.97 |
| Raqqa Type One | | 12.74 | 5.1 | 1.57 | 70.87 | 3.42 | 4.52 | 0.06 | 0.29 | 0.51 | 0 | Henderson et al. 2004 | 1.13 | 6.04 |

| | | | | | | | | | | | | | | |
|----------------|--|---------------|----------|----------|---------------|--------------|----------|----------|----------|----------|---|-----------------------|------|------|
| Raqqa Type One | | 15 .0 5 | 0. 97 | 3.4 2 | 67 .1 9 | 0. 7 3 | 10 .9 | 0. 07 | 0 | 0.4 7 | 0 | Henderson et al. 2004 | 0.09 | 4.49 |
| Raqqa Type One | | 14 .1 7 | 1. 98 | 2.8 7 | 69 .5 6 | 1. 2 8 | 8. 51 | 0. 05 | 0. 09 | 0.4 8 | 0 | Henderson et al. 2004 | 0.23 | 3.77 |
| Raqqa Type One | | 14 .7 3 | 6. 2 | 1.5 1 | 68 .6 | 2. 8 2 | 4. 32 | 0. 07 | 0. 18 | 0.4 7 | 0 | Henderson et al. 2004 | 1.44 | 6.67 |
| Raqqa Type One | | 14 .5 1 | 6. 24 | 1.5 3 | 68 .7 8 | 2. 7 5 | 4. 35 | 0. 07 | 0. 21 | 0.4 9 | 0 | Henderson et al. 2004 | 1.43 | 7.40 |
| Raqqa Type One | | 13 .1 6 | 0. 5 | 3.1 4 | 71 .7 6 | 0. 4 6 | 9. 49 | 0 | 0 | 0.3 3 | 0 | Henderson et al. 2004 | 0.05 | 6.78 |
| Raqqa Type One | | 13 .9 6 | 4. 52 | 1.7 | 69 .1 5 | 3. 0 9 | 4. 41 | 0. 07 | 1. 3 | 0.6 | 0 | Henderson et al. 2004 | 1.02 | 6.07 |
| Raqqa Type One | | 12 .9 2 | 0. 44 | 3.0 3 | 73 .6 3 | 0. 4 4 | 8. 16 | 0. 05 | 0 | 0.3 1 | 0 | Henderson et al. 2004 | 0.05 | 3.58 |
| Raqqa Type One | | 14 .6 2 | 4. 75 | 2.5 8 | 64 .0 6 | 2. 5 9 | 7. 31 | 0. 11 | 1. 97 | 0.8 9 | 0 | Henderson et al. 2004 | 0.65 | 5.50 |
| Raqqa Type One | | 12 .7 6 | 0. 68 | 3.2 1 | 73 .1 6 | 0. 5 8 | 8. 17 | 0. 05 | 0 | 0.4 | 0 | Henderson et al. 2004 | 0.08 | 4.62 |
| Raqqa Type One | | 13 .1 3 | 3. 51 | 2.5 7 | 69 .7 | 3. 1 3 | 5. 52 | 0. 13 | 0. 14 | 1.0 6 | 0 | Henderson et al. 2004 | 0.64 | 4.83 |
| Raqqa Type One | | 12 .6 7 | 5. 48 | 1.4 2 | 71 .7 7 | 2. 6 | 4. 15 | 0. 06 | 0. 53 | 0.4 5 | 0 | Henderson et al. 2004 | 1.32 | 4.45 |
| Raqqa Type One | | 14 .6 4 | 3. 75 | 3.8 8 | 65 .2 7 | 3. 1 2 | 6. 47 | 0. 15 | 0. 15 | 1.4 2 | 0 | Henderson et al. 2004 | 0.58 | 5.14 |
| Raqqa Type One | | 15 .3 | 0. 58 | 3.1 7 | 71 .1 | 0. 5 1 | 7. 77 | 0. 06 | 0 | 0.3 2 | 0 | Henderson et al. 2004 | 0.07 | 5.41 |
| Raqqa Type One | | 13 .0 7 | 4. 16 | 2.0 6 | 70 .7 2 | 2. 2 | 4. 49 | 0. 08 | 1. 04 | 0.8 7 | 0 | Henderson et al. 2004 | 0.93 | 4.19 |
| Raqqa Type One | | 14 .5 3 | 6. 53 | 1.4 7 | 67 .5 3 | 2. 9 2 | 5. 05 | 0 | 0. 54 | 0.4 5 | 0 | Henderson et al. 2004 | 1.29 | 3.57 |
| Raqqa Type One | | 14 .7 4 | 0. 91 | 3.3 9 | 69 .3 4 | 0. 7 3 | 9. 51 | 0. 07 | 0 | 0.5 5 | 0 | Henderson et al. 2004 | 0.10 | 4.75 |

| | | | | | | | | | | | | | | |
|----------------|--|---------------|----------|----------|---------------|--------------|---------------|----------|----------|----------|---|-----------------------|------|------|
| Raqqa Type One | | 13 .7 6 | 5. 32 | 2.2 7 | 67 .3 2 | 2. 8 3 | 6. 14 | 0. 11 | 0. 23 | 0.9 1 | 0 | Henderson et al. 2004 | 0.87 | 5.44 |
| Raqqa Type One | | 13 .5 1 | 3 | 1.0 5 | 69 .0 2 | 2. 4 9 | 7. 48 | 0. 05 | 1. 75 | 0.3 | 0 | Henderson et al. 2004 | 0.40 | 6.31 |
| Raqqa Type One | | 14 .7 6 | 4. 22 | 2.6 9 | 64 .4 | 2. 5 2 | 8. 45 | 0. 1 | 0. 84 | 0.9 8 | 0 | Henderson et al. 2004 | 0.50 | 3.63 |
| Raqqa Type One | | 14 .0 8 | 3. 69 | 0.8 7 | 67 .5 2 | 2. 4 | 8. 4 | 0 | 1. 34 | 0.2 8 | 0 | Henderson et al. 2004 | 0.44 | 3.61 |
| Raqqa Type One | | 14 .2 4 | 4. 61 | 5.3 2 | 59 .5 3 | 3. 3 5 | 8. 27 | 0. 2 | 0. 83 | 2.2 9 | 0 | Henderson et al. 2004 | 0.56 | 7.74 |
| Raqqa Type One | | 14 .4 6 | 0. 59 | 3.1 1 | 69 .7 5 | 0. 5 7 | 10 .0 4 | 0 | 0 | 0.3 7 | 0 | Henderson et al. 2004 | 0.06 | 5.72 |
| Raqqa Type One | | 13 .6 6 | 0. 49 | 3.0 2 | 73 .0 6 | 0. 4 2 | 7. 73 | 0. 05 | 0 | 0.3 4 | 0 | Henderson et al. 2004 | 0.06 | 6.47 |
| Raqqa Type One | | 15 .4 3 | 0. 45 | 2.8 8 | 71 .1 3 | 0. 4 4 | 8. 32 | 0 | 0 | 0.2 5 | 0 | Henderson et al. 2004 | 0.05 | 4.61 |
| Raqqa Type One | | 14 .3 | 4. 19 | 2.6 3 | 65 .7 2 | 3. 6 6 | 6. 56 | 0. 13 | 0. 44 | 1.1 4 | 0 | Henderson et al. 2004 | 0.64 | 3.80 |
| Raqqa Type One | | 12 .1 1 | 3. 04 | 1.1 6 | 69 .7 6 | 2. 3 | 7. 94 | 0. 06 | 2. 07 | 0.4 3 | 0 | Henderson et al. 2004 | 0.38 | 5.48 |
| Raqqa Type One | | 14 .9 2 | 3. 11 | 1.5 6 | 67 .4 8 | 3 | 6. 47 | 0. 09 | 1. 41 | 0.6 9 | 0 | Henderson et al. 2004 | 0.48 | 7.61 |
| Raqqa Type One | | 12 .4 3 | 0. 77 | 3.1 3 | 73 .6 6 | 0. 5 5 | 7. 87 | 0. 05 | 0 | 0.4 | 0 | Henderson et al. 2004 | 0.10 | 6.41 |
| Raqqa Type One | | 15 .2 5 | 0. 53 | 3.1 2 | 71 .1 7 | 0. 5 2 | 7. 86 | 0 | 0 | 0.3 3 | 0 | Henderson et al. 2004 | 0.07 | 6.63 |
| Raqqa Type One | | 13 .7 | 0. 51 | 3.0 8 | 71 .1 2 | 0. 4 7 | 9. 68 | 0 | 0 | 0.2 9 | 0 | Henderson et al. 2004 | 0.05 | 3.80 |
| Raqqa Type One | | 13 .3 2 | 3. 3 | 0.8 8 | 68 .7 8 | 2. 5 4 | 8. 12 | 0. 06 | 1. 43 | 0.3 1 | 0 | Henderson et al. 2004 | 0.41 | 5.01 |
| Raqqa Type One | | 12 .9 1 | 0. 54 | 3.1 5 | 72 .5 8 | 0. 5 6 | 8. 81 | 0. 08 | 0 | 0.5 3 | 0 | Henderson et al. 2004 | 0.06 | 4.68 |

| | | | | | | | | | | | | | | |
|----------------|--|-------|------|------|-------|------|-------|------|------|------|---|-----------------------|------|------|
| Raqqa Type One | | 12.88 | 0.48 | 3.12 | 71.84 | 0.46 | 9.71 | 0 | 0 | 0.31 | 0 | Henderson et al. 2004 | 0.05 | 4.74 |
| Raqqa Type One | | 13.86 | 0.54 | 2.66 | 73.23 | 0.47 | 7.75 | 0.05 | 0 | 0.43 | 0 | Henderson et al. 2004 | 0.07 | 6.16 |
| Raqqa Type One | | 13.11 | 4.58 | 1.55 | 71.02 | 2.97 | 4.22 | 0.07 | 0.75 | 0.5 | 0 | Henderson et al. 2004 | 1.09 | 4.80 |
| Raqqa Type One | | 13.45 | 1.43 | 2.95 | 70.06 | 1.06 | 9.31 | 0.06 | 0.17 | 0.6 | 0 | Henderson et al. 2004 | 0.15 | 7.35 |
| Raqqa Type One | | 13.95 | 5.03 | 1.77 | 68.21 | 2.99 | 4.55 | 0.09 | 1.62 | 0.63 | 0 | Henderson et al. 2004 | 1.11 | 5.91 |
| Raqqa Type One | | 13.6 | 1.41 | 2.99 | 70.46 | 0.97 | 8.83 | 0.07 | 0.17 | 0.53 | 0 | Henderson et al. 2004 | 0.16 | 5.67 |
| Raqqa Type One | | 12.67 | 4.46 | 2.02 | 70.82 | 2.88 | 5.01 | 0.09 | 0.21 | 0.86 | 0 | Henderson et al. 2004 | 0.89 | 5.32 |
| Raqqa Type One | | 14.43 | 0.69 | 3.2 | 68.23 | 0.52 | 11.44 | 0 | 0 | 0.44 | 0 | Henderson et al. 2004 | 0.06 | 5.84 |
| Raqqa Type One | | 13.21 | 0.48 | 3.18 | 71.92 | 0.49 | 9.32 | 0 | 0 | 0.33 | 0 | Henderson et al. 2004 | 0.05 | 6.38 |
| Raqqa Type One | | 15.91 | 0.61 | 3.14 | 70.13 | 0.54 | 7.97 | 0.05 | 0 | 0.37 | 0 | Henderson et al. 2004 | 0.08 | 7.54 |
| Raqqa Type One | | 12.55 | 0.47 | 3.1 | 73.61 | 0.44 | 8.41 | 0 | 0 | 0.26 | 0 | Henderson et al. 2004 | 0.06 | 4.83 |
| Raqqa Type One | | 14.54 | 0.61 | 3.21 | 70.48 | 0.61 | 8.84 | 0 | 0 | 0.43 | 0 | Henderson et al. 2004 | 0.07 | 6.89 |
| Raqqa Type One | | 13.2 | 0.53 | 3.21 | 72.1 | 0.49 | 8.89 | 0 | 0 | 0.35 | 0 | Henderson et al. 2004 | 0.06 | 5.02 |
| Raqqa Type One | | 13.94 | 1.86 | 2.79 | 70.2 | 1.03 | 8.6 | 0.06 | 0.12 | 0.43 | 0 | Henderson et al. 2004 | 0.22 | 4.87 |
| Raqqa Type One | | 13.74 | 1.23 | 2.98 | 70.66 | 0.86 | 8.77 | 0.07 | 0.15 | 0.65 | 0 | Henderson et al. 2004 | 0.14 | 5.00 |
| Raqqa Type One | | 13.25 | 3.23 | 0.86 | 69.01 | 2.51 | 8.08 | 0.06 | 1.41 | 0.26 | 0 | Henderson et al. 2004 | 0.40 | 4.87 |

| | | | | | | | | | | | | | | |
|----------------|--|---------------|----------|----------|---------------|--------------|---------------|----------|---------------|----------|---|-----------------------|------|-----------|
| Raqqa Type One | | 13 .3 2 | 3. 87 | 2.0 4 | 68 .5 3 | 3. 3 5 | 4. 96 | 0. 1 | 1. 8 | 0.8 6 | 0 | Henderson et al. 2004 | 0.78 | 4.84 |
| Raqqa Type One | | 13 .4 5 | 1. 34 | 2.8 3 | 71 .1 1 | 0. 8 4 | 8. 9 | 0. 07 | 0. 07 | 0.4 2 | 0 | Henderson et al. 2004 | 0.15 | 5.51 |
| Raqqa Type One | | 13 .4 | 1. 32 | 2.9 7 | 69 .9 4 | 0. 8 8 | 9. 79 | 0. 07 | 0. 15 | 0.5 2 | 0 | Henderson et al. 2004 | 0.13 | 3.94 |
| Raqqa Type One | | 13 .7 3 | 2. 32 | 3.5 3 | 67 .3 1 | 2. 3 | 8. 27 | 0. 12 | 0. 13 | 1.2 1 | 0 | Henderson et al. 2004 | 0.28 | 5.77 |
| Raqqa Type One | | 14 .2 6 | 0. 52 | 4.6 2 | 69 .9 1 | 0. 4 8 | 8. 75 | 0 | 0. 05 | 0.2 1 | 0 | Henderson et al. 2004 | 0.06 | 4.83 |
| Raqqa Type One | | 15 .0 1 | 4. 28 | 4.2 4 | 62 .0 3 | 3. 3 8 | 7. 63 | 0. 19 | 0. 19 | 1.7 1 | 0 | Henderson et al. 2004 | 0.56 | 4.48 |
| Raqqa Type One | | 12 .8 6 | 3. 83 | 1.0 8 | 67 .3 9 | 2. 5 8 | 8. 98 | 0. 06 | 1. 49 | 0.4 | 0 | Henderson et al. 2004 | 0.43 | 5.77 |
| Raqqa Type One | | 14 .7 3 | 3. 72 | 4.2 2 | 63 .8 4 | 3. 4 1 | 7. 01 | 0. 16 | 0. 06 | 1.5 4 | 0 | Henderson et al. 2004 | 0.53 | 3.92 |
| Raqqa Type One | | 14 .6 4 | 4. 63 | 3.6 5 | 63 .6 6 | 2. 6 4 | 7. 54 | 0. 15 | 0. 51 | 1.2 9 | 0 | Henderson et al. 2004 | 0.61 | 12.5 1 |
| Raqqa Type One | | 15 .7 4 | 3. 08 | 3.2 6 | 62 .9 3 | 2. 4 9 | 7. 85 | 0. 12 | 1. 8 | 1.0 2 | 0 | Henderson et al. 2004 | 0.39 | 3.98 |
| Raqqa Type One | | 14 .3 3 | 0. 69 | 3.4 2 | 69 .1 3 | 0. 5 5 | 10 .4 3 | 0. 05 | 0 | 0.4 1 | 0 | Henderson et al. 2004 | 0.07 | 12.7 9 |
| Veh Ardasir | | 16 .9 | 4. 27 | 1.8 3 | 58 .8 | 3. 8 3 | 5. 8 | 0. 17 | 0. 03 6 | 0.9 | 0 | Henderson et al. 2004 | 0.74 | 54.5 2 |
| Veh Ardasir | | 14 .3 | 4. 13 | 2.8 8 | 60 .2 | 3. 3 4 | 6. 41 | 0. 24 | 0. 04 7 | 1.4 8 | 0 | Mirti et al. 2009 | 0.64 | 38.6 5 |
| Veh Ardasir | | 14 .9 | 4. 17 | 2.8 5 | 59 .4 | 3. 4 | 6. 54 | 0. 24 | 0. 05 | 1.4 8 | 0 | Mirti et al. 2009 | 0.64 | 16.5 6 |
| Veh Ardasir | | 14 .2 | 3. 82 | 2.7 2 | 62 .1 | 2. 9 8 | 6. 39 | 0. 23 | 0. 04 7 | 1.4 5 | 0 | Mirti et al. 2009 | 0.60 | 5.68 |
| Veh Ardasir | | 15 .7 | 3. 34 | 1.7 9 | 59 .5 | 3. 6 8 | 5. 16 | 0. 18 | 0. 03 7 | 0.9 | 0 | Mirti et al. 2009 | 0.65 | 5.61 |
| Veh Ardasir | | 14 .4 | 4. 14 | 2.8 5 | 58 .3 | 3. 8 4 | 6. 11 | 0. 16 | 0. 04 3 | 1.2 7 | 0 | Mirti et al. 2009 | 0.68 | 5.14 |

| | | | | | | | | | | | | | | |
|-------------|--|----------|----------|----------|----------|--------------|----------|---------------|---------------|----------|---|-------------------------|------|-----------|
| Veh Ardasir | | 15 .1 | 0. 42 | 2.1 3 | 65 .7 | 0. 4 2 | 7. 46 | 0. 05 1 | 0. 24 | 0.5 | 0 | Mirti et al. 2009 | 0.06 | 2.85 |
| Veh Ardasir | | 17 .6 | 8. 12 | 2.1 3 | 56 .9 | 3. 2 5 | 5. 09 | 0. 11 | 0. 03 4 | 0.6 8 | 0 | Mirti et al. 2009 | 1.60 | 5.33 |
| Veh Ardasir | | 17 .6 | 7. 66 | 1.2 8 | 59 .4 | 3. 3 4 | 4. 65 | 0. 05 2 | 0. 03 4 | 0.3 7 | 0 | Mirti et al. 2009 | 1.65 | 28.3 9 |
| Veh Ardasir | | 15 .4 | 4. 93 | 2.2 9 | 59 .4 | 3. 3 1 | 6. 26 | 0. 15 | 0. 03 1 | 0.9 4 | 0 | Mirti et al. 2009 | 0.79 | 2.96 |
| Veh Ardasir | | 16 .1 | 0. 7 | 2.1 | 66 .5 | 0. 5 9 | 5. 7 | 0. 11 | 0. 13 | 0.6 1 | 0 | Mirti et al. 2009 | 0.12 | 6.44 |
| Veh Ardasir | | 16 .7 | 0. 64 | 1.8 8 | 65 .2 | 0. 4 3 | 6. 49 | 0. 1 | 1. 04 | 0.5 6 | 0 | Mirti et al. 2009 | 0.10 | 8.31 |
| Veh Ardasir | | 12 .6 | 3. 21 | 1.8 7 | 65 .9 | 4. 3 8 | 5. 36 | 0. 12 | 0. 02 5 | 0.7 8 | 0 | Mirti et al. 2009 | 0.60 | 4.68 |
| Veh Ardasir | | 16 | 4. 03 | 2.3 7 | 66 .6 | 4. 0 7 | 6. 46 | 0. 18 | 0. 04 | 1.2 2 | 0 | Mirti et al. 2009 | 0.62 | 5.18 |
| Veh Ardasir | | 17 .8 | 5. 99 | 3.8 4 | 49 .4 | 3. 6 4 | 8. 83 | 0. 27 | 1. 75 | 2.4 8 | 0 | Mirti et al. 2009 | 0.68 | 8.20 |
| Veh Ardasir | | 17 .5 | 4. 72 | 2.5 1 | 57 .4 | 4. 3 8 | 6. 95 | 0. 17 | 0. 04 4 | 1.2 6 | 0 | Mirti et al. 2009 | 0.68 | 5.56 |
| Veh Ardasir | | 15 .5 | 4. 12 | 1.3 8 | 64 .7 | 3. 3 9 | 4. 86 | 0. 11 | 0. 02 4 | 0.6 1 | 0 | Mirti et al. 2009 | 0.85 | 5.60 |
| Veh Ardasir | | 14 .6 | 0. 62 | 2.4 9 | 66 .5 | 0. 4 6 | 7. 59 | 0. 06 8 | 1. 12 | 0.4 | 0 | Mirti et al. 2009 | 0.08 | 3.74 |
| Veh Ardasir | | 12 .9 | 0. 54 | 2.8 4 | 67 .2 | 0. 7 1 | 7. 96 | 0. 06 7 | 0. 51 | 0.3 8 | 0 | Mirti et al. 2009 | 0.07 | 5.58 |
| Veh Ardasir | | 18 .4 | 8. 18 | 1.7 9 | 56 | 3. 1 | 5. 19 | 0. 07 6 | 0. 04 2 | 0.5 4 | 0 | Mirti et al. 2009 | 1.58 | 6.24 |
| Veh Ardasir | | 16 .1 | 4. 3 | 1.6 9 | 58 .4 | 3. 9 | 7. 62 | 0. 08 2 | 0. 04 5 | 0.5 7 | 0 | Mirti et al. 2009 | 0.56 | 4.50 |
| Veh Ardasir | | 13 .5 | 3. 8 | 2.6 4 | 65 | 2. 9 4 | 6. 06 | 0. 24 | 0. 04 1 | 1.3 6 | 0 | Mirti et al. 2009 | 0.63 | 3.57 |
| Veh Ardasir | | 16 .6 | 7. 17 | 1.8 1 | 64 .3 | 2. 5 7 | 6. 33 | 0. 09 1 | 0. 07 3 | 0.8 2 | 0 | Mirti et al. 2009 | 1.13 | 7.72 |
| Veh Ardasir | | 14 .2 | 4. 75 | 3.0 8 | 60 .7 | 4. 2 | 6. 73 | 0. 19 | 0. 04 6 | 1.5 6 | 0 | Mirti et al. 2009 | 0.71 | 3.70 |
| Veh Ardasir | | 13 .8 | 0. 66 | 1.8 5 | 66 .3 | 0. 5 9 | 8. 75 | 0. 09 7 | 0. 03 4 | 0.5 9 | 0 | Mirti et al. 2009 | 0.08 | 7.34 |
| Veh Ardasir | | 17 .5 | 5. 95 | 1.5 2 | 56 .8 | 3. 9 4 | 6. 77 | 0. 07 2 | 0. 03 7 | 0.5 3 | 0 | Mirti et al. 2009 | 0.88 | 9.31 |
| Veh Ardasir | | 17 | 8. 41 | 0.9 5 | 59 .2 | 2. 9 7 | 8. 26 | 0. 12 | 0. 61 | 0.4 5 | 0 | Mirti et al. 2009 | 1.02 | 5.12 |

| | | | | | | | | | | | | | | |
|----------------|---------------|------|------|------|-------|------|------|-------|-------|------|-------|-------------------|------|------|
| Veh Ardasir | | 17.9 | 7.9 | 1.01 | 59.8 | 3 | 4.86 | 0.062 | 0.43 | 0.37 | 0 | Mirti et al. 2009 | 1.63 | 5.38 |
| Veh Ardasir | | 16.4 | 6.28 | 0.97 | 61 | 2.41 | 7.3 | 0.066 | 0.5 | 0.39 | 0 | Mirti et al. 2009 | 0.86 | 9.21 |
| Veh Ardasir | | 14.5 | 5.32 | 1.16 | 64 | 1.9 | 4.1 | 0.058 | 0.42 | 0.91 | 0 | Mirti et al. 2009 | 1.30 | 6.59 |
| Veh Ardasir | | 16.9 | 4.44 | 1.79 | 63.3 | 3.9 | 5.09 | 0.13 | 0.031 | 0.78 | 0 | Mirti et al. 2009 | 0.87 | 6.08 |
| Veh Ardasir | | 15.4 | 3.77 | 2.4 | 63.4 | 3 | 6.68 | 0.19 | 0.042 | 1.15 | 0 | Mirti et al. 2009 | 0.56 | 8.56 |
| Outliers | | | | | | | | | | | | | | |
| Nishapur | Emerald Green | 0.23 | 0.46 | 0.68 | 25.1 | 0.3 | 1.5 | 0.01 | 0 | 0.23 | 70.7 | Wypyski | | |
| Rayy (AH) R.28 | Emerald Green | 0 | 0 | 0 | 26.09 | 0 | 0 | 0 | 0 | 0 | 73.32 | Author | | |